The Bulletin of
The Canadian Association
of Physicists

Vol. 32 No. 3
Congress Issue 1976

Bulletin de
l'Association canadienne
des physiciens

Vol. 32 no. 3
Numéro du Congrès 1976

Physics in Canada

La Physique au Canada

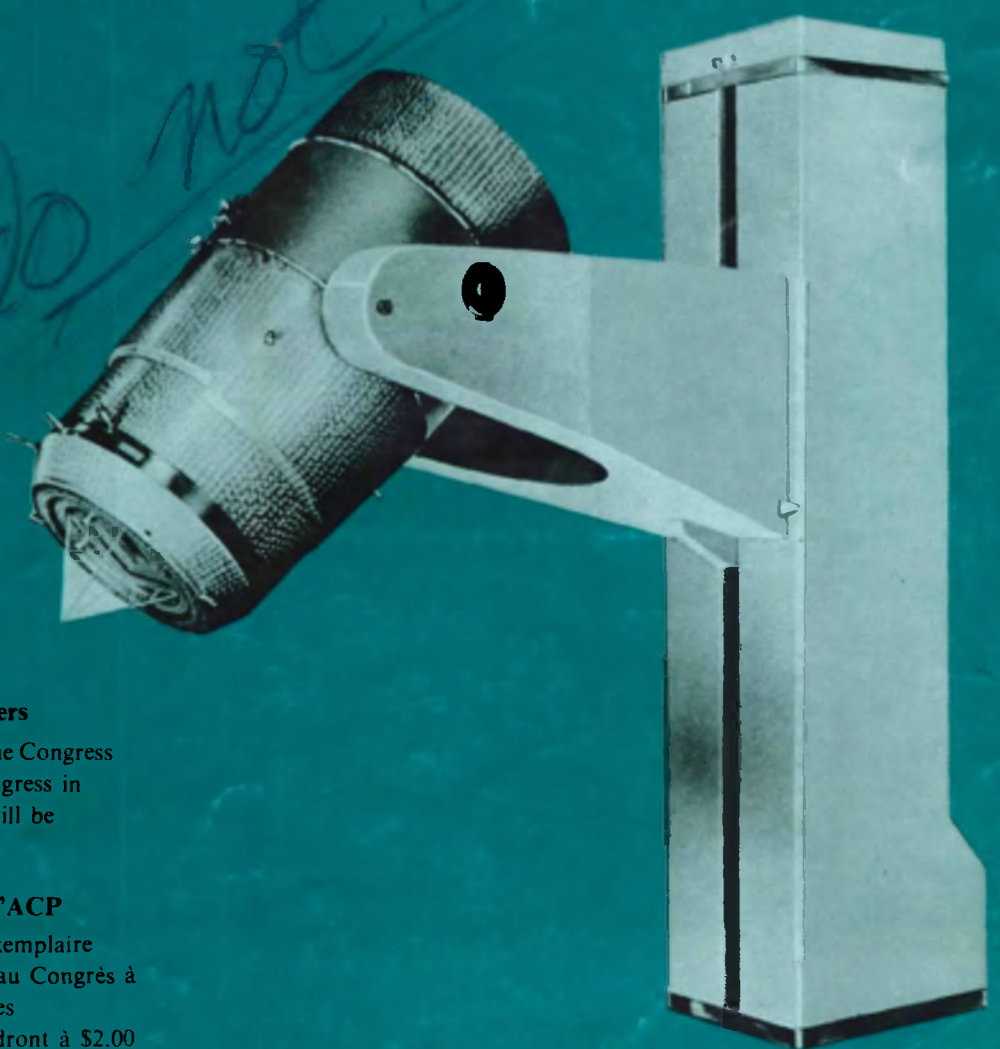

Notice to CAP Members

Bring this free copy of the Congress Issue to the annual congress in Québec: other copies will be available at $2.00 each.

Avis aux membres de l'ACP

Veuillez apporter cet exemplaire gratuit du programme au Congrès à Québec. Des exemplaires supplémentaires se vendront à $2.00 chacun.

A sophisticated 512* line FFT SPECTRUM ANALYZER for less than $7000?

YES!

Princeton Applied Research, a recognized leader in signal processing instrumentation, introduces the Model 4512 FFT Real Time Spectrum Analyzer.

FEATURES:

- dc-10Hz to dc-40kHz in 12 analysis ranges (dc-0.5Hz; dc-100kHz optional)
- Real time to 16kHz (FFT analysis in 35ms)
- 1024 input points
- 12-bit input A/D
- Spectral averaging
- Transient capture
- LED cursor reads out frequency *and* amplitude
- Scope, plotter and computer compatible outputs
- Simultaneous display of signal and spectrum
- Anti-aliasing filters (-120 db/octave)
- Field portable
- Small size
- Price; $6,900 (excludes scope)
- * 2048-line expanded memory option available at extra cost

Before commiting your dollars on a more expensive spectrum analyzer, why not check into PARC's new Model 4512 FFT Real Time Spectrum Analyzer. For additional information about how the Model 4512 fits your application, write or call:

Princeton Applied Research Corporation
P. O. Box 2565, Princeton, New Jersey 08540
Phone: 609/452-2111 Telex: 84-3409

In Canada: Contact Allan Crawford Associates Ltd.
Ottawa 613-829-9651
Montréal 514-670-1212
Vancouver 604-980-4831

335

**The Bulletin of
The Canadian Association
of Physicists**

Vol. 32 No. 3
Congress Issue 1976

Physics in Canada

**Bulletin de
l'Association canadienne
des physiciens**

Vol. 32 no. 3
Numéro du Congrès 1976

La Physique au Canada

Editorial Address:
English Copy:
R.L. Clarke
Physics Department
Carleton University
Ottawa, Ontario, K1S 5B6

Adresse de la Rédaction:
Textes français:
Gilles Lamarche
Département de Physique
Université d'Ottawa
Ottawa, Ontario, K1N 6N5

SUBSCRIPTION RATE/ABONNEMENT PAR AN $10.00
ADVERTISING, SUBSCRIPTIONS AND CHANGE OF ADDRESS/PUBLICITÉ, ABONNEMENT ET CHANGEMENT D'ADRESSE

Canadian Association of Physicists
Association Canadienne des Physiciens
Suite 903, 151 Slater Street
Ottawa, Ontario, K1P 5H3
Phone: (613) 237-3392

OFFICERS OF THE ASSOCIATION/BUREAU DE DIRECTION

COUNCIL/CONSEIL: 1975-76

*President	A.E. Douglas	National Research Council, Ottawa
*Past President	A.H. Morrish	University of Manitoba
*Vice-President	R.J.A. Levesque	Université de Montréal
*Vice-President Elect	H.E. Johns	Ontario Cancer Institute
*Honorary Secretary-Treasurer	J.S. Fraser	A.E.C.L., Chalk River
Director - Members	D.H. Jelly	Communications Research Centre, Ottawa
Director - Affiliates	G.R. Mason	University of Victoria
Director - Students	D. Verner	Université Laval
Director - Corporate Members	J.A. Courtney	Nicolet Canada Limited
Editor	R.L. Clarke	Carleton University

DIVISION CHAIRMEN

Aeronomy and Space Physics	D.J. McEwen	University of Saskatchewan
Atomic and Molecular Physics	T. Oka	National Research Council, Ottawa
Canadian Geophysical Union	D.I. Gough	University of Alberta
Condensed Matter Physics	D.R. Taylor	Queen's University
Medical & Biological Physics	J.R. Cunningham	Ontario Cancer Institute
Nuclear Physics	J.B. Warren	University of British Columbia
Optical Physics	C. Richard	Institut de Recherche de l'Hydro-Québec
Particle Physics	H.C.S. Lam	McGill University
Physics Education	D.C. Baird	R.M.C., Kingston
Plasma Physics	A.J. Alcock	National Research Council, Ottawa
Theoretical Physics	R.T. Sharp	McGill University

COUNCILLORS/CONSEILLERS

British Columbia and Yukon	K.E. Rieckhoff	(1)	Simon Fraser University
	D.F. Measday	(2)	University of British Columbia
Alberta	L.L. Cogger	(1)	University of Calgary
	J.A. Kernahan	(2)	University of Alberta
Saskatchewan and Manitoba	R.C. Barber	(1)	University of Manitoba
	K.V. Paulson	(2)	University of Saskatchewan
Ontario - Southwest	D.E. Brodie	(1)	University of Waterloo
	J.W. McConkey	(2)	University of Windsor
Ontario - Central and North	G.I.A. Stegeman	(1)	Erindale College, U. of Toronto
	L.D. Reed	(2)	C.D.I.E.M., Downsview
Ontario - East	J.P. Jan	(1)	National Research Council, Ottawa
	D.C. Baird,	(2)	R.M.C., Kingston
Quebec	J.M. Gagné	(1)	Ecole Polytechnique, Montréal
	C. St-Pierre	(2)	Université Laval
New Brunswick and Newfoundland	F.A. Weil	(1)	Université ce Moncton
	H. Kiefte	(2)	Memorial University of Newfoundland
Nova Scotia and Prince Edward Island	B.L. Blackford	(1)	Dalhousie University
	E.W. Grundke	(2)	St. Francis Xavier University
At large	R.E. Green	(1)	A.E.C.L., Chalk River
	R. Carbonneau	(2)	C.R.D. Valcartier
EDITOR - CANADIAN JOURNAL OF PHYSICS	P.R. Wallace		McGill University
EXECUTIVE SECRETARY/SECRETAIRE EXECUTIF	M.L. Jento		

*Member of Executive Committee (Revised By-Laws 1973, Art. V, Sec. 2)
(1) Term ends June ~~1976~~ 1977; (2) Term ends June ~~1977~~ 1978

CORPORATE MEMBERS - 1976 / MEMBRES CORPORATIFS - 1975

ALLAN CRAWFORD ASSOCIATES LIMITED
AUTOMATIC ELECTRIC (CANADA) LIMITED
BARRINGER RESEARCH LIMITED
BELL CANADA
BELL-NORTHERN RESEARCH LIMITED
BRUKER SPECTROSPIN (CANADA) LIMITED
CANADIAN GENERAL ELECTRIC CO. LIMITED
CANADIAN THIN FILMS LIMITED
COMPUTING DEVICES OF CANADA LIMITED
DOW CHEMICAL OF CANADA LIMITED
EALING SCIENTIFIC LIMITED
EDWARDS HIGH VACUUM (CANADA) LIMITED
ELECTROVERT LIMITED
ERIE TECHNOLOGICAL PRODUCTS OF CANADA
GULF OIL CANADA LIMITED
INSTITUT DE RECHERCHE DE L'HYDRO-QUEBEC
LUMONICS RESEARCH LIMITED
NICOLET CANADA LIMITED
ONTARIO HYDRO
POLYSAR LIMITED
RADIONICS LIMITED
RCA LIMITED
VARIAN ASSOCIATES OF CANADA LIMITED
WELWYN CANADA LIMITED

McGILL UNIVERSITY
MEMORIAL UNIVERSITY OF NEWFOUNDLAND
UNIVERSITY OF OTTAWA
UNIVERSITY OF SASKATCHEWAN
UNIVERSITY OF WATERLOO

CONGRES CONJOINT ACP-APS-SMF 1976 CAP-APS-SMF JOINT CONGRESS

RENSEIGNEMENTS GENERAUX

Le trente-et-unième congrès annuel de l'Association Canadienne des Physiciens se tiendra conjointement avec l'American Physical Society et la Sociedad Mexicana de Fisica. Il aura lieu du lundi 14 juin au jeudi 17 juin 1976, à la cité universitaire de l'université Laval, à Ste-Foy en banlieue de Québec.

Le département de Physique se réjouit de commencer son deuxième tiers de siècle d'existence en acceuillant ce congrès nord-américain des physiciens. L'Université Laval, pour sa part, a un long passé historique. C'est en 1852 qu'elle obtenait sa Charte mais elle doit sa naissance au Séminaire de Québec qui fut fondé en 1663 par Mgr de Montmorency Laval.

Guide pour l'arrivée

Les participants qui voyagent en voiture se dirigeront vers le boulevard Laurier à partir du pont Laporte. En suivant ce boulevard (qui change deux fois de nom), ils verront la cité universitaire à leur gauche (2½ milles du pont) puis atteindront le Château Frontenac, situé à l'intérieur des murs du Vieux Québec (7 milles du pont). Le long de ce boulevard, on trouve au moins une vingtaine d'hôtels et de motels entre le Pont Laporte et l'entrée de l'université Laval.

Il y a 7 milles entre l'aéroport et la cité universitaire et le taxi est le moyen de transport le plus approprié. Le tarif est d'environ $7.00. Une limousine fait le trajet entre l'aéroport et le Château Frontenac ($2.50 par personne). Cette limousine s'arrête à quelques hôtels et, sur demande, en face de la Cité universitaire.

Ceux qui ont réservé aux résidences universitaires se rendront au Pavillon Lemieux où se trouve le bureau des résidences (voir le plan ci-joint). Ce bureau est ouvert 24 heures par jour. Toutes les chambres des résidences sont simples et le coût est de $10. par jour. Des chambres adjacentes sont disponibles à prix réduit pour les familles.

Ceux qui ont fait leur réservation au Château Frontenac, ou à tout autre hôtel, doivent obtenir confirmation au préalable de l'hôtel.

En cas de difficulté, on pourra rejoindre le comité local au numéro 418-656-2658 avant le congrès, et au bureau de l'inscription, 418-656-9670 durant le congrès.

Transport Local

L'autobus urbain no 8 mène au Centre-ville. Il faut une correspondance avec le no 11 ou le no 7 pour se rendre au Château Frontenac. Deux importants Centres commerciaux se trouvent à ½ mille des résidences universitaires; on s'y rend facilement à pied.

Des autobus nolisés sont prévus pour les activités sociales du jour. Ces autobus partiront du pavillon de Koninck et feront un bref arrêt devant le Pavillon Lemieux.

GENERAL INFORMATION

The thirty-first annual Congress of the Canadian Association of Physicists will be held jointly with the American Physical Society and the Sociedad Mexicana de Fisica, from Monday June 14 to Thursday June 17, 1976 on the campus of Laval University located in Ste-Foy, a suburb of Québec City.

As it enters its 34th year, the Physics Department is especially happy to welcome physicists from all over North America to this tripartite congress. The history of Laval University dates back to the founding of the Séminaire de Québec in 1663 by Mgr Montmorency Laval. It received its charter in 1852.

Arrival Orientation

By car - From the Laporte bridge take Laurier Boulevard. The University campus is on the left hand side of the road, generally East about 2½ miles from the bridge. Continue along the boulevard (which changes name twice) to the Château Frontenac (7 miles from the bridge) which is located inside the walls of Old Québec. There are some 20 hotels and motels along the Boulevard between the bridge and the Château Frontenac.

By Air - The University campus is 7 miles from the aeroport. Taxis, fare approximately $7.00, are recommended. A limousine service operates between the aeroport and the Château Frontenac (Fare $2.50 /Person). Stops are made at some hotels and, on request, opposite the Cité Universitaire.

Persons who have reserved accommodation in the university residences should proceed directly to the residence office in the Pavillon Lemieux (see map) which is open 24 hours a day. Single rooms only are available, at $10. per day. Families may be accommodated in adjacent rooms at reduced rates.

Reservations at the Château Frontenac and other hotels should be confirmed directly with the hotel.

In case of difficulty the Local Committee may be contacted before the congress at (418) 656-2658, or at the Registration Desk (418) 656-9670, during the Congress.

Local Transportation

City bus No. 8 goes to the centre of the city. Transfer to No. 11 or 7 for the Château Frontenac. There are two large shopping centres within easy walking distance (½ mile) of the University residences.

Chartered buses have been laid on for the social events; they will depart from the Pavillon de Koninck with a brief stop in front of the Pavillon Lemieux.

Inscription

Toutes les activités principales du congrès se dérouleront au Pavillon de Koninck. Le bureau d'inscription pour le congrès sera situé au local 1231 et sera ouvert aux heures suivantes:

dimanche, 13 juin	14 h 00 - 21 h 00	
lundi, 14 juin	8 h 30 - 17 h 00	
mardi, 15 juin	8 h 30 - 17 h 00	
mercredi, 16 juin	8 h 30 - 17 h 00	

Les frais d'inscription sont établis comme suit:

Membre de l'ACP, APS ou SMF	$25.00
Non-membres	$30.00
Enseignants d'école secondaire ou CEGEP et étudiants prégradués.	$ 3.00

Les personnes qui accompagnent les délégués sont aussi priées de s'inscrire; dans ce cas il n'y a aucun frais d'inscription.

Les billets pour le banquet et pour les diverses activités sociales seront en vente au bureau d'inscription.

Les repas

Les repas seront servis à la cafétaria du pavillon Pollack aux heures suivantes:

dimanche:		17 h 00 - 18 h 30
sur semaine:	petit déjeuner	7 h 15 - 9 h 30
	déjeuner	11 h 30 - 13 h 30
	diner	17 h 00 - 18 h 30

Le coût pour les 3 repas est d'environ $7.00.

La salle "La Résille" du pavillon Pollack est un "steak house" avec permis d'alcool. Les heures des repas sont:

déjeuner:	11 h 30 - 14 h 00	
diner :	17 h 00 - 19 h 00	

Le café-terrasse du pavillon Pollack offre un service de bar et des mets froids de 11 h 00 à 01 h 00.

Au pavillon de Koninck, on trouvera des machines distributrices à l'étage 0, ainsi qu'un bar au café-terrasse situé sous la tente dans la cour intérieure ouvert de 10 h 00 à 17 h 30.

Les amateurs de bonne cuisine à prix modique pourront profiter des déjeuners d'affaires offerts dans les meilleurs restaurants. Les gourmets trouveront facilement satisfaction à Québec. Une liste de bons restaurants sera fournie.

Stationnement

Lors de l'inscription, on pourra se procurer au coût de $2.50 une vignette valable sur les espaces de stationnement à panneau indicateur de couleur rouge. Sans cette vignette, les visiteurs doivent utiliser les stationnements orangés pour lesquels le tarif est horaire avec un maximum de $1.50 au-delà de 2h½.

Registration

The Pavillon de Koninck is the centre of congress activities. The Registration Desk will be located in Room 1231 and will be open as follows:

Sunday, June 13th	14 h 00 - 21 h 00	
Monday, June 14th	8 h 30 - 17 h 00	
Tuesday, June 15th	8 h 30 - 17 h 00	
Wednesday, June 16th	8 h 30 - 17 h 00	

The registration fees are:

Member: CAP, APS, SMF	$25.00
Non-Members	$30.00
High School and CEGEP Teachers and Undergraduate students	$ 3.00

Persons accompanying delegates are also asked to register. There is no registration fee for companions.

Tickets for the banquet and other social events may be purchased at the Registration Desk.

Arrangements for Meals

Meals will be available in the cafeteria of the Pavillon Pollack:

Sunday		17 h 00 - 18 h 30
Weekdays:	Breakfast	7 h 15 - 9 h 30
	Luncheon	11 h 30 - 13 h 30
	Dinner	17 h 00 - 18 h 30

The cost of 3 meals a day is approximately $7.00.

"La Résille", the steak house in the Pavillon Pollack is licensed and meals are served as follows:

Luncheon	11 h 30 - 14 h 00	
Dinner	17 h 00 - 19 h 00	

The café-terrasse, open from 11 h 00 to 01 h 00, is also located in the Pavillon Pollack and offers bar service and cold plates.

In the Pavillon de Koninck, food vending machines are located on Floor 0. The covered café-terrasse in the courtyard offers bar service.

Business luncheons at reasonable prices are available in most good restaurants. Québec has a variety of excellent restaurants to delight the epicure. A list of good restaurants will be included in the registration kit.

Parking

At the time of registration persons requiring parking may purchase stickers, valid in the "red" parking lots, for $2.50. Others will have to park in the orange, hourly, parking areas - Maximum $1.50 /day after 2½ hours.

Comité local / Local Committee

Président	Claude St-Pierre	Chairman
Vice-président	Gabriel Bédard	Vice-Chairman
Secrétaire-Trésorier	Yvan Chassé	Secretary-Treasurer
Hébergement	Yvan Chassé	Accommodation
Salles de conférences et services	Robert Lalande	Lecture rooms & Services
Expositions et exposants	Gabriel Bédard	Exhibition & Exhibitors
Inscription	Rodolfo J. Slobodrian	Registration
Publicité et information	H.H. Arsenault	Publicity & Information
Programme local et banquet	Paul Koenig	Local programs & Banquet
Représentant du Service des Relations publiques	Mademoiselle L. Marquis et/ou J.-M. Carpentier	Public relations Representative
Représentant de U.C.G.	M.K. Seguin	C.G.U. Representative
Représentant de Vie Etudiante	Robert Tremblay	Student representative

Pour tout renseignement concernant le congrès et les activités sociales et en cas de difficulté, on s'adressera, pendant le congrès, au bureau de l'inscription, salle 1231 du Pavillon de Koninck, Téléphone: 656-9670.

For information about the Congress and social events and in case of difficulty during the Congress, contact the Registration Desk, room 1231, Pavillon de Koninck, Telephone: 656-9670.

Les services de placement de l'A.C.P. seront à la salle 1248, le bureau de la presse à la salle 1249, et le bureau de l'exécutif de l'ACP à la salle 1252 du Pavillon de Koninck.

The CAP Placement Service will be located in Room 1248, the Press in Room 1249, and the CAP executive office in Room 1252, all in the Pavillon de Koninck.

EXPOSITION PAR LES MANUFACTURIERS ET LES EDITEURS

Un vaste choix d'appareils scientifiques et de volumes techniques ou d'enseignement seront en exposition et les représentants manufacturiers seront à la disposition des congressistes. Les loges des exposants se trouvent dans le Hall central face aux auditorium des étages 1 et 2. On trouvera ci-joint la liste des exposants en date du 15 avril. Notez bien les heures d'ouverture de l'exposition:

MANUFACTURERS AND PUBLISHERS EXHIBITION

A wide selection of scientific equipment and of scientific and technical books will be exhibited. Manufacturers' representatives will also be on hand to meet the delegates. The exhibitors' booths are located in the lobbies outside the session rooms on the 1st and 2nd floors. The exhibitors as of April 15 are listed on page viii. The exhibition will be open:

lundi le 14 juin	13 h 00 - 18 h 00	Monday, June 14
mardi le 15 juin	10 h 00 - 18 h 00	Tuesday, June 15
mercredi le 16 juin	10 h 00 - 18 h 00	Wednesday, June 16

Café et Rafraichissements

Le café sera servi durant les pauses de l'avant-midi et de l'après-midi aux deux extrémités des halls des étages 1 et 2.

Refreshments

Coffee will be available mid-morning and mid-afternoon at both ends of the lobbies on the 1st and 2nd floors.

VISITE DES LABORATOIRES DE RECHERCHE

Les activités de recherche du département de physique sont concentrées dans quatre domaines: physique atomique et moléculaire, physique nucléaire, optique et laser, et astronomie. Tous les laboratoires sont situés au pavillon Vachon. On peut y voir notamment plusieurs sélecteurs d'électrons de type monocinétrons, un laser de 5 gigawatts de puissance

RESEARCH LABORATORIES OPEN HOUSE

The research activities of the Physics Department are divided into four main fields: atomic and molecular physics, nuclear physics, optics and lasers, and astronomy. All the laboratories are located in the Pavillon Vachon. Of special interest are several electron monochrometors, a 5 gigawatt peak power laser, optical processer set-ups and an 8 MV

instantanée, des montages de traitement optique de l'information et un accélérateur Van de Graaff de 8 MV. Les visites se feront de façon rotative. Un horaire sera présenté au tableau d'affichage et au tableau vidéo.

On pourra aussi visiter les laboratoires de géophysique au département de Géologie situé au 4ème étage du Pavillon Pouliot.

Van de Graaff accelerator. Tours will be arranged on a rotating basis. The schedule will be posted on the Notice Board and will be shown on the video screen.

The geophysics laboratories in the Geology Department, 4th floor, Pavillon Pouliot, will also be open to visitors.

ACTIVITES SOCIALES

Québec est une ville touristique des plus intéressantes. Seule ville fortifiée d'Amérique, ses remparts, ses vieilles maisons, ses rues étroites, ses champs de bataille font partie de son histoire. Son caractère français ne fait qu'ajouter un cachet de plus à son charme.

Une visite du Vieux Québec à pied est très fortement recommandée. On ne manquera pas non plus de visiter la Place Royale. Il existe aussi un service de visite de la ville et des environs en autobus. Les dames voudront sans doute profiter de l'occasion pour visiter les boutiques.

Lors de l'inscription, on vous remettra ce qui suit:

1) Une carte de la ville de Québec
2) Un dépliant "Québec vu à pied"
3) Un guide sur Québec et ses environs
4) Une liste annotée des restaurants.

SOCIAL EVENTS

Québec, the only fortified city on the North American continent, is a fascinating tourist attraction; the ramparts, old houses, narrow streets and battlefields all form part of its history. The French character of the city adds to its charm.

A walking tour of Old Québec is a must. One should also see Place Royale. Bus tours of the city and vicinity are available. Ladies will no doubt wish to visit the boutiques.

The registration kit will include:

1) A map of Québec City
2) A pamphlet describing a walking tour of Québec
3) A guide to Québec and the surrounding area
4) An annotated list of restaurants

VISITES SPECIALES

Trois excursions ont été organisées en collaboration avec des guides experts. Les réservations doivent être faites au moins 24 heures à l'avance. Les autobus partiront du pavillon de Koninck et feront un arrêt devant le pavillon Lemieux.

Excursion 1: *Québec photogénique*
lundi le 14 juin

Visite des sites photogéniques de la ville de Québec. On s'arrête à de nombreux endroits charmants. On pourra aussi contempler la ville dans toute sa splendeur du sommet du plus haut édifice.

Durée: 3 heures. Coût: $3.00
Départ à 13 h 45 du Pavillon de Koninck.

Excursion 2: *Québec historique*
mardi le 15 juin

La civilisation française en Amérique du Nord vue à travers son architecture, sa sculpture, sa peinture, son orfèvrerie et ses arts mineurs. On visite le Musée du Québec, le Séminaire, le Couvent des Ursulines. Déjeuner dans un restaurant pittoresque ou libre. Puis visite de la Place Royale, de l'Eglise Notre-Dame des Victoires puis de la Maison Chevalier et de la Maison des vins où il y aura dégustation.

Durée: 5 heures. Coût: $6.00 déjeuner non inclus
Départ à 9 h 30 du Pavillon de Koninck.

SPECIAL TOURS

Three tours have been organized in consultation with expert guides. Reservations must be made at least 24 hours in advance. Buses will leave from the Pavillon de Koninck with a stop in front of the Pavillon Lemieux.

Tour 1: *Picturesque Québec*
Monday June 14

Tour of the picturesque areas of Québec. Stops at a number of delightful places of interest. Panoramic view of the city from its highest building.

Duration: 3 hours. Cost: $3.00
Departure: 13 h 45 from Pavillon de Koninck.

Tour 2: *Historical Québec*
Tuesday June 15

The French culture in North America - its architecture, sculpture, painting, precious metal artwork and crafts. The tour includes visits to the Musée du Québec, the Seminary and the Ursuline Convent. Luncheon in a picturesque restaurant or one of your choice, followed by visits to Place Royale, Notre-Dame des Victoires church, then to Maison Chevalier and the Maison des vins for a winetasting.

Duration: 6 hours. Cost $6.00 luncheon excluded
Departure: 9 h 30 from Pavillon de Koninck.

Excursion 3: *L'Ile d'Orleans*
mercredi le 16 juin

L'Ile d'Orléans est renommée pour la beauté de ses paysages, son caractère champêtre, ses vieilles fermes et l'art unique de ses églises d'époque. Arrêts prévus à tous les endroits particulièrement intéressants. Déjeuner dans l'ancien moulin benal (public par opposition à seigneurial) de St-Laurent. Un circuit inoubliable.

Durée: 6 heures. Coût $6.00 déjeuner non inclus
Départ à 9 h 30 du Pavillon de Koninck.

Tour 3: *Ile d'Orleans*
Wednesday June 16

Ile d'Orleans is famous for its beautiful countryside, rustic atmosphere, old farms and the unique architecture of its old churches. Stops are scheduled at all the most interesting places. Luncheon in the old St-Laurent communal mill. An unforgettable tour.

Duration: 6 hours. Cost $6.00 luncheon excluded
Departure: 9 h 30 from Pavillon de Koninck.

Sports et loisir

Le Pavillon de l'Education physique et des sports (PEPS) est extrêmement bien équipé. Il possède, entre autres, une piste intérieure et une piscine olympique. En raison des nombreuses compétitions qui s'y déroulent, il n'est pas possible d'annoncer à l'avance les heures d'ouverture au public. Celles-ci seront affichées au babillard et au tableau vidéo.

Recreational Facilities

The Pavillon de l'Education Physique (PEPS) is very well equipped with, among other things, an indoor track and an olympic swimming pool. It is not possible to indicate in advance when these facilities will be open to the public because of the large number of competitions that it accommodates. The times will be posted on the Bulletin Board and the video screen.

Réception et banquet: Mercredi le 16 juin

Le Recteur de l'Université Laval, le Dr Larkin Kerwin, recevra les congressistes à une réception à 17 h 30 au jardin géologique près du Pavillon Pollack, ou en cas de pluie au Grand Salon du Pavillon Pollack.

Le banquet aura lieu en la salle de bal du Château Frontenac à 19 h 30. Le prix (vins inclus) est de $15.00 par personne. On doit acheter son billet avant 10 h le mardi. Le nombre de places est limité et l'on vous conseille de vous procurer votre billet dès l'inscription.

Reception & Banquet: Wednesday June 16

The Rector of Laval University, Dr Larkin Kerwin, will give a reception for delegates and their companions at 17 h 30 in the Geological Gardens adjacent to the Pavillon Pollack. In the event of rain the reception will be held in the Grand Salon of the Pavillon Pollack.

The Banquet will follow at 19 h 30 in the ballroom of the Château Frontenac. The cost (wine included) is $15.00 per peron. Tickets must be purchased before 10 h 00 on Tuesday. As the number of tickets is limited you would be well advised to purchase your ticket (s) when you register.

Soirée d'acceuil:

Un bar-rencontre aura lieu le dimanche 13 juin 1976 de 20 h 00 à 22 h 00 dans le Grand Salon du Pavillon Pollack. C'est une excellente occasion de rencontrer les membres du département et de retrouver de vieilles connaissances.

Mixer: Sunday June 13

Meet the members of the Physics Department and renew old acquaintances at the Bar-rencontre in the Grand Salon, Pavillon Pollack, from 20 h 00 to 22 h 00.

PLACEMENT SERVICE

The Placement Service Committee will maintain a bulletin board during the week of the Congress on which recent lists of available positions as compiled by the Committee will be displayed. The same area will be available as a communications centre for those wishing to advertise new job openings, or by members who are presently seeking employment.

PLAN DE LA CITÉ UNIVERSITAIRE

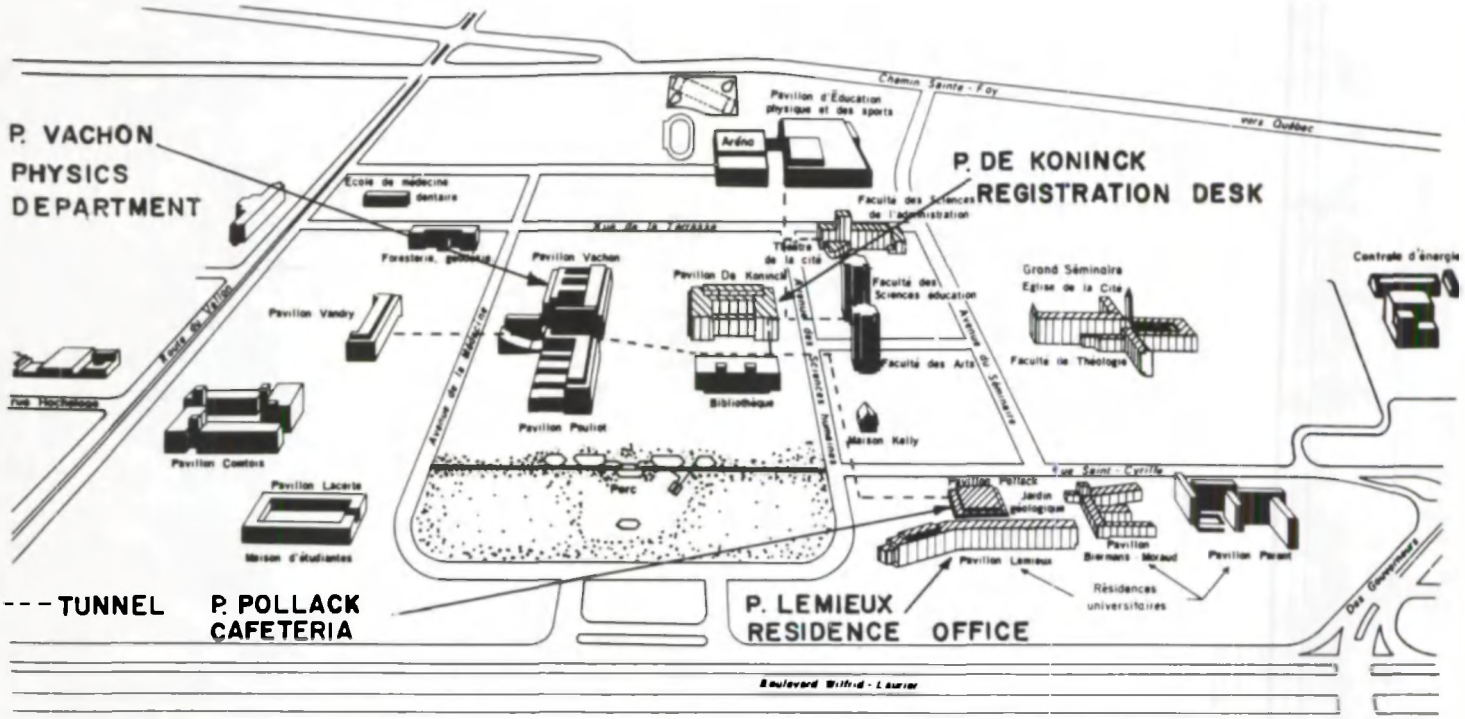

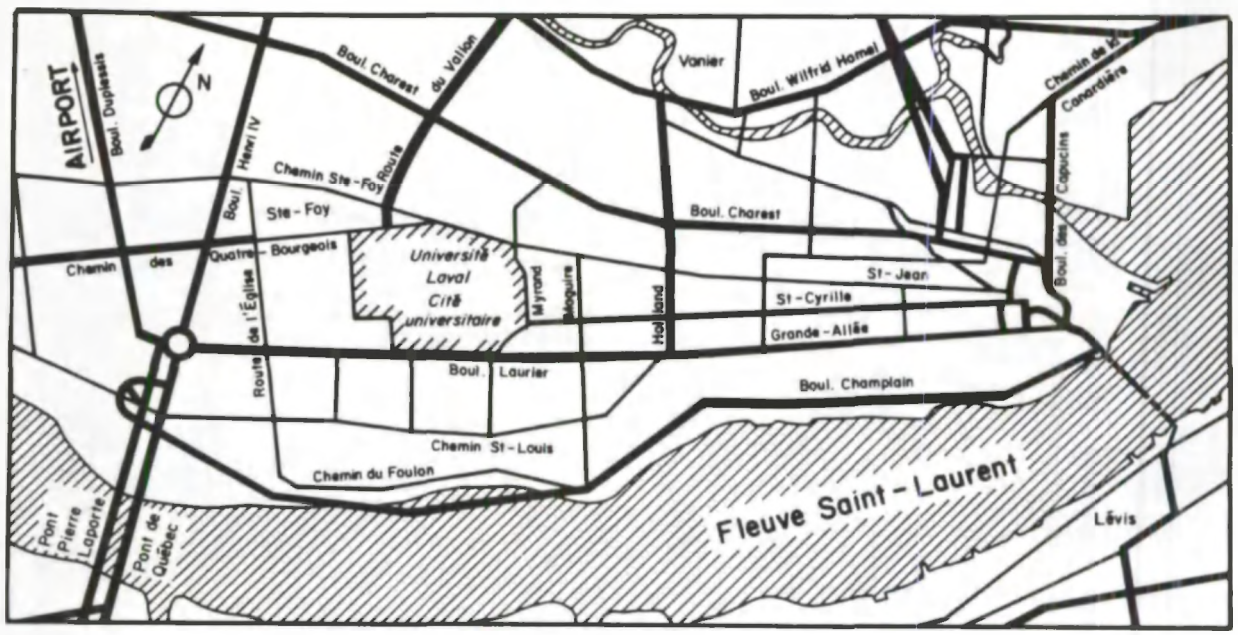

QUEBEC METROPOLITAIN

CANADIAN ASSOCIATION OF PHYSICISTS MEDALLISTS 1976
LAUREATS DE L'ASSOCIATION CANADIENNE DES PHYSICIENS 1976

CAP Medal for Achievement in Physics

~~Jan Van Kranendonk~~
A.H. MORRISH.

Herzberg Medal

~~John Christopher~~ Hardy
H.B. WALKER.

CANADIAN ASSOCIATION OF PHYSICISTS PRIZE EXAM 1976
RESULTATS DE L'EXAMEN DE L'ASSOCIATION CANADIENNE DES PHYSICIENS 1976

118 29

~~Eighty-three~~ students from ~~nineteen~~ universities competed ~~this year.~~ The exam was administered by ~~H.G. Calkin~~ of Dalhousie University, Halifax. ~~An alphabetical list of the first ten contestants with the names of the first [redacted] prize-winners in order of rank is given below:~~

Richard Adler	University of Alberta
Kevin Hamilton	Queen's University - FIRST PRIZE
William Hsieh	University of British Columbia
Ross Male	University of Waterloo
Gilbert Morin	Ecole Polytechnique
Kirk Olynyk	Simon Fraser University
Jacques Richer	Université de Montréal - DEUXIEME PRIX
Stanley Shadick	University of Saskatchewan
Lorne Whitehead	University of British Columbia - THIRD PRIZE
Mark Wise	University of Toronto
Ian Youle	Dalhousie University

FUTURE CONGRESSES
CONGRES FUTURS

~~1977 - University of Saskatchewan, Saskatoon, June 20-23~~
1978 - University of Western Ontario, London, June 12-15
1979 - University of British Columbia, Vancouver, June 18-21
1980 - McMaster University, Hamilton June 16-19
1981 - Dalhousie University, Halifax

CONGRES CONJOINT ACP-APS-SMF 1976 CAP-APS-SMF JOINT CONGRESS

LISTE DES EXPOSANTS/LIST OF EXHIBITORS
En date du 15 Avril 1976

Manufacturiers et Représentants/Manufacturers and Suppliers

AIRCO TEMESCAL

ALLAN CRAWFORD ASSOCIATES LIMITED

APTEC ENGINEERING LIMITED/L'INGENIERIE APTEC LIMITEE

CANADIAN VACUUM EQUIPMENT COMPANY LIMITED

CESCO ELECTRONICS LIMITED/CESCO ELECTRONIQUE LIMITEE

DATACOMP ELECTRONICS LIMITED

FISHER SCIENTIFIC COMPANY LIMITED

JANIS RESEARCH COMPANY INC.

LAKE SHORE CRYOTRONICS INC.

LUCTOR CANADA LTD

MINNESOTA VALLEY ENGINEERING

NICOLET INSTRUMENT CORPORATION

NUCLEAR DATA INC.

THE OPTIKON CORPORATION LIMITED/LA CORPORATION OPTIKON LIMITEE

RADIONICS LIMITED

S.H.E. CORPORATION

VARIAN ASSOCIATES OF CANADA LTD

Editeurs/Publishers

ADDISON-WESLEY (CANADA) LIMITED

HOLT, RINEHART AND WINSTON OF CANADA LIMITED

W.B. SAUNDERS COMPANY CANADA LIMITED

Geophysique/Geophysics

SOQUEM (SOCIETE QUEBECOISE D'EXPLOITATION MINIERE)

EARTH PHYSICS BRANCH
ENERGY MINES AND RESOURCES CANADA

DIRECTION DE LA PHYSIQUE DU GLOBE
ENERGIE, MINES ET RESSOURCES CANADA

LISTENERS, SPEAKERS, AND SESSION CHAIRMEN

SPECIAL INSTRUCTIONS FOR TIMED PAPERS

To make the adoption of timed papers successful, the cooperation of the audience, speaker, and session chairman are imperative.

LISTENERS

1) Arrive at a lecture theatre promptly before the next paper is to begin. If this is not possible, take a seat quietly enough so that the paper can begin on schedule.

2) Leave a session unobtrusively, probably either during or at the end of the question and answer period.

SPEAKERS

1) Make your slide projection arrangements before the start of your paper, probably before the start of your session.

2) Be ready to start your talk on time.

3) Pace your talk to end well before the next talk begins: about 3 minutes for a contributed paper and about 10 minutes for an invited paper.

4) Answer questions and perhaps comments as completely and briefly as made necessary by the response of the audience.

5) Obey your chairman's instructions.

6) Most important, practise giving your talk BEFORE the meeting. Remember, you are the ambassador of your department and institution, and you will be judged by your audience.

CHAIRMEN:

1) Get to the session room about half an hour before your session begins. Check that all needed projection and auxiliary equipment are present and operational. Check that your speakers are healthy, and above all, present.

2) Start each paper right on time.

3) Make sure each speaker stops talking well before the next paper begins.

4) Keep the after paper delivery periods interesting, lively, and productive. If no one asks a question, you ask one (or more), and get the audience involved. After all, you are an expert, and this is why you were appointed session chairman. Read the papers in your session over before the session. If necessary, prepare comments and questions. If the audience has more than enough to contribute to fill the between paper gap, then keep quiet.

5) Do not let any discussion period get out of hand, either on the speaker's or the questioner's side.

6) If no one appears to give a paper, then either close the session until the time of the next scheduled speaker or else use the time imaginatively, perhaps begin a discussion of earlier papers.

7) Under no circumstances may the order of giving the papers differ from that given in the program, even though you may, in your wisdom, see a better arrangement than that determined by the program committee.

INVITED SPEAKERS/CONFERENCIERS INVITES

ADLER, J.G., *University of Alberta;* HD1: The Study of Organic Molecules on Surfaces by Electron Tunnelling
AHLSTROM, H.G., *Laser Plasma Interaction Group - Lawrence Livermore Laboratory;* GA1: Laser Plasma Interaction Experiments for Fusion
ANDERSON, H., *University of Chicago;* EI5: Deep Inelastic Muon Scattering
BERKO, S., *Brandeis University;* DD1: Measurement of the "Lamb Shift" of the first Excited State of Positronium
BOYD, G.M., *Concordia University;* DF2: Gaming and Simulations as Motivators
BUGG, D.V., *Queen Mary College, London and TRIUMF;* DA1: Nucleon-Nucleon Elastic Scattering
CAMPBELL, C., *University of Minnesota;* CC4: The Registered Phases of Helium Monolayers
CARNEGIE, R., *Carleton University;* EI4: $K\pi$ and $K\pi$ π Results from a 13 GeV $K^{\pm}p$ Experiment
CHASSE, Y., *Université Laval;* DF4: Enseignement individualisé en physique à Laval
CHENG, Y.C., *Xerox Research Centre of Canada Ltd;* EE2: Surface Physics Research in Industry
CLINE, D., *University of Wisconsin;* EI1: Excitation of New States of Matter by High Energy Neutrinos
CROZIER, E.D., *Simon Fraser University;* AC1: Structural Determinations of Condensed Matter Using Synchrotron Radiation
DUPUY, M., *Canada Department of External Affairs;* BJ2: Canadian Nuclear Export Sales Policies
FEINBERG, G., *Columbia University;* HA4: Neutral Current Effects in Muonic Atoms
GOLDSTEIN, S., *University of Maryland;* BI3: Ion Induced Pinching and Intense Ion Currents
GREENWOOD, T., *Political Science, M.I.T;* BJ1: The Nuclear Industry, Nuclear Proliferation and International Approaches to Control
GRIFFIN, A., *University of Toronto;* CF2: Surface Magnetism and Surface Spin Waves in Itinerant Ferromagnets
HAMEL, P.E., *Atomic Energy Control Board, Ottawa;* BJ3: Nuclear Waste Management
HARTMAN, G., *Xerox Research Centre of Canada Limited;* EE3: Research in Electrophotography
HELAVA, J., *M.I.T.,* BI1: High Density Operation of Alcator
HENDERSON, D., *Laser Theory Group, Los Alamos Scientific Laboratory;* GA2: Laser Plasma Interaction
HERSKIND, B., *Niels Bohr Institute, Copenhagen, Denmark, and Chalk River Nuclear Laboratories, Canada;* AA2: Studies of Heavy Ion Fusion Reactions from Gamma-Ray Multiplicity Measurements
HERZBERG, G., *National Research Council of Canada;* AB1: Optical Spectra of Molecular Ions
HUEBNER, R., *Argonne National Laboratory;* CB2: Apparent Oscillator Strength Densities from the Electron Energy Loss Measurements
IZATT, J.R., *Université Laval;* DE1: Optically Pumped Far Infrared Lasers
JAMES, A.N., *University of Alberta, TRIUMF;* DA2: Nucleon-Nucleon Interactions in Nuclei; a survey of the prospects for direct investigations
JENSEN, R., *Laser Isotope Separation Group - Los Alamos Scientific Laboratory;* GA3: Laser Isotope Separation Experiments at LASL
JOHNSON, K., *M.I.T.;* BF3: The M.I.T. Model for Structure of Hadrons
JONES, A.V., *Herzberg Institute of Astrophysics, N.R.C.;* ED1: Modelling of Electron Aurora
KABIR, P., *University of Virginia;* HA3: Symmetry Properties of Atomic and Nuclear Interactions
KALMAN, C.S., *Concordia University;* DF3: Cultural Influences on Physicists
KARL, G., *University of Guelph,* EG2: Speculations on Quarks
KERWIN, L., *Université Laval;* DF1: Physics Education: Some Personal Views
KORNELSEN, E.V., *National Research Council, Ottawa;* HB1: Interaction of Helium with Vacancies in Metals
KUEHNER, J.A., *McMaster University;* HA1: Use of Tensor Polarized Deuterons to Measure Spin and Parity
LESSARD, L., *McGill University;* AA1: Nuclear Fission Studies with On-Line Mass Spectrometers
MACFARLANE, M.H., *Argonne National Laboratory;* AA3: Heavy Ion Reactions
MADDEN, R.P., *National Bureau of Standards, Washington, D.C.;* AC2: Atomic and Molecular Experiments Using Synchrotron Radiation
MANDEL, L., *University of Rochester;* BG1: Superradiance and Optical Free Induction
MARMET, P., *Université Laval;* CB3: Les spectres des états électroniques des atomes mesurés par électroionisation; ED3: Electron Impact Production of Highly Excited (12-25 eV) Atmospheric Gases
MATTHEWS, J.A.J., *Michigan State University;* EI3: Particle Search Results from Fermilab
MCDONALD, R.D., *Solid State Chemistry Department, Canada Wire & Cable Limited;* AF2: Fibre Optics Communication Technology
MEYER, J., *University of British Columbia;* BI4: Mixing and Stimulated Scattering of Light in Plasmas and Other Refractive Media
MICHEL, L., *Institut des Hautes Etudes Scientifiques, Bures sur Yvette, France et Centre de Recherche Mathématique, Université de Montréal;* EG1: Broken Symmetries
MOSHINSKY, M., *Universidad de Mexico;* CF1: Group Theory and Collective Motions in Nuclei
NESBET, R.K., *IBM Research Laboratories, San Jose, California;* CB4: Low Energy Electron Impact Excitations of Atoms
NORTON, P.R., *Atomic Energy of Canada Limited;* AC4: The Use of Photoemission in Surface Research
O'DONNELL, P.J., *University of Toronto;* BF1: Meson Decay Rates
OVERHAUSER, A., *Purdue University;* HA2: Fundamental Experiments with a Neutron Interferometer
PASSELL, L., *Brookhaven National Laboratory;* CC2: Elastic and Inelastic Neutron Scattering from Monolayers
PAUL, D.A.L., *University of Toronto;* CB1: Recent Experiments with Electrons Plus and Minus
PICKAR, K.A., *Bell-Northern Research;* EE1: The Physics of Integrated Circuit Lithography
REDWINE, R., *LAMPF;* DA3: Pion Nuclear Total Cross-Section
ROSNER, S.D., *University of Western Ontario;* DF5: The Unitary Transformation: The Keller Modular Approach to Teaching Physics
RYAN, D.G., *McGill University;* EI2: Measurement of the $\bar{K}^{\pm} \rightarrow K^{0} \gamma$ Radiative Decay
SANDOVAL, A., *University of Marburg and Lawrence Berkeley Laboratory;* AA4: Central Collisions of Relativistic Heavy Ions
SARGENT, C.P., *M.I.T;* DA4: Electron Scattering at the MIT-Bates Linear Accelerator
SCHIFF, H.I., *York University;* AB2: Laboratory Studies of Ion-Molecule Reactions of Interest in Interstellar Regions; ED4: Laboratory Studies of $O(^1D)$ Reactions of Atmospheric Interest
SKARSGARD, H., *University of Saskatchewan;* BI2: Turbulent Heating ^{2} of a Large Toroidal Plasma
SPILLER, E., *IBM Corporation, New York;* AC3: New Applications of the Vacuum UV
STEWART, G.A., *University of Pittsburgh;* CC3: Phase Changes in Nitrogen Monolayers
SVENSSON, E.C., *Atomic Energy of Canada Ltd., Chalk River, Ontario;* HB2: Neutron Scattering Studies of the Dynamical Structure of Liquid ^4He
THADDEUS, P., *Columbia University;* AB3: Molecular Ions in Interstellar Space
TIMUSK, T., *McMaster University;* HB3: Far-Infrared Studies of Excitons and the Electron-Hole Liquid in Germanium
UMEZAWA, H., *University of Alberta;* BF2: Symmetry Rearrangement and Vortex Solution
WAKSBERG, M.A., *Laboratoire de Recherche, RCA Limited;* AF1: La communication au moyen du laser
WEBB, M.B., *University of Wisconsin;* CC1: Leed Investigations of Noble Gas Films
WOODS, R.C., *University of Wisconsin;* AB4: Laboratory Microwave Spectra of Molecular Ions
ZIPF, C., *University of Pittsburgh;* ED2: Extreme UV Auroral Excitation, Predictions and Observations

PROGRAM SUMMARY

RESUME DU PROGRAMME

The letter code of the session, the starting time, the location and the topics of each session are given in order. All sessions will be held in the Pavillon de Koninck ~~unless otherwise indicated~~. PHYSICS BLDG.

(The personal names are those of invited speakers).

SUNDAY, JUNE 13

	19:30	AA	CAP COUNCIL

MONDAY, JUNE 14

AA	9:00	1C	Nuclear Physics 1 - Heavy Ions; LESSARD, HERSKIND, MACFARLANE, SANDOVAL
AB	9:00	0B	Molecular Ions of Astrophysical Interest; HERZBERG, SCHIFF, THADDEUS, WOODS
AC	9:00	1B	Synchrotron Radiation; CROZIER, MADDEN, SPILLER, NORTON
AD	9:00	2B	Surface, Thin Films, Whiskers
AE	9:00	2D	Astrophysics and Statistical Mechanics
AF	9:00	2E	Optics 1 - Communications, Difraction, Holography; WAKSBERG, MCDONALD
AG	9:00	2C	Phase Transitions, Statistical Physics, Liquids
AH	9:00	1A	Geophysics - Electromagnetic Methods 1
AI	9:00	2F	Laser Produced Plasmas
BA	13:30	1C	Few Nucleon Systems
BB	13:30	1B	Nuclear Fission and Photonuclear Reactions
BC	13:30	2C	Molecular Physics
BD	13:30	2A	Optical Properties of Solids
BE	13:30	2B	Electrical Properties of Solids 1
BF	13:30	2D	Elementary Particles - Theory; O'DONNELL, UMEZAWA, JOHNSON
BG	13:30	2E	Optics 11 - Quatum Optics; MANDEL
BH	13:30	1A	Geophysics - Electromagnetic Methods 11
BI	13:30	2F	Plasma Physics Symposium; HELAVA, SKARSGARD, GOLDSTEIN, MEYER
BJ	20:00*	1112	Nuclear Exports and Nuclear Waste Management; GREENWOOD, DUPUY, HAMEL *Pavillon Pouliot

TUESDAY, JUNE 15

CA	9:00	1B	Nuclear Reactions and Scattering
CB	9:00	2A	Electroexcitation Symposium; PAUL, HUEBNER, MARMET, NESBET
CC	9:00	1C	Structure and Excitations of Monolayer Films; WEBB, PASSELL, STEWART, CAMPBELL
CD	9:00	2B	Electrical Properties of Solids 11
CE	9:00	2C	Elementary Particles - Experiments
CF	9:00	2D	Theoretical Physics 1; MOSHINSKY, GRIFFIN
CG	9:00	2E	Nuclear Structure A < 100
CH	9:00	1A	Geophysics - Paleomagnetism
CI	9:00	2F	Laser Interactions, Diagnostics, Dynamics
DA	13:30	1C	Nuclear and Particle Physics at Intermediate Energies; BUGG, JAMES, REDWINE, SARGENT
DB	13:30	1B	Atomic Physics 1
DC	13:30	2A	Electrical Properties of Solids 111
DD	13:30	2B	Positrons; BERKO
DE	13:30	2D	Optics 111 - Lasers; IZATT
DF	13:30	0B	Physics Education Symposium; KERWIN, BOYD, KALMAN, CHASSE, ROSNER
DG	13:30	2C	Condensed Matter - Theory
DH	13:30	1A	Continental Crust and Mathematical Geophysics
DI	13:30	2E	ARCS, RF Plasma
	16:45	2B	Division of Aeronomy and Space Physics
	16:45	1B	Division of Atomic and Molecular Physics
	16:45	1A	Canadian Geophysical Union - A Joint Division of CAP/GAC
	16:45	2A	Division of Condensed Matter Physics
	16:45	1C	Division of Nuclear Physics
	16:45	2D	Division of Optical Physics
	16:45	2F	Division of Particle Physics
	16:45	0B	Division of Physics Education
	16:45	2E	Division of Plasma Physics
	16:45	2C	Division of Theoretical Physics
DJ	19:00	0B	L'Enseignement de la physique au Québec

WEDNESDAY, JUNE 16

EA	9:00	1B	Nuclear Structure A > 100
EB	9:00	1C	Nuclear Techniques and Instrumentation
EC	9:00	2A	Atomic Physics II
ED	9:00	2B	Atmospheric and Space Physics; JONES, ZIPF, MARMET, SCHIFF
EE	9:00	2C	Solid State Physics Research in Industry; PICKAR, CHENG, HARTMAN
EF	9:00	2D	Magnetic Properties of Solids
EG	9:00	2E	Theoretical Physics II; MICHEL, KARL
EH	9:00	1A	Geodesy
EI	9:00	2F	Elementary Particles - Experiments; CLINE, RYAN, MATTHEWS, CARNEGIE, ANDERSON
FA	14:00	1C	CAP Presidential Address; DOUGLAS

THURSDAY, JUNE 17

GA	9:00		Séance Plénière, Interaction Laser - Matière; AHLSTROM, HENDERSON, JENSEN Théâtre de la cité universitaire,Pavillon des Sciences de l'administration
HA	13:30	1B	Nuclear Physics II - Selected Topics; KUEHNER, OVERHAUSER, KABIR, FEINBERG
HB	13:30	1C	Condensed Matter Symposium; KORNELSEN, SVENSSON, TIMUSK
HC	13:30	2A	Magnetic Resonance, Relaxation, Mossbauer
HD	13:30	2B	Superconductivity; ADLER
HE	13:30	2C	General Physics
HF	13:30	1A	General Geophysics
HG	13:30	2D	Plasma-Magnetic Confinement, Waves, Instabilities
HH	13:30	2E	Biophysics
HI	13:30	2F	Lattice Dynamics
HJ	13:30	0B	Paleomagnetism II
	17:00	AA	C.A.P. Council

SUNDAY, JUNE 13, 1976
ROOM 2A
19:30

CAP COUNCIL

Chairman: A.E. Douglas

MONDAY, JUNE 14, 1976
ROOM 1C
Chairman: G. EWAN

NUCLEAR PHYSICS I - HEAVY IONS

9:00
AA1 Nuclear Fission Studies with On-Line Mass Spectrometers
L. LESSARD, *McGill University*

9:45
AA2 Studies of Heavy Ion Fusion Reactions from Gamma-Ray Multiplicity Measurements.
B. HERSKIND, *Niels Bohr Institute, Copenhagen, Denmark, and Chalk River Nuclear Laboratories, Canada.*

10:30
AA3 Heavy Ion Reactions
M.H. MACFARLANE, *Argonne National Laboratory*

11:15
AA4 Central Collisions of Relativistic Heavy Ions
A. SANDOVAL, *University of Marburg and Lawrence Berkeley Laboratory*

MONDAY, JUNE 14, 1976
ROOM 0B
Chairman: T. Oka

MOLECULAR IONS OF ASTROPHYSICAL INTEREST

9:00
AB1 Optical Spectra of Molecular Ions
G. HERZBERG, *National Research Council of Canada*

9:45
AB2 Laboratory Studies of Ion-Molecule Reactions of Interest in Interstellar Regions
H.I. SCHIFF, *York University*

10:30
AB3 Molecular Ions in Interstellar Space
P. THADDEUS, *Columbia University*

11:15
AB4 Laboratory Microwave Spectra of Molecular Ions
R.C. WOODS, *University of Wisconsin*

MONDAY, JUNE 14, 1976
ROOM 1B
Chairman: K.A. Pickar

9:00
AC1 Structural Determinations of Condensed Matter Using Synchrotron Radiation
E.D. CROZIER, *Simon Fraser University*

The intense, collimated, continuum radiation emitted by synchrotrons is ideally suited for extended X-ray absorption fine structure (EXAFS) studies of condensed matter. EXAFS is the oscillation in the absorption coefficient on the high energy side of the X-ray absorption edges which can extend 1000 ev beyond the edge. The oscillation is dominated by the interference of the photoelectron scattered by atoms in the immediate neighbourhood of the absorbing atom. Current theory and experimental work is reviewed which shows that EXAFS can yield the distance, number, and nature of co-ordinating atoms in crystalline and disordered materials as well as provide a measure of thermal and structural disorder effects. EXAFS studies of inorganic gases, metals, semiconductors, metalloproteins and catalytic systems are discussed. Also discussed are the structural implications of our recent EXAFS measurements as a function of temperature of two component semiconductor systems in the amorphous and liquid states. The measurements were made using the synchrotron radiation from SPEAR, Standord's e^+e^- storage ring.

9:45
AC2 Atomic and Molecular Experiments Using Synchrotron Radiation
R.P. MADDEN, *National Bureau of Standards, Washington, D.C.*

The importance of synchrotron radiation for far UV-x-ray physics is now recognized on a global basis, as evidenced by the present world-wide interest in the development of "dedicated" sources. The area of physics where the applications of synchrotron radiation have received the greatest publicity is solid state physics, due to the greater volume of work in that area. Never-the-less atomic and molecular physics experiments have been performed from the earliest application of synchrotron radiation. In this presentation I will review a number of atomic and molecular physics experiments, complete or on-going, which have explcited the unique properties of synchrotron radiation.

10:30
AC3 New Applications of the Vacuum UV
E. SPILLER, *IBM Corporation, New York*

The high intensity from synchrotron radiation sources has stimulated much research in the vacuum uv during the last decade. Applications of this spectral range can now be expected in many different fields such as astronomy and space optics, biology and medicine and manufacturing. We will review in this paper recent work towards such applications and discuss possible developments for the future. Topics covered are x-ray lithography and x-ray micrography, the possible design of imaging devices using multilayer coating and the applications of x-ray waveguides. X-ray lithography is used to fabricate submicron devices from an original electron beam generated mask. In x-ray micrography a replica of a biological specimen is obtained in an x-ray resist and viewed in a scanning electron microscope. Both techniques use the wavelength region between 5 and 100 Å and are capable of a resolution close to 50 Å with exposure times under one second if synchrotron radiation is used. In both techniques the x-rays produce a 1:1 image, magnification is provided by the electron microscope. X-ray imaging with magnification has traditionally been achieved using reflection at grazing incidence. Recent work in multilayer coatings has shown that reasonable reflectivities can also be obtained at normal incidence. High quality imaging elements (mirror telescopes, microscopes, etc.) using the new coatings should be possible for all wavelengths between 50 Å and 1500 Å. The field of integrated optics offers some imaging techniques not available in conventional optics; the successful propagation of x-rays in waveguides promises the transfer of these imaging techniques to the x-ray field.
The different techniques discussed in this paper are in quite different development stages. While x-ray lithography and micrography are ready to be used the other applications still require extensive research. The availability of strong synchrotron radiation makes this development worthwhile. We can also expect a mutual stimulation of the different techniques as for example, the use of x-ray lithography for the production of x-ray waveguides. The ideal light source for the applications would be a dedicated electron storage ring with an electron energy between 0.5 and 1 GeV.

11:15
AC4 The Use of Photoemission in Surface Research
P.R. NORTON, *Atomic Energy of Canada Limited*

The use of ultraviolet and X-ray photoemission techniques in studying the properties of surfaces will be illustrated by reference to chemisorption, physisorption and implantations on or in the basal planes of single crystal metal samples. A combination of inert gas resonance lamp and suitable filters can produce monochromatic vacuum-UV radiation and experimental results on the carbon monoxide-nickel system will be used to illustrate the advantages of a tunable light source.

MONDAY, JUNE 14, 1976
ROOM 2B
Chairman: D. Shewchun J. Marton

9:00
AD1 Intéraction des Plasmons de Surface et d'Interface dans les Structures MOS.* A. CAILLE ET M. BANVILLE, Univ. de Sherbrooke. -- Le gaz d'électrons à deux dimensions à l'interface entre un isolant et un semiconducteur dans la couche d'inversion d'une structure MOS donne naissance à un mode collectif du type plasmon dont la fréquence tend vers zéro à la limite des grandes longueurs d'onde. Ce mode n'a pas été mis en évidence expérimentalement. L'électrode métallique de la structure MOS , à la limite macroscopique, possède deux modes plasmons de surface: le mode tangentiel et le mode normal. L'intéraction entre le mode plasmon d'interface et les modes plasmons de surface modifie de façon importante les modes de plasmon de surface de l'électrode semimétallique. Cette intéraction suggère l'étude par des méthodes optiques du plasmon d'interface à l'aide des plasmons de surface couplés.

* Subventionnée par un octroi du C.N.R.C.

9:15
AD2 N_2 Monolayers on Graphite. T. T. CHUNG and J. G. DASH, U. of Washington--Calorimetric measurements of N_2 monolayers on Grafoil have been made in the regions recently explored by neutron diffraction.[1] The T≈50K transition between the $\sqrt{3}$ registered structure and a disordered phase involves approximately symmetric specific heat anomalies of ∿ 2K FWHM, and the peak positions shift slightly with increasing coverage in the range $0.3<x<0.7$. Above x≈0.7 the peaks become progressively asymmetric and shift more rapidly to higher T, tending toward the results of Butler, Huff, Toth and Stewart at higher coverage.[2] There are no other sharp anomalies in the explored range 30K<T<70K. The combined neutron and calorimetric data therefore indicate a second order transition between low-T registered and high-T disordered regimes. We believe that the system changes continuously from registered islands with extended short range order to a fluid, with no sharp distinction between solid, liquid and gaseous phases. The contrast between this system and others such as Ne may be due to molecular orientation[3] combined with effects of substrate structure.

[1]Kjems, et al., Phys. Rev. B13, 1446 (1976).
[2]Butler, et al., Phys. Rev. Lett. 35, 1718 (1975).
[3]Bourdon, et al., Phys. Rev. Lett. 35, 544 (1975).

9:30
AD3 Trap Density in Annealed InSb MOS Capacitors.* C.W. FISCHER, Univ. of Guelph - Anodic oxides grown on InSb exhibit passivating and insulating properties permitting field effect studies. However, the "as grown" oxides have an oxide - InSb interface trap density of approximately 10^{11} cm^{-2}. The trap density is measured by building MOS capacitors, plotting the differential capacitance versus voltage curve and noting the difference in voltage, at a fixed capacitance, between the curves for increasing and decreasing voltage. The electrical properties of the oxide, specifically the conductivity, and trap density are strongly dependent upon the post oxidation treatment. Results of several post oxidation annealing cycles in vacuum, N_2 and H_2 will be presented and compared with the "as grown" oxides.

*Supported by the National Research Council.

9:45
AD4 **Brillouin Scattering From Thin Film Optical Waveguides.*** **G.I. STEGEMAN, N. ROWELL and V. SO, Univ. of Toronto - The Brillouin spectrum of a thin (0.4μm) glass film deposited on a substrate has been observed using multi-pass Fabry-Perot interferometry. This film acts as a single mode integrated optics waveguide with the result that the incident light is guided by, and confined to the film. The broad spectrum observed normal to the film surface arises from scattering by a phonon continuum characterized by a constant projection of the sound wavevector in the plane of the film. (Momentum conservation in this acousto-optic interaction occurs in the plane of the film only, but not perpendicular to the film surface.) There is evidence which indicates that the presence of the surface changes the thermal population of the sound modes relative to the infinite medium case. It was found from a preliminary analysis of the spectrum that the C_{11} elastic constant of the film is smaller than that of the bulk glass material.**

*Research supported by the National Research Council

10:00
AD5 Properties and Disorder of Vacuum - Deposited Solids: a New Basic Relationship. P. S. VINCETT, Xerox Research Centre of Canada, Mississauga, Ontario, G. G. ROBERTS, New Univ. of Ulster, Coleraine, N.Ireland, and W. A. BARLOW, ICI Corporate Labs, Runcorn, England.--A wide variety of vacuum-deposited materials (including anthracene, phthalocyanine, Se, ZnO, ZnTe, ZnSe and CdS) have been shown to exhibit rather sharply optimised properties when the temperatures T_s of the substrate during deposition are near 0.34 of the normal boiling points of the deposited materials[1]. We have studied anthracene in detail, and have shown that the rapid variation of properties correlates with a reduction of structural disorder in the films. Furthermore, for a narrow range of T_s near the optimum, there is evidence that regions having unusual (and probably not close-packed) crystal structures may be formed. We show that these observations can be quantitatively interpreted if we assume that optimum films are formed when any disordered (probably glassy) regions of the growing films can just boil against the pressure of the impinging vapour flux.

[1]P. S. Vincett, W. A. Barlow and G. G. Roberts, Nature 255 542 (1975)

10:15
AD6 Plasmon Induced Desorption from Stainless Steel Surface.* S. K. SEN and R. P. GUPTA, Univ. of Manitoba.-- The positive ion spectra from the 304-stainless steel surface bombarded by a 1.5 keV electron beam have been observed with a modulated potential difference type (cylindrical) analyzer. The peaks at 3.3, 7.8 and 17.1 eV in the spectrum have been explained as due to desorption of O_2^+, N_2^+ and $C_3H_7^+$ respectively, the energy for the process being available from the decay of 19 eV plasmons in the stainless steel sample.[1] It is believed to be a new observation with considerable promise of useful applications in surface science.

[1]S.K. Sen, R.P. Gupta and W.H. Chung, Surface Science, 1976 (in press).

*Work supported by the NRC - Canada.

10:30
AD7 Optical Excitation of Surface Plasmons in Layered Media*. G.J. KOVACS and G.D. SCOTT, Univ. of Toronto --The Method of frustrated total reflection (FTR) can be used to optically excite electromagnetic surface plasma waves (SPW) at a metal-dielectric interface. Most work to date, using evanescent coupling, has been to study SPW on bulk on single thin film samples. We report the excitation of SPW by FTR at interfaces of a three-layered system, involving Ag-MgF_2-Ag sandwiched between glass

and air. Roughness of the evaporated MgF_2 surface is found to increase with film thickness and this roughness has a pronounced effect on the SP resonance. A cermet is imagined to form at the MgF_2-Ag interface and its effective optical constants can be evaluated using the Maxwell-Garnet theory. If this cermet is treated as a separate layer in the structure then excellent agreement is obtained between calculated and experimental wave-vectors of SPW in the system.

* Supported by the National Research Council of Canada

10:45
AD8 Realisation de Photo-Systèmes Semi-Conducteurs-METAL.* R. ARSENAULT et G. BOIVIN, LROL, Univ. Laval. -- On décrit des systèmes photographiques en couches minces utilisant l'iodure de plomb comme matériau photo-décomposable rendu plus sensible par "doping" avec cuivre. Un système Fabry-Pérot photo-décomposable est réalisé directement par correction de phase. Un autre système comprend l'évaporation simultanée de l'iodure de plomb et du cuivre. Ces systèmes ne requièrent pas de développement et de l'information supplémentaire peut être ajoutée sur une plaque déjà exposée. Les caractéristiques de ces systèmes seront présentées.

* Subventionné en partie par le Conseil National de Recherches du Canada.

11:00
AD9 Observation of Oxygen Atoms (^3P) Adsorbed on Quartz Surface.* N. PAPP, Univ. Laval and K.P. LEE, Univ. of N.B. -- In gas flow E.S.R. studies of the discharge produce of molecular oxygen, a new spectrum of weak satellite lines was observed, in addition to the spectra which are due to free atoms or molecules in the gas phase. It is shown that these extraneous resonance lines were due to physically adsorbed O-atoms on the glass surface which enclosed the gas, and arguments will be presented to suggest that the perturbation of the energy levels of the adsorbed atoms is due to electrostatic surface fields which are known to exist in interfacial regions.

* Supported by the National Research Council.

11:15
AD10 Role of Interfacial Layer in MIS Type Solar Cells.* R. SINGH and J. SHEWCHUN, McMaster Univ. -- A renewed interest is presently centered on Schottky barrier solar cells with an interfacial layer. Low cost and low temperature, as well as the possible adaptability to polycrystalline material make the device suitable for future large scale terrestrial applications. A performance improvement in Schottky barrier solar cells is obtained when a interfacial layer of proper thickness is present, as this eliminates the pinning effects and it gives a significantly higher open circuit voltage with a minimal increase in the series resistance. In this paper we shall discuss the role of the interfacial layer in such solar cells based on the concept that they are minority carrier non-equilibrium MIS tunnel diodes.[1,2]

1. M.A. Green, F.D. King and J. Shewchun, Solid St. Electron. 17, 551 (1974).

2. J. Shewchun, M.A. Green and F.D. King, Solid St. Electron. 17, 563 (1974).

* Work supported by the National Research Council of Canada.

11:30
AD11 Excitation of Surface Plasmons on Spherical Voids in a Metal by Fast Electrons. J. C. ASHLEY, Oak Ridge National Lab.*, and T. L. FERRELL, Appalachian State U.- In studies of voids in metals using fast electrons, an inelastic process that may occur is the excitation of surface plasmon modes on the void surface. The cross section for this inelastic process is calculated with the void approximated by a spherical bubble in an electron gas. The probability for this process is compared with that for volume plasmon excitation. With a reasonable choice for the density of voids in the metal, it is shown that the excitation by fast electrons of surface plasmon modes on a void should be experimentally observable.

*Operated by UCCND for ERDA.

11:45
AD12 Dynamic Coupling Between an Adsorbed Argon Monolayer and a Graphite Substrate.† A. D. NOVACO*, Lafayette C.--A simple model is used to estimate the extent to which certain phonon modes in an argon monolayer are coupled to the phonon modes in a graphite substrate. The model maintains most of the physics of the actual system but greatly simplifies the lattice dynamics. It is found that such coupling is important only over a small region of the Brillouin zone. The effect of this coupling on the inelastic neutron scattering from this system[1] will be discussed. For typical scattering geometries, it is found that this coupling has only minor importance. Thus one can associate a component of the scattering intensity with the motion of the film alone, and this component is simply the total intensity minus the background intensity due to the graphite substrate.

†Work supported by NSF.
*Guest scientist at Brookhaven National Laboratory.
[1] H. Taub, L. Passell, J. K. Kjems, K. Carneiro, J. P. McTague, and J. G. Dash, Phys Rev Letters 34. 654 (1975) and unpublished.

12:00
AD13 Theory of Surface Paramagnetic Spin Waves in Exchange-Enhanced Metals*. A. GRIFFIN and G. GUMBS, University of Toronto--We have computed the transverse dynamic spin susceptibility of a metal slab, assuming a constant magnetic field H_0 normal to the surfaces. The exchange interaction between electrons has a finite range λ ($< \lambda_F$) and the boundaries give rise to classical specular scattering, without any spin flips. The dispersion relation for the slab spin wave modes is analogous to the one recently discussed[1] for $H_0 = 0$, except that it involves the non-interacting bulk transverse susceptibility. We find that the bulk spin wave mode $\omega_B(q_\parallel, q_z = 0)$ is shifted upward and becomes a surface spin wave, localized near the boundaries over a distance δ. It is analogous to a surface plasmon or surface zero sound. All previous discussions assumed $\lambda = 0$, in which case the surface spin wave mode becomes the uniform CESR mode. The degree of localization and frequency shift strongly increase (for a given λ) with the amount of exchange enhancement (I).

*Supported by NRC of Canada.

[1] E. Zaremba and A. Griffin, Can.Journ.Phys. 53, 891 (1975)

12:15
AD14 The use of a ^{6}Li Beam for Surface Layer Analysis.
J. L'ECUYER, C. BRASSARD, C. CARDINAL, L. DESCHENES, Y. JUTRAS et J. P. LABRIE, Laboratoire de Physique Nucléaire, Université de Montréal. -- Light elements ($A < 20$) present at the surface of materials are notoriously difficult to detect and profile by conventional techniques such as Rutherford back scattering. We have taken advantage of the high Q value of ^{6}Li reactions to obtain very clean p and α spectra coming from such light elements even in the presence of a thick heavy element backing. Using a ^{6}Li beam in the range of 4.5 to 7 MeV, we have taken spectra at forward and backward angles with and without absorbers in front of our silicon detectors. From these measurements, sensitivity and depth resolution for various nuclei have been extracted and will be discussed.

MONDAY, JUNE 14, 1976
ROOM 2D
Chairman: G. Michaud

9:00

AE1 A Disk Instability Model For Planetary Spacings. T. G. PHILLIPS, Bell Labs, Murray Hill, New Jersey 07974--The most rapidly growing density wave instability for a uniform disk is used to roughly predict planetary initial condensation radii for an approximate model of the presolar nebula. Most solar planetary positions can be fitted to two simple linear relations, indicating that collapse may have taken place in two stages. The first stage is derived by the collapse of typical interstellar material and the second stage is a Jean's instability caused by the physical process of molecular hydrogen dissociation in the central condensation of the first stage. Jupiter's position is anomalous and it is suggested that it was formed in a bar fragmentation process between the disk collapse stages. An attempt is made to superpose the instability formalism on the more realistic presolar disk of Cameron and Pine, where it is found that the outer planet spacings are predictable.

9:15

AE2 The $^{42}Ca(p,\gamma)$ Reaction and its Role in Stellar Nucleosynthesis. A.E.VLIEKS, C.W.CHENG and J.D.KING, Scarborough College/U.of Toronto -- The total cross section for the $^{42}Ca(p,\gamma)$ reaction has been measured from 0.7 to 5.5 MeV using the residual radioactivity of the product nucleus. Stellar reaction rates, $N_A\langle\sigma V\rangle$, at several temperatures of Astrophysical interest, and cross sections will be presented and compared with theoretical calculations.[1]

[1]S.E.Woosley, W.A.Fowler, J.A.Holmes, and B.A. Zimmerman, OAP-422 (August 1975).

9:30

AE3 Surface Abundances of Stars and Accretion of Interstellar Matter.* MICHAEL J. NEWMAN, California Institute of Technology and RAYMOND J. TALBOT, JR., Rice University.—It has recently been pointed out[1] that the suggestion[2,3] that the occurrence of Ice Ages could be triggered by the accretion of interstellar matter by the sun in the dense clouds of the Galactic spiral arms could significantly ease the solar neutrino problem through enhancement of the heavy element abundance of the solar surface. In the present work we explore the consequences of accretion of interstellar matter by the Hoyle-Lyttleton-McCrea mechanism for stars other than our sun. The well-known correlation between heavy element abundance and kinematics, the metal-poor nature of the halo stars, the deficiency of metal-poor dwarfs in the disk, and several other observed features of the chemical composition of stellar surfaces can be simply understood in this picture. Possible observational tests of these ideas will be discussed.

*Supported in part by the NSF [MPS71-02670 A05, AST75-01398 A01] at Caltech and [AST74-20076 A01] at Rice U.

[1]M.J. Newman and R.J. Talbot, Jr., submitted to Nature.
[2]W.H. McCrea, Nature 255, 607 (1975).
[3]F. Hoyle and R.A. Lyttleton, Proc. Cambridge Phil. Soc. 35, 405 (1939).

9:45

AE4 Atomic and Cosmological Constants. B. KIVEL, AERL, Everett, Ma., USA. --Atomic and cosmological constants are related using general relativity and Dirac's hypothesis of large numbers. We make the important distinction between the physical constants that are independent of the cosmological environment and those which can be derived. c and h are invariant and independent of cosmology. The local cosmological parameters of the universe are its radius R, mass M, and the number of mass elements N. From general relativity the gravity constant $G = c^2R/2M$. We assume that the large ratio $e^2/Gm^2 = \eta^2\sqrt{N}$ based on the need for an inhomogeneous cosmology to define acceleration and mass. The derived quantities are: G, $m_e = M/N$, $e = \eta c\sqrt{(RM/2)}/N^{3/4}$, $r_e = \eta^2 R/2\sqrt{N}$, $\alpha = \eta^2 \pi RM/hN^{3/2}$. The cosmology parameter values $R = 1.5 \times 10^{28}$ cm. $M = 10^{56}$ g, $N = 10^{83}$, $\eta = 10/3$ give the correct values for the derived constants.

10:00

AE5 Dynamics of an Open Lattice Universe.* DIETER R. BRILL and JAMES ISENBERG, Univ. of Maryland. -- Lattice Universes are cosmological solutions of the Einstein equations which are approximately homogeneous and isotropic in the large, but consist of a finite number of Schwarzschild masses. The well-known construction[1] of closed lattice universes by the Schwarzschild cell method is here extended to obtain a lattice universe of open topology. The continuum limit of this lattice universe is the "flat" Friedman universe. The cells are typically cubical and have 3-torus symmetry. The constraints of general relativity imply that the extrinsic curvature K_{ij} of the spacelike surfaces must be non-vanishing. In order to model the cells from the Schwarzschild solution we therefore need spacelike surfaces in the Schwarzschild spacetime for which $K_{ij} \neq 0$; for simplicity we choose $K = K_i{}^i = \text{const.}$ These K = const. slices of the Schwarzschild solution will be discussed, and it will be shown how to fit them approximately into a lattice universe. The large-scale dynamics of this universe will be compared to that of the flat Friedman universe which it approximates.

*Supported in part by the National Science Foundation.
[1]Lindquist and Wheeler, Revs. Mod. Phys. 29, 432 (1957)

10:15

AE6 Electric and Magnetic Energy Density Transport Equations in Hydromagnetism, Part II. KEITH L. MCDONALD, P. O. Box 2433, Salt Lake City, Utah.—We write the vector potential $\underline{A}(\underline{r},t)$ into the previous expression[1] for $\underline{E} = \partial\underline{E}/\partial t$, where $\underline{E} = -\mu\dot{\underline{A}}/c$, $\underline{B} = \nabla\times\mu\underline{A}$ so that $\underline{A}$ includes the potential of the net electric charges and $K(\underline{r})$, μ, σ are now variables with $\underline{B}=\mu\underline{H}$, $\underline{D}=K\underline{E}$, $\nu_m=c^2/4\pi\mu\sigma$. Integrating with respect to time we obtain, aside from stationary and static fields, the defining differential equation $\nu_m\nabla\times\mu^{-1}\nabla\times\mu\underline{A} - \underline{v}\times\mu\underline{A} + \dot{\underline{A}} = [\nu_m c^{-1}\underline{D} + \rho_m\underline{v}/\mu\sigma] = 0$, the bracket vanishing by quasi-stationarity. For this gauge choice, $\nabla\cdot(K\mu\underline{A}) = -4\pi c\rho_E$. Forming the curl, with μ constant, there results the induction equation $\partial\underline{B}/\partial t = \nu_m\nabla^2\underline{B} + \nabla\times(\underline{v}\times\underline{B}) + \nu_m\nabla\log\sigma\times(\nabla\times\underline{B}) + \mu\nabla\times[\cdots]$. The amplification term $\nabla\times(\underline{v}\times\underline{B})$ equals $-\underline{B}\nabla\cdot\underline{v} + \underline{B}\cdot\nabla\underline{v} - \underline{v}\cdot\nabla\underline{B}$. Transposing the convection term then gives $d\underline{B}/dt = \cdots$. Multiply by $\underline{H}$ to obtain $\underline{H}\cdot\partial\underline{B}/\partial t = \frac{1}{4}\pi\partial U_B/\partial t = \cdots$, which may be modified by use of the equality $2\underline{v}\cdot\nabla\underline{B}\cdot\underline{H} = \underline{v}\cdot(\underline{H}\cdot\underline{B}\underline{v}) - (\underline{H}\cdot\underline{B})\nabla\cdot\underline{v}$. Add the convection term $\frac{1}{4}\pi\underline{v}\cdot\nabla U_B = \cdots$ to get $dU_B/dt = -2U_B\nabla\cdot\underline{v} + (4\pi)^{-1}\underline{B}\cdot\nabla\underline{v}\cdot\underline{H} + (4\pi)^{-1}\nu_m\underline{H}\cdot\nabla^2\underline{B} + (4\pi)^{-1}\underline{H}\cdot\nu_m\nabla\log\sigma\times(\nabla\times\underline{B}) + (4\pi)^{-1}\underline{B}\cdot\nabla\times[\cdots]$, since $\underline{B}\cdot\nabla\underline{B}\cdot\underline{v} - \underline{v}\cdot\nabla\underline{B}\cdot\underline{B} = \underline{v}\cdot(\nabla\times\underline{B})\times\underline{B}$, and the bracket again vanishes. One may also write $\nu_m\underline{H}\cdot\nabla^2\underline{B} = -\nu_m\mu(\nabla\times\underline{H})^2 + \nu_m\nabla\cdot(\underline{B}\times\nabla\times\underline{H}) = -4\pi(\underline{J}^2/\sigma + \nu_m\nabla\cdot\underline{J}\underline{B}/c)$, deleting electric displacement terms $-\sigma^{-1}(2\underline{J}\cdot\dot{\underline{D}} + \dot{\underline{D}}^2/4\pi) - \nu_m\nabla\cdot(\dot{\underline{D}}c)/c$, on the right. This establishes the well-known association of the Joule heating term with the diffusion term. The defining equation for $\underline{A}$, with $\nabla\cdot\underline{A} = 0$, is known.

[1]Keith L. McDonald, Bull. A. P. S., 21, No. 4 (1976).

10:30

AE7 On the Theory of Hydrodynamical Fluctuations. R. PERALTA-FABI and L.S. GARCIA-COLIN, Univ. Autónoma Metropolitana, Iztapalapa, Mexico.-- The microscopic fluctuating mass and current density are used as variables in Mori's[1] generalized hydrodynamical scheme. The fluctuating stress-stress tensor correlation function is calculated explicitly at zeroth order in time for an inhomogeneous fluid. Landau and Lifshitz's[2] phenomenological theory for the fluctuating stress tensor is recovered as a special case.

1. Mori, H.,Prog. Theoret. Phys. (Kyoto) 33, 423 (1965).

2. Laudau, L. and Lifshitz, E.M., Fluid Mechanics. Addison-Wesley. Mass. (1959).

10:45

AE8 The Structure of Binary Solution Microclusters. C. H. Walker, Clark College and Patrick Hamill, NASA-Ames Research Center. The traditional description of the kinetics of phase change in a binary mixture of condensable vapors (homogeneous heteromolecular nucleation theory) has been based largely upon the capillarity approximation along with various schemes for dealing with possible composition inhomogeneities, especially near the surface (surface enrichment). When coupled with the drastic densitiy gradients common to microclusters, the estimation of the contribution of such inhomogeneities to the free energy of formation becomes a difficult task. To ascertain which, if any, of the proposed methods of dealing with this problem are realistic, we have used Monte Carlo techniques to simulate the behavior of small clusters of two atomic species interacting through various pair potentials for a range of compositions and and cluster sizes. We shall present some of these results and compare them with the theoretical predictions.

11:00

AE9 Evaluation of the Free Energy and Specific Heat Expansions for the Classical Vector Model of Ferromagnetism in General Spin Dimensionality. P. S. ENGLISH and D. L. HUNTER, St. F. X. Univ.-- The high temperature series for the free energy and specific heat for the Classical Vector model have been evaluated explicitly as rational functions of the spin vector dimensionality. The resulting series agree with previous results for the Ising model (D=1) and the classical Heisenberg model (D=3), but the present work has extended the series for the latter model. The series for D=3 has been independently evaluated as far as the 13th term in an appropriate temperature variable, as a check on our general results.

MONDAY, JUNE 14, 1976
ROOM 2E
Chairman: R. Tremblay

OPTICS I - COMMUNICATIONS, DIFFRACTION, HOLOGRAPHY

9:00

AF1 La communication au moyen du laser
M.A. WAKSBERG, *Laboratoire de recherche, RCA Ltd.*

9:45

AF2 Fibre Optics Communication Technology
R.D. MCDONALD, *Solid State Chemistry Department, Canada Wire & Cable Ltd.*

10:30

AF3 Etude de l'Homogénéité des Fibres Optiques en Microscopie Interférentielle par Double "Shearing"* -- P.G. VERLY et J.W.Y. LIT, LROL, Univ. Laval.-- Il est très important de pouvoir contrôler de façon non-destructive le profil d'indice de réfraction et l'homogénéité des fibres utilisées en communications optiques. La microscopie interférentielle par "shearing" simple possède déjà des propriétés très intéressantes sous cet aspect. Nous allons montrer qu'on peut également extraire de l'information sur l'épaisseur optique de la fibre en microscopie interférentielle par double "shearing", avec en vue une amélioration de la précision.

* Subventionné en partie par le Conseil National de Recherches du Canada.

10:45

AF4 Propriétés de Rétroaction d'une Nouvelle Forme de Structure Périodique.* A.D. ROCHETTE et J.W.Y. LIT, LROL, Univ. Laval.-- En optique intégrée, les propriétés de structures périodiques ont été utilisées à différentes fins. Ainsi, des méthodes d'agir périodiquement sur une onde confinée dans un guide diélectrique ont été développées, d'où on a réalisé plusieurs types de composantes. De notre côté, nous avons expérimenté, à l'aide d'un simulateur micro-onde, une nouvelle forme de structure périodique. Elle a été étudiée en tant que guide tridimensionnel, élément focalisant et composante à rétroaction distribuée. La modulation périodique dans le guide plan diélectrique est obtenue en plaçant des éléments métalliques sur la surface de ce dernier. Pour une période donnée de cette modulation, nous pouvons sélectionner une fréquence de l'onde guidée où on a un effet de rétroaction par la structure étudiée. Les résultats obtenus sur cette nouvelle forme de structure périodique, en tant que composante à rétroaction distribuée, seront discutés dans cet exposé.

* Subventionné par le Ministère de la Défense Nationale (CRDV).

11:00

AF5 Annular and Radial Focusing Systems for Laser Processing.* M. RIOUX, P.A.BELANGER and R. TREMBLAY, LROL, Laval Univ. -- A spherical lens and an axicon are combined to form an optical system producing a ring-shaped focalisation pattern. The diameters of the rings at the focal point depend on the angle of the axicon and on the focal length of the lens. The diffractional analysis of the lens-axicon combination when illuminated by a uniform plane wave and by a gaussian laser beam is presented. This type of focalisation is well suited for a system where a laser beam is used to drill holes. Variation of this combination can be made with a reflecting axicon to obtain a radial focalisation pattern. Experiments with an annular and a radial focusing system will be presented.

* Supported by the National Research Council of Canada and by the Education Department of Quebec.

11:15

AF6 Application de la théorie des ondes de bord à l'étude des systèmes d'iris en cascade. G. OTIS, J.-L. LACHAMBRE et P. LAVIGNE, Centre de Recherches pour la Défense, Valcartier.-- Nous présentons une nouvelle formulation pour l'étude des systèmes d'iris en cascade soumis à la radiation incidente d'un faisceau laser. L'analyse des propriétés diffractionnelles de ces systèmes repose ici sur la théorie des ondes de bord[1], qui permet de traiter à l'aide de rayons lumineux les diverses contributions qui composent le champ diffracté. Les formules dérivées pour le calcul du champ transverse sont valides partout, et convergent particulièrement bien près de la frontière géométrique de l'ombre. Ces formules trouvent une application directe à l'étude des résonateurs optiques, et à la conception de systèmes de focalisation à iris.

[1] G. Otis, J. Opt. Soc. Am., 64, 1545 (1974).

11:30

AF7 Les courbes caractéristiques de la plaque Kodak 649 F utjlisée comme détecteur en holographie*. J. COUTURE, R.A. LESSARD et A. BOIVIN, Université Laval. - En holographie, la disposition relative des pièces optiques par rapport à la plaque, le rapport en intensité des faisceaux de référence et d'objet et le coefficient de transmission en amplitude de l'hologramme ont été les trois premiers points à être déterminés, car ils devaient être contrôlés pour permettre un bon enregistrement des informations optiques. En effet, si à la reconstruction, les réseaux élémentaires préalablement enregistrés diffractent efficacement l'énergie incidente, l'image holographique sera suffisamment lumineuse pour être observée. Cependant, si nous voulons employer la plaque pour contrôler quantitativement la qualité des images, nous devrons, lors de l'enregistrement, en connaître tous les paramètres. Ainsi, nos expériences ayant montré que la densité des plaques dépendaient de la façon d'enregistrer les hologrammes, nous avons alors tracé les courbes du noircissement de la plaque en fonction des situations d'enregistrement. Nous présenterons une classification des courbes caractéristiques et discuterons nos résultats.

* Subventionné par le CNR du Canada.

11:45

AF8 Interférence de deux enregistrements holographiques spatialement indépendants*. M. LAROSE, R.A. LESSARD, A. BOIVIN, Université Laval. - Le codage optique spatial consistant à enregistrer plusieurs signaux en des portions indépendantes du milieu enregistreur, est maintenant une méthode bien connue en holographie multiplex. En voulant appliquer cette technique à l'interférométrie holographique, certains auteurs[1] ont démontré l'impossibilité de faire interférer les reconstructions de deux des hologrammes constituants s'ils n'ont pas été enregistrés sur la même portion de l'émulsion ou sélectionnés par une même pupille. Etant en désaccord avec leur conclusion, nous avons entrepris une étude approfondie de ce processus interférométrique. Nous avons reproduit holographiquement des expériences classiques d'interférométrie en vue d'expliquer leurs difficultés. Nous expliquerons qualitativement le phénomène et présenterons les résultats expérimentaux obtenus.

[1] R. DANDLIKER, E. MARON, F.M. MOTTIER, Opt. Commun. 6, 368 (1972).

* Subventionné par le CNR du Canada.

12:00

AF9 Etude des propriétés d'imagerie de quelques pupilles.* M. PARADIS, R.A. LESSARD et A. BOIVIN, Université Laval. - L'holographie multiplex à codage du faisceau-objet utilise des masques pupillaires pour coder les différentes informations optiques avant leur enregistrement sur la plaque photographique. Nous avons tenté de trouver des configurations pupillaires permettant un codage rapide de ces informations tout en garantissant une bonne résolution. Nous avons trouvé une description théorique de la figure de diffraction produite par trois de ces pupilles ainsi qu'une évaluation de l'énergie encerclée comprise dans cette figure. Nous présenterons la figure de diffraction de ces trois ouvertures et en discuterons leur description théorique. Enfin, une brève discussion de la distribution énergétique sur la résolution viendra compléter la présentation.

* Travail subventionné par le CNR du Canada.

12:15

AF10 Near-Field Diffraction by a Disk.* C.L. ANDREWS, I. CHUNG, and L.F. LIBELO, SUNY at Albany.--We have measured the near-field diffraction pattern on the axis, shadow side, for a plane polarized electromagnetic wave incident normally on the surface. The wavelengths were 3.5 and 10.0 cm. Scans were made from the surface to a distance of two disk diameters for 70 disks of diameters ranging from 0.04 to 2.00 wavelengths. The precision of the electrical measurements $|E|^2/|E_\infty|^2$ was ± 1.0% of $|E_o|^2$ of the incident wave. This is the first time that magnetic measurements have been reported in this region. Our estimated precision of $|H|^2/|H_\infty|^2$ is ± 4%. The improved precision was obtained by use of probe-antennas with dimensions less than 0.05 wavelengths. We used leads of carbon impregnated Teflon from the probe to an electronic electrometer. For the first resonant size of disk, we observed a maximum in $|E|^2/|E_\infty|^2$ of 1.54 at a distance of 0.65 diameter and a maximum in $|H|^2/|H_\infty|^2$ of 1.6 at the surface. We submit these measurements in anticipation that someone will compute the axial diffraction pattern from the exact theory of Meixner and Andrejewski.

* Work supported by Naval Surface Weapons Center, White Oak, Silver Springs, Maryland.

MONDAY, JUNE 14, 1976
ROOM 2C
Chairman: J.D. Betts

9:00
AG1 Renormalization Group Solution of the One-Dimensional Ising Model with a Magnetic Field.* WEI-TOU NI, National Tsing Hua University, Hsinchu, Taiwan, Republic of China. — Nauenberg's[1] renormalization group approach is applied to the one-dimensional Ising model with a magnetic field. A rapidly convergent infinite series expansion for the free energy (per spin), f(K,H), is obtained as follows:

$$f(K,H) = \ln\{e^{K}[\cosh H + (\sinh^2 H + e^{-4K})^{1/2}]\}$$
$$= \ln 2 + \sum_{n=1}^{\infty} \frac{K^{(n)}}{2^n} + \sum_{n=0}^{\infty} \frac{1}{2^{n+1}} \ln \cosh H^{(n)}$$

where $K \equiv J/kT$, $H \equiv B/kT$, $K^{(i)} = \frac{1}{4}\ln[\cosh(2K^{(i-1)} + H^{(i-1)}] + \frac{1}{4}\ln[\cosh(2K^{(i-1)} - H^{(i-1)}] - \frac{1}{2}\ln\cosh H^{(i-1)}$

and $H^{(i)} = H^{(i-1)} + \frac{1}{2}\ln\cosh(2K^{(i-1)} + H^{(i-1)}) - \frac{1}{2}\ln\cosh(2K^{(i-1)} - H^{(i-1)})$.

*Supported in part by the National Science Council, Republic of China.

[1] M. Nauenberg, J. Math. Phys. 16, 703 (1975).

9:15
AG2 The Non-Commutativity of Thermal and Structural Averages. H.A. BROWN and W.F. PARKS, University of Missouri-Rolla--Consider a Heisenberg ferromagnet with exchange between neighbors varying randomly because of dilution, amorphous structure, or other cause. There are then two averages to be taken: the thermal average for a given structural configuration and the average over configurations, taken in that order. If taken in the opposite order, the configuration average gives a Hamiltonian, for example, dependent on average parameters to use in finding the thermal average. The two procedures lead to significantly different results. It is argued that the second may be preferable when one deals with cluster theories involving only a small number of interacting spins. Some specific results are obtained, using both procedures, to support the contention.

9:30
AG3 The Effect of Gravity on the Rayleigh Linewidth of a Fluid Near its Critical Point. B. N. MILLER and H. K. LEUNG, Texas Christian University.--The effect of the earth's gravity on the Rayleigh linewidth, Γ, of a simple fluid near its critical point has been investigated in detail. It is found that the earth's fluid significantly influences linewidth measurements to the extent that it is difficult to compare available data with current theories. Due to gravity the universal curve of the scaled linewidth is separated into a family of curves depending on external parameters, regardless of the particular theory used. The ability to distinguish between the prediction of the mode-mode coupling and decoupled mode theories, while only slight in the field free case, is enhanced by the strong density gradient. It is found that the different theories result in plots of Γ vs. temperature that have different shapes, resulting in a viable method of selection.

9:45
AG4
Electric Anomalies at the Phase Transition in FeS, J.R. GOSSELIN, M.G. TOWNSEND and R.J. TREMBLAY, Dept. of Energy, Mines and Resources, Ottawa, Canada, K1A 0G1. The conductivity and thermoelectric power of single crystals of $Fe_{0.996}S$ have been recorded at temperatures between 80° and 600°K. The results show that the material is probably a p-type semiconductor at low temperature and a not-well-behaved metal above the phase transition at $T_{\alpha} \simeq 420$°K. A qualitative band model is suggested. There is a small sharp peak in the thermoelectric power at T_{α} that we believe is the real origin of two reported apparently anomalous effects. They are: a voltage at T_{α}, purportedly due to diffusion of free electrons at an interface between the low and high temperature phases[1], and a pyroelectric current with a sharp peak at T_{α}[2]. From symmetry considerations we show that the report of ferroelectricity below T_{α} in FeS[2] is unfounded.

1. T. Takahashi and O. Yanada, J. Phys. Chem. Solids 37, 161 (1976).

2. C.B. van den Berg and J.E. van Delden, Phys. Stat. Solidi, 36, K89 (1969).

10:00
AG5 Phase Transition in Ammonium Sulphate as Studied by Paramagnetic NH_4^+ Probes.* M. FUJIMOTO, L.A. DRESSEL and T.J. YU, Univ. of Guelph, Ontario--To study the model proposed by Sawada, Takagi and Ishibashi[1] for the phase transition in ammonium sulphate at ~50°C, we carried out EPR experiments on NH_4^+ radicals at ammonium sites. The ^{14}N hyperfine tensor has a well-defined unique axis thereby representing ammonium orientation in librational motion. The following conclusions have emerged from the EPR results. (1) The phase transition is first-order. (2) At the transition point molecular reorientation takes place to allow coupling of pseudo-spins associated with the two ammonium sublattices. This displacive reorientation occurs in a A_g-mode, and the pseudo-spin interaction is responsible for the simultaneous softening of a polar B_{1u} mode. (3) In the polar phase NH_4^+ axes split into two orientations symmetrical with respect to (001) plane. The sublattice polarization may be interpreted as ordering of pseudo-spins between these two directions, however, the Stark splitting in the Lorentz field was not resolved to deal with the polarization.

[1] A. Sawada et al, J. Phys. Soc. Japan 34, 748 (1973).
*Supported by N.R.C. of Canada.

10:15
AG6 Kinetics of Calcite-Aragonite Transformation.* N.S. BRAR and H.H. SCHLOESSIN, Univ. of Western Ontario. --The transformation of calcite to aragonite as a function of pressure and temperature observed by different workers, shows noticeable differences. These differences are due to such factors as shear stresses, grain size, impurities etc. of the starting material. The present series of experiments investigate the transformation rate of calcite single crystals. Pressure and temperature conditions are set so that crystals are well within the aragonite stability field, and, in each run, different times (1/4-8 hours) are allowed for the transformation to occur. The volume fractions of partial transformation are determined from x-ray peak intensity ratios. Preliminary results at a pressure 20 Kb and temperature 600°C are consistent with a $t^{\frac{1}{2}}$ law, which confirms that it is a diffusion controlled transformation. The results are discussed in terms of diffusion coefficient and activation energy as well as size and shape of the nuclei.

*Supported by National Research Council of Canada.

10:30
AG7 Phase Transformation in $Hg_{2.86}AsF_6$ and $Hg_{2.91}SbF_6$.* A. VAN SCHYNDEL, B. CUTFORTH and W.R. DATARS. McMaster U.-- Phase transitions have been observed in $Hg_{2.86}AsF_6$ and $Hg_{2.91}SbF_6$ metallic compounds using differential thermal analysis and resistivity measurements.[1] The transition occurs over the temperature range 220-240 K in $Hg_{2.86}AsF_6$ and 210-245 K in $Hg_{2.91}SbF_6$ upon warming from 180 K. The transition shows hystereses effects and upon cooling occurs in the temperature range 245-180 K. These results will be compared with other electrical and optical properties which exhibit one dimensional properties.

*Research supported by the National Research Council of Canada.

[1] W.R. Datars, B.D. Cutforth, A. van Schyndel and R.J. Gillespie, Bull Am. Phys. Soc. 20, 439 (1975).

10:45
AG8 Positron and Positronium Annihilation in Benzene Solutions. S. Y. Chuang and S. J. Tao, New England Institute.-- Positron annihilation in nitrobenzene and manganese oleate solutions in benzene at both liquid and solid states was studied by using both lifetime and angular correlation methods. A long life time component ($\tau_2 \sim 1.3$ nsec) was found in the lifetime spectrum for the solid state of a nitrobenzene solution in benzene but not the liquid state. No narrow component was observed in the angular correlation curves for the same sample at both liquid and solid states. The values of τ_2 and I_2 for manganese oleate solutions in benzene increase appreciably as it changes from the solid to the liquid state. A large narrow component was found in the angular correlation curve for a manganese oleate solution in benzene at the liquid state as well as the solid state. The results are discussed.

11:00
AG9 An Improved Perturbation Theory of Liquid Structure. W.R. CONKIE and D.S. HALL, Queen's Univ.--The perturbation theory approach of Chandler et al[1] to the calculation of properties of classical fluids has enjoyed considerable success. Another approach has been to impose thermodynamic self-consistency in deriving integral equations for the pair distribution function[2]. A characteristic of the perturbation approach is that the virial coefficients obtained are not accurate. The reasons lie in the methods used which use an expansion in ξ, the range of the 'blip' function, which is not a density expansion. The self-consistent approach can be combined with the perturbation approach to give accurate virial coefficients and an accurate equation of state. This will be illustrated by results for inverse power potentials.

[1] H.C. Anderson, J.D. Weeks and D. Chandler, Phys. Rev. A4, 1597 (1971).

[2] P. Hutchinson and W.R. Conkie, Mol. Phys. 24, 567, (1972).

11:15
AG10
Structure and Properties of $V_{1+x}P_{1-x}O_{5-c/2}$ Glasses* B. Jordan and C. Calvo, Dept. of Physics, McMaster Univ. -- Glasses of composition $V_{1+x}P_{1-x}O_{5-c/2}$, with $0 \leq x \leq 0.6$ were prepared from melts of differing proportions of V_2O_5 and P_2O_5 and their structure studied by x-ray scattering. A model for the glass structure is proposed, based on layers like those found in crystalline α-VPO_5. For $x > 0$, vanadium substitutes for phosphorus on tetrahedral sites. Stacking faults of frequency 1/2 provide adequate prediction of the density. If polarons are excluded from the tetrahedral vanadium sites, the x dependence of the reported Seebeck coefficient behavior and conductivity extrema[1] is largely removed.

* Supported by a grant from the National Research Council of Canada.

[1] G.S. Linsley et al., J. Non-Crystalline Solids, 4, 208 (1970).

11:30
AG11 Solution of the Mean Spherical Approximation Integral Equation for the Density Profile of a Hard-Sphere Fluid Near a Wall. D. HENDERSON, IBM, San Jose, CA, E. WAISMAN, INTI, Buenos Aires, Argentina, and J. L. LEBOWITZ, Yeshiva University, New York.-- Recently, the mean spherical approximation (MSA) integral equation has been reformulated by Henderson, Abraham, and Barker[1] so as to be appropriate for a fluid near a wall. We have solved these equations for the case of hard spheres where the direct correlation function (DCF) for the wall-fluid interaction decays exponentially outside the wall and have obtained expressions for the density profile of the hard-sphere fluid near the wall. In this paper we outline this solution and empirically choose the two parameters in the DCF outside the wall so as to give the correct thermodynamic properties of a hard-sphere fluid near a wall. The resulting density profile is in good agreement with recent machine simulations.

[1] D. Henderson, F. F. Abraham, and J. A. Barker, Mol. Phys. (in press).

11:45
AG12 Direct Measurement of the Void Fraction of a Two-Phase Fluid by Nuclear Magnetic Resonance. G.F. LYNCH, A.E.C.L., Chalk River, and S.L. SEGEL, Queen's University. Application of nuclear magnetic resonance (NMR) to the direct measurement of void fractions of two-phase fluids has been studied. With this technique, the effective density of the fluid is determined by monitoring the NMR signal strength from a particular nuclear species in the liquid. The results, from experiments on both static and flowing systems, establish the linearity of the method for the full range ($0 \rightarrow 1$) of void fractions, independent of the mass distribution of the liquid, and demonstrate the feasibility of using NMR as a direct method for void-fraction measurements in two-phase systems.

MONDAY, JUNE 14, 1976
ROOM 1A
Chairman: E. Gaucher

9:00
AH1
COTRAN - An all digital time domain airborne EM system for low level high resolution surveys, A. R. Barringer, Barringer Research - The author will discuss the COTRAN" (COrrelation of TRANsients) airborne prospecting technique, which utilises a frequency modulated pulse and digital micro-programmed mini-computer to eliminate the use of a towed bird and to allow operation at low terrain clearance. This system provides analog outputs for in-flight monitoring and digital for ground processing. The computer derives an optimum match between data and reference waves, giving great flexibility and a choice of relatively simple data output or a complex analysis, covering both the measurement of conductivity and conductor orientation.

9:15
AH2
Airborne EM Mapping. A. BECKER & C. ST-HILAIRE - Multifrequency airborne electromagnetic data can be automatically interpreted to yield information useful for the mapping of overburden. The desired parameters such as thickness and conductivity are derived from the phase-amplitude characteristics of the secondary field. Before an interpretation can be made however, it is imperative to remove the effects of aircraft altitude variations from the data. This correction can be made quite accurately on a computer with the aid of algorithms specially designed for this purpose.

9:30
AH3
Resistivity Mapping with the Dighem Airborne Electromagnetic System, D.C. FRASER, Dighem Ltd. - Airborne electromagnetic measurements in areas of conductive terrain often are ineffective because of the large amount of geological noise. Such noise produces a continuous waveform on the output recording device, rather than the discrete anomalies characteristic of bedrock conductors in resistive terrain. A homogeneous earth algorithm can be used to transform the AEM data into apparent resistivity. Contoured apparent resistivity maps from DIGHEM data have proven useful in indentifying zones of bedrock conductivity in areas of high surface conductivity.

9:45
AH4 Mapping of the Conductivity and Thickness of Surficial Layers by the Tridem Airborne Electromagnetic System, Harold O. Seigel, Scintrex Ltd. - The Tridem airborne electromagnetic system comprises three totally independent fixed configuration units operating simultaneously on frequencies of 500, 2000 and 8000 Hz. The coils are coplanar, with their axes 18 metres apart and in the direction of flight. In-phase and quadrature electromagnetic responses are recorded. For overburden mapping a computer programme has been developed which automatically determines the thickness and conductivity of the layer. Useful quantitative information may be derived for overburden conductivities of less than 4×10^{-4} to greater than 4 mhos/metre. This information is useful in mapping the distribution of overburden types as well as the location and quality of groundwater.

10:00 Crustal Conductivity Anomalies related to major Fracture Zones. D.I. GOUGH, U. of Alberta and P.A. CAMFIELD, Earth Phys. Branch, E.M.R. - The use of large two-dimensional arrays of three component magnetometers to record time-varying geomagnetic fields, in the period range 10-1440 minutes, has led to the discovery of several major fracture zones in the Earth's lithosphere. Such fracture zones have anomalously high electrical conductivity, probably associated with saline water and with conductive minerals such as graphite. Currents induced in the Earth are concentrated in such conductive zones and may be mapped by a magnetometer array. Three examples will be discussed, in the North American Central Plains, in the St. Lawrence Valley and in a southern extension of the African Rift Valleys.

10:15
AH6 A Numerical Study of the Topographic Effect on Electromagnetic Fields in a Three-Dimensional Conductivity Model. V. RAMASWAMY, F.W. JONES, University of Alberta and H. DOSSO, University of Victoria - The Topographic effect on electromagnetic fields in a three-dimensional conductivity model is investigated using a finite-difference numerical method. The model is that of a conducting block buried in the host Earth beneath a conducting hill. The altitude effect as well as the effect of conductivity of the hill has been studied by comparing the results for the field components at the surface of the hill with those at the surface of a flat half-space. The results indicate that both altitude and the hill conductivity influence the behaviour of the electromagnetic fields. For certain traverses beyond the edge of the block, it is seen that the variations in some field components are mainly due to the topographic effect and that the contribution from the block itself is negligible.

10:30
AH7 Using Numerical Models to Better Understand EM Prospecting, G. F. WEST, Univ. of Toronto. - Numerical modelling programs have been devised by quite a number of researchers and many results from their programs are available. While many of the studies are not directly comparable with actual prospecting field data and therefore not directly helpful to interpreters, they do help one gain a better understanding of how various EM systems work and which characteristics of the ground are most important in determining response. A crucial question is whether the observed local anomalies are due to localized eddy current induction or the gathering of regionally induced currents. The question of where a two-dimensional model can be applied is linked to this problem.

10:45
AH8 Radiohm Mapping of Permafrost*, B.W. Powell, McGill University
Radiohm surveys were carried out at three test sites along the Mackenzie Valley. Reformulation of the radiohm data into a "permafrost index" is shown to be effective in mapping the distribution of discontinuous permafrost. A simple two layer, single frequency interpretation was employed to estimate thickness of the permafrost without a prior assumption of the permafrost resistivity. Two solutions are found to exist and the use of scatter diagrams is demonstrated to determine which solution is valid. Results are found to be in reasonable agreement with control information.

*Supported by N.R.C. and D.E.M.R.

AH 10
AH 11

11:00
AH9 VLF Electromagnetic Mapping of Gold Bearing Structures, R.S. MIDDLETON - This paper describes an unique application of electromagnetics for mapping geological structures containing gold deposits. Most gold deposits, unlike massive sulphide base metal deposits are not directly detectable with geophysical methods because the metal contents are extremely low in the 1-5 PPM au range and the quartz host rock does not have contrasting physical properties with the surrounding country rock. However, structures such as faults, shears and contacts which control the implacement of gold bearing veins are often weakly conductive and therefore can be detected with VLF electromagnetic methods using both the secondary magnetic field and the ratio of the electric and magnetic field to measure the resistivity of the ground. Examples of mapping tropically weathered gold bearing zones in central America and classic saddle reef structures in anticlinal domes in Nova Scotia are presented.

MONDAY, JUNE 14, 1976
ROOM 2F
Chairman: R. Nodwell

LASER PRODUCED PLASMAS

9:00
AI1 COCO-II - A 100 J, ns Pulsed CO_2 Laser for Laser-Target Irradiation Studies. M.C. RICHARDSON, N.H. BURNETT, G. ENRIGHT, P. BURTYN and K. LEOPOLD, N.R.C. -- The design and operating characteristics of a new high power, dual beam CO_2 laser capable of output energies in excess of 100 J with a 1 ns pulse are described. The system basically consists of an actively mode-locked oscillator, a pulse selection, isolation and magnification stage followed by preamplification and amplification by 8 cm and 20 cm aperture UV preionized atmospheric pressure CO_2 gas discharges. A method for spectral control of the oscillator by injection of a low power c.w. CO_2 laser beam will be discussed as well as a fast plasma isolator for protection of the GaAs switch and improvement of the pulse contrast ratio. Beam propagation parameters and focussing conditions on target will be described.

9:15
AI2 X-Ray Emission from a CO_2 Laser-Produced Plasma. G.D. ENRIGHT, N.H. BURNETT, M.C. RICHARDSON, N.R.C. and D.J. NAGEL, N.R.L., Washington, D.C. -- A 1 ns pulse of radiation from a CO_2 laser (COCO-II) has been used to irradiate slab targets with power densities exceeding 10^{14} watts/cm^2. The intensities and the spectra of the x-rays emitted from the resulting plasmas contain valuable information about the temperature and density of the electrons. We have observed characteristic line emission from H-like and He-like ions of Al and Mg. Preliminary analyses of these spectra have indicated an electron temperature of approximately 2 KeV. Various detector and filter combinations have also been employed to observe the continuum x-ray spectrum and its dependence on the power density of the incident laser radiation.

9:30
AI3 Synchronized Single Pulses from Mode-Locked TEA CO_2 and Nd:glass Lasers. I.V. TOMOV, R. FEDOSEJEVS*, M.C. RICHARDSON, and W.J. ORR. N.R.C.-- A system is described which produces a subnanosecond Nd:glass laser which is synchronized to the 1 ns CO_2 laser pulse from the COCO-II laser system. The pulse synchronization is reproducibly better than 0.4 ns. This has been achieved with the aid of an actively mode-locked Nd:glass ring laser with variable dynamic Q-control. By controlling both the formation and buildup of the initial noise pulses within the laser cavity, the buildup of a very short pulse within the resonator is precisely controlled. The single pulse from a mode-locked TEA CO_2 laser is used to trigger a spark gap and switch out the subnanosecond pulse from the Nd:glass cavity. Exact synchronization is obtained by driving the active mode-locking elements for both lasers from the same RF oscillator.

* University of Toronto.

9:45
AI4 Subnanosecond Interferometry of CO_2 Laser-Produced Plasmas. R. FEDOSEJEVS*, I.V. TOMOV, M.C. RICHARDSON, N.R.C. -- A single pulse from a synchronized mode-locked Nd:glass laser system is upconverted and used to investigate plasmas formed by the 1 ns CO_2 laser pulse from the COCO-II laser system. By means of a folded-wavefront interferometer an integrated two-dimensional electron density profile is obtained which, because of cylindrical symmetry, can be transformed into a complete three-dimensional profile. The use of a synchronized subnanosecond pulse at 5300A permits both time resolution within the nanosecond interaction period of the laser and plasma, and observation of the plasma at the critical density surface of the CO_2 laser radiation. The interferometer system will be described and preliminary results presented.

*University of Toronto.

10:00
AI5 Passive Mode-Locking of Pulsed Lasers Using the Optical Kerr Effect. K. SALA*, M.C. RICHARDSON, and N.R. ISENOR*, N.R.C. -- A theoretical and experimental description is given of a novel technique which enables passive Q-switching and mode-locking of pulsed high power lasers. The technique is based upon a device termed the optical Kerr effect modulator (OKEM) which employs the optical Kerr effect in a two-fold way to produce both phase and amplitude modulation. The OKEM method of passive mode-locking offers a number of key advantages over the more common method of passive mode-locking employing saturable dyes and a discussion is presented which compares the two techniques with respect to questions of stability, frequency selectivity, and versatility.

* University of Waterloo.

10:15
AI6 Interferometric Determination of the Parameters of Shocks Formed by High Intensity Laser Radiation Incident on Thin, Solid Targets. J.C. SAMSON and A.J. ALCOCK, N.R.C. -- Optical interferometric observations of the expansion of plasma in the unloading of shock-heated materials from the back of thin targets allows the direct determination of the fluid velocity u behind the shock, and the thermal velocity v of the plasma ions. In the laboratory frame, we assume that the density of the unloading front obeys an adiabatic, fluid expansion of the form $\rho_{max}(t)\ \exp[-|\vec{r}-\vec{u}t|^2/(R+vt)^2]$ where r is radial position, R is the radius of the focal spot, the time t = 0 marks the beginning of unloading, and $vt >> R$. Some applications of the technique to shocks formed by 0.6943 and 1.06 μm laser light, with pulse durations from nanoseconds to tens of nanoseconds, focussed on suspended particles and thin fibers (thickness < 100 μm), will be presented.

10:30
AI7 Comparaison entre la distribution du courant émis et celle de l'illumination pour une cible irradiée par laser. P. KIEFFER, M.G. DROUET, R. BOLTON, G. SAINT-HILAIRE, Z. SZILI, Direction Sciences de base, IREQ, Varennes, Québec, Canada, J0L 2P0; H. PEPIN, B. GREK, A. THIBAUDEAU, INRS-Energie, Varennes, Québec, Canada, J0L 2P0, et K. TREPANIER, C.R.D.V., Valcartier, Québec, Canada, J0A 1R0 -- La distribution du flux laser sur une cible et celle du courant émis par la cible à la suite de cette irradiation ont été mesurées. Un laser au verre dopé au néodyme (4 J, 30 ns) et une cible de cuivre ont été utilisés et les mesures ont été effectuées dans l'air à 0.3 torr à l'aide de fils-sondes et de photodétecteurs localisés dans la cible. Les mesures de courant confirment l'existence d'une cathode centrée sur l'axe laser entourée d'une anode annulaire. La structure de la distribution du courant à la cathode correspond à la structure de la distribution de flux laser. L'amplitude maximum du courant, atteinte à la fin de l'illumination, suggère que la source est du type thermionique. La distribution de courant à l'anode initialement en 1/r évolue en raison d'une expansion probable des lignes de courant dans le plasma laser devant la cible.

10:45
AI8 Evidence pour la diffusion du champ magnétique dans le plasma-laser. R. BOLTON, M.G. DROUET, G. SAINT-HILAIRE, P. KIEFFER, Z. SZILI, Direction Sciences de base, IREQ, Varennes, Québec, Canada, J0L 2P0; H. PEPIN, B. GREK, A. THIBAUDEAU, INRS-Energie, Varennes, Québec, Canada, J0L 2P0, et K. TREPANIER, C.R.D.V., Valcartier, Québec, Canada, J0A 1R0 -- Dans un plasma créé par l'impact sur une cible, d'un faisceau laser CO_2 (4 J, 1.7 ns), nous avons mesuré l'amplitude du champ magnétique B, qui y est produit, en fonction de la distance à la cible. Les mesures ont été effectuées dans l'argon à 0.1 torr. Dans l'espace étudié - de 5 à 30 mm de la cible à 45° par rapport à l'axe laser - on observe une variation progressive de la forme et de l'amplitude de l'impulsion de champ magnétique qui satisfait l'hypothèse d'une diffusion du champ devant la cible et non pas celle de la propagation d'un front tel que proposé par d'autres auteurs.

11:00
AI9 Mesures simultanees de courant et de champ magnétique dans un plasma produit par laser. M.G. DROUET, R. BOLTON, G. SAINT-HILAIRE, P. KIEFFER, Z. SZILI, Direction Sciences de base, IREQ, Varennes, Québec, Canada, J0L 2P0; H. PEPIN, B. GREK, A. THIBAUDEAU, INRS-Energie, Varennes, Québec, Canada, J0L 2P0, et K. TREPANIER, C.R.D.V., Valcartier, Québec, Canada, J0A 1R0 -- Le plasma est créé à l'impact, sur une cible de cuivre, d'un faisceau laser CO_2 (4 J, 1.7 ns) ou d'un faisceau laser au verre dopé au néodyme (4 J, 30 ns) dans les gaz CO_2, Ar, He, N_2 ou air entre 10^{-3} et 10^3 torrs. Des fils-sondes, dans la cible, permettent la mesure de la distribution de courant émise par la cible[1] et des sondes inductives, celle du champ magnétique dans le plasma. Les montées des impulsions de courant, I, et de champ magnétique, B, sont simultanées, suggérant l'existence d'une seule source pour I et B. De plus, B décroît moins vite que I confirmant une expansion, dans le plasma, des contours du champ B. La forte dépendance de B sur la pression du gaz n'est pas observée dans le cas du courant émis par la cible irradiée par l'impulsion laser à 1.06 μm.

[1] M.G. Drouet, R. Bolton, Phys. Rev. Lett., March 15, 1976.
M.G. Drouet, H. Pépin, Appl. Phys. Lett., April 15, 1976.

11:15
AI10 Infrared Emission From CO_2 Laser Produced Plasmas. B. Grek,* H. Pepin and T.W. Johnston, I.N.R.S. Energie. The spectrum of emission in the vicinity of 10 μm., from a plasma produced by a 1.6 nsec, 5 joule pulse on polyethylene targets is studied as a function of laser power and scattering angle. The backscattered radiation is frequency shifted in a manner that indicates that specular reflection dominates for energy fluxes less than 10^{12}W/cm^2, but that for higher powers stimulated scattering from acoustic modes dominates. The spectral shape and angular dependance of the 10 μm. emission also indicates that parametric decay is an important absorption mechanism of the incident laser radiation.

*Part of this was performed while this author was at D.R.E.V.

11:30
AI11 Mesures du ravonnement-X dans l'interaction laser-CO_2, cibles solides.* H. PEPIN, B. GREK, T.W. JOHNSTON, INRS-Energie, U. du Québec, F. RHEAULT, Gentec, Québec--L'émission X d'un grand nombre de matériaux irradiés par un laser CO_2-TEA de 4J - 1.8nsec[1] a été étudiée. Les résultats suivants seront présentés: énergie X émise suivant les matériaux et suivant l'énergie laser, spectre haute résolution avec crystal de Bragg incluant les raies, spectre basse résolution avec la méthode des absorbants jusqu'à 10 kev, photographie-X du plasma.

[1] F. Rheault, J.L. Lachambre, P. Lavigne, H. Pépin, H. Baldis, Rev. Sci. Inst. 46, 1244 (1975).
*Recherche subventionnée par l'A.C. Laser du M.E.Q.
+Adresse actuelle: INRS-Energie, Varennes

11:45
AI12 Angular Distributions of Laser-Plasma X-Ray & Fast Electron Efficiencies.* C.E. VIOLET and J. PETRUZZI, Lawrence Livermore Lab.--Angular distributions of the x-ray and fast electron efficiencies of laser-produced plasmas have been measured. Incident laser pulses of two different wave lengths were provided by Nd-glass (1.06μ) and CO_2 (10.6μ) lasers in separate experiments. X-ray and electron fluences were measured with silicon surface-barrier detectors. Discrimination between the X-rays and electrons was achieved using electron sweeping magnets. The planar targets were of thin CH_2 and parylene. In the CO_2 laser experiments the fast electron efficiencies were strongly peaked anti-parallel to the incident pulse and significantly greater than the x-ray efficiencies. These effects were present but much weaker in the Nd-glass laser experiments.

*Prepared for U. S. Energy Research and Development Administration under contract No. W-7405-Eng-48 and the Defense Nuclear Agency.

AI13 (voir HF 9)

MONDAY, JUNE 14, 1976
ROOM 1C
Chairman: R.G. Slobodrian

13:30
BA1 Analyse des Réactions ^{3}He(d,d)^{3}He et ^{3}He(d,p)^{4}He Entre 15 et 40 MeV.* R. ROY†, H. E. CONZETT, R. M. LARIMER, F. N. RAD+ et F. SEILER‡, Lawrence Berkeley Laboratory.--La section efficace différentielle et le pouvoir d'analyse vectoriel iT_{11} de la diffusion élastique ^{3}He(d,d)^{3}He à six énergies incidentes de deutons entre 15 et 40 MeV ont été analysés dans le cadre du modèle optique. Un accord satisfaisant est obtenu entre les calculs et les données expérimentales en - dessous de 30 MeV. Diverses variations des paramètres semblent confirmer la distribution en énergie des coefficients d'expansion en polynomes de Legendre d'une analyse antérieure[1]. Ces paramètres permettent, par des calculs en ondes distordues, de reproduire convenablement certaines données de la réaction ^{3}He(d,p)^{4}He avec ou sans coupure inférieure dans l'intégrale radiale de recouvrement.

[1]R. Roy et al., 4th Int. Symp. on Polar. Phenom. in Nucl. Reac., Zurich, Swiss, Aout 1975, sous presse.
*Travail supporté par U.S. Energy Research Dev. Admin.
†Boursier postdoctoral du CNR, à présent au Département de Physique, Université Laval, Québec.
†A présent au Bates Linear Acce., Middelton, Mass, 01949
‡A présent à l' Université de Bâle, Suisse.

13:45
BA2 Nouvelle confirmation de la mesure de deutons à haute énergie dans la réaction ^{3}He + ^{3}He. *
R. PIGEON, M. IRSHAD et R.J. SLOBODRIAN, Laboratoire de Physique Nucléaire, Département de Physique, Université Laval, Québec, G1K 7P4. La réaction ^{3}He + ^{3}He a fait l'objet d'une étude[1] et des résultats positifs ont été publiés récemment[2]. La mesure à 20°_{lab} a produit une section efficace moyenne $d^2\sigma/dEd\Omega = 2.2 \pm 0.6$ nb MeV sr^{-1}, en bon accord avec la valeur de la ref. 2. Des mesures avec une cible d'air et une cible vide ont démontré que les deutons observés avec la cible d'^{3}He ne proviennent pas des réactions (^{3}He,d) avec des impuretés de la cible ou avec les fenêtres de la cellule gazeuse. La possibilité que les protons de la réaction ^{3}He (τ,p) ^{5}Li produisent une réaction (p,d), a été éliminée après une mesure de la réaction ^{2}H (τ,p) ^{4}He.
*Ce travail a été appuyé en partie par la CCEA du Canada et par le Ministère de l'Education du Québec.

[1]R. Pigeon et al., Problèmes à petit nombre de corps ... Presses de l'Université Laval, Québec (1975) 434.
[2]R.J. Slobodrian, R. Pigeon et M. Irshad, Phys. Rev. Lett. 35 (1975) 19.

14:00
BA3 *Deuteron Spin-Tensor Moments in n-p Radiative Capture**. S.F.J. WILK, Univ. of Manitoba--Calculations of the energy and angular dependence of the deuteron spin-tensor moments for the reaction n(p,d)γ are presented and discussed. These calculations were performed for the Lomon-Feshbach[1] boundary condition model B.C.M. in addition to the Reid[2] and Tabakin[3] potential models, in order to cover a wide range of D-state probabilities for the deuteron (i.e. Reid: 6.5%, B.C.M.: 5.2% and Tabakin: 3.2%). The results demonstrate the need for experimental data to resolve the long standing uncertainty as to the tensor character of the nucleon nucleon interaction.

*Supported in part by the AECB of Canada.

[1] E.L. Lomon and H. Feshbach, Annals of Physics 48, 94 (1968).
[2] R.V. Reid Jr., Annals of Physics 50, 41 (1968)
[3] F. Tabakin, Annals of Physics 30, 51 (1964).

14:15
BA4 ANALYSIS OF AN ANGULAR DISTRIBUTION OF p-n FINAL STATE INTERACTION FROM THE ^{2}H(p,pn)^{1}H REACTION AT Ep = 12.5 MeV. E. ANDRADE, Instituto de Física, Universidad Nacional Autonoma de México, D. MILJANIC, Institute Ruder Boskovic, Zagreb Yugoslavia and G. C. PHILLIPS, Rice Univ. Houston, Texas. Proton-neutron coincidences from the p + d$\rightarrow$p + n + p reaction, with the proton and the neutron counters located on the same side of the axis, were measured in the angular range $15^{\circ} \lesssim \theta_n = \theta_p \lesssim 45^{\circ}$. The data have been analized using the Ebenhöh code (EC)[1], which solves the three particle Faddeev equations exactly for separable, S-wave, spin dependent N-N interactions. The N-N potential is of the Yamaguchi form.

1. W. Ebenhöh, Nucl. Phys. A191(1972)97.
*Supported in part by the U.S. Atomic Energy.

14:30
BA5 Three Body Breakup in the ^{6}Li(^{3}He,pα)α Reaction and the Resonant State of ^{5}Li. K. RAMAVATARAM*, R. LARUE, and R. GAGNON, University Laval, Quebec; W.G. DAVIES, G.C. BALL, and A.J. FERGUSON, AECL Chalk River, Ontario and R.E. WARNER, Oberlin College, Oberlin Ohio.--We have performed a kinematically complete experiment to study the three-body breakup of the ^{6}Li(^{3}He,pα)α reaction. A 36 MeV ^{3}He beam from the Chalk River MP Tandem Accelerator was used to bombard an isotopically enriched ^{6}Li target. Protons and alphas were detected in coincidence for 10 different coplanar geometries of two Si counter telescopes. We have identified peaks in the spectra corresponding to the 16.7, 20.2, and 22.6 MeV states of ^{5}Li. A comparison of the results with earlier work[1,2] on the resonant states of Li and with theoretical calculations[3] will be presented.

*Work supported by the Atomic Energy Control Board of Canada.
[1]D.J. Plummer et. al. Nucl. Phys. A 174 (1971) 274
[2]H.T. King, W.E. Meyerhof and R.G. Hirko, Nucl. Phys. A 178 (1972) 337.
[3]K. Ramavataram and S. Ramavataram, Nucl. Phys. A 147 (1970) 293.

14:45
BA6 Elastic Scattering Differential Cross Sections for ^{3}He(p,p)^{3}He: Precise Measurements Between 19 and 48 MeV*. B.T. MURDOCH, A.M. SOURKES and W.T.H. van OERS, Univ. of Manitoba and RONALD E. BROWN, Univ. of Minnesota--Precision measurements of $d\sigma_{el}/d\Omega$ for ^{3}He(p,p)^{3}He were made at the University of Manitoba cyclotron. Elastically scattered protons were detected at 5° intervals for θ_{LAB}=10° to 170°, with eight values of E_p from 19.6 to 47.6 MeV. A left-right averaging method served to cancel out first-order geometrical errors. Total relative errors are typically 2%; absolute errors, 1%. These results, along with existing total reaction cross

section and polarization data can be used to extend the low-energy phase-shift analysis of Hale et al[1] to this energy range.

* Supported in part by the AECB of Canada and by the NRC of Canada.

1 G.M. Hale, J.J. Devaney, D.C. Dodder and K. Witte, Bull. Am. Phys. Soc. 19, 506 (1974).

15:00

BA7 Small Angle Elastic p-^{3}He Scattering at Intermediate Energies. A.W. STETZ, J.M. CAMERON, R. McCAMIS, C.A. MILLER, G.A. MOSS, and G. ROY, Univ. of Alberta; C.A. GOULDING, B. MURDOCH, W.T.H. van OERS, Univ. of Manitoba; J.G. ROGERS, TRIUMF--We have measured elastic p-^{3}He differential cross sections at a range of laboratory angles from 4° to 15° and at 200, 350, and 500 MeV incident proton energy. The experiment made use of solid state detectors to measure the energy of the recoiling α particles and multiwire proportional counters to determine the proton scattering angles. The data show strong destructive coulomb-nuclear interference at 200 MeV followed by increasing forward cross section and slope at higher energies.

15:15

BA8 Optical Model Analysis of P + ^{4}He Scattering at Intermediate Energies. R.H. McCAMIS, S.W-L. LEUNG, J.M. CAMERON, and H.S. SHERIF, Univ. of Alberta, Edmonton--Available data on cross section and polarization in the elastic scattering of protons on ^{3}He in the energy range 150-600 MeV are analyzed using a conventional optical model potential. Reasonable fits are obtained for the forward angle data. Inclusion of a Majorana exchange term explains the behavior of the large angle cross sections; the data seem to indicate, however, that this term is unimportant for proton energies in the neighborhood of 300 MeV. The effect of the exchange term on the large angle polarization is less pronounced. One interesting feature of the results is that the data seem to invariably require a large imaginary spin orbit potential.

15:30

BA9 New Results on Elastic Scattering of Alpha Particles by Protons. § J. OOSTENS, M. VAN DEN BOSSCHE and L. VU HAI, CEA-SATURNE (FRANCE), J. BERGER, J. DUFLO, L. GOLDZAHL, F. PLOUIN, CNRS-SATURNE (FRANCE) G. BIZARD, C. LEBRUN, CNRS-U. DE CAEN (FRANCE), F. FABBRI, P. PICOZZA AND L. SATTA, CNEN-FRASCATI (ITALY). -- Recently acquired data obtained with alpha particles from the Saclay Synchrotron Saturne confirm at 6.00 GeV/c the backward peak reported earlier at lower momentum[1]. At 5.08 GeV/c, data taking has been completed in the region where double and triple scattering contribute. A mild interference structure is seen. Our data will be compared with recent theoretical models.

§ Submitted by B. THEVENET

[1]VIth International Conference on Nuclear Structure and High Energy Physics. Santa Fe, June 1975, Abstracts VI.B.16 and 17.

15:45

BA10 Observation of Neutron Hole States in Nuclei W.J. MCDONALD, J.M. CAMERON, D.A. HUTCHEON, A.N. JAMES*, P. KITCHING, and C.A. MILLER, Univ. of Alberta, TRIUMF. E.D. EARLE, AECL, Chalk River.- The $^{12}C(p,pn)\ ^{11}C$ reaction has been observed and compared with $^{12}C(p,2p)^{11}B$ using 400 MeV incident protons from the TRIUMF cyclotron. These results are from a preliminary measurement in which the protons were detected in a range telescope ($\Delta Ep \sim 7$ MeV), while the neutrons were observed by time of flight over a 2m path. The time resolution for neutrons was 0.5 ns to yield $\Delta E_n \sim 7$ MeV also. Thus the neutron separation energy was determined to about 10 MeV. This was adequate to separate s and p neutron hole states in ^{11}C. With the aid of a thin counter in front of the neutron detector charged particles were identified so that (p,2p) events could be observed at the same time. Two broad peaks were observed in the separation energy spectrum for neutrons and compared with the corresponding peaks for protons from the (p,2p) reaction. The peak which corresponded to the p state disappeared at zero momentum transfer as expected while that attributed to the s state did not.

* On leave from the University of Liverpool.

16:00

BA11 Quasi Elastic Knockout of Deuterons from ^{12}C. D.A. HUTCHEON, A.N. JAMES*, P. KITCHING, W.J. MCDONALD, C.A. MILLER, Univ. of Alberta, TRIUMF. G.A. MOSS, W.C. OLSEN, D.M. SHEPPARD, A.W. STETZ, Univ. of Alberta. J.G. ROGERS, TRIUMF.- The TRIUMF proton beam has been used to investigate the reaction ^{12}C (p, pd) in a kinematically complete experiment. The energies of the outgoing particles were measured in two five inch diameter by three inch thick NaI(Tl) crystals. The particles were identified by determining their energy loss in thin plastic passing counters and the production angles measured using multiwire proportional chambers. With incident protons of 400 MeV the overall energy resolution of the system was about 6 MeV. About 50,000 (p, pd) events were obtained with several different kinematic conditions.

* On leave from the Univ. of Liverpool.

16:15

BA12 Photoproduction of Positive Pions from Deuterons Near Threshold.* B. CHASAN, E.C. BOOTH, R. BLAIR, and R. CARTER, Boston U., A. BERNSTEIN, P. BOSTED, and W. TURCHINETZ, MIT--The excitation function for the reaction $\gamma + d \rightarrow 2n + \pi^+$ has been measured for end point photon energies 1-6 MeV above threshold using the bremsstrahlung beam of the MIT Bates Linear Accelerator. The method employed was based on detection of the high energy ($E_o \gtrsim 52$ MeV) positrons emitted by the decay muons, all of which stop in the reaction target. Detection was done with a counter telescope gated on immediately after beam pulses. The results have been compared with the calculation of Tzara[1], who has pointed out the relevance of the reaction as a test of the impulse approximation. Preliminary analysis indicates good agreement with his total cross-section result for a value of the neutron-neutron scattering length which is in rough agreement with the currently accepted one.

*Work supported by ERDA and by NSF.

[1]Tzara, Nuclear Physics. A256 381 (1976).

16:30

BA13 A Triton Beam for Medium Energy Physics. § G. BIZARD, J.L. LAVILLE, C. LE BRUN, J.F. LECOLLEY, F. LEFEBVRES, A. OSMONT, R. REGIMBART and J.C. STECKMEYER, Un. of Caen (France), J. BERGER and L. GOLDZAHL, CNRS Saturne, Saclay (France), J. OOSTENS, Dept. Saturne, Saclay (France) and C. SCHAERF, Un. of ROMA (Italy). -- A quite usable alternative to an accelerated triton beam has been developped at Saturne : ^{4}He are accelerated to 5.08 GeV/c, and undergo break up shortly after extraction, on a 10 cm long piece of lucite. The resulting tritons are peaked in the forward direction and have momenta centered at 3/4 of the incident Alpha momentum. The tritons are transported by a magnetic channel including two bending magnets and four quadrupoles. A 20 mm momentum slit selects a 60 MeV/c (FWHM) bite of the break up spectrum. 6 10^7 tritons per machine pulse are focussed into a spot 50 mm wide by 15 mm high at the Hydrogen target.

§ Submitted by B. THEVENET.

MONDAY, JUNE 14, 1976
ROOM 1B
Chairman: W.K. Sherman

13:30

BB1 On the Mass Asymmetry in the Radium Region. H. SCHULTHEIS, F. GONNENWEIN, R. SCHULTHEIS, and K. WILDERMUTH, Tuebingen Univ., W. Germany--In low-energy fission experimental mass distributions are symmetric for compound nuclei with $Z \leq 85$ and asymmetric for those with $Z \geq 88$. Contrary to the conventional classification (according to the charge number of the parent nucleus) an analysis of the deformation energy in terms of cluster contributions confirms early suggestions that the neutron number N = 132 determines the mass asymmetry in the Radium region: Only isotopes heavier than N = 132 should fission asymmetrically. Due to the lack of suitable targets in that region an experimental test of the (N=132)-hypothesis is difficult to perform. The bombardment of Pb-targets with heavy ions is suggested.

13:45

BB2 Some Estimates of Fragment Deformations and Excitations at Scission.* R. SCHULTHEIS and H. SCHULTHEIS, Tuebingen Univ., W. Germany--The calculated potential energy of spheroidal fragments at scission is compared with the experimental fragment excitation and kinetic energies. By treating pre-scission collective and internal excitations and post-scission Coulomb excitations as adjustable parameters certain upper and lower limits have been obtained for the following quantities at scission: the fragment deformations, the energy of collective vibrations and internal excitations and the deviation of the resulting scission configuration from the path of minimum energy.

* Submitted by F. GÖNNENWEIN.

14:00

BB3 Study of Proton Induced Fission of ^{238}U.* K.C. CHAN, B.P. PATHAK, L. NIKKINEN and L. LESSARD, McGill University.--The isotopic distributions of indium and gallium were obtained for the reaction $^{238}U(p,f)$ at proton energies between 35 and 100 MeV with an on-line mass spectrometer. The energy dependence of the most probable masses and of the widths of the distributions will be compared with the rubidium and cesium values reported previously. The distributions of the gallium isotopes which have been observed for the first time with this method will be used together with the distributions of the complementary fragments (Pm), previously measured by radiochemical methods[1], to obtain information on the reaction mechanism.

[1]J.L. Galinier, Ph.D. Thesis, Chemistry Department, McGill University, 1975 (unpublished).

*Work supported by the Atomic Energy Control Board.

14:15

BB4 Preliminary search for a low viscosity trajectory to fission*. the neckin-in. P. AMIOT, Université Laval, Québec, G1K 7P4. The viscosity coefficient in nuclear fission in really a tensor, η, defining a dissipation function $\sim \frac{1}{2} \dot{\alpha}^T \eta \dot{\alpha}$, Where α is the column vector of the deformation coordinates. Recent theoretical estimates of the average η[1] in the fissioning process yield larger values than suggested by experimentally observed Kinetic energies of fragments. On the basis of a schematic single particle model we suggest that the tensor η defines a favored, low viscosity direction defining a trajectory which proceeds from the (second) saddle to scission by pure necking-in. This trajectory is important mainly for the heavy actinides and it is argued that it coincide with that found on the adiabatic energy surface of Mustapha et al[2]. Such a trajectory was first suggested by J.J. Griffin[3].

* Supported in part by the Conseil National de la Recherche (Canada).

1) S.E. Koomin and J.R. Nix, 1976, Phys. Rev. C13, 209.

2) M.G. Mustapha, U. Mosel and H.W. Schmitt, 1973, Phys. Rev. C7, 1519.

3) J.J. Griffin, IAEA-SM-122/200, IAEA Proc. Conf. on Phys. and Chem. of Fission, Vienna, 1969.

14:30

BB5 Photofission with Monochromatic Photons. B. PICH, T.E. DRAKE, Univ. of Toronto* W. KNOWLES, AECL, Chalk River Nuclear Labs.--A 4800 wire proportional counter for the detection of fission fragments was constructed by alternating 96 sets of wire planes with 1/32" aluminium plates coated with thin films of $^{232}ThO_2$ and $^{238}UO_2$. This counter was used with the University of Illinois Bremsstrahlung Monochromator and C.W. Microtron to measure photofission yields with monochromatic photons. The counter construction and performance characteristics are described.

*Supported by the National Research Council of Canada.

14:45

BB6 Electrofission of Heavy Elements.* A. KERNOHAN, T.E. DRAKE, L. PAI and A. CHUNG, Univ. of Toronto--Electrofission yield curves for electron energies of 32-44 Mev were obtained for ^{206}Pb, ^{207}Pb, ^{208}Pb and ^{209}Bi using aluminized Makrofol detectors. The curves were fitted with a statistical model of the fission process and values for the saddle point level density parameters and the fission barriers were obtained. A strong resonance-like feature was discovered in the ^{206}Pb yield curve. Preliminary work was done on ^{184}W which indicates no dependence of the pairing energy on the nuclear surface.[1]

[1]U. Mosel, Phys. Rev. C.6, 971 (1972).

*Supported by the National Research Council of Canada.

15:00

BB7 Radiative Capture Reactions Leading to Mass-15 Nuclei. W. DEL BIANCO, S. KUNDU and J. KIM. Univ. de Montreal. The reactions $^{12}C(^3He,\gamma)^{15}O$ and $^{11}B(\alpha,\gamma)^{15}N$ have been experimentally studied over the incident-particle-energy range from 6 to 18 MeV. The γ-rays have been detected with a 9" x 9" NaI crystal surrounded by a plastic scintillator operated in anticoincidence. In both reactions, the differential cross section at $\theta_{lab} = 90°$ is about a factor 50 smaller than the corresponding $^{14}C(p,\gamma_0)^{15}N$ cross section. The structure observed in the yield curves will be compared with that measured in the $^{14}C(p,\gamma_0)^{15}N$ and $^{13}C(d,\gamma_0)^{15}N$ reactions and with theoretical calculations.

1 M.H. Harakeh, P. Paul. H.M. Kuan and E.K. Warburton Phys. Rev, C12, 1410 (1975).

* Supported by a grant from the National Research Council of Canada.

15:15

BB8 Study of Giant Dipole Resonances in ^{29}P by (p,γ) Reaction*. S.T. LIM†, M.D. HASINOFF and D.F. MEASDAY, University of British Columbia, Vancouver, B.C.-- The reaction $^{28}Si(p,\gamma)^{29}P$ has been investigated over the giant dipole resonance region. Gamma yields have been measured for transitions to the ground and the first five excited states using a 10" x 10" NaI spectrometer[1]. The strengths of different channels in terms of the classical dipole sum are compared with the structure of the low-lying states in ^{29}P.

[1]M.D. Hasinoff, S.T. Lim, D.F. Measday and T.J. Mulligan Nucl. Instr. & Meth. 117, 375 (1974).

*Work supported in part by the National Research Council of Canada and the US Atomic Energy Commission.

†Present Address: AECL, Chalk River Nuclear Laboratories Chalk River, Ontario.

15:30

BB9 Photoneutron Cross Sections for Osmium Isotopes† B. L. BERMAN, R. A. ALVAREZ, D. D. FAUL, and P. MEYER, Lawrence Livermore Lab.--We have measured the photoneutron cross sections for $^{188,189,190,192}Os$ from the (γ,n) threshold to 30 MeV and for ^{186}Os from 11 to 19 MeV, using monoenergetic photons from the annihilation in flight of fast positrons from the LLL Electron-Positron Linac. The photon energy resolution ranged from 300 to 400 keV over the energy range of the experiment. Isotopically enriched powdered-metal osmium samples were used. The objective of this experiment was to test the recent theoretical prediction[1] of a nuclear phase transition, from prolate deformed to γ-unstable between the ^{188}Os and ^{190}Os nuclei. Values for integrated cross sections and branching ratios for multiple-neutron-emission cross sections were obtained as well.

†Work performed under the auspices of the U.S. Energy Research and Development Administration.

[1]R. Sedlmayr, M. Sedlmayr, and W. Greiner, Nucl. Phys. A232,465 (1974).

15:45

BB10 Ground and First Excited State Transitions in the $^{208}Pb(\gamma,n)$ Reaction. N.K. SHERMAN, K.H. LOKAN, C.K. ROSS and H.M. FERDINANDE*, Physics Division, National Research Council, Ottawa, Canada--By repeating our previous photoneutron time-of-flight measurements[1] at 300 keV intervals of bremsstrahlung end-point energy we have obtained the first excited state cross section $d\sigma_1/d\Omega$ for the $^{208}Pb(\gamma,n)$ reaction, in addition to remeasuring the ground state cross section $d\sigma_0/d\Omega$ from 8 MeV to 16 MeV. Below 8.5 MeV, where the features in $d\sigma_0/d\Omega$ can be compared with other measurements, there is good agreement. Our earlier discovery of a resonance at 9 MeV is confirmed, and is strong evidence against an EO interpretation. Above 10 MeV, we find $d\sigma_1/d\Omega$ to be about twice $d\sigma_0/d\Omega$, consistent with E1 absorption.

[1]N.K. Sherman, H.M. Ferdinande, K.H. Lokan and C.K. Ross, Phys. Rev. Lett. 35, 1215 (1975).

*N.A.T.O. Postdoctoral Fellow, Rijksuniversiteit te Gent, Belgium.

16:00

BB11 Ground State Transitions from the Giant Dipole Resonance. K.H. LOKAN, N.K. SHERMAN and C.K. ROSS, Physics Division, National Research Council, Ottawa, Canada, and H.M. FERDINANDE, Rijksuniversiteit te Gent, Belgium--Photoneutron energy spectra have been measured by time-of-flight methods at 1 MeV bremsstrahlung energy intervals between 10 MeV and 25 MeV for the isotopes ^{209}Bi, ^{197}Au, ^{181}Ta and ^{115}In. Each of these nuclei yields raw spectra containing a peak which corresponds to ground state neutrons from the giant dipole resonance. This peak is unexpected. It indicates that the ground state decay channel is favoured over many other possible channel adjacent to it in energy. A qualitative explanation is that removal from these nuclei of one neutron by a direct interaction with the photon does not greatly affect the nuclear potential in which the remaining nucleons move, so that the combined wave function for these spectator nucleons has a large overlap with the ground state of the A-1 nucleus.

16:15

BB12 Photoneutron Reaction on Lead at 9 MeV. J. F. McPHF and W.V. PRESTWICH, McMaster Univ. --

The photoneutron reaction on natural lead has been investigated at 9 MeV incident photon energy. Neutron spectra and cross sections have been obtained using monochromatic photons from neutron capture and a high resolution ^3He detector.

MONDAY, JUNE 14, 1976
ROOM: 2C
Chairman: R.M. Lees

MOLECULAR PHYSICS

13:30

BC1 Collisional Transfer of Rotational Energy in Methanol and OCS.* L. J. RETALLACK and R. M. LEES, Univ. of New Brunswick-- Collision-induced rotational transitions have been studied for CH_3OH and OCS by steady-state microwave double resonance. An M-resolved experiment on the $(4_0\text{-}3_1)_p\text{-}(2_1\text{-}3_0)_s$ four-level system of CH_3OH in the presence of a Stark field is described in which collisional transfer is observed between individual M-substates of pump and signal levels. For pure CH_3OH, the collisional preferences are $\Delta M=0, \pm 1$, and the relative signal intensities are consistent with a simplified dipole-dipole model of the collisional interaction. In CH_3OH-He and CH_3OH-H_2 mixtures, transitions with $|\Delta M|>1$ are seen, indicating a higher-order interaction. For OCS, our initial results are interesting, but a clear picture of the collisional preferences has not yet emerged. Measurements will be reported for the $(3\text{-}2)_p\text{-}(1\text{-}0)_s$, $(4\text{-}3)_p\text{-}(1\text{-}0)_s$ and $(4\text{-}3)_p\text{-}(2\text{-}1)_s$ systems, in pure OCS and in OCS-CH_3OH, OCS-He and OCS-H_2 mixtures.

*Supported by the National Research Council.

13:45

BC2 The Role of Short Range Repulsive Potential in Molecular Collision Broadening. R. P. SRIVASTAVA, and H. R. ZAIDI, University of New Brunswick, Fredericton, N. B., Canada.--A general expression for the pressure broadened line width is derived, using a short range isotropic repulsive potential of the form $1/r^n$ along with the dominant anisotropic interaction potential. The short range potential eliminates the need for a

cutt off at small impact parameters. Further to our earlier work,(1) we have obtained some new results for CO_2. Using a single value for n and the quadrupole moment, Q, we obtain good agreement for CO_2 IR as well as Raman lines. (In previous calculations(2,3) different values of Q had been used in order to obtain agreement with the experimental data). Hence, it appears, that the contribution of the short range interaction is significant in CO_2, and information about it can be obtained from the collision broadening data.

[1]R. P. Srivastava and H. R. Zaidi, DAMP Meeting of CAP, Fredericton, N. B. (November 1975).
[2]C. G. Gray and J. Van Kranendonk, Can. J. Phys. 44, 2411 (1966).
[3]G. Yamamoto, M. Tanaka and T. Aoki, JQSRT 9, 371 (1969).

14:00

BC3 Multi-Photon Hole-Burning in CH_3F. J. REID and T. OKA, Herzberg Inst. of Astrophysics, N.R.C.C., Ottawa -- It is well known that intense laser radiation can burn holes in the Doppler profile of an absorption line. As the laser frequency is tuned through the centre of the molecular transition, a Lamb dip is obtained. We have investigated these hole-burning processes by placing a cell containing $^{13}CH_3F$ in a CO_2 laser cavity. The 9.4 μm P(32) CO_2 laser line is used to saturate the R(4,3) transition in $^{13}CH_3F$. A second CO_2 laser is used to monitor the absorption profile. We report the first direct observation of velocity-tuned multi-photon hole-burning[1]. These observations will be linked to recent theoretical work on the line shape of Lamb dips.

[1]S.M. Freund, M. Römheld and T. Oka, Phys. Rev. Lett. 35, 1497 (1975).

14:15

BC4 Determination of Differential "Free-Free Cross Sections" in Intense Laser Fields.* A. WEINGARTSHOFER, St. Francis Xavier University, Antigonish, N. S.--A "free-free transition" in a strong laser field is described by the following equation

$$e^-(\vec{p}_i) + h\nu + A(\vec{p}_i') \longrightarrow e^-(\vec{p}_f) + A(\vec{p}_f')$$

where an incoming free electron, $e^-(\vec{p}_i)$ absorbs a photon hν from the laser beam and thereby changing its energy and momentum, $e^-(\vec{p}_f)$, in such a manner that after the transition the electron is again free. The third collision partner A, an atom or molecule, is important to absorb the momentum of the photon. This is a three-beam experiment (electron, molecular, and laser) which we have been planning and are now ready to perform. We would like to discuss the experimental difficulties and the nature and importance of expected results in this novel experiment.

* Work supported by the National Research Council of Canada.

14:30

BC5 The Electronic Absorption Spectrum of NH_2. J.W.C. JOHNS, D.A. RAMSAY and S.C. ROSS, Herzberg Inst. of Astrophys., Ottawa. - The earlier analysis[1] of the $\tilde{A}^2A_1$-$\tilde{X}^2B_1$ absorption system of NH_2 has been considerably extended, especially at the long wavelength end of the spectrum (6500-9500Å). All the low-lying vibronic levels of the excited state have been identified up to $v_2' = 8$. These levels are: 010(K=0), 020(K=1), 030 (K=0,2), 040(K=1,3), 050(K=0,2,4), 060(K=1,3,5), 070 (K=0,2,4,6) and 080(K=1,3,5,7). Large perturbations (≈200 cm^{-1}) have been observed between some of these levels and high vibrational levels of the ground state. Accurate molecular constants have been obtained for the ground state and for the first level involving the bending vibration ($v_2'' = 1$).

[1]K. Dressler and D.A. Ramsay, Phil. Trans. Roy. Soc. (London) 251A, 553, 1959.

14:45

BC6 The Infrared Spectrum of Nitroxyl. J.W.C. JOHNS and A.R.W. McKELLAR, Herzberg Inst. of Astrophysics, N.R.C.C., Ottawa -- The high resolution and sensitivity of intracavity laser absorption spectroscopy are especially useful for studying infrared spectra of unstable molecules. We have detected and analyzed the ν_3 bands (N-O stretch) of HNO and DNO in the 6.4 μm region using laser Stark spectroscopy. The HNO (DNO) is produced by the reaction of H (D) atoms with NO in a continuous flow through an absorption cell inside the cavity of a CO laser. Molecular transitions are tuned into resonance with the fixed frequency laser lines ($^{12}C^{16}O$, $^{13}C^{16}O$, and $^{12}C^{18}O$) by means of the Stark effect. Many lines not due to nitroxyl are also observed; in the case of HNO, most of these are due to NH_3. Inclusion of the Coriolis coupling between ν_3 and the nearby ν_2 bending vibration is necessary for the HNO analysis, but not for DNO where the two vibrations are more widely separated.

15:00

BC7 Overlap Parameters of the H_2-H_2 Molecular Pairs from the Absorption Spectra of the Collision-Induced Fundamental Band of H_2.* S. P. REDDY, G. VARGHESE+ and R. D. G. PRASAD, Memorial Univ. of Newfoundland.--The collision-induced fundamental infrared absorption band of H_2 in the pure gas at 77, 196, and 298 K has been recorded for a number of gas densities up to 60 amagat. An analysis of the absorption profiles was performed by assuming appropriate line shapes and the characteristic half-width parameters δ_λ and δ_c of the short-range overlap transitions and δ_q (and $\delta_{q'}$) of the long-range quadrupolar transitions were determined. From this analysis the contributions to the intensity of the band from the overlap- and quadrupolar- interactions were separated. The overlap parameters λ and ρ giving respectively the magnitude and range of the induced overlap dipole moment of the H_2-H_2 molecular pairs were then determined by obtaining the best fit of the calculated overlap part of the binary absorption coefficients as a function of temperature to the experimental values of the overlap part.

*Supported by the National Research Council of Canada.
+On leave from the University of Zambia.

15:15

BC8 The Electron Impact Excitation Spectrum of HD.* A. WEINGARTSHOFER and E. M. CLARKE, St. Francis Xavier University, Antigonish, N. S.--We report here results for HD which are an extension of published work on H_2[1] and D_2[2]. To be discussed is primarily the isotopic effect in this series of molecules. In particular we will compare their threshold excitation spectra which are composed exclusively of triplet states. In the region of ionization we have observed a remarkable isotopic effect for HD which presumably arises on account of predissociation. We express our appreciation to Dr. D. A. Ramsay, of the Herzberg Institute of Astrophysics, for a generous donation of HD.

[1,2]A. Weingartshofer et al, J. Phys. B, 8, 1552 (1975) and L278 (1975).

* Work supported by the National Research Council of Canada.

15:30
BC9 Absolute Intensity and Effective Band Center Frequency of the First Overtone Band of CO. G. CHANDRAIAH, Memorial Univ. of Newfoundland.--Recently we have presented the preliminary experimental results regarding the absolute intensity measurement of the 2-0 band of CO, using essentially the Wilson-Wells technique[1]. Now, we have extended the studies to determine the intensity of the band from the measurement of the intensities of several, well resolved, self-broadened, P-branch lines by the method of equivalent widths for Lorentz lines. Absorption cells of different path lengths and a number of CO gas pressures below 1 atmosphere were used. Wing and base corrections were made for the measured equivalent widths to obtain accurate results. The effective band center frequency ω_{2-0} was calculated from the measured intensities of liens with higher J-values and the band intensity of 2.11 cm^{-2} agt^{-1}. Our value found for the effective band center frequency is in good agreement with the previous value obtained by direct method[2]. The value of the square of the rotationless matrix element and the magnitude of the dipolement coefficients M_2 have also been obtained.

[1]G. Chandraiah, DAMP Annual Meeting, 1975; UNB, Fredericton.
[2]C.L. Korb, R.H. Hunt, and E.K. Plyler, J. Chem. Phys. 48, 4252

15:45
BC10 The Electric Quadrupole Interaction of ^{181}Ta in K_3HfF_7. L.M. LOWE and W.V. PRESTWICH, McMaster Univ. --

The electric quadrupole interaction of ^{181}Ta in the heptafluorate compound of hafnium, K_3HfF_7 was measured by the differential perturbed angular correlation (DPAC) method. The results are discussed in comparison with previous DPAC work[1] on another compound containing the heptafluorohafnate ion, $(NH_4)_3HfF_7$.

1) E. Gerdau, J. Birke, H. Winkler and J. Braunsfurth. Z. Physik 263, 5 (1973).

16:00
BC11 Détermination Optique du Second Coefficient Viriel Diélectrique d'un Gaz.* J.M. ST-ARNAUD et T.K. BOSE, Univ. Que. (Trois-Rivières).-- Nous pouvons mesurer directement la partie induite (B_{IND}) du second coefficient viriel d'un gaz. Avec un interféromètre laser et deux cellules identiques en série, nous mesurons l'indice de réfraction (n) en fonction de la pression. Après avoir rempli la cellule A et mesuré n_A, nous faisons le passage du gaz de la cellule A vers la cellule B, attendons la stabilité et mesurons la variation d'indice (Δ). Nous recommençons le processus de B → A. Ce faisant, nous obtenons directement B_{IND} en établissant la valeur moyenne pour les 2 passages à une pression donnée. Nous présentons les résultats obtenus pour le CH_4.

* Subventionnée par le C.N.R. et le Min. Educ. Qué..

16:15
BC12 "Forbidden" Rotational Transitions between Different Spin Modifications. K. LALITA and T. OKA, Herzberg Inst. of Astrophysics, N.R.C.C., Ottawa -- Polyatomic molecules of astrophysical interest such as H_2O, NH_3, CH_4, H_2O^+, NH_2 etc. have nuclear spin modifications which, similar to ortho- and para-modifications of hydrogen, do not convert to each other easily through radiative and collisional processes. Thus in discussing molecular equilibrium in astronomical objects, different spin modifications have been treated as separate molecules. In this paper we examine theoretically to what extent this is justified. Magnetic Hamiltonian terms which are invariant with respect to permutations of identical nuclei (that is, exchanges of cartesian and spin coordinates of identical particles) but not invariant with respect to exchange of spin coordinates alone are identified; mixing due to these terms is calculated. Radiative transitions are caused by intensity borrowing through these mixing terms, and collisional transitions are caused by adiabatic passage through the avoided crossing region.

16:30
BC13 Some Anomalies in the NeI (744—736 Å) Photoelectron Spectra of N_2O.* M. J. WEISS, Department of Physical Chemistry, The Hebrew University, Jerusalem, Israel.—The NeI 744/736 Å photoelectron spectra of N_2O is reported for the $\tilde{X}\ ^2\Pi$ state of N_2O^+. The spectra in general do not show any autoionization behavior to the extent reported for CO_2 and CS_2[1]. There is an apparent 'enhancement' of the 101 level by the 744 Å line. In contrast to HeI 584 Å PES, the intensity ratio for the 100 and 001 levels are reversed when excited by NeI 736 Å radiation. In addition to the 101 level, other modes are excited by NeI radiation, notably the 201 and 102 modes. These modes have not been previously reported for HeI (584 Å) radiation. The spectra can be explained within the framework of direct ionization as well as excitation of an autoionizing Rydberg level having one vibrational component of the B state as its series limit.

*Work supported by Grants from the Israel Academy of Sciences and the U.S.-Israel Binational Science Foundation.
[1]J. E. Collin and P. Natalis, Int. J. Mass Spectry. Ion Phys. 1, 121 (1968).

16:45
BC14 Review of Laser Oriented Research in HCl Kinetics. DAVID W. HOWGATE, U.S. Army Missile Command, Redstone Arsenal, AL.--The visibility of gaseous hydrogen chloride (HCl) as a viable infrared laser candidate system, along with the projected nonresonant transfer of vibrational energy from molecular hydrogen to HCl, has spurred renewed research activity in the critical area of HCl kinetics and vibration transfer. Programs addressed include: (1) shock tube and shock tube/shock tunnel measurements of vibrational energy transfer in the H_2/HCl molecular system, (2) vibrational energy transfer and modeling with application to molecular gas lasers, (3) stimulated Raman and laser fluorescence measurements for the H_2/HCl system, (4) multiquantum relaxation processes in HCl, (5) theory of molecular collisions and vibrational relaxation with application to HCl. The state-of-the-art will be summarized, and the efforts of some leading contributors will be identified.

17:00
BC15 Exact Rate-Equation Study of Coupled Vibrational Relaxation and Radiative Decay in Molecular Systems.* V. SESHADRI and V.M. KENKRE, U. of Rochester-- Simultaneous vibrational relaxation and radiative decay in the harmonic oscillator model of a meloecule are studied using a generalized Montroll-Shuler equation,[1,2] and exact solutions in closed form are obtained for the time dependent probabilities of occupation of individual vibrational levels for several physical initial distributions like Boltzmann, Poisson, Laguerre, and δ-function. Closure relations involving Franck-Condon factors are derived, the radiative decay rate for individual vibrational levels is shown to be linear in the energy, and emission and absorption line shapes are calculated for several cases including an initial Boltzmann distribution in the electronic ground-state.

[1]E.W. Montroll and K.E. Shuler, J. Chem. Phys. 26, 454 (1957)
[2]V. Seshadri and V.M. Kenkre, Phys. Letters A (to be published)

MONDAY, JUNE 14, 1976
ROOM 2A
Chairman: T. Timusk

13:30

BD1 Mobility of Hydrogen in MgO under the Influence of Radiation. Y. CHEN, M. M. ABRAHAM, L. C. TEMPLETON, Solid State Division, Oak Ridge National Laboratory, Oak Ridge, TN 37830, H.T. TOHVER, University of Alabama, Birmingham, Al.--The distribution of hydrogen between substitutional sites (V_{OH}^{-} or V_{OH}^{+} centers) and $Mg(OH)_2$ precipitates in MgO single crystal depends on the thermal treatment of the crystal. Using infrared absorption measurements, it is shown that substitutional hydrogen as monitored by the 3296 cm^{-1} band, while not mobile at room temperature, becomes exceedingly so under the influence of ionizing radiation. Under electron irradiation, the mobility of substitutional hydrogen is a strong function of the temperature at which the irradiations are carried out, being greater at higher temperature. The decay of the 3296 cm^{-1} band is attended by increases in the V^{-}-center coloration and $Mg(OH)_2$ infrared absorption. A mechanism for the displacement of the substitutional hydrogen will be discussed.

*Operated by Union Carbide Corporation for the USERDA.

13:45

BD2 Centers in Particle-Irradiated Single Crystals of Tetragonal GeO_2.* L. A. KAPPERS, M. STAPELBROEK and O. R. GILLIAM, Univ. of Conn., and B. H. ROSE, Brookhaven National Lab.--A single, almost isotropic ESR line with $g_{\parallel}=1.9987$ and $g_{\perp}=1.9977$ is observed in single crystals of tetragonal GeO_2 following electron or reactor irradiations. The same resonance has been observed previously in reactor-irradiated polycrystalline samples and was attributed to an F^{+} center.[1] Optical absorption bands are observed at 3.8 eV and 2.5 eV in the single crystal samples for $E \perp c$. Illumination in the 3.8-eV band at 77 K enhances both the 2.5-eV optical band and the F^{+} center ESR signal while a decrease in the 3.8-eV band is observed. An isochronal pulse anneal reveals that the enhanced 2.5-eV band and ESR signal are thermally stable up to 400 K. The original intensities can be restored by a 546-nm bleach. These results suggest that the 2.5-eV band can be assigned to the F^{+} center and that the 3.8-eV band can be assigned to an F center absorption.

[1] R. A. Weeks, in Recent Advances in Science and Technology of Materials, ed. by A. Bishay (Plenum, New York, 1974), Vol. I, p. 27.

14:00

BD3 ESR of a Radiation-Induced Defect in NaN_3.* R. H. BARTRAM and L.A. KAPPERS, Univ. of Conn.--A relatively weak ESR spectrum is observed in single crystals of NaN_3 after u.v. or x-ray irradiation at 77 K. This spectrum, which has an anisotropic g value and exhibits a resolved 5-line hyperfine structure in some orientations, corresponds to a single unpaired electron interacting equally with two spin-one nuclei, in three inequivalent sites. Presumably the defect involves a molecular fragment comprising two or more nitrogen atoms, but its spectrum is clearly different from the N_2^{-} ESR spectrum described by Gelerinter and Silsbee.[1] The spectrum anneals over a wide temperature range above 200 K, but is still observable after warming briefly to 270 K.

*Supported by ARO-D, Grant DA-ARO-D-31-124-71-G35.

[1] E. Gelerinter and R.H. Silsbee, J. Chem. Phys. 45, 1703 (1966).

14:15

BD4 The Impurity Band in Si(P).* J.A. Rostworowski and M. Eswaran, Univ. of British Columbia -- The photoluminescent spectrum of phosphorus-doped silicon at dopant concentration ranging from 5.0×10^{17} to 1.1×10^{19} at low excitation intensities are dominated by the recombination of an electron in the impurity band and a free hole. For impurity concentrations below the metal-semiconductor transition a first principle calculation of the emission lineshape in the Hubbard model shows good agreement with experiment.

[1] J.A. Rostworowski, M.L.W. Thewalt and R.R. Parsons, Solid State Commun. 18, 93, (1976)

*Supported by the National Research Council.

14:30

BD5 Electron-Hole Droplets in Metallic Si(P).* R.R. Parsons, J.A. Rostworowski and B. Bergersen, Univ. of British Columbia -- The photoluminescent spectrum of phosphorus-doped silicon at dopant concentrations ranging from 1.2×10^{17} cm^{-3} to 4×10^{19} cm^{-3} is studied as a function of excitation power. Luminescent bands are attributed to recombination of carriers inside an electron hole droplet. Comparison is made between theoretical and experimental charge carrier densities and threshold energy as a function of dopant concentration.

[1] R.E. Halliwell and R.R. Parsons, Can. J. Phys. 52, 1336 (1974).

*Supported by the National Research Council.

14:45

BD6 Bound Excitons in Silicon.* M. Thewalt, G. Kirczenow, R.R. Parsons, Univ. of British Columbia -- The photoluminescent spectrum of excitons bound to neutral impurities is studied in silicon. The line widths of the phonon-assisted radiative transitions is explained in terms of the spatial extent of the complexes and the wavevector dependence of the phonon energies. The no-phonon line in Si(P) is beyond the resolution limits of our monochromator (0.075 meV.).

*Supported by the National Research Council.

15:00

BD7 Raman Study of Layered Crystals.* D.G. MEAD and J.C. IRWIN, Simon Fraser Univ.--The Raman spectra of a number of group IV (Zr), group V (Nb, Ta) and group VI (W) transition metal dichalcogenides have been investigated in the temperature region from 20 to 500 K. Discontinuities in the resistivity as a function of temperature have previously been observed[1] in several of these compounds and the results interpreted in terms of charge density waves. Raman spectra have been obtained from both the commensurate and incommensurate phases of several of these compounds and the temperature dependence of the vibrational structure studied. In particular spectra obtained from the incommensurate phase

of 1T-TaS_2 consisted of a featureless continuum. However upon transition into the commensurate phase below 190°K sharp phonon lines appeared in the spectrum. These results indicate the formation of a superlattice and several other compounds have been investigated for similar behaviour.

[1]J.A. Wilson, F.J. Di Salvo and S. Mahajan, Phys. Rev. Letters 32, 882 (1974).

*Work supported by the National Research Council of Canada.

15:15

BD8 Indices of Refraction of GaSe and GaS.* T.A. McMATH and J.C. IRWIN, Simon Fraser Univ.--The real parts of the ordinary and extraordinary indices of refraction of the birefringent (uniaxial) layer structure semiconductors GaSe and GaS have been measured in the wavelength range 4,000 to 10,000 Å. Two techniques were employed: the least deviation of various laser lines through small angle prisms with polarization either parallel or perpendicular to the crystal optical axis, and the determination of the wavelength and interference order of the fringes resulting from multiple internal reflections of white light in the thin parallel-sided samples. The results are compared to values previously obtained by other workers and in contrast to the measurements of Akhundov et al.[1] the crystals are unambiguously shown to be optically negative.

[1]G.A. Akhundov, S.A. Musaev, A.E. Bakhyshev, N.M. Gasanly, and L.G. Musaeva, Sov. Phys. Semicond. 9, No. 1, 94 (1975).

*Supported by the National Research Council of Canada.

15:30

BD9 Optical Transmission near the Fundamental Absorption edge in Cu_2O, J. M. Reyes and F. L. Weichman, Univ. of Alberta, Edmonton, Alberta.--Optical transmission in Cu_2O from 0.6 to 1μ was studied as a function of crystal growth conditions (oxygen partial pressure and temperature). Thermal quenching at high oxygen pressures produced an oxygen rich surface layer (CuO). The surface layer produced an apparent absorption edge at about 1.7 eV compared in the Cu_2O at ≈ 2.04 eV. The broad absorption band near the fundamental absorption edge of Cu_2O, normally attributed to a broad distribution of localized states or associated with the 0.7 and 0.8 μ luminescence centres, is shown to be largely due to this surface layer.

15:45

BD10 Optical Properties of Aggregated Noble Metal Films* VO-VAN TRUONG and G.D.SCOTT, Univ. of Toronto--The optical properties of aggregated gold, silver and copper films have been studied in the spectral range from 0.35 to 1.0 micron. In order to develop relatively large size aggregates of regular shape, the films were formed by evaporation on a hot substrate and annealed at 300°C. From the measurements of reflectance and transmittance, the effective optical constants of the aggregated films were calculated and compared with the values given by a rotational ellipsoid model. The particles forming the films are considered to be of the rotational ellipdoid shape and they behave like dipoles under the action of the applied field. Consequences of this theoretical model are discussed together with the influence of the substrate on the optical properties. Measurements of film structure parameters were also made and satisfactory agreement was obtained between theory and experiment for the filling factor and the average height of particles. Aspects of the film properties, when p-polarized incident light is used, are also discussed.

*Supported by the National Research Council of Canada.

16:00

BD11 Two-Phonon absorption Spectra of CdTe.* E. BATALLA, E.S. KOTELES and W.R. DATARS. McMaster U.--Far-infrared absorption spectra of CdTe were investigated at 15 K and 50 K using a high-resolution Fourier-transform spectrometer. Van Hove singularities were identified with the aid of two-phonon sum and overtone density-of-states curves calculated from a 14-parameter shell model. The parameters were taken from a fit to earlier neutron diffraction data. Many of the prominent features of the absorption spectra are assigned to pairs of phonons on the hexagonal face of the Brillouin zone while phonon pairs at Γ, X and L generally contribute only minor features to the spectra.

*Research Supported by the National Research Council of Canada.

16:15

BD12 Photoemission from Cu, Ag, and Au Valence Bands Using 32 - 280 eV Synchrotron Radiation.* J. STÖHR, F. R. MCFEELY, G. APAI, P. WEHNER, R. S. WILLIAMS, and D. A. SHIRLEY, Lawrence Berkeley Lab.--Photoemission from the valence bands of polycrystalline Cu(3d) and Ag(4d) was studied in the photon energy range 50 - 175 eV. Strong changes in the detailed shape of the spectra were observed in the region 50 eV ≤ hν ≤ 70 eV for Cu and 100 eV ≤ hν ≤ 150 eV for Ag. The photoexcitation cross-section for Ag 4d was studied in the range 32 ≤ hν ≤ 250 eV and is found to exhibit a pronounced Cooper minimum at hν = 140 eV. Angle-resolved photoemission from single crystals of Cu and Au(5d) was observed along the [100] and [111] directions for 32 eV ≤ hν ≤ 280 eV. Dramatic differences were found between the two directions and strong variations with energy were observed even above hν = 100 eV. The above results are discussed in terms of cross section effects arising from the angular and radial parts of the transition matrix element and/versus surface effects such as momentum broadening in the final state.

*Work performed at the Stanford Synchrotron Radiation Project (SSRP).

BD13

BD14

BD15

MONDAY, JUNE 14, 1976
ROOM 2B
Chairman: J.L. Brebner

13:30
BE1 Tunneling, Landau Level Spectra and Te Vacancy States in PbTe. D. C. TSUI and P. H. SCHMIDT, Bell Labs., Murray Hill, NJ 07974--The lack of carrier freeze-out in n-type PbTe has been explained by Parada and Pratt[1] as due to Te vacancies, contributing two electrons per vacancy without forming bound states in the energy gap. Each vacancy produces four doubly degenerate levels in the conduction band continuum, two of which may lie several tens meV above the band edge. We have studied the tunneling characteristics and the Landau level spectra of Au-PbTe tunnel junctions and found no evidence for any resonant levels within 70 meV above the conduction band edge. In this talk, we discuss these results and their relevance to the Te vacancy levels.

[1]N. J. Parada and G. W. Pratt, Jr., Phys. Rev. Lett. 22, 180 (1969).

13:45
BE2 Warm Electrons in Semiconductors. S. ZUKOTYNSKI and H. NAKAGAWA, University of Toronto. - The principal of equal a priori probabilities is used to deduce a trial function for the transport equation. The transport equation is solved and the distribution function for warm electrons is obtained. A comparison with experimental data for Ge and Si is carried out. It is found that for departures from ohms law of up to 40% the agreement between observed and calculated drift velocities is excellent.

14:00
BE3 Hall Mobility in Strontium Titanate at High Temperatures[1]. G. PERLUZZO and J. DESTRY, Université de Montréal. We report on an experimental investigation of Hall mobility in the polar semiconductor $SrTiO_3$, in the temperature range where thermal energies are comparable to the energies of the interacting phonon modes. We find, for all crystals measured, i.e. for charge densities from 9.6×10^{20} cm^{-3} to 4.1×10^{17} cm^{-3}, a mobility decreasing with increase in temperature for 300 K < T < 650 K, from ~ 5 cm^2 volt^{-1} sec^{-1} at room temperature to ~ 1.5 cm^2 volt^{-1} sec^{-1} at 650 K. A slight dependence of mobility on charge density is observed, in that the crystals with higher charge density have the higher mobility. Finally, we interpret our results in terms of existing large polaron transport theory.

1. Work supported by Le Ministère de l'Education du Québec and National Research Council of Canada.

14:15
BE4 High Pressure Dielectric Properties of $Pb(Zr,Ti)O_3$ Ceramics.* G.W. TIMCO and H.H. SCHLOESSIN, Dept. of Geophysics, U.W.O.-The dielectric constant, k, dissipation factor, D, and ferroelectric-paraelectric transition temperature, T*, have been measured as a function of temperature (20-300°C) in the pressure range 20-56 kbar for two ceramics of the donor doped PZT-5 series. Initial application of pressure results in a large decrease in k. For PZT-5H, T* decreased linearly at rates of -3.9, -4.1 and -4.6°C/kbar for the three samples studied. For PZT-5A, T* decreases non-linearly with a point of inflection in the T*-p curve at ~30 kbar. PZT-5H shows the typical k-T peak broadening with increasing pressure. In the case of PZT-5A, however, the k-T peak "sharpens" above ~30 kbar and becomes pressure insensitive at pressures >40 kbar. The initial large decrease in k is attributed to 90° domain reorientation relative to the direction of the maximum deviatoric stresses in the initial stage of non-hydrostatic stress distribution. The broadening of the k-T curves may be related to the distribution of residual microstresses inherited from the manufacturing processes.

*Supported by the National Research Council of Canada.

14:30
BE5 The Forward Current-Voltage Characterizations of Single Crystal Cu_2O-Cn diodes. K.T. CHEE and F.L. WEICHMAN, Univ. of Alberta.--The forward current-voltage characteristics of Cu_2O-Cu diodes, made from single crystal Cu_2O, were measured. When fitted to steady state SCL theory, it was found that, in general, two types of localized states must be postulated for Cu_2O: a) discrete localized energy states, usually associated with low resistivity ($\rho < 10^6$ Ω-cm) crystals b) a continuous energy level distribution of the localized states in higher resistivity ($\rho > 10^7$ Ω-cm) crystals. Vacuum annealling at high temperatures is used to control the resistivity of the Cu_2O through changes in defect concentration.

14:45
BE6 The relationship between iron content and the electrical conductivity of some North American micas. J. P. CRINE, M. R. WERTHEIMER and A. YELON, Ecole Polytechnique, Montreal. - The electrical conductivity σ of various North American micas has been measured at room temperature and electric field strengths ranging from 10^2 to 5×10^4 V cm^{-1}. All samples displayed ohmic behaviour under these conditions. It is shown that the conductivity varies with iron content, as reported earlier by Davidson and Yoffe[1]. However, this variation occurs over two very different regimes: a rapid rise in σ with % Fe below approximately 5%, and a much slower rise above this concentration. We find that σ varies exponentially with Fe^{3+} concentration; contrary to Davidson and Yoffe's suggestion, it appears to depend only weakly upon titanium content.

[1]A. T. Davidson and A. D. Yoffe, Phys. Stat. Solidi 30, 741 (1968).

15:00
BE7 Free Carrier Absorption in Tellurium S. ADES and C.H. CHAMPNESS, Electrical Eng. Dept., McGill Univ. --The variation of room temperature absorption coefficient α with wavelength λ has been determined between 4 and 20 microns in tellurium from measurements of transmittance and reflectance on single crystal samples. Above about 8 microns for $E \perp c$, a quadratic dependence on λ has been observed in intrinsic material, which is found to be consistent with the free carrier absorption theory of Schmidt.[1] With assumed values for the intrinsic carrier concentration, the electron-to-hole mobility ratio and the hole effective mass, comparison with the theory has yielded a room temperature effective mass ratio for electrons of 0.16. From measurements with $E \parallel c$ on a sample moderately doped with antimony, the hole concentration was estimated. This concentration, together with the deduced electron effective mass, was used to account for the measured values of α for $E \perp c$. Some preliminary experiments have also been carried out in tellurium on second harmonic generation produced by 10.6 micron radiation from a T.E.A. CO_2 laser. This will be briefly described.

[1]H. Schmidt, Zeit. f. Phys. 139, 433, 1954

15:15
BE8 Electrical Studies in the Reverse Direction of Te-Se-Cd Structures. M. EL AZAB and C.H. CHAMPNESS, Electrical Eng. Dept., McGill University--Electrical measurements have been made on Te-Se-Cd layer-structures in the reverse direction. The structures were fabricated with the selenium in the form of a monocrystalline film in the (0001) plane. A characteristic variation of the small signal differential capacitance, at fixed reverse bias, with frequency (in the range of a few cycles/sec to one megacycle/sec) was measured on several unformed samples with different chlorine content and prepared in slightly different ways. The observed characteristics could be explained by trapping effects in the space charge layer. A simple model which accounts for the observed results is presented and different parameters for the dominant traps are estimated. The trap density calculated according to the model is consistent with the measured variation of capacitance as a function of biasing voltage taken on the same samples.

15:30
BE9 Photovoltaic Effect in a Te-Se-CdO Structure M. ALTMEJD and C.H. CHAMPNESS, Electrical Eng. Dept., McGill Univ.--The photovoltaic effect has been studied in Te-Se-CdO layer structures containing a thin monocrystalline film of trigonal selenium. The structures were fabricated by first evaporating selenium on to a monocrystalline tellurium substrate maintained at 145°C and then depositing the counter electrode by reactive sputtering from a cadmium target in an atmosphere of 0.1 torr of argon with a trace of air. Examination of the counter electrode by reflection high energy electron diffraction has confirmed it to be CdO. Similar examination of the selenium film has confirmed its monocrystallinity. Open circuit voltage at high illumination was found to be about 0.5 volt, which is about the magnitude of the diffusion potential determined from differential capacitance measurements on the same structures. Measurements of the responsivity over the wavelength range 3,500 to 8,000 A have been carried out and the quantum efficiency determined.

15:45
BE10 Electronic Transport in $La_{1-x}Sr_xVO_3$ and $La_{1-x}Sr_xCrO_3$.* J. B. WEBB and M. SAYER, Queen's Univ. --A great deal of interest in the electronic properties of the highly conducting oxide ceramics has developed recently due to their possible technical application as electrodes in MHD generating stations. The perovskites such as lanthanum strontium vanadate and chromite, exhibit conductivities comparable with many of the metallic alloys to temperatures >2100K. The electrical conductivity of $La_{1-x}Sr_xVO_3$ ($0 \leq x \leq 0.4$) has been measured in the temperature range $160 \leq T \leq 1600$K. For small or zero values of x, the material behaves like a conventional impurity semiconductor with conduction resulting from the excitation of carriers from localised states 0.14 eV above the valence band edge. For values of $x > 0.05$, the conductivity is essentially determined by the strontium concentration with the mobility remaining essentially constant at $0.15 cm^2/V\text{-}s$. For $x > 0.2$ a metal-nonmetal transition of the Anderson type occurs. The conductivity of $La_{1-x}Sr_xCrO_3$ in the same temperature interval is given for comparison.

*Supported by the National Research Council.

16:00
BE11 Magnon Drag and the Thermopower of $(GeTe)_{1-x}(MnTe)_x$ Ferromagnetic Semiconductors* A. CAFARO and W.B. MUIR, McGill University.--In an effort to detect the magnon drag contribution to the thermopower of a degenerate ferromagnetic semiconductor a detailed investigation of the thermopower of two $(GeTe)_{1-x}(MnTe)_x$ alloys having x=0.01 and 0.05 has been made. These alloys order ferromagnetically[1] at 2.3 and 9°K respectively thus allowing thermopower measurements above and below the Curie temperature. After correction for phonon drag the data showed no trace of a change in the thermopower at the Curie temperature. This gives an estimated upper limit to the magnon drag thermopower of less than 0.2μV/°K in this material.

[1]R.W. Cochrane, M. Plischke and J.O. Ström-Olsen, Phys. Rev. B9, 3013, 1974.

*Supported by the National Research Council of Canada.

16:15
BE12 Electrical Resistivity of Aℓ-B Composites Between 78K to 400K. D. ABUKAY, K. V. RAO, S. ARAJS, and Y. D. YAO, Department of Physics, Clarkson College of Technology, Potsdam, N.Y. 13676.--The electrical resistivity (ρ) of composites of commercial Aℓ(6061)-B,* containing 60 volume % B fibers of diameter of 0.008 in., have been studied as a function of temperature (T) between 78 and 400K. The slope of ρ vs T curve is considerably large for the transverse (B fibers perpendicular to the electric current) than for longitudinal case. The results will be discussed from the viewpoint of existing theories for electrical conduction processes in composite materials.

* Materials obtained from Commonwealth Scientific Corporation, Alexandria, Va.

MONDAY, June 14, 1976
ROOM 2D
Chairman: G. Karl

13:30
BF1 Meson Decay Rates
P.J. O'DONNELL, *University of Toronto*

14:00
BF2 Symmetry Rearrangement and Vortex Solution
H. UMEZAWA, *University of Alberta*

14:30
BF3 The M.I.T. Model for Structure of Hadrons
K. JOHNSON, *M.I.T.*

15:00
BF4 A Suggestion Regarding Nuclear Forces. C. SHARP COOK, U. of Texas at El Paso.--I propose a nucleon model in which the forces of the nuclear interaction need not necessarily be short range, but can possibly have the same basic r^{-2} radial dependence found for gravitational and electrostatic forces, except that the nuclear interaction has a much larger force constant. The basis for this proposal is an assumption that the true nuclear force is not that which is observed external to a nucleon but is the force between the nucleon core and its meson cloud. The externally observed force is then shielded by the neutralizing effect of the meson cloud. In this form the true nuclear force could have its r^{-2} characteristics but still show a Yukawa-type potential or other appropriate potential external to the nucleon.

15:15
BF5 Pion Decay in a Simple Model.* L. RESNICK and J.H. KIM, Carleton U.-- The pion is considered a bound state due to strong interactions of a quark-anti-quark pair. The decays $\pi^0 \to \gamma\gamma$, $\pi^+ \to \mu^+\nu_\mu$ and $\pi^+ \to e^+\nu_e\gamma$ are calculated to lowest order in the weak and electromagnetic interactions, and compared with experiment.

* Supported in part by the National Research Council.

15:30
BF6 The New Scaling Hypothesis of Dao et al[1] and the Breaking of Feynman Scaling at Asympototic Energies.* R.J. YAES Memorial University of Newfoundland, Canada. We have shown that the assumption that scaling in the mean[1], KNO scaling, limited p_T and the slow rise of multiplicity with energy, all remain valid at asymptotic energies for which $p_L >> p_T, m$, leads to a scaling law for the inclusive distribution of the form $F(p_L,s) = \langle n\rangle \phi(\langle n\rangle x)$, $x = 2p_L/\sqrt{s}$, which is obviously inconsistent with ordinary Feynman scaling, $F(p_L,s) = f(x)$. Consequently it has been shown[2] that scaling in the mean could be used to explain the violation of Feynman scaling at x = 0 recently found at the CERN ISR.

*Work supported in part by the National Research Council of Canada.

[1] F. T. Dao et al, Phys. Rev. Lett. 33 389 (1974).
[2] W. Ernst and I. Schmitt, Bielefeld Preprint Bi-75/26.

15:45
BF7 Composite model of hadrons and Zweig-Iizuka rule M. BANDO, McMaster Univ.--A new composite model for hadrons is proposed. A hadron consists of certain number of constituent particles, which are described as relativistic independent particles moving in a central potential. Characteristic features of hadron decay phenomena are well explained in this framework.[1] Further we introduce a residual interaction between the constituent particles such that the PCAC treatment for hadron decays follows and also qualitative features of mass splittings of ps and V mesons are reproduced. The residual interaction is also constrained such that the Zweig-Iizuka rule for the case of the vector mesons follows. It turns out that this residual interaction leads to a considerable deviation from the Iizuka-Zweig rule in the case of the ps mesons. The decays of new particles will be investigated on this line of thought.

1) M. Bando, T. Kugo and S. Tanaka, Prog. Theor. Phys. 53 (1975), 544

M. Bando, S. Tanaka and M. Tova, Prog. Theor. Phys. 55 (1976), 169

16:00
BF8 Regge Model of A_1, A_2, and A_3 Meson Production in $\pi^\pm p$ Collisions. RICHARD A MORROW, Univ. of Maine.--For present purposes it is assumed that the A-mesons are produced as localized systems with well-defined quantum numbers, even though the A_1 and A_3 might not show all the characteristics of bone fide resonances. An attempt is then made to fit data on charged A_1, A_2, and A_3 production in $\pi^\pm p$ collisions for incident pion momenta in the range 10 to 40 GeV/c using a Regge pole model with Pomeron and degenerate f°-ρ exchanges. The Regge residues used are those extracted from a dual resonance model (B_6) and appropriately generalized to include abnormal couplings. Fits are made to the total cross sections, the t-distributions, and the spin-density matrix elements. It is found that a consistent treatment of all three reactions requires the Pomeron to be incoherent with the f°-ρ and to lie on a trajectory of small slope.

16:15
BF9 THE RULE $\Delta\vec{J}=1$ FOR DECUPLET PRODUCTION. M.G.DONCEL, P.MINNAERT and L. MICHEL I.H.E.S. 91440 Bures-sur-Yvette, FRANCE

Study of polarization effects is necessary for discovering simple and fundamental laws for the dependence on angular momentum transfer. In reactions of the type

$$0^- + 1/2 \to 1^- + 3/2$$

the angular momentum change of the baryon could be obtained both angular momentum transfers $\Delta\vec{J}=1$ and $\Delta\vec{J}=2$. We have analyzed all the published data on the 19 measurable polarization parameters between 3 and 13 Gev. We found that $\Delta\vec{J}=2$ is completly suppressed. We shall present our geometrical plots (proposed several years ago) for the data of the different published experiments

MONDAY, JUNE 14, 1976
ROOM 2E
Chairman: G.I.A. Stegeman

13:30
BG1 Superradiance and Optical Free Induction
L. MANDEL, *University of Rochester*

14:15
BG2 Mesure de la Fréquence de la Transition Hyperfine non Perturbée des Atomes de Rb^{85} M. TETU, R. FORTIN J.-Y. SAVARD et J. VANIER, Un. Laval. - La fréquence de la transition hyperfine des atomes de Rb^{85} libres a été mesurée à l'aide d'un maser à jet. L'inversion des populations est produite par pompage optique dans un ballon de stockage revêtu d'un enduit de parafine. La valeur obtenue est 3,035,732,441 ± 5 Hz. Les principales perturbations affectant cette mesure sont les déplacements de la fréquence dus à la lumière de pompage, à la désyntonisation de la cavité, à l'effet Doppler, au champ magnétique, aux interactions d'échange de spins et finalement aux interactions avec la paroi du ballon. Un autre résultat intéressant est la mesure absolue du déplacement de cette fréquence par les interactions que subissent les atomes de Rb^{85} avec une paroi de "paraflint". Le coefficient de déplacement mesuré est - 175 ± 25 Hz-cm à 72°C.

14:30
BG3 Effet de Paroi dans le Maser H et la Fréquence Hyperfine de l'Atome d'Hydrogène. Jacques VANIER, Robert LAROUCHE, Roger BROUSSEAU, Un. Laval. - Dans une première étape, on a mesuré le déplacement de la fréquence hyperfine de l'atome d'hydrogène dû aux collisions avec la paroi de teflon du ballon de stockage dans un maser H. On a mesuré la différence de fréquence Δf entre un maser H expérimental et un autre maser étalon. Trois ballons de diamètres différents ainsi que deux types de teflon (FEP 120, TFE 42) ont été utilisés dans le maser expérimental. On a ainsi déterminé la valeur absolue de l'effet de paroi du maser étalon. Dans une seconde étape, la fréquence d'un oscillateur à quartz, asservie en phase au signal du maser étalon, a été mesurée par comparaison aux signaux de la chaîne de navigation LORAN C contrôlée par des étatons atomiques au césium. Une mesure sur dix jours, à une précision de l'ordre de 0.5 μsec, donne une exactitude de $\pm 5 \times 10^{-13}$. La fréquence hyperfine obtenue est 1,420, 405,751.772 ± 0.002. Ce résultat est en accord avec d'autres résultats publiés. Les différentes sources d'erreurs et corrections appliquées sont examinées en détails. D'autres approches de mesures pouvant donner plus de précision sont discutées.

14:45
RG4 L'aspect Fréquence dans un Système à Trois Niveaux. G. BUSCA, Un. Laval.- On dérive des équations générales pour les populations et les cohérences dans un système à trois niveaux soumis à deux perturbations cohérentes. Dans le cas d'une double résonance optique-microonde et pour lumières de faible intensité, on trouve le "light-shift" ordinaire. Pour des raies optiques saturées la courbe du gain de la raie microonde montre un minimum qui est fonction de la fréquence d'excitation optique. On étudie l'application de ses effets au transfert de la stabilité de fréquence. On présente aussi des résultats expérimentaux relativement à une expérience de double résonance microonde-radiofréquence: l'effet Zeeman dans le maser au Rb^{87}.

15:00
BG5 Fluorescence and Transmission of Chlorophyll A Excited by a Q-Switched Ruby Laser.* P.ARSENAULT and M.M. DENARIEZ-ROBERGE, LROL, Laval Univ. -- An evaluation of the chlorophyll two-photons cross-section σ_{02} at 6943 Å was deduced from an antistoke excitation of its fluorescence as already described by Herman et al.[1] and Danilov et al.[2]. But their initial formula giving the variation of the fluorescence intensity as a function of the laser excitation intensity has been modified for taking into account the important singlet-triplet energy transfer . We obtained $\sigma_{02} = 1.26 \cdot 10^{-43} cm^4/sec$. This high value may be justified by resonance effects. An estimation of the absorption cross-section from the first excited singlet is also obtained from transmission measurement à 6943 Å as a function of the laser intensity. We find σ_{12} of the order of $1.26 \cdot 10^{-16} cm^2$.

[1] J.P. Herman and J. Ducuing. Opt.Commun., 6, 101(1972).
[2] V.V. Danilov, Y.T. Mazwenko and S.I. Vorontsova. Opt. Commun., 9, 283 (1973).

* Supported by the National Research Council of Canada.

15:15
BG6 Tunable UV-radiation produced by stimulated Raman scattering.* H. MENNICKE, J. MEYER and T. SINNOTT, Univ. of British Columbia.-- High order anti-Stokes Raman lines can be produced by irradiation of liquid nitrogen with the focused beam of a giant pulse ruby laser. By mixing the ruby light with that of a tunable dye laser tunable anti-Stokes lines have been produced. In the case the ruby light pumps the molecules into the first vibrational level, while the dye laser stimulates the anti-Stokes transitions.

15:30
BG7 Experimental Study of some Rapid Relaxation in HITC*. M.M. DENARIEZ-ROBERGE, G.NIYONIZEYE et L.TURGEON Univ. Laval. - Rapid relaxations in HITC were measured in different solvents by two different approaches. In our first set up, delay between absorption of a mode-locked ruby laser light and emission were measured with the help of a delay line and an optical Kerr effect obturator . The delay was found to vary as the cubic root of the solvent viscosity. In the second experiment, recovery time of the absorption after saturation was tested. The saturation was obtained by a single pulse of a mode-locked ruby laser. Variation of the transmission with time is then probed with a low energy beam and a variable delay. Only incident pulses of about the same energy are considered. In some solvents, as acetone, absorption from excited states is found to be important during the duration of the mode-locked pulse.

* Supported by the National Research Council of Canada and the Defence Research Establishment.

15:45
BG8 Multiphoton Excitation Processes Between Vibrational States of Molecules. V.E. MERCHANT and N.R. ISENOR, Univ. of Waterloo.--An approximation method has been developed to evaluate the perturbation theory expressions for the probabilities of two and three photon transitions amongst low-lying vibrational levels of diatomic and polyatomic molecules. The sum over intermediate rotational states is performed for a general case and the sum over intermediate vibrational states for a few particular cases. It is shown that two and three photon processes should be observable with available infrared lasers. The accuracy of the calculation is limited by the lack of reliable data for electronic transition dipole moments.

MONDAY, JUNE 14, 1976
ROOM 1A
Chairman: E. Gaucher

13:30
BH1 Vertical Loop EM vs Horizontal Loop EM under Canadian Precambrian Conditions, J.S. DOWSETT - Both vertical and horizontal loop EM techniques have been used in both detailed ground electromagnetic surveys and as a follow-up tool to airborne electromagnetic surveys for many years in the search for massive sulphide deposits in the Precambrian of Canada. This paper presents one view of the criteria utilized in selecting the techniques to be used.

13:45
BH2 The Application of EM Methods in Mining Drill Holes, A.V. Dyck - An extensive testing and evaluation program has been carried out by the Geological Survey of Canada in cooperation with several mining companies. All available borehole EM systems have been tested at a variety of sites throughout Canada, together with borehole IP and magnetometer equipment. A number of practical problems were encountered; however the data collected shows that borehole EM systems are capable of detecting ore zones lying as much as one hundred feet from the hole. In conclusion, borehole EM surveys can contribute significantly to an exploration program.

14:00
BH3 Geoprove EMR-14: A new Multi-spectral E.M. System for Determining Stratification of the Ground, MRINAL K. GHOSH, Geoprobe Ltd., - GEOPROBE EMR-14 is a fourteen-channel ground E.M. system for applications in determining (small scale and large scale) stratification of the ground. This system covers a frequency range of 5Hz to 45,000 Hz. This system consists of a portable transmitting station and a portable receiving station There is no physical cable connection between them. Ground stratification may be investigated from a depth of 10 feet to 4,000 feet. Presence of up to four layers in the ground may be identified. Exact thickness and real electrical conductivities of the layers are estimated using GEOPROBE EMR-14 system. Test results obtained using this system have been confirmed by drillings. Applications of GEOPROBE EMR-14 are very broad. Primary applications are detection of geothermal energy resources, ground-water reservoirs, and shallow oil and gas reservoirs, determination of overburden thicknesses, depth of basement complexes, thickness of permafrost layers, etc.

14:15
BH4 Electromagnetic Non-Contacting Ground Conductivity Mapping J.D. McNEILL, Geonics Limited The theory and some case-histories are presented for an inductive electromagnetic technique for determining terrain conductivity to depths of approximately 50 meters. Ground probes are not required & virtually any type of terrain can be rapidly surveyed by a one or two man crew, depending on the depth required. The technique uses a dipolar transmitter and receiver with intercoil spacing chosen so that the resultant induction number is much less than unity. The instruments read conductivity directly, and the penetration depth is determined by the intercoil spacing over a wide range of terrain conductivity.

14:30
BH5 Applications des mesures EM transitoires. Y. LAMONTAGNE, Univ. de Toronto-- On a étudié l'utilité des mesures EM sur une grande gamme de fréquences (30 Hz à ~ 10 kHz) au moyen d'un systeme spécialement conçu (UTEM) qui mesure les champs magnétique et électrique. L'onde simple (triangulaire) émise et l'échantillonnage logarithmique produisent des données simples à interpréter. On reconnait les conducteurs simples tels que dykes, sphères, blocs, etc.., autant par la manière dont leur anomalie décroit dans le temps que par sa forme en plan. Les cas plus compliqués dus à la présence d'uneroche encaissante, zone ou mort-terrain conducteurs autour d'un excellent conducteur se reconnaissent aux modifications typiques qu'ils produisent au début de la réponse transitoire. Dans les cas de sondage vertical, on a pu trouver directement, par ordinatrice, les modèles stratifiés qui satisfont les données. Certaines mesures de terrain montrent que des effets de polarisation provoquée accompagnent souvent la réponse EM des conducteurs métalliques, surtout celle du champ électrique. Il semble que ces effets de PP soient causés par la circulation de courants induits d'un conducteur métallique à un conducteur électrolytique voisin.

14:45
BH6 Electromagnetic Induction via a Magnetometer Array in a Tectonically-Active Region of Quebec: Preliminary Results. P.A. CAMFIELD, Energy Mines and Resources.--In summer 1975, Earth Physics Branch operated an array of 23 borrowed Gough-Reitzel geomagnetic variometers in the Saguenay-Parc des Laurentides area north of Quebec City. The object was to study the crustal and upper mantle electrical conductivity in this region of relatively high seismicity and rapid downward crustal movement. Visual inspection of magnetograms of substorms and shorter-period events recorded simultaneously across the array does not appear to detect effects due to order-of-magnitude lateral conductivity contrasts reported by Bailey et al.[1] Such contrasts would thus have to be considerably more than one order of magnitude to perturb magnetograms. Contour maps of Fourier coefficients of the time series and transfer functions will be used to separate anomalous fields due to internal currents from the large external source fields.

[1]Bailey, Edwards, Garland, Kurtz and Pitcher, J. Geomag. Geoelectr. 26, 125-146 (1974).

15:00
BH7 Radar Probing of Salt Rock, R. R. Unterberger - The author has done several mapping surveys in salt mines using radar waves. He will speak about them and outline further applications of the technique.

15:15
BH8 An Analogue Model Study of Electromagnetic Induction for Islands Situated Near a Coastline. W. NIENABER, H.W. DOSSO, Univ. of Victoria, L.K. LAW, Dept. of Energy, Mines and Resources, Victoria, and F.W. JONES and V. RAMASWAMY, Univ. of Alberta - The behavior of time varying electromagnetic fields near an island situated in a shallow ocean is investigated using a scaled analogue model. To examine the effect of the shape of the island, square and circular island models are used. To study the effect of a coastline, various model island-coastline distances are treated. Electric and magnetic field components for various traverses over the islands and coastline are presented.

MONDAY, JUNE 14, 1976 PLASMA PHYSICS SYMPOSIUM
ROOM 2F
Chairman: T.W. Johnston

13:30
BI1 High Density Operation of Alcator
J. HELAVA, *M.I.T.*
Operation of Alcator has extended to a peak density of 6.6×10^{14} cm^{-3} at a toroidal field of 75 kG. The energy replacement time, $\tau_E = \frac{3}{2} \langle nK (T_i - T_e) \rangle$. plasma volume/VI, over the operating range has been found to be proportional to n, with a weak dependence on q and no explicit dependence on I or B_T. Operation at high density is made possible by: (1) production of a sufficiently clean vacuum and wall conditions to permit $Z_{eff} \lesssim 1$; and (2) the high value of ohmic heating power density permitted by the large value of B_T/R. Thus, the density limit can be increased only by a further increase of current at constant q. The discharges obtained at the highest densities are characterized by: (1) the plasma being opaque to energetic neutrals; (2) the electrons and ions nearly in equilibrium; and (3) the energy confinement time roughly in numerical agreement with neoclassical theory. Thus we obtain a new regime of tokamak operation. In addition to discussion of the confinement time and density limit, we will discuss measurements of the impurities and effective Z.

14:45
BI2 Turbulent Heating of a Large Toroidal Plasma
H. SKARSGARD, *University of Saskatchewan*

15:00
BI3 Ion Induced Pinching and Intense Ion Currents
S. GOLDSTEIN, *University of Maryland*

In the past few years modeling of electron and ion flow pattern in large aspect ratio diodes has advanced to the stage of finding self-consistently two dimensional solutions, uniquely defined by the physical boundary conditions of the diode. The solutions are used to construct a physical model of the time dependent evolution of electron and ion flow using four distinct phases:
(1) Electron flow at low voltages (re-examination of the Child Langmuir theory and correcting it for self magnetic field effects)
(2) The weak pinch phenomenon at high voltages
(3) Collapsing of the weak pinch due to time dependent ion emission from the anode leading to very tight pinch formation.
(4) Steady state pinched electron flow and enhanced ion current.
Using this model,[1] most of the experimental data[2] may be explained. In addition the model predicts that the ion current is enhanced by the aspect ratio R/D (R - cathode radius, D - anode cathode gap) over the Langmuir bipolar prediction. Recent experiments[3] are in agreement with the theoretical predictions. For large aspect ratio diodes the proton current may thus be larger than the electron current. A scheme is presented for the spherical focusing of these large ion currents for pellet irradiation with spherical symmetry. Preliminary experiments indicate that electrons do pinch in spherical diodes.

[1] Shyke A. Goldstein and Roswell Lee, Phys. Rev. Lett. 35, 1079 (1975).
[2] A. E. Blaugrund and G. Cooperstein, Phys. Rev. Lett. 34, 461 (1975).
[3] A. E. Blaugrund, G. Cooperstein, J. R. Boller and S. A. Goldstein, Bull. Am. Phys. Soc. 20, 1252 (1975).

15:45
BI4 Mixing and Stimulated Scattering of Light in Plasmas and Other Refractive Media
J. MEYER, *University of British Columbia*

MONDAY, JUNE 14, 1976 NUCLEAR EXPORTS AND NUCLEAR WASTE MANAGEMENT
ROOM 1112 Pavillon Pouliot
Chairman: H.R. Glyde

20:00
BJ1 The Nuclear Industry, Nuclear Proliferation and International Approaches to Control
T. GREENWOOD, *Political Science, M.I.T.*

20:45
BJ2 Canadian Nuclear Export Sales Policies
M. DUPUY, *Canada Department of External Affairs*

21:30
BJ3 Nuclear Waste Management
P.E. HAMEL, *Atomic Energy Control Board, Ottawa*

TUESDAY, JUNE 15, 1976
ROOM 1B
Chairman: W.J. MacDonald

9:00
CA1 Half-Off-Shell t-Matrix Elements for a Class of Equivalent Potentials. B. RAM and J. SHIRLEY, New Mexico State Univ.--Given a central hard-core local potential V(r) we construct a variety of energy-dependent potential functions of the form V(E,r) = V(E)f(r); each of these, when used in the S-wave Schroedinger equation reproduces for c.m. energy E $\leq$ 70 MeV, the total scattering cross-section $\sigma(E)$ produced by V(r) when used in the Schroedinger equation in all partial waves. These potentials are all equivalent for two-body total scattering. We then compare half-off-shell t-matrix elements for these potentials. We do this for two shapes of potentials--hard core square well, and exponential--which are pertinent to Λ-N scattering. A major purpose is to later use these potentials in nuclear matter calculations to determine the extent to which off-shell effects are important.

9:15
CA2 Polarization in the ^{6}Li (^{3}He,p) ^{8}Be reaction * M. IRSHAD, C. RIOUX, J. ASAI, R. PIGEON and R.J. SLOBODRIAN, Laboratoire de Physique Nucléaire, Département de Physique, Université Laval, Québec G1K 7P4, Canada. Angular distributions of proton polarization and differential cross section have been measured for the reaction ^{6}Li (^{3}He,p) ^{8}Be leading to the ground and the first excited states in ^{8}Be. The measurements were made at a ^{3}He incident energy of 14 MeV. The measurement of proton polarization were accomplished using the silicon polarimetry facility at Université Laval [1]. The results have been compared with the predictions of distorded-waves theory. DWBA calculations using spectroscopic amplitudes obtained from shell model wave functions generated from two-body matrix elements of Cohen and Kurath [2] pertaining to 1p-shell are not able to account for the measurements.

*Work supported in part by the Atomic Energy Control Board of Canada and the Ministry of Education of Québec.

[1] M. Irshad, S. Sen, R. Pigeon and R.J. Slobodrian, Fourth International Symposium on polarization Phenomena in Nuclear Reactions, Zürich 1975.

[2] S. Cohen and D. Kurath, Nucl. Phys. 73, 1 (1965).

9:30
CA3 Tensor Analyzing Power Measurements in the ^{40}Ca(d,α)^{38}K Reaction at 0°. D. T. PETTY, P. G. IKOSSI, J. A. KUEHNER and J. SZUCS, McMaster Univ.--The tensor analyzing power near 0° was measured in the ^{40}Ca($\vec{d}$,α)^{38}K reaction at incident beam energies of 7.5, 7.75 and 8.0 MeV. The alpha particles from the reaction were momentum analyzed with an Enge split-pole magnetic spectrograph and detected on the focal plane with a position-sensitive gas proportional counter. With this system, a resolution of about 20 keV was obtained. States in ^{38}K from 1.7 to 4.0 MeV in excitation were observed and are assigned either natural or unnatural parity depending on the values of T_{20}.[1]

[1] J.A. Kuehner, P.W. Green, G.D. Jones and D.T. Petty, Phys. Rev. Lett. 35, 423 (1975).

9:45
CA4 Analysis of ^{130}Te(p,p$_1$) on Analog Resonances. J.L. FOSTER, R., Univ. de Sao Paulo, Brazil, T.V. RAGLAND, Purdue Univ., Lafayette, Indiana, and J.P. MARTIN, L. LESSARD* and S. GALES†, Univ. de Montreal, Canada.--Analysis of cross-section and polarization measurements to proton inelastic scattering on isobaric analog resonances in the ^{130}Te+proton system is carried out through the addition of a resonant scattering matrix to a coupled channel scattering matrix using program JUPITOR[1]. Neutron orbital coupling to the 2^+ state in the wave functions of the parent states in ^{131}Te is thus determined.

1 T. TAMURA, Rev. Mod. Physics 37 (1965) 679, ORNL 4152 unpublished.

* Foster Radiation Laboratory, McGill Univ., Montreal, Canada.

† Institut de Physique Nucleaire, Orsay, France.

10:00
CA5 ft-Values of T=1/2 Mirror Nuclei.* G. AZUELOS and J. KITCHING, McGill University.--Precision measurements have been performed of the half-lives and branching ratios of most of the T=1/2 mirror beta decays. The differences between the Gammow-Teller and the isoscalar magnetic moment matrix elements have been calculated on a shell model basis for decays up to the end of the sd shell. The possibility of extracting the axial-vector coupling constant in nuclei on the basis of these results is discussed.

*Work supported by the Atomic Energy Control Board.

10:15
CA6 The Density Expansion of the Kinetic Energy.* M. BRACK, S.U.N.Y. at Stoney Brook and B. K. JENNINGS, McMaster Univ. - For a uniform fermi gas the kinetic energy density goes as the spatial density, ρ, to the five-thirds power. For an inhomogenous gas correction terms must be added. Within an extended Thomas-Fermi model we derive corrections which include not only a Weizsäcker-like term but also further correction terms. This expression for the kinetic energy, τ, is:

$$\tau = \frac{\hbar^2}{2m}\int d^3r \left\{ \frac{3}{5}(3\pi^2)^{2/3}\rho^{5/3} + \frac{(\nabla\rho)^2}{36\rho} + \frac{\rho^{1/3}}{6480(3\pi^2)^{2/3}} \left[8\left(\frac{\nabla\rho}{\rho}\right)^4 - 27\left(\frac{\nabla^2\rho}{\rho}\right)\left(\frac{\nabla\rho}{\rho}\right)^2 + 24\left(\frac{\nabla^2\rho}{\rho}\right)^2 \right] \right\}.$$

The validity of this expression is discussed using specific examples.

*Work supported in part by National Research Council of Canada.

10:30
CA7 The Influence of Virtual Δ States on the Binding Energy of Nuclear Matter.* Y. NOGAMI, McMaster U.-- Several authors have examined the effect of virtual Δ (1236) states on the saturation properties of nuclear matter within the framework of lowest-order Brueckner theory.[1-3] It has been found that the inclusion of Δ does not change the usual tendency of the saturation points to lie in a narrow band in the energy-density plane that does not contain the empirical saturation point. At the normal density, the binding energy is reduced by the Δ-effect by several MeV. On the other hand basically the same problem has been investigated through the three-body force which arises due to virtual Δ states. Recently, Grange et al[4] have shown in the latter approach that the Δ-effect increases the nuclear matter binding, although only by about 1 MeV or less. We will clarify the nature of the difference between the two approaches. The difference

stems from the treatment of three-body correlations.

*Supported by the National Research Council of Canada

[1] B.D. Day and F. Coester, Preprint
[2] T.K. Dahlblom and L.E.W. Smulter, Preprint
[3] A.M. Green and P. Haapakoski, Nucl. Phys. A 221 (1974) 429.
[4] P. Grange et al, Phys. Letters 60B (1976)237.

10:45

CA8 Investigation of the Reorientation Effect in ^{76}Se and ^{80}Se. R.LECOMTE, J.BARRETTE, M.BARRETTE, G.LAMOUREUX, P.PARADIS, and S.MONARO, Lab.de Phys. Nucl., Université de Montréal. -- Measurements of the Coulomb excitation probabilities of the first 2^+ states in ^{76}Se and ^{80}Se have been made with ^{4}He and ^{16}O projectiles. The measurements yield for Q_{2+} and $B(E2;0^+ \rightarrow 2^+)$: (-0.34 ± 0.07)e b or (-0.15 ± 0.07)e b and $(0.422 \pm 0.005)e^2b^2$ for ^{76}Se; $(+0.32 \pm 0.07)$e b or $(+0.51 \pm 0.07)$e b and $(0.238 \pm 0.004)e^2b^2$ for ^{80}Se. The first Q_{2+} values are for constructive interference, the second values are for destructive interference. The different sign of Q_{2+} in ^{76}Se and ^{80}Se is a clear evidence for a prolate to oblate shape transition in these nuclei. This is in disagreement with recently published data on the Se nuclei [1,2]. Preliminary measurements on ^{78}Se and ^{82}Se indicate that the shape transition occurs in ^{78}Se with 44 neutrons.

1) S.L.Heller and J.N.Friedmann, Phys.Rev. C10, 1509 (1974).
2) U.Ardouin et al., Phys.Rev. C12, 1745 (1975).

11:00

CA9 Investigation of the Reorientation Effect in ^{94}Mo, ^{96}Mo, ^{98}Mo, and ^{100}Mo.
P. PARADIS, G. LAMOUREUX, R. LECOMTE, and S. MONARO, Lab. de Phys. Nucl., Université de Montreal. -- Thin targets of ^{94}Mo, ^{96}Mo, ^{98}Mo, and ^{100}Mo have been bombarded by 8 MeV alpha-and 36.0 (or 36.5) MeV ^{16}O particles. The Coulomb excitation of the first 2^+ levels was observed by resolving the elastically and inelastically backward scattered particles in four surface barrier detectors placed at $\pm 157.5^\circ$ and $\pm 172.5^\circ$. The results are: $B(E2, 0^+ \rightarrow 2^+)$ in e^2b^2 units (0.196 ± 0.003) (^{94}Mo); (0.270 ± 0.004) (^{96}Mo); (0.266 ± 0.005) (^{98}Mo); and (0.511 ± 0.009) (^{100}Mo). The Q_{2+} values, in barns, are: (-0.13 ± 0.08) or $(+0.01 \pm 0.08)$; (-0.20 ± 0.08) or $(+0.04 \pm 0.08)$; (-0.20 ± 0.09) or $(+0.16 \pm 0.09)$; and (-0.42 ± 0.09) or (-0.10 ± 0.09). The first values are for constructive interference and the second values are for destructive interference.

11:15

CA10 Exchange in the Optical Model*. N.E. DAVISON and F. VOSNIAKOS, Cyclotron Lab. Univ. of Manitoba--Existing proton elastic scattering data for ^{16}O, ^{40}Ca and ^{208}Pb at several proton energies have been analyzed for evidence that exchange plays an important role in the optical description of elastic scattering. Data were analyzed with an optical model in which the real central and absorptive potentials are multiplied by terms of the form $1+C_L(-1)^\ell$ which simulates exchange[1] coefficients C_R (for real central potential) and C_I (for absorptive potential) are adjustable parameters which determine the strength of the exchange. Significant improvements in the fits to the data are obtained, but the parameters C_R and C_I have a complex dependence on incident proton energy.

[1] G.W. Greenlees et al, Phys. Rev. C6, 2057 (1972).

* Supported by the AECB of Canada.

11:30

CA11 Proton Elastic Scattering From ^{24}Mg. D. HASELL, N.E. DAVISON, B. MURDOCH, A.SOURKES and W.T.H. van OERS, Cyclotron Lab. Univ. of Manitoba--Existing values of the energy dependence of optical parameters suggest that there may be significant variations from nucleus to nucleus. In order to extend the study of energy dependence to other nuclei differential cross section angular distributions for proton elastic scattering from ^{24}Mg have been measured at incident proton energies from 20.0 to 45.0 MeV in 50 MeV steps. Data were collected in 2.5° steps at forward angles and in 5.0° steps at backward angles. Uncertainties in the relative cross sections less than 2%. Data have been analyzed using a standard optical model and the energy dependences of the optical model parameters have been extracted. Results are compared with those obtained for other nuclei.

* Supported by the AECB of Canada

11:45

CA12 Total Proton Reaction Cross Section for Ti and B Between 20 and 50 MeV. T.N. NASR, A.M. SOURKES, W.T.H. VAN OERS, Cyclotron Lab., Department of Physics, Univ. of Manitoba. Using a variation of the standard attenuation technique[1] and a tightly collimated and momentum analyzed proton beam, total reaction cross sections, σ_R, were measured for Ti and B, each at eight incident proton laboratory energies between 20 and 50 MeV at the University of Manitoba Cyclotron Laboratory. The Ti cross sections are presented along with existing reaction data[2] and compared with optical model predictions for σ_R obtained from analyses of differential-elastic and total reaction cross section data for titanium. The B data are compared with σ_R of the nearby elements Be and C[3]. The B and Ti results are also compared to predictions of the opaque-nucleus model.

1. R.F. Carlson et al, Nucl. Instr. Methods 123, 509 (1975)
2. J.J.H. Menet et al, Phys. Rev. C4, 1114 (1971); J.F.Dicello et al, Phys. Rev. 157, 1001 (1967).
3. R.F.Carlson et al, Phys. Rev. C10, 2237 (1974).

12:00

CA13 Isomeric Cross Sections for 14.8 MeV Neutrons in Medium and Heavy Mass Nuclei.*† G. N. SALAITA and S. L. SOTHRAS, Southern Methodist U.--The cross section for the production of isomeric states via the (n,p) and (n,2n) reactions in Selenium Rubidium, Palladium, Barium, Cerium, Neodymium, Samarium, Erbium, Rhenium and Platinum at 14.8 MeV neutrons were measured. Isomeric activities with half lives in the seconds range were studied using the cyclic activation technique. Long lived isomeric and ground state activities were investigated through conventional activations method using Ge(Li) detector γ-ray spectroscopy. Monitors of known cross section values and with half lives close to activities under investigation were used. The present cross section values for ^{139m}Ce and ^{141}Nd are in excellent agreement with the more recent precise data[1]. For ^{168}Er(n,2n)^{167m}Er only one measurement has been reported. The cross sections for the reactions ^{135}Ba(n,2n)^{137m}Ba and ^{185}Re(n,p)^{185m}W given here, to our knowledge, have been reported for the first time.

*Submitted by JEFF D. CHALK, III
†Work supported by the Robert A. Welch Foundation

[1] S.M. Qaim, Nucl. Phys. A224, 319(1974).

TUESDAY, JUNE 15, 1976 — ELECTROEXCITATION SYMPOSIUM
ROOM 2A
Chairman: J.D. Carette

9:00
CB1 Recent Experiments with Electrons Plus and Minus
D.A.L. PAUL, *University of Toronto*

9:45
CB2 Apparent Oscillator Strength Densities from the Electron Energy Loss Measurements
R. HUEBNER, *Argonne National Laboratory*

10:30
CB3 Les spectres des états électroniques des atomes mesurés par électroionisation
P. MARMET, *Université Laval*

11:15
CB4 Low Energy Electron Impact Excitations of Atoms
R.K. NESBET, *IBM Research Laboratories, San Jose, California*

TUESDAY, JUNE 15, 1976 — STRUCTURE AND EXCITATIONS OF MONOLAYER FILMS
ROOM 1C
Chairman: ~~J.G. Dash~~ M.B. Webb

9:00
CC1 Leed Investigations of Noble Gas Films
M.B. Webb, *University of Wisconsin*

9:45
CC2 Elastic and Inelastic Neutron Scattering From Monolayers
L. PASSELL, *Brookhaven National Laboratory*

10:30
CC3 Phase Changes in Nitrogen Monolayers
G.A. STEWART, *University of Pittsburgh*

Precision heat capacity measurements provide an effective probe for examining the existence of phase changes in heavy gas monolayers which adsorb at temperatures near 100K. When used in combination with vapor pressure measurements, heat capacity experiments (a) locate the phase boundaries and (b) determine whether the associated transition is first or higher order. The combined use of these thermal techniques will be discussed for a variety of monolayer transitions and will be illustrated for the particular case of nitrogen adsorbed on exfoliated graphite where a transition corresponding to loss of registry with the hexagonal basal plane has been observed using neutron diffraction[1]. The thermal studies[2] indicate that this nitrogen transition is of higher order (no latent heat) and suggest that it may be of the classical second order type. Specifically, the constant area heat capacity exhibits an abrupt drop near 80K. Such a heat capacity signature at constant area cannot uniquely specify the transition order but with ancillary vapor pressure information a first order transition (coexisting phase) appears ruled out. Evidence for the existence of similar transitions in heavy noble gas monolayers will be discussed.

1. J. K. Kjems, et al., Phys. Rev. B13, 1446 (1976).
2. D. M. Butler, et al., Phys. Rev. Lett. 35. 1718 (1975).

11:15
CC4 The Registered Phases of Helium Monolayers
C. CAMPBELL, *University of Minnesota*

TUESDAY, JUNE 15, 1976
ROOM 2B
Chairman: A.T. Stewart

9:00
CD1 Deviations from Matthiessen's Rule in Cold-worked Aluminum Alloys* J. A. ROWLANDS and S. B. WOODS, Univ of Alta.--Previous electrical resistivity measurements[1] on cold-worked pure Al in the temperature range 1-30K showed that a decrease in the temperature dependent resistivity is sometimes associated with an increase in the the residual resistivity, ρ_o, brought about by cold-work. The explanation for these results, or indeed for the general behaviour of Al alloys,[2] is not clear. Measurements on alloys in various stages of cold-work and with ρ_o =71 and 200nΩ cm when annealed have been made. These new results will be discussed in light of the various scattering mechanisms in Al.

[1]J A Rowlands and S B Woods, J. Phys. F. 5, L100 (1975)
[2]A D Caplin and C Rizzuto, Aust. J. Phys. 24, 309 (1971)

*Supported, in part, by the National Research Council of Canada.

9:15
CD2 Resistance Minima in Pd-Pt Alloys*. J. A. ROWLANDS and S. B. WOODS, Univ of Alta.--The electrical resistivity of Pd-Pt has been measured[1] for several concentrations and was found to have some unexpected features, the most interesting of which was a barely resolved minimum at ~ 3K in a Pd-43at%Pt alloy. The suggested explanation was a temperature dependent impurity resistivity rather than the Kondo effect. The precision offered by a new resistance bridge[2] has permitted us to make a more systematic study of these minima below 20K. Resistors made from these alloys show exceptional promise as stable, thermoelectric-free low-temperature comparison standards.[3]

[1]P Blood and D Greig, J.Phys.F. 2, 79 (1972)
[2]R P MacMartin and N L Kusters, IEEE IM-15, 212 (1966)
[3]J A Rowlands and S B Woods, J.Sci.Instrum. (Submitted)

9:30
CD3 The de Haas-van Alphen Phase in Zn Needles. P. L. LI and B. E. PATON, Dal. Univ. - The Lifshitz-Kosevich (LK) formula of de Haas-van Alphen effect (dHvA) predicts that the absolute amplitude is proportional to $\left(\frac{\partial^2 S}{\partial k_{\parallel}^2}\right)^{-1/2}$ and the phase is $\pi/4$. Fourier analysis has been applied to the torque measurement in the Zn needle Fermi surface. The experimental results indicate that the dHvA phase is independent of field as LK predicted. However, when the magnetic field is near to the c-axis, the dHvA phase is significantly smaller than the LK value. When the magnetic field is tipped away from the c-axis, i.e., $\theta \simeq 50^0$, the dHvA phase agrees with the LK value of $\pi/4$. This new information supports the model proposed by Stark[1] for the monster arm and needle regions of the Fermi surface. The absolute amplitude may contain an additional term $\left(\frac{\partial^4 S}{\partial k_{\parallel}^4}\right)$ and the phase will then be between $\pi/4$ and $\pi/8$ which is consistent with the experimental results.

[1]R. W. Stark, Phys. Rev. 135A, 1698 (1964).

9:45
CD4 Waveshape Analysis of the Zinc Needle Oscillations using the Fast Fourier Transform. W. A. ROGER, P. L. LI, B. E. PATON, A. M. SIMPSON, Dal. Univ. - Quantum oscillations from the needle orbit in zinc have been measured in the de Haas-van Alphen (dHvA) torque and the ultrasonic velocity. Harmonics were separated and individually regenerated using the fast Fourier transform, without knowledge of the parameters in the LK formula. The Dingle temperature, breakdown field H_0, effective g-factor, and dHvA phase were determined from the regenerated data by the usual method. It was found that the effective g-factor differed from previously reported[1] values, and the experimental dHvA phase was less than the theoretical value when the field was near [0001].

[1]W. J. O'Sullivan and J. E. Schirber, Phys. Rev. 162, 519 (1967); g = 170.

10:15
CD5 g-Factor Measurements in Sb Using the de Haas-van Alpen Effect* P. H. HILL and J. VANDERKOOY, Univ. of Waterloo--The dHvA effect in Sb observed by the field modulation technique in magnetic fields up to 11.8 Tesla was used to determine the g-factors of holes and electrons in the trigonal-bisectrix and binary-bisectrix planes. Measurements were made at 1.3 K with Dingle temperatures of less than 1 K to obtain g-factor values directly from spin-splitting of the oscillations. The use of high fields, low temperatures and annealed specimens permitted the determination of up to four g-factors other than just those relating to the lowest masses. Values for the lowest masses in the binary-bisectrix plane are in excellent agreement with those obtained by McCombe and Seidel[1], using magnetothermal oscillations. It is found that sample quality deterioriates with each thermal cycling, unless care is taken in mounting.

[1]B. McCombe and G. Seidel, Phys. Rev. 155, 633 (1966).

*Supported by the National Research Council of Canada.

10:00
CD6 de Haas-van Alphen Effect in MgHg. A. E. DUNSWORTH, National Research Council of Canada -- The de Haas-van Alphen effect has been measured in the four-valent β brass compound MgHg. The two bands observed have been studied in detail. The Fermi surface of the first band is a closed, butterfly shaped piece which has been inverted to give the Fermi surface radii. The second band Fermi surface is a large multipliconnected sheet similar to the second band surface of CuZn. This surface supports a multitude of frequency branches having areas ranging from 0.5 to 15 kT. Cyclotron masses have also been measured. The observations are explained well by the LMTO band structure of Skriver.[1]

[1] H.L. Skriver, to be published.

10:30

CD7 Stress Dependence of the Fermi Surface of Nb* N. SANFORD and E. FAWCETT, Univ. of Toronto--Using the method of oscillatory magnetostriction and de Haas-van Alphen torque, we have measured the uniaxial stress dependence of the hole ellipsoids and "jungle gym" of the Fermi surface of niobium. The value, $\partial \ln A/\partial \sigma \sim 2 \times 10^{-6} \text{bar}^{-1}$ for the ellipsoids is roughly constant with change in field orientation, and is consistent with the values for the ellipsoids in Mo and W according to an empirical scaling law.

*Research supported by the National Research Council of Canada.

10:45

CD8 Fermi Surface of Tungsten under Uniaxial Strain* M.J.G. LEE, J. PERZ, D.J. STANLEY** and R. GRIESSEN, Univ. of Toronto--The dependence of several cross sections of the Fermi surface of tungsten on uniaxial strain has been measured by the combined oscillatory magnetostriction and torque method, and by the combined sound velocity and torque method. The response of the Fermi surface of tungsten to a general homogeneous strain field has been calculated in the spherical muffin tin approximation by an extention of the band structure method of Korringa, Kohn and Rostoker. A simple model, in which it is assumed that the phase shifts of the interaction between the conduction electrons and the metal lattice depend only on the dilation associated with the strain field, gives generally good agreement with the data.

*Research supported by the National Research Council of Canada.

**Present address: c/o Materials Physics Division, AERE, Harwell, Didcot, Oxfordshire, OXX11 ORA, England.

11:00

CD9 Fermi Surface of Pt_3Sn. J.-P. JAN and A. WENGER,* National Research Council, Ottawa, and H. L. SKRIVER, N.R.C., Ottawa and Kamerlingh Onnes Laboratory, Leiden. --Experiments by the de Haas-van Alphen effect, and a band structure calculation by the LMTO method, including spin-orbit splitting, show that the Fermi surface of Pt_3Sn (simple cubic $AuCu_3$ structure) consists of cylindrical hole tubes along ΓX (<100> direction) compensating two nested closed electron sheets centered at R. An influence of composition has been observed on the closed sheets. The shape of the sheets, obtained by inversion of the dHvA data, suggests magnetic breakdown when the magnetic field is in and near the <110> direction; five of the seven possible breakdown orbits are clearly observed.

*Now at Straumann Res. Inst., Waldenburg, Switzerland

11:15

CD10 Cyclotron Resonance Measurements in Sb at Far Infrared Frequencies.* C. S. KANG and J. VANDERKOOY, Univ. of Waterloo--We have measured the surface impendance of antimony at 337 μm and 311 μm in magnetic fields up to 11.8 Tesla, using an HCN laser. Voigt configuration is used in the binary-bisectrix plane, with a Faraday measurement along the trigonal axis. The data reveal cyclotron resonance in the retarded regime, with several spin shifted resonances. A large sharp dielectric anomaly at about 7 T and the disappearance of some cyclotron resonance at higher fields may be associated with hybrid resonances and plasma effects. Several orientations show spatial resonances dependent on sample thickness. Our spectrometer allows accurate measurements of relative surface impedance using bolometric techniques, but field modulation studies are not possible in such an experiment due to interference from magnetocaloric effects.

*Supported by the National Research Council of Canada.

TUESDAY, JUNE 15, 1976
ROOM 2C
Chairman: D. Kessler

ELEMENTARY PARTICLES - EXPERIMENTS

9:00

CE1 Measurement of Pion Production Cross sections at TRIUMF. G.R. MASON, G.A. BEER, E.L. MATHIE, and L.P. ROBERTSON, University of Victoria, and D.A. BRYMAN A. OLIN, and J.S. VINCENT, TRIUMF --Cross sections for the production of low energy positive pions at backward angles from targets of carbon and copper were measured at TRIUMF, Vancouver, for proton bombarding energies between 400 and 500 MeV. The techniques will be described and results presented. The results do not show the relatively large cross section previously observed for carbon by Lillethun[1].

[1] Lillethun, E., Phys. Rev. 125, 665 (1962).

9:15

CE2 An Upper Limit on the 2-Photon Decay of the 2S Level in Light Muonic Atoms*. A.L. Carter, M.S. Dixit†, E.P. Hincks, Carleton Univ., C.K. Hargrove, R.J. McKee, H. Mes, N.R.C. (Canada), R.T. Siegal, R.E. Welsh, J.R. Kane, M. Eckhause, C. Cox, M. Rushton, G. Dodson, William and Mary College.--It has been suggested[1,2], that low-Z muonic atoms should be very sensitive to parity violation caused by neutral current effects. Targets of Li, LiH, Be, BeH_2, B, and $B_{10}H_{14}$ were irradiated in the muon channel at the Space Radiation Effects Laboratory. Two Ge detectors, in a delayed coincidence arrangement, were used to observe the 2-photon decay of the 2S levels in muonic Li, Be, and B. Preliminary analysis of the data yield results consistent with little or no delayed 2-photon events. Upper limits for 2-photon decay of the 2S levels in these targets will be presented.

[1] J. Bernabeu, T.E.O. Ericson and C. Jarlskog, CERN-report TH. 1853.

[2] G. Feinberg, M.Y. Chen, Phys. Rev. D10, 3789, 1974.

*Supported by N.R.C. (Canada) through the Institute of Particle Physics, N.S.F., State of Verginia.
†Now at the University of Victoria.

9:30

CE3 A High Pressure Cryogenic Optical Spark Chamber with High Spatial Resolution* J. R. PEKELSKY and R. W. MORRISON, Carleton University, and F. VILLA, SLAC.-- A small neon-helium filled optical spark chamber that can be cooled to liquid nitrogen temperature and pressurized to 21 atm. has been tested in the 9 Gev/c pion beam at SLAC. The improvement in spatial resolution due to the increased gas density is examined at several pressure/temperature combinations and the results compared with the predictions of diffusion theory. Data on the optical quality of the spark, the spark formation time and the effect of the applied high voltage pulse at various gas densities and isobutane admixtures is also presented. The results from a prototype high pressure spark chamber (up to 21 atm.) operated near threshold (minimum spark energy mode) are also discussed.

* Supported by the National Research Council of Canada through the Institute of Particle Physics.

9:45
CE4 Further Tests of Vacuum Polarization Theory with Muonic Atoms*. J.S. Wadden, A.L. Carter, M.S. Dixit†, E.P. Hincks, D. Kessler, Carleton Univ., C.K. Hargrove, R.J. McKee, H. Mes, National Research Council of Canada. H.L. Anderson, Univ. of Chicago, and A. Zehnder‡, Cal. Inst. of Technology.--We have previously reported[1] the first results of our latest precision measurements of muonic atom transition energies chosen to test vacuum polarization corrections. We now report further measurements of transitions between 130 keV and 440 keV in muonic Ca, Sn, Ba, Au, TI and Pb. The accuracy has been improved by carefully studying possible systematic effects. The results are in good agreement with the latest calculations.

[1]M.S. Dixit et al., Phys. Rev. Lett. 35, 1633 (1975).

*Supported by N.R.C. (Canada) through the Institute of Particle Physics, N.S.F. and E.R.D.A.

†Now at the University of Victoria.

‡Now at ETH, Zurich, Switzerland.

10:00
CE5 New Measurement of the π^- Mass*. H. Mes, C.K. Hargrove, E.P. Hincks, R.J. McKee, National Research Council of Canada, A.L. Carter, M.S. Dixit†, M. K. Sundaresan, J.S. Wadden, P.J.S. Watson, Carleton Univ., H.L. Anderson, Univ. of Chicago, A. Zehnder‡, Cal. Inst. of Technology.--Using the same techniques recently employed[1] in precision measurements of muonic atom transitions, several pionic atom transition energies have been measured for which all corrections can be calculated to high precision. From these we deduce the π^- mass to be 139,572.1 ± 2.1 keV/c^2. Assuming equality of the π^+ and π^- masses and using the latest measured value[2] of the muon momentum in π^+ decay, the upper limit (90% confidence level) of the muon neutrino mass is 1.04 MeV/c^2.

[1]M.S. Dixit et al., Phys. Rev. Lett. 35, 1633 (1975).

[2]M. Daum et al., Phys. Lett. 60B, 380 (1976)

*Supported by N.R.C. (Canada) through the Institute of Particle Physics, N.S.F. and E.R.D.A.

†Now at the University of Victoria.

‡Now at ETH, Zurich, Switzerland.

10:15
CE6 Panofsky Ratio in Hydrogen and Deuterium.* M.D. HASINOFF, D. BERGHOFER, R. MACDONALD, D.F. MEASDAY, M. SALOMON, J. SPULLER and T. SUZUKI, Univ. of B.C. J.K.P. LEE, McGill Univ., J-M POUTISSOU and R. POUTISSOU, Univ. de Montréal. -- Two large NaI detectors have been used to detect γ-rays emitted when negative pions are stopped in liquid hydrogen. A stop rate of 15,000 π^-/sec was obtained for a 50 MeV beam from the TRIUMF M9 channel. A preliminary analysis of less than 20% of our data yields a Panofsky Ratio i.e. $P = \omega(\pi^- p \to \pi^0 n)/\omega(\pi^- p \to \gamma n)$ of 1.56 ± 0.04. For deuterium, π^0 production for stopped π^- has never been observed; prior results give $K < 0.7\%$. New results will be presented if available.

*Supported by the National Research Council of Canada.

10:30
CE7 Application d'un modèle de Regge utilisant l'Hypothese d'Additivité des Quarks aux Reactions $\pi^+ p \to \omega\Delta^{++}(1230)$ et $\pi^+ p \to \rho\Delta^{++}(1230)$.† J. BEAUFAYS, C.N. KENNEDY, A.W. KEY, H.N. MERDJANIAN, P.D. ZEMANY, Univ. of Toronto; H. GORDON, K.W. LAI, Brookhaven Nat. Lab.--L'hypothèse d'additivité des quarks fournit des contraintes sévères pour les amplitudes et donc, pour les éléments de matrice densité. Appliquée aux quasi-réactions $\pi^+ p \to \rho\Delta^{++}(1230)$ et $\pi^+ p \to \omega\Delta^{++}(1230)$, celle-ci présente un bon accord avec les resultats expérimentaux à 10 GeV/c. Ainsi, les contraintes entre amplitudes sont utilisées pour effectuer un fit utilisant un modèle absorptif de Regge.

†Work supported in part by National Research Council of Canada.

10:45
CE8 Production of High Mass Resonances in the reactions $\pi^+ p \to \pi^+ p \pi^+ \pi^- (\pi^0)$ at 10.3 GeV/c.* P.D. ZEMANY, C.N. KENNEDY, A.W. KEY and H.N. MERDJANIAN, Univ. of Toronto: H. GORDON and K.W. LAI, Brookhaven Nat. Lab.--A structure at 1880 MeV has been observed in the $\pi^+ p$ invariant mass distributions produced from the reactions $\pi^+ p \to \pi^+ p \pi^+ \pi^- (\pi^0)$. Cuts on the $\pi^+ p$ Jackson decay angle and the mass of the $\pi^+\pi^-\pi^0$ enhance the structure. A fit to the $\pi^+ p$ mass distribution gives a mass and width of (1879 ± 12, 200 ± 50) MeV. The estimated cross section for $\pi^+ p \to \Delta^{++}(1880)\,\pi^+\pi^-$ ($\pi^+ p \to \Delta^{++}(1880)\,\omega^0$) is 50 (25) μb.

11:00
CE9 Production of $\Sigma^+(1385)$ $K^{*0}(890)$ in $\pi^+ p$ Interactions at 10.3 GeV/c.† D. GILBERT, M. GODDARD, A. KEY, Univ. of Toronto; H. GORDON, K. LAI, Brookhaven Nat. Lab.--Density matrix elements for the quasi-two body process $\pi^+ p \to \Sigma^+(1385)\,K^{*0}(890)$ are presented and compared with theoretical models. Invariant mass distributions in the channel $\Lambda K\pi\pi$ are shown and the resonant structure is fitted with Breit Wigners plus background.

†Work supported in part by National Research Council of Canada.

11:15
CE10 Resonance Production in the Reaction $\pi^+ p \to \pi^+\pi^+\pi^+\pi^+\pi^- n$ at 10.3 GeV/c.* C.N. KENNEDY and A.W. KEY, Univ. of Toronto; H. GORDON and K.W. LAI, Brookhaven Nat. Lab.--The production of several resonant states from the reaction $\pi^+ p \to \pi^+\pi^+\pi^+\pi^+\pi^- n$ at 10.3 GeV/c incident pion momentum is discussed. This reaction has not been extensively studied in the past due to the difficulty of extracting it from the background. The manner in which this problem has been overcome is also discussed.

*Work supported in part by the National Research Council of Canada.

11:30
CE11 Measurement of K* Resonances from the Reaction $K^+ p \to K^+ p$ at 6.0 GeV/c.* S. PITLUCK, C.H. HALLIWELL, L. BIRD, D. KESSLER, R.W. MORRISON, D. MOWBRAY and T. OHSKA, Carleton University, Ottawa; C.K. HARGROVE, E.P. HINCKS, R.J. McKEE and H. MES, Physics Division, National Research Council, Ottawa; D.G. STAIRS and J. TRISCHUK, McGill University, Montreal, Que.--We are studying the reaction $K^+ p \to K^+ p$ at 6.0 GeV/c at B.N.L. in the Medium Energy Separated Beam of the AGS. Recoil protons near the Jacobean peak enter a telescope which incorporates spark chambers to measure angles and plastic scintillators to measure energy (E) and dE/dX. The K* decay products are observed with planar and cylindrical spark chambers subtending a large solid angle at the LH target. Making use of the K^0_S V from the successive decays $K^{*+} \to K^0 \pi^+$, $K^0_S \to \pi^+\pi^-$ the reaction was reconstructed with a 3C fit at the $K^+ p$ vertex. The well known K*(890) and K*(1420) resonances are observed along with new evidence for the K*(1760).

*Supported by N.R.C. (Canada) through the Institute of Particle Physics.

TUESDAY, June 15, 1976
ROOM 2D
Chairman: A. Boivin

9:00
CF1 Group Theory and Collective Motions in Nuclei
M. MOSHINSKY, *Universidad de México*

9:45
CF2 Surface Magnetism and Surface Spin Waves in Itinerant Ferromagnets
A GRIFFIN, *University of Toronto, Toronto, Canada*

10:30
CF3
On The Localizability Of The Neutrino.
G. BURDET, M. PERRIN. Université de Montréal.--

The embedding of the two-dimensional extended Schrödinger algebra in the conformal algebra allows to define a two-dimensional "Galilean" position operator for massless particles.

The components of this position operator in the "transverse plane" are explicitely constructed by using the zero-mass discrete spin U.I.R. U^{+}_{0} of the Poincaré group which can be extended in an unique way to the most degenerate discrete series of U.I.R. of SU(2,2). The so-obtained expressions are identical to two of the components of the position operator independently obtained by J. Bertrand and E. Angelopoulos et al. following the Mackey technic.

The above results are extended to the neutrino Weyl Theory. The maximal kinematical invariance algebra of the massless Dirac equation is the conformal algebra, more exactly the extension to the conformal algebra of the Poincaré representations $D \oplus U^{+}_{0}$ where D is the so-called Dirac (finite dimensional) representation of the Pincaré group. Then a two-component position operator is constructed which states that in some sense neutrinos are localizable.

10:45
CF4 Splitting Schemes for the Numerical Solution of a Two-Dimensional Vlasov Equation, M. SHOUCRI and R.R.J. GAGNE, Laval Un.- Splitting schemes have been successfully applied for the numerical solution of a two-dimensional Vlasov equation. Results obtained using two different methods are compared. The first method consists in expanding the distribution function in velocity space in terms of Hermite polynomials, and integrating the resulting hyperbolic differential equation successively in the x and y directions. The second method consists of a direct integration of the Vlasov equation in phase space. It has been found that the method of direct integration is more accurate, more stable and more economic than the Hermite polynomials expansion method.

11:00
CF5 *Vibration and surface modes of one-dimensional crystal.* L. Andrade, M. Alvarez. *Facultad de Ciencias-Universidad Nacional Autónoma de México.- The vibration and surface modes of one-dimensional crystals are calculated with interatomic interactions that include next-necrest neighbor, using the method of Cheng. Localized surface modes with the displacements amplitudes exponentially damped away from the surface can occur under certain conditions. The frequencies are determined by the strength of the various crystals parameters.*

11:15
CF6 Vibration and interface modes of one-dimensional crystals. L. Andrade, J. Borau. Facultad de Ciencias-Universidad Nacional Autonoma de México.- Using essentially the Cheng's model of surface modes of one-dimensional crystals we calculated the frequencies of the vibrational and interface modes of two identical one-dimensional semi-infinite crystals in close contact. Localized interface modes with the displacement amplitudes exponentially damped away from the interface can occur under certain conditions. The frequencies are determined by the strength of the various crystals parameters.

11:30
CF7 A Unified Approach for Deriving Kinetic and Coarse Grained Equations in Non-Equilibrium Statistical Mechanics. J. L. DEL RIO, Escuela Superior de Fisica y Matemáticas, I.P.N., and L. S. GARCIA-COLIN, Universidad Autonoma Metropolitana, Iztapalapa, México 13, D. F.
A unified method for deriving exact kinetic equations for the coarse-grained distribution function and the time evolution equations for the coarse grained variables of a many body system is presented. In the case of kinetic equations, the well known results of Mori[1] and Zwanzig[2] are recovered as special cases. Furthermore, it is shown that they differ only by the way in which the system is prepared at the initial time. Yet, they are related to one another as Schroedinger and Heisenberg's pictures are in quantum mechanics. With respect to coarse grained equations we find the exact time evolution equations. We show that in the Markoffian limit these equations reduce to those used recently by Mori et al[1].

1. H. Mori, Fujisaka and Shigematsu, Prog. Theor. Phys. 51, 109 (1974).
2. R. Zwanzig, Phys, Rev. 124, 983 (1961).

CF 8

TUESDAY, JUNE 15, 1976
ROOM 2E
Chairman: R.E. Azuma

9:00
CG1 Alpha Particle Model of ^{12}C.* M VALLIERES, McMaster University, Hamilton, Ont. and H. T. COELHO, U. of Pernambuco, Brazil - Using the hyperspherical approach we have solved for the 0^+ states of ^{12}C in a three-boson model, using the Ali-Bodmer[1] α-α interaction, with the repulsive strength adjusted to reproduce the excited state energy. The monopole transition and the form factor for elastic and inelastic electron scattering are examined. The shape of the 3-α wavefunction for both the ground and excited state is analysed; in the former a high probability for a triangular shape is found while the latter does not exhibit any particular shape.

([1]) S. Ali and A. R. Bodmer Nuc. Phys. 80 (1966) 99

(*)supported by N.R.C. (Canada)and CNP_q (Brazil)

9:15
CG2 Resonance Structure in ^{14}N at 9.13 MeV.* R. W. KRONE, E. F. GOLDBERG AND J. RAYMER, University of Kansas.--The resonance structure of ^{14}N at 9.13 MeV has been reexamined to determine whether there is evidence for two closely lying states as proposed by Fortune *et al.*[1] Using the $^{13}C(p,\gamma)$ reaction, detailed gamma ray spectra were observed over this energy range showing that there are a number of weak branches in addition to the ground state transition previously reported. Evidence will be presented that show that one of these branches has maximum yields at E_p = 1.701 and 1.710 MeV whereas all the other branches show resonant yield at E_p = 1.701 MeV only. Angular distribution measurements of the ground state transition will be presented. These indicate that the previous 2^- assignment of this state is in question.[2]

*Supported in part by the University of Kansas General Research Fund.
[1]H.T. Fortune, H.G. Bingham, D.J. Crozier and J.N. Bishop, Phys. Rev. C, 11, 302 (1975).
[2]R.W. Detenbeck, J.C. Armstrong, A.S. Figuera and J.B. Marian, Nucl. Phys., 72, 552 (1965).

9:30
CG3 Search for the T = 2 Level in ^{26}Al.* D. W. HEIKKINEN, I. D. PROCTOR and F. S. DIETRICH, Lawrence Livermore Laboratory--Using the previously measured[1,2,3] mass of the T_z = 2 nucleus ^{26}Na the excitation energy of its analog in ^{26}Al can be estimated to be approximately 13.6 MeV. We have searched in this region of excitation energy using the isospin forbidden $^{25}Mg(p,p)$ and $^{24}Mg(d,p$ reactions. In addition the $^{25}Mg(p,\gamma)$ reaction has been studied looking for the allowed γ decay of the 3^+ T = 2 level via low-lying T = 1 levels. Results of the excitation function measurements will be presented showing a large number of resonances in the charged particle channels but relatively few in the γ-ray work. The possible identification of the T = 2 level will be discussed.

*Work performed under the auspices of the U.S. Energy Research and Development Administration, W-7405-Eng-48.
[1]G.C. Ball, et al., Phys. Rev. Lett. 28, 1069,1497 (1972)
[2]E.R. Flynn and J.D. Garrett, Phys. Rev. C9, 210 (1974)
[3]C. Thibault,et al., Phys. Rev. C12, 644 (1975)

9:45
CG4 Resonance at E_{cm} = 12.9 MeV in the $^{12}C(^{16}O,n)^{27}Si$ Reaction. G.RAO, P.TARAS, B.HAAS*, J.C.MERDINGER*, S.LANDSBERGER†, P.PARADIS, R.LECOMTE and S.MONARO, Lab.de Phys.Nucl., Univ.de Montreal -- Time-of-flight spectra of neutrons from the $^{12}C(^{16}O,n)^{27}Si$ reaction have been measured using two 17.8 x 5.1 cm. NE213 detectors and a flight path of 1.5m. These spectra show a resonance at E_{cm}=12.9 MeV. A further measurement with a flight path of 8.5 m indicates that two levels in ^{27}Si are predominantly populated at the resonance energy. n-γ coinc.experiments indicate five new levels in ^{27}Si in the energy range of 3.8 to 7.8 MeV excitation energy and with spins ranging from 9/2 to 17/2. The possibility of the resonance having a quasi-molecular structure is being examined. However, preliminary analysis of proton and deuteron exit channels do not show any strongly correlated resonances at this energy.
* Permanent address: C.R.N., Strasbourg, France.
† Permanent address: Physics Department, Concordia University, Montreal, Canada.

10:00
CG5 Search for $(f_{7/2})^{-3}$ Configuration States in ^{45}Ca.* H. NANN, E. KASHY and D. MUELLER, Mich. State U.--Angular distributions of the $^{48}Ca(^3He,^6He)^{45}Ca$ reaction have been measured at 70 MeV bombarding energy. Several states in ^{45}Ca up to an excitation energy of 4.5 MeV are strongly excited. Since, except for the $7/2^-$ state the $(f_{7/2})^{-3}$ configurations have seniority 3, these states are not strongly excited in single-nucleon transfer reactions, but are expected to be strong in the three-neutron pick up reaction. A comparison with states observed in the $^{44}Ca(d,p)^{45}Ca$ reaction[1] gives evidence for the $(f_{7/2})^{-3}$ configuration of these states.

*Supported by the U.S. National Science Foundation.
[1]Rapaport, Dorenbusch and Belote, Phys. Rev. 156,1255(1967).

10:15
CG6 Spectra of Odd-Mass A = 51-55 Nuclei.* I.P. JOHNSTONE and H. G. BENSON, Queen's Univ.--The possible occurrence of "intruder states" in odd-mass A = 51-55 nuclei has been investigated by calculating the energy levels arising from specific n-particle, m-hole configurations relative to the ^{56}Ni core, using when necessary truncation based on a weak-coupling model. The calculations reproduce the bands of neutron-hole states observed in ^{53}Cr and ^{55}Fe, and predict that four-hole states are among the lowest excited states of ^{55}Co. The theoretical spectra contain many levels which to date have not been isolated, including three $^7/_2^-$ states below 3 MeV in ^{51}Ti and several high-spin states below 5 MeV in ^{53}Cr and ^{55}Fe.

*Supported in part by the National Research Council of Canada.

10:30
CG7 A Shell Model Study of the Cobalt Nuclei* T. TAYLOR and R.G. SUMMERS-GILL, McMaster Univ. - - Binding energies and spectroscopic factors of low-lying states of cobalt nuclei with $55<A<60$ have been calculated in a 1f2p shell-model configuration space assuming an inert ^{56}Ni core. Single particle energies were determined empirically from the binding energies of states of $^{55-57}$Ni. Both Kuo-Brown (KB) and modified surface delta interaction (MSDI) two-body matrix elements were considered. The KB calculations are a dramatic failure. On the other hand, the MSDI reproduces the experimentally observed properties surprisingly well with only a few well understood exceptions.

*Work supported in part by the National Research Council of Canada.

10:45
CG8 Population of the M1 1^+ Levels in ^{58}Co via the ^{58}Fe(p,n) Reaction,* C. WONG and S. GRIMES, Lawrence Livermore Laboratory and V. MADSEN, Oregon State University--Using time-of-flight techniques and a 29.6 m flight path at 0° we have investigated the population of 1^+ levels in ^{58}Fe(p,n) at 20.2 MeV bombarding energy. The relative (p,n) 1^+ intensities at 0° are compared with the ^{58}Ni(t,^{3}He)^{58}Co results[1] and the electron scattering measurements[2] for populating the T>M1 1^+ analog states in ^{58}Ni. The unexpected result is that the (p,n) 1^+ strengths closely resembles that seen in (e,e'); on theoretical grounds, one would expect only agreement between the (t,^{3}He) and (e,e') strengths. The close agreement in (p,n) and (e,e') would indicate that the four neutrons beyond the $f_{7/2}$ shell in ^{58}Fe are predominantly in the $f_{5/2}$ orbit.

*Work performed under the auspices of the U.S. Energy Research and Development Administration, W-7405-Eng-48.
[1]E.R. Flynn and J.D. Garrett, Phys. Rev. Lett. 29, 1748 (1972).
[2]R.A. Lindgren, preprint (to be published).

11:00
CG9 The ^{71}Ga(^{3}He,D)^{72}Ge Reaction.* E.E. HABIB and Z. PREIBISZ, Univ. of Windsor.-Energy levels in ^{72}Ge were investigated by means of the ^{71}Ga(^{3}He,D)^{72}Ge reaction at an incident energy of 24 MeV. The angular distribution of the deuterons were analysed using the DWBA formalism and the spectroscopic strengths of many levels determined. Pure $\ell = 1$, $\ell = 3$ and $\ell = 0$ as well as mixed $\ell = 1 + 3$ and $\ell = 2 + 4$ transfers have been observed. The results are analysed in terms of the pairing model.

* Supported by the National Research Council of Canada

11:15
CG10 β-Decay Studies of Some Rb Isotopes Using a Superconducting Solenoid β Spectrometer.* D.M. REHFIELD, L. LESSARD, G. BAVARIA and R.B. MOORE, McGill University.--The β-decay of the uranium fission products ^{88}Rb, ^{89}Rb, ^{90}Rb and ^{91}Rb, produced by the McGill synchrocyclotron external beam and separated by an on-line mass spectrometer, were studied with an IG detector mounted in a superconducting solenoid. The end-point energy for the well-known decay was reproduced, and the end-points for ^{88}Rb, ^{90}Rb and ^{91}Rb will be reported. In addition, ^{77}Rb, ^{78}Rb and ^{80}Rb, produced by (p,xn) reactions on Kr gas, were obtained by the high-speed extraction system. Nuclear masses extracted from this data, as well as some information on branching ratios for these β-decays will be discussed. Comparisons with Garvey-Kelson mass formulas will be made.

*Work supported by the Atomic Energy Control Board.

11:30
CG11 Nuclear Masses of $1g_{9/2}$ Nuclei.* S.I. HAYAKAWA, J. MISKIN, K.C. CHAN and R.B. MOORE, McGill University.--Study of nuclear masses in the region of $40 \leq Z, N \leq 50$ gives a unique opportunity for investigating pairing energy differences between proton pairs and neutron pairs, Coulomb energy systematics and linear dependence of isospin in the mass equation, because the shell effects are expected to be minimal. We are presently measuring beta end-point energies of ^{91}Tc, ^{89}Nb, ^{88}Nb and ^{87}Nb. The data will be analyzed in conjunction with other known masses in this region, and the results will be presented.

*Work supported by the Atomic Energy Control Board.

11:45
CG12 The Study of States in ^{95}Tc.* K.A. MARSHALL, W.B. COOK, J.V. THOMPSON, M.W. JOHNS, McMaster U.--The decay of states populated in ^{95}Tc following the (α,2n) reaction on ^{93}Nb has been studied. Excitation functions were taken using beam energies from 17 to 27 MeV. Gamma-gamma coincidence and angular distribution experiments were performed at 26 MeV, partially confirming recent work.[1,2] New levels have tentatively been placed at 1310, 2231, 2907, and 3113 keV, and additional gamma rays have been placed in the published level schemes. Spin assignments have been made to levels with excitation energies up to 4 MeV.

[1]T. Shibata, T. Itahashi and T. Wakatsuki, Nucl. Phys. A237, 382 (1975).
[2]D. Hippe, B. Heits, H.W. Schuh, K.O. Zell, H.G. Friederichs and P. van Brentano, Z. Physik A273, 349 (1975).

*Research Supported by the National Research Council of Canada.

TUESDAY, JUNE 15, 1976
ROOM 1A
Chairman: J. Roy

9:00
CH1 Alteration Textures of Basaltic Titanomagnetites from Puerto Rico. D. J. PLASSE. Dalhousie University - Crack and granulation textures of sea floor titanomagnetites from Puerto Rico are very similar to textures observed in deep sea basaltic titanomagnetites. On the basis of x-ray diffraction, scanning electron microscopy, and electron microprobe analyses, titanite (sphene) is the dominant mineral in Puerto Rican crack and granulation textures. The Puerto Rican titanite textures appear to have pseudomorphed previously well developed "ferri-rutile" granulation texture during a zeolite grade metamorphic event. Pseudomorphing requires that Ca and Si were mobile components. Granulation of titanomagnetites may be a sensative indicator of a hydrothermal alteration, whereas cracking seems to be a stress feature. Titanite alteration is likely to occur at 300°C. "Ferri-rutile" alteration may occur at temperatures of 100°C to 200°C.

9:15
CH2 Paleomagnetism of Archean Rock Units and Mineralization of the Noranda Area, Quebec. J. W. LONDRY and D. T. A. SYMONS, Dept. of Geology, Univ. of Windsor - A paleomagnetic study was made of 435 cores from 87 sites representing Keewatin mafic and acidic volcanics, Timiskaming sediments, Haileyburian type diorites, Algoma acidic intrusives, and mineralization and associated alteration in the Noranda area. Alternating-field cleaning was used to isolate a stable remanence for the Keewatin volcanics and Timiskaming sediments was secondary. The diorites which contain concordant mixed primary directions as shown by a contact test. Therefore, a pole position of 89.6°W, 73.2°N (9.5°, 10.2°) was calculated for these four rock types. The Algoman intrusives give a similar pole of 94.2°W, 69.6°N (7.7°, 8.1°) suggesting that they were emplaced soon after the diorite. Alternatively, migrating late Kenoran isotherms affected all the remanence directions to give a regional crescentic polarity pattern. The mineralization pole of 302.2°W, 81.3°N (11.3°, 14.8°) is statistically different from the previous poles. This suggests that the mineralization was emplaced after the Algoman acidic intrusives but before the diabase dikes. These poles fit the Archean polar wander path for the Superior Province.

9:30
CH3 A Possible Archean Paleopole from the Shelley Lake Granite. D.J. DUNLOP, K.L. BUCHAN, Geophysics Laboratory, Univ. of Toronto--The Shelley Lake granite is a sill-like intrusion into Archean metasediments and gneisses of the Quetico gneiss belt, western Superior structural province. It is conformable with the rocks it intrudes and with the nearby Shebandowan volcanics and appears to be an early intrusion subsequently deformed along with the country rock during the Kenoran orogeny. Aeromagnetic anomaly interpretation suggests a steep dip (about 70°) to the south-east. Cleaned magnetization directions fall in two groups. The first group (27 normal, 11 reverse magnetizations) has a well-defined mean ($k = 69.8$, $\alpha_{95} = 5.2°$) giving a paleopole at 69°E, 76.5°N, in the general area of the Matachewan and Stillwater poles. This component seems to be a metamorphic overprint of Kenoran age (≈ 2500 my). The second group (2 normal, 8 reversed) is more scattered but corresponds to a pole near 160°W, 5°S or, after structural correction, near 127°W, 17°S. Although poorly defined, this pole is near the Archean-age pole of the Kirkland Lake volcanics[1] at 136°W, 22°S. Similar magnetizations of possibly Archean age are found in widely separated areas of the nearby Wabigoon volcanic subprovince.

1 R.H. Ridler, J.H. Foster, GSA/GAC Abstracts with Programs, 7, 844, 1975.

9:45
CH4 An orogenic pulse at 2,200 my. W.A. MORRIS, Earth Physics Branch, EMR., Ottawa--Track 5 and Hairpin 50 define the apparent polar wander path relative to Laurentia for the interval -2500 to -1800 Ma. By distinguishing and separating primary magnetizations and overprints together with radiometric data it is possible to recognise a sequence of stratigraphic, tectonic and intrusive events which affected a large portion of the present Canadian shield. At approximately 2,300 my till like rocks (Huronian and equivalents) were deposited in a number of small basins marginal to the Superior Province. Subsequently these sediments were deformed and metamorphosed by a major orogenic pulse at approximately 2,200 my. Finally, the intrusion at 2150 my of a large number of dykes probably signalled the onset of another cycle of rifting, sedimentation and orogenesis.

10:00
CH5 Paleomagnetic Investigation of the Nimish Greenstones, Labrador. SEGUIN, MAURICE K.-, Département de Géologie, Université Laval, Québec G1K 7P4, Canada.- This paleomagnetic study is centered on the Nimish formation which consists of basic and intermediate lava flows and agglomerates containing fragments of iron formation. It involves a total of 80 specimens from 28 sites. Both thermal and AF cleaning techniques were used to isolate the residual remanent component. The dispersion of the poles is smaller when using AF demagnetization than thermal treatment. The paleopole position obtained after AF demagnetization is 121°W , 30°S ($\alpha_{0.95}$=13.8°, d_m=14.1°, d_p=7.3°, K=34) and the polarity of most of the samples is normal even though reversal occurs frequently in the process of AF demagnetization. The paleopole position obtained after thermal treatment is 093°W, 06°S ($\alpha_{0.95}$=21.5°, d_m=25.4°, d_p=20.6°, K=26) and the polarity of almost all the samples is normal. The analysis of the results and their comparison with data published suggest that the thermal treatment allows the determination of the initial thermoremanent component which would yield an age of extrusion of the order of 2200 m.y. The AF demagnetized results would give the paleopole position related to the Hudsonian orogeny (1750-1800 m.y.)

10:15
CH6 Application of combined analysis of gravity and magnetic anomalies to the Sept Iles anorthosite A.K. GOODACRE Earth Phys. Br. - If the ratio of magnetization contrast to density contrast is constant throughout an anomalous source which is magnetized in a uniform direction, the direction of the total magnetization vector can be obtained from a knowledge of the gravity and magnetic anomaly fields. Combined analysis of the intense, nearly circular, gravity and magnetic anomalies over the gabbroic anorthosite south of Sept Iles, Quebec suggests that the azimuth and inclination of the total magnetization vector are approximately -53 (±14) degrees and 67 (±10) degrees respectively (standard deviation given in brackets). The direction of the remanent magnetization vector depends upon whatever value is adopted for the Koenigsberger ratio, Q, but, if Q = 0.25 (a value suggested by rock magnetism data kindly supplied by the Geological Survey of Canada) the virtual palaeomagnetic pole is located at 10°N; 155°W. This location is near palaeomagnetic poles obtained from 1200 to 1400 my old rocks elsewhere in the Canadian Shield.

10:30
CH7 The Great Conglomerate Test. H.C. PALMER, U.W.O. London, H.C. HALLS and L.J. PESONEN, Univ. of Toronto--Oriented cores, field-drilled from 210 mafic volcanic pebbles are evenly distributed among four sites within

the Middle Keweenawan Copper Harbor Conglomerate, northern Michigan. All sites show a marked departure from randomness of NRM directions indicating that the conglomerate has been partially remagnetized along a direction with westerly declination and shallow downward inclination. One site, analysed in detail, shows that about 50% of the pebbles are stable to AF demagnetization up to 1000 oe. The other 50% yield directions which progressively move along great circle paths. The remagnetization circles so obtained intersect at a point (D=270°, I=+20°) which gives the direction of the secondary component. The swinging samples have NRM intensities ($3x10^{-5}$ to $3x10^{-4}$ emu/cc) and NRM directions with $\beta<70°$ where β is the angle between the NRM direction and that of the secondary component. Stable samples tend to have higher NRM intensities (3x10-4 to $3x10^{-3}$ emu/cc) and $\beta>70°$. These relations suggest that the secondary component is a CRM.

10:45

CH8 . . . . . .New Paleomagnetic and Paleointensity Results from Keweenawan Intrusives and Baked Contact Rocks. LAURI J. PESONEN and HENRY C. HALLS, Department of Geology, University of Toronto, Ontario. - A new paleomagnetic pole (Lat. 49.0°N, Long. 215.8°E, dp = 5.6°, dm = 6.6°, N = 15) has been obtained from 15 Keweenawan reversely magnetized diabase dikes in Baraga and Marquette Counties, northern Michigan. This pole determination supercedes an earlier one by Graham (1953) which was based on results from only 2 dikes without magnetic cleaning. The new pole position suggests that the Baraga dikes are correlative with the reversely magnetized Logan sills and dikes on the north side of Lake Superior. Thellier-Thellier paleointensity measurements on magnetically reversed and normal Keweenawan intrusives and baked contact rocks suggest a higher paleointensity for the reversed epoch (mean of 23 specimens = 0.77 oe, range 0.29 to 1.36 oe) compared to the younger normal one (mean of 7 specimens = 0.56 oe, range 0.28 to 0.79 oe). Although results are tentative, because specimen response to the Thellier method is often complex, they are consistent with the hypothesis of apparent polar wander during the formation of the Logan Loop.

11:00

CH9 Paleomagnetism, Petrochemistry and K-Ar dating of Sudbury Dikes. B.A. MERZ, A. HAYATSU AND H.C. PALMER U.W.O., London, Ont.--In the Lake Panache region, Sudbury diabase dikes cross the Grenville Front and can be traced for a short distance into the Grenville Province. Within the Southern Province the dikes have a mean paleomagnetic direction of 264, +01 ($\alpha95$ = 3½) and a spread in apparent ages from 1100-1600 my. Approximately 1 mile in advance of the Front directions change to 112, +26 ($\alpha95$ = 6); apparent ages are scattered with some anomalously old apparent ages. Further into the Grenville Province ages are typically Grenville - i.e., 850-1100 my. A short dike segment in the Grenville Front region is characterized by a paleomagnetic direction of 125, +59, K-Ar apparent ages in the 430-500 my range and tholeiitic chemistry rather than the distinctly alkali-olivine basalt chemistry which typifies all the other Sudbury dikes.

11:15

CH10 Paleomagnetism of Silurian and Devonian Rocks from Newfoundland. P.L. LAPOINTE, Earth Physics Branch, EMR., Ottawa--In central Newfoundland Botwood group sediments (red beds of Silurian age) are intruded by the Mount Peyton diorite body. The Mount Peyton body is a two-phase intrusion; the initial phase is dioritic and probably dated at 420 m.a., the second phase is granitic and probably dated at 375 m.a. The Botwood group and the Mount Peyton were sampled for paleomagnetic study. Specimens of red beds of the Botwood group were cleaned using thermal, Af and chemical demagnetization techniques, they yield very stable single magnetization with a direction (231 + 69 pole 95E 20S). The Mount Peyton samples (subjected to Af and Thermal cleaning) yield two directions one associated with the dioritic phase (080,-50 pole 62E 17S) and the other with granitic phase (063, +84 141E 53S). Based on these new data the lower paleozoic data for North America are reviewed and a preliminary polar path is proposed.

11:30

CH11 La position stratigraphique de sédiments carbonifères de Minudie Point, Nouvelle Ecosse. J.L. ROY, Dir. Phys. Globe.--Des traitements chimiques, thermiques et par champ alternatifs indiquent que ces roches sédimentaires ont conservé leur aimantation initiale acquise lentement et progressivement pendant la déposition et la diagénèse subséquente. A 8 des 9 sites, un changement de polarité eut lieu au début du procédé d'aimantation avec le résultat que l'aimantation produite pendant les premières phases du procédé ne peut nous fournir une détermination fidèle du champ de l'époque. Cependant, il est possible par analyse vectorielle de déterminer la direction de la dernière phase d'aimantation qui eut lieu aprés le renversement. Cette direction tombe d'accord avec la direction obtenue à l'autre site où la plupart des phases d'aimantation survinrent dans un champ de même polarité. La direction moyenne (174°,+21; α_{95}=6°) concorde bien avec la direction du groupe d'Hopewell dont l'âge est aux bornes du Pennsylvanien-Mississippien. Cette similitude de directions et surtout le fait qu'une polarité négative a été enregistrée indiquent que l'aimantation fut acquise avant la longue période de polarité positive du Carbonifère supérieur-Permien. Ces grès sont donc probablement pré-Cumberland i.e. d'âge Canso ou Riversdale.

11:45

CH12 Paleomagnetic Results from Some Quaternary Sediments in B.C. and Their Bearing on Geomagnetic Secular Variation, C.J. OBERG and M.E. EVANS, U. of Alberta, I.E.P.P. - Magnetic remanence has been determined from 37 horizons spread throughout a 7m section of floodplain silt near Lumby, B.C. Radiocarbon dates indicate that the section represents about 9000 years with a base at about 31,000 years B.P. The magnetic vectors are tightly grouped (α_{95} = 1.5°) but regular oscillations in the direction of the magnetic vectors occur. However, there is no evidence for the very marked geomagnetic excursion reported from Lake Mungo, Australia, which supports the view that such features are not global in extent. Maximum entropy analysis of magnetic vectors mapped onto the complex plane reveals marked peaks in the power spectrum at periods of about 800, 2100 and 6000 years. The shorter periods exhibit a strong clockwise sense of rotation implying westward drift of non-dipole components. The 6000 year component implies easterly drift but alternative explanations may be possible.

12:00

CH13 Paleomagnetism of DSDP Leg 37 Basement Rocks. J. M. Hall and D. J. PLASSE. Dalhousie University - Over 400 sub samples of oceanic basement have been tested for paleomagnetic properties. Basalts show: 1) Average NRM intensity is very close to $40x10^{-4}$emu cm^{-3} and varies randomly with depth 2) Average induced magnetization, at 3% of stable remanence, is negligible 3) cleaned magnetic inclinations are consistantly shallow in 3 of 5 holes, tightly grouped according to lithologic unit, and in one hole record a polarity reversal. These data suggest a source depth varying between 600 m and 2.5 km for sea floor magnetic anomalies, and that episodic volcanism is likely to produce layer 2.

TUESDAY, JUNE 15, 1976
ROOM 2F
Chairman: H. Skarsgard

9:00
CI1 Bleaching Absorption Fronts and Beam Propagation in Laser Heated Solenoids. N.H. BURNETT, N.R.C., and A.A. OFFENBERGER, Univ. of Alta. -- It is shown that the propagation velocity of bleaching laser driven heating waves in the supersonic mode is governed by the requirement that the bleached plasma maintains an optical thickness of unity. Simple analytic considerations indicate that under constant intensity irradiation the length of the bleached column will increase as $L \propto t^{3/5}$. An analytic expression for the minimum intensity necessary to prevent the occurence of axial motion and shock formation will be derived. The results will be compared to the predictions of a one dimensional Lagrangian computer code. Simulation results will also be discussed for the head on collision of two near supersonic heating waves.

9:15
CI2 Interprétation des premiers résultats obtenus sur un plasma-focus produit par une impulsion laser CO_2. G. SAINT-HILAIRE et Z. SZILI, Direction Sciences de base, IREQ, Varennes, Québec, Canada, J0L 2P0 -- Nous avons déjà montré[1] qu'un plasma-focus peut être produit par laser en focalisant le faisceau, à l'aide d'un miroir toroïdal approprié, sur une ligne circulaire à la surface interne d'une cible annulaire (cible de cuivre, 1 cm de diamètre intérieur). Le plasma-focus produit par une impulsion laser CO_2 (50 ns, 50 J) est étudié à l'aide d'un interféromètre axial ($n_e = 1.6\ 10^{18} cm^{-3}$). De plus, l'évolution temporelle de la luminosité du plasma est mesurée pour différentes positions radiales, et permet d'établir un modèle simple de l'écoulement de plasma dans la cible annulaire. Ce modèle suppose que les collisions sont insuffisantes pour permettre la thermalisation au sein du plasma-focus. La température ionique équivalente est initialement de 1 keV, mais ne dépasse guère 4 eV à l'instant du maximum de densité électronique. On estime que plus de 10% de l'énergie de l'impulsion laser se retrouve en énergie cinétique du nuage de plasma.

[1] G. Saint-Hilaire and Z. Szili, 1976 IEEE International Conference on Plasma Science, Austin, Texas, (May 24-26).

9:30
CI3 Fluctuation Spectra in Plasmas Stimulated by Subthreshold Pumps.* J.N. LEBOEUF and T.W. JOHNSTON. INRS-Energie, Univ. du Québec, Varennes, Qué.--Earlier theory[1] is used to calculate fluctuation spectra. Even well below threshold, large enhancements ($\sim 10^3$) of the plasma line are evident with a structure which is a convolution of the normal plasma line and the usual low-frequency feature aliased by the pump to the plasma frequency. This type of aliasing will also be present for magnetoplasmas and for saturated fluctuations. Effects of electron-to-ion temperature ratio, pump frequency, pump power and wave vector resolution are presented.

[1] J.N. Leboeuf, T.W. Johnston, Can. J. Phys. 53 (21), 2387-2405 (1975).

9:45
CI4 Optical Mixing in a Plasma near the Plasma Frequency.* L. A. GODFREY and R. NODWELL, Univ. of British Columbia.-- A description will be given of an experiment to detect the enhanced light scattering cross-section in a plasma due to the optical mixing of two light beams who's frequency difference is near the plasma frequency. The light beams are provided by two tuneable dye lasers which have been developed for high spectral brightness. A high current Helium plasma jet is used as the plasma source.

10:00
CI5 Semiconductor Reflection Switching of High Power CO_2 Laser Radiation. A.J. ALCOCK, P.B. CORKUM, J.C. SAMSON and D.J. JAMES*, N.R.C. -- Carrier densities sufficiently high to reflect 10 μm radiation can be produced by illuminating the surface of a semiconductor with intense visible or near infrared laser radiation. Experiments carried out on germanium with nanosecond duration pulses of 0.7 μm or 1.06 μm radiation have demonstrated the rapid onset of complete reflection and subsequent absorption of an incident 10.6 μm beam. This technique provides an effective means of synchronizing a CO_2 laser pulse with the output of a shorter wavelength laser and has also permitted the selection of a single 1-2 joule pulse from the output of an injection mode-locked CO_2 oscillator.

*Dept. of Applied Physics, Univ. of Hull, Hull, England

10:15
CI6 Quantitave Schlieren System employing Neutral Density Wedges. C. HUMPHRIES and B. AHLBORN, Univ. of British Columbia.- In this schlieren system the probing laser beam is attenuated by a neutral density wedge (instead of the usual knife edge) so that the intensity is proportional to the deflection angle, which in turn is proportional to the density gradient. Time integration of the attenuated probe beam intensity yields the absolute refractive index variation across moving objects. The device is tested by measuring the density jump across a Mach 9 shock wave. Diffraction effects are practically eliminated in this schlieren system.

10:30
CI7 Positron Annihilation Diagnostics for Plasmas.* U.O. ZIEMELIS and B. AHLBORN, Univ. of British Columbia.- The feasibility of using positrons to probe plasmas has been investigated. The analysis of γ-rays resulting from positron annihilations with plasma electrons may yield information about the momentum distribution, temperature and number density of these electrons. Various techniques, including measurement of positron lifetimes, annihilation line widths, 2γ angular correlation and beam spread will be discussed with special reference to conditions in Tokamak and laser fusion plasmas. Optimum conditions for these measurements require complete thermalization of the probe positrons with the plasma electrons. Calculations indicate that this condition is satisfied in a fully ionized hydrogen plasma with $T_e > 10eV$ and $10^9 < N_e(cm^{-3}) < 10^{26}$ for positrons from a ^{22}Na source.

10:45
CI8 Thermal Blast Waves.* B. AHLBORN and S. ARIGA, Univ. of British Columbia.-- We have developed a model to describe blast waves in which the energy transfer by radiation and/or conduction dominates over the energy transfer by shock heating and adiabatic cooling (Taylor-Sedov blast waves). This model distinguishes three phases in the blast wave development, the initial supersonic phase, the short lasting detonation like phase and the final subsonic phase in which one has a small hot core (radius r_H) and a shock envelope (radius r_S). The blast wave energy E_o can be found in this late phase from $E_o = \text{const.}\ r_H^3 \cdot V_S^2 \cdot \rho_1$ where ρ_1 is the density outside and V_S the shock front velocity. Other parameters (such as enthalpy, pressure particle velocity and thermal response law) may be obtained from the front velocity at the detonation point, which can be well determined on smear camera traces of the blast wave.

11:00
CI9 Multiple Shock Compression.* B. ARMSTRONG and B. AHLBORN, Univ. of British Columbia.-- In order to study some of the hydrodynamic conditions required for laser fusion with homogenious D-T pellets we have generated successive shock waves with an ablasion surface driven by a tylored power pulse. This flow field was generated in an electrothermal shock tube and the shock interaction region was studied with a smear camera. Density increases well beyond the compression of a single strong shock were reached, but the driving heat wave seems to approach sonic conditions, where no further shock can be launched, so that there will be an upper limit for the compression in this experiment.

*This work was supported by the Atomic Energy Control Board.

11:15
CI10 Characteristics of a Pyro-electric Vidicon for recording pulsed 10.6 μm Radiation. W.J. SARJEANT, H.A. BALDIS and A.J. ALCOCK, N.R.C. -- Although a limited number of techniques exist for the direct recording of spatial intensity variations at the CO_2 laser wavelength, the pyroelectric vidicon appears to be the only available high sensitivity room-temperature detection device[1] for this application. The characteristics of a pyro-electric vidicon as a means of recording pulsed 10.6 μm radiation have been investigated using an English Electric P8090 tube in conjunction with a special television camera.[2] Using this system energy densities as low as 50 μJ/cm have been recorded with a spatial resolution of ∿5 line pairs/mm. Additional data on linearity, dynamic range and long term stability will be presented.

[1]K.B. Mitchell, T.F. Stratton and P.B. Weiss, Appl. Phys. Letts. 27, 11 (1975).

[2]Modified version of a camera kindly provided by P.B. Weiss, Los Alamos Scientific Laboratory.

11:30
CI11 Investigation des Caractéristiques Spectrales d'un Laser CO_2 Syntonisable et Multi-Atmosphérique. D.F. ROLLIN* et A.J. ALCOCK, C.N.R.C. -- La conversion élévatrice de la fréquence dans la proustite a déjà été appliquée à la détermination précise de la longueur d'onde des lignes d'émission des lasers CO_2.[1] L'expérience décrite ici utilise le mixage de radiations de 10.6 et 1.06 μm dans la proustite pour déterminer la longueur d'onde ainsi que la largeur de ligne d'un laser syntonisable CO_2 à excitation transverse fonctionant à une précision de l'ordre de 10-15 atm. La radiation de 1.06 μm est produite par un laser Nd:Yag à déclenchement actif qui est contraint à osciller sur un mode longitudinal unique. Un tel oscillateur permet de réduire l'apport de la radiation de 1.06 μm au spectre de la radiation a fréquence convertie dont la largeur de bande peut être déterminée à l'aide d'un interférometre de Fabry-Pérot accoupli à un tube de conversion de l'image.

*Univ. Carleton

E.K. Pfitzer, H.D. Riccius and K.J. Siemsen, Optics Communications 3, 277 (1971).

11:45
CI12 Injection Mode-Locking of Flashlamp Pumped Dye Lasers. H.D. MORRISON*, P.B. CORKUM and A.J. ALCOCK, N.R.C. -- Experiments carried out with TEA CO_2 lasers[1] have already demonstrated that the temporal characteristics of a low energy pulse, or train of pulses, can be transferred to a much higher energy pulse train by means of injection mode-locking. The applicability of this technique to other laser systems is of considerable interest and an initial experiment involving a dye laser has been reported recently.[2] In the past the individual pulse energies, available from mode-locked dye lasers, have been limited to the microjoule range however injection mode-locking offers the possibility of obtaining low divergence pulses at significantly higher energies. In the present paper experiments carried out with two flashlamp pumped dye lasers will be described.

*University of Waterloo.

[1]P.A. Belanger and J. Boivin, Physics in Canada, 30, 47 (1974); IEEE J. Quantum Electron. QE-11, 730 (1975).

[2]E.I. Moses, J.J. Turner and C.L. Tang, Appl. Phys. Letts., 28, 258 (1976).

TUESDAY, JUNE 15, 1976
ROOM 1C
Chairman: J.B. Warren

NUCLEAR AND PARTICLE PHYSICS AT INTERMEDIATE ENERGIES

13:30
DA1 Nucleon-Nucleon Elastic Scattering
D.V. BUGG, *Queen Mary College, London and TRIUMF*

14:15
DA2 Nucleon-Nucleon Interactions in Nuclei; a survey of the prospects for direct investigations
A.N. JAMES, *University of Alberta, TRIUMF*

15:00
DA3 Pion Nuclear Total Cross-Section
R. REDWINE, *LAMPF*

15:45
DA4 Electron Scattering at the MIT-Bates Linear Accelerator
C.P. SARGENT, *Massachusetts Institute of Technology*

TUESDAY, JUNE 15, 1976
ROOM 1B
Chairman: P.D. Marchand

ATOMIC PHYSICS I

13:30
DB1 Range and Projected Range Calculations at Low Energies.* B. M. LATTA and P. J. SCANLON, Queen's Univ. --Several reported experimental range measurements indicate that the Lindhard Scharff Schiott (LSS) theory underestimates the projected range at low ε values[1]. The LSS calculations are based on a free-atom interaction potential. We show that the use of an interaction potential appropriate for a solid target[2] yields theoretical projected ranges that are in better agreement with the low ε experimental data.

[1]H. Oetzmann, A. Feuerstein, H. Grahmann, and S. Kalbitzer, Phys. Lett. 55A, 170 (1975).

[2]B. M. Latta and P. J. Scanlon, Phys. Rev. A10, 1638 (1974).

*Supported by Atomic Energy Control Board of Canada.

13:45
DB2 Fermi's Calculation of Minimum Dipole Moment for Electron Binding.* J. E. TURNER, Health Physics Division, ORNL, Oak Ridge, TN 37830 -- In 1966-67 four independent investigations led simultaneously to the result that a minimum value, 0.639 ea_0, of the dipole moment is required to bind an electron to a static electric dipole. It was subsequently learned that this result was published in 1947 by Fermi and Teller without a derivation.[1] The author has found a numerical solution in Fermi's notebooks at the University of Chicago Library. This solution will be presented.

*Research sponsored by the Energy Research and Development Administration under contract with Union Carbide.

[1]E. Fermi and E. Teller, Phys. Rev. 72, 406 (1947).

14:00
DB3 The Three-body bound-state with Coulomb Forces*. R.K. BHADURI, A.K. DUTTA and Y. NOGAMI, McMaster U.-- Recently, we have applied the Feshbach-Rubinow (FR) approximation to the 3-body bound-state problem with Coulomb forces.[1] In this method, the space-symmetric three-body wave-function is assumed to depend on a single nonnegative variable $R=\frac{1}{3}(\eta_1 r_1+\eta_2 r_2+\eta_3 r_3)$, where the η_i's are variational parameters, r_1 is the interparticle distance between particles 2 and 3, and likewise for r_2 and r_3. The problem then reduces to solving a single differential equation, which can be done analytically for Coulomb forces. For helium atom and helium-like ions, the numerical accuracy of the above method is found to be comparable to that of solving a large number of coupled equations in the K-harmonics approach.[2] Encouraged by this, we propose an extension of the FR method to take better account of the interparticle correlations, and yield a better estimate of the binding energy.

[1]R.K. Bhaduri and Y. Nogami, Phys. Rev. A (June, 1976)
[2]R.M. Shoucri and B.T. Darling, Phys. Rev. A12,2272(1975)

*Supported by the National Research Council of Canada.

14:15

DB4 Etude de l'émission ionique secondaire négative du cuivre et de quelques-uns de ses alliages par impact d'ions positifs de cesium. P. VALLERAND et M. Baril, Univ. Laval.-- Nous avons entrepris l'étude de l'émission ionique secondaire en utilisant les ions Cs^+ comme projectile dans le faisceau primaire. Nos résultats démontrent qu'il est nécessaire d'effectuer les mesures à un vide poussé (~ 10^{-8} torr). Nous comparerons l'émission négative de cuivre pur avec celle de ses alliages. Nous discuterons de l'utilisation éventuelle du modèle thermodynamique d'Andersen. Certaines mesures sur les éléments contenus en faible concentration montrent que l'émission est renforcée pour certains éléments (P, Al, Fe, Sn, Ni) et atténuée pour d'autres (Zn, Pb).

14:30

DB5 Theoretical Interpretation of Neon Autoionization Spectrum.* J. LANGLOIS and J. M. SICHEL, Univ. Laval and Univ. de Moncton — Autoionizing states of neon corresponding to a double excitation of the 2p shell have been observed by photon, heavy ion and electron impact. We have calculated the energy of many such states by a frozen-core super-position-of-configurations method in which the excited orbitals, occupied or virtual are represented by Slater orbitals orthogonalized to each other and to Hartree-Fock core orbitals. We have considered $3s^2$, 3s3p, 3s3d, $3p^2$ and 3p3d excitations and obtained a precision of the order of 0.1 eV. In cases where several values of intermediate angular moments are consistent with the final symmetry, we have determined the best coupling sheme. Based on these calculations we propose interpretations for several observed structures in terms of neutral and negative-ion states.

*Research supported by the Canadian National Research Council.

14:45

DB6 Ionisation du CO_2 par impact électronique. N. BUSSIERES et P. MARMET, Département de Physique, Université Laval.--Des faisceaux croisés d'électrons et de molécules sont utilisés pour produire des ions CO_2^+. Ceux-ci traversent un filtre quadrupolaire pour être ensuite détectés, amplifiés par un multiplicateur d'électrons puis comptés par un analyseur à canaux multiples. Un mini-ordinateur permet d'effectuer des redressements par lissage sur les courbes d'ionisation produites; ce traitement met en évidence les structures dues à des niveaux neutres autoionisants et à des niveaux de l'ion négatif. La région allant du seuil à 19.5 eV est examinée. Le seuil d'ionisation a pour valeur 13.83 ± 0.05 eV. Les structures observées se rattachent en particulier à des niveaux de Rydberg convergeant vers les limites B (18.07 eV) et C (19.38 eV).

Nous remercions le Conseil National des Recherches du Canada ainsi que le Gouvernement du Québec pour avoir fourni des octrois essentiels à la réalisation de ce projet.

15:00

DB7 Forces d'oscillateur des raies de résonance Kr VII et du Kr VIII. E.J. KNYSTAUTAS ET R. DROUIN, Laboratoire de l'accélérateur Van de Graaff, C.R.A.M., et Département de chimie, Université Laval, Québec, Canada G1K 7P4.--Les vies moyennes des premiers états excités dans le Kr VII et le Kr VIII ont été mesurées à l'aide de la méthode faisceau-lame. Les effets des cascades ainsi que de la détérioration rapide de la cible sur les résultats sont discutés. Les forces d'oscillateur des raies de résonance sont calculées à partir de ces mesures, et elles sont comparées aux valeurs extrapolées et calculées dans leurs séquences iso-électroniques respectives (Cu I et Zn I). Nos mesures permettent une extrapolation aux éléments de ces mêmes séquences présents comme impuretés dans les réacteurs à fusion.

15:15

DB8 Spectroscopie par détection de métastables.* E. BOLDUC et P. MARMET, Université Laval.--Des variations ont été observées dans la section efficace d'excitation des états métastables de l'hélium, du néon et de l'argon. Elles ont permis de mesurer l'énergie et, dans certains cas, la vie d'états neutres et négatifs de ces atomes. Plusieurs des états détectés, ont pu être identifiés, aussi bien dans la région d'énergie située sous le seuil d'ionisation qu'au-dessus du seuil. Les mesures ont été prises à l'aide d'un instrument construit pour la spectroscopie par électroionisation(1). L'utilisation du redressement par lissages(2) a permis de mettre en évidence certaines des structures.

(1) E. Bolduc, J.J. Quéméner et P. Marmet, J. Chem. Phys. 57, 1957 (1972).
(2) E. Bolduc, J.J. Quéméner et P. Marmet, Can. J. Phys. 49, 3095 (1971).

Subventionné par le C.N.R.C. et le M.E.Q.

To be presented by H. Weingartshofer

15:30

DB9 The Eighth Spectrum of Selenium: Se VIII. Y.N. JOSHI, Th. A. M. VANKLEEF* and H. BENSCHOP*, St. F. X. University.--The spectrum of Selenium was photographed in the region 90Å - 600Å using a triggered vacuum spark source. On the basis of new measurements, the Eighth Spectrum has been revised and extended. Energy level calculations by parametric method and the intensity calculations from transition probabilities confirm the analysis.

Recent extensions in the Sixth and Seventh Spectrum of Selenium (Se VI and Se VII) will also be discussed.

* Permanent address: Zeeman Laboratory, The University of Amsterdam, The Netherlands.

15:45

DB10 Broadening of Lithium Lines.* A. J. BARNARD and D. C. STEVENSON, Univ. of British Columbia.-- The broadening of the neutral lithium line at 4603 A is of some interest, since it has a forbidden component that shows up in dense plasmas. We have calculated the line profile at different densities using the impact approximation for the electrons and the quasi-static approximation for the ions. The line shape has also been measured in a pulsed arc in helium with lithium added to the electrodes. The temperature and the electron density could be determined from the intensity and widths of the helium lines. The Li I 4603 A line from this source was observed to be about twice as wide as calculated and this is probably due to the large optical thickness of the plasma. To check this interpretation the measurement is being repeated with a sufficiently cooler and hence optically thin plasma. Other lithium lines will also be studied.

TUESDAY, JUNE 15, 1976
ROOM 2A
Chairman: W.R. Datars

13:30
DC1 Electrical Conduction in Epoxy Composites Containing Graphite Fibers. K. W. TSE, W. TEOH, SIGURDS ARAJS, and K. V. RAO, Department of Physics, Clarkson College, Potsdam, N.Y. 13676 -- Electrical resistivity (ρ) of unidirectional composite bars consisting of graphite (or carbon) fiber bundles imbedded in an epoxy resin matrix and cured at 175C have been studied as a function of temperature between 78K and 300K. The samples contain about 60 volume % of fibers of the following origin: Celenese Celion GY-70, Hercules Type A, Stockpole Fibers Panex 30, and Union Carbide Thornel 300. All the ρ vs T curves monotomically decrease with increasing temperatures. The results will be discussed using the current models of electrical conduction in composite materials.

13:45
DC2 Electrical Resistivity of Metglasses 2605 and 2605A Between 78K and 1000K. N. TEOH, W. TEOH, SIGURDS ARAJS, and P. B. HARWOOD, Department of Physics, Clarkson College, Potsdam, N.Y. 13676.--Electrical resistivity (ρ) of amorphous ferromagnets $Fe_{80}B_{20}$(Allied Chemical Metglass 2605) and $Fe_{78}Mo_2B_{20}$(2605A) have been determined as a function of temperature (T) between 78K and 1000K. Metglass 2605A exhibits a maximum in the ρ vs T curve at 190 ± 5K and a minimum at 236 ± 5K. Such anomalies in the amorphous state are absent in Metglass 2605. For warming rates of about 8K/hr the crystallization starts at about 630K for Metglass 2605 and at approximately 680K for Metglass 2605A. Anomalies in ρ vs T curves at the ferromagnetic Curie temperatures in either amorphous or crystalline state are extremely small.

14:00
DC3 Equivalent Circuit Model for the Pb/PbO Cell. P.M. MOONEY, Vassar College.-- The Pb/PbO solid electrolyte cell consists of a thin layer of tetragonal PbO anodized on a lead substrate with a silver electrode on the oxide surface. Several models for charge transport in the cell have been proposed. This research included the measurement of the I-V curve for the cell under steady conditions and measurements of the current as a function of time when a step voltage was applied to the cell. These data were interpreted in terms of an equivalent circuit which is valid for some cells. It appears that under reverse bias conditions only the cell surface and the silver electrode respond to changes in applied voltage and that the surface of the cell is relatively highly conducting even when the cell is not illuminated. Houston's model for charge transport is essentially correct for cells for which this equivalent circuit is valid.

14:15
DC4 Open orbits in ReO_3.* F.S. RAZAVI and W.R. DATARS. McMaster U.-- Open orbits have been observed in the metal compound ReO_3 for the first time. The open orbits were detected using an angle modulation technique with an induced torque magnetometer in a superconducting magnet at field values of 30-55 kOe. Numerous open orbits were detected for magnetic field directions in the (110) plane that was studied. There are primary open orbits along <100> directions, secondary open orbits along <110> directions plus many higher order open orbits. Two-dimensional open-orbit regions were also observed. The results show that the γ Fermi surface sheet of ReO_3 is open along <100> directions as predicted by Matthiess[1] by an augmented plane wave calculation.

[1] L.F. Matthiess, Phys. Rev. 181, 987 (1969).

14:30
DC5 K-effect and Clustering in the Spin-glass System $(Pd_{0.5}Ag_{0.5})_{1-x}Fe_x$ Alloys. K.THYGESSEN, K.V.RAO & S.ARAJS* Clarkson Coll. and J.I.BUDNICK & T.J.BURCH, Univ. Conn.-- For some concentrations in alloys like Ag-Pd, Au-Pd etc., the elec. resis. is found to initially decrease and then increase with further straining. In Pd-Ag alloys, this well known K-effect dominates for a conc. range 30-60 at% Ag.[1] It is precisely in this matrix composition range that $(Pd_{1-x}Ag_x)_{0.99}Fe_{0.01}$ alloys exhibit a spin-glass behaviour In order to understand the role of clusters in these systems we have studied the strain-effect on the elec. resis. of $(Pd_{0.5}Ag_{0.5})_{1-x}Fe_x$ alloys for x= 0,0.005,0.01,& 0.02. Contrary to what is observed for the matrix, in alloys with Fe, the resistivity increases for small strains and then follows the matrix behaviour at larger strains. The magnitude of this initial increase in resistivity is found to depend on the Fe conc. We explain this to be the effect of the initial breaking of clusters (thus providing more scattering centers) dominating over those due to the competing mechanisms originating from the localized deformation potential and increasing defects.

* Supported by NSF.
1 W.H.Aarts & A.S.Houston-Macmillan, Acta Met. 5 525 1957
2 J.I.Budnick, V.Cannella & T.J.Burch, AIP Conf 18 307 1974

14:45
DC6 Skew scattering in the Spin Glass AuFe. S.P. McALISTER and C.M. HURD, Natl. Res. Coun. Can. - We have measured the anomalous skew component of the Hall resistivity of polycrystalline AuFe alloys in the spin glass regime, both as a function of applied field and temperature. The applied field perturbs the spin glass transition so that it is no longer sharp, but can be observed in fields ~0.1T.

15:00
DC7 Magnetic and Electrical Properties of non-ferro-Magnetic Ternary Cr-Fe-V system. K.V.RAO* L.HEDMAN, H. GUDMUNDSSON & H.U.ASTRÖM, Roy.Inst.Tech. Sweden.-- It has been suggested that Fe impurities in Cr, known to form local moments weakly coupled to the host, at conc. ~3 at% are antiferromagnetically arranged around 4K with a mag. moment considerably smaller ($1.4\mu_B$) than in its para-state ($2.2\ \mu_B$)[1]. In addition, Cr with Fe impurities >2 at% exhibit a large first-order jump in the elec.resis. Pressure studies on this system concluded that the nature of this magnetic transition is P-I-C type.[2] Our mag. Sus. and elec. resis. studies on Cr+3 at% Fe with additions of 0.5 & 1 at% V indicate: Addition of V sharply suppresses the I-C transition; the magnetic moment of Fe impurity remains a constant all the way down to 2K, while it is because a fraction of the Fe atoms, which are almost nearest-neighbours, are antiferromagnetically ordered below T_N, one observes the apparent difference in the magnetic moments between the paramagnetic and the ordered states.

* Permanently at: Clarkson College, Potsdam. N.Y.
1 Y.Ishikawa, R.Tournier & J.Filippi, J.Phys.Chem.Solids 26, 1727 (1965)
2 R.Nityananda, A.S.Reshamwala and A.Jayaraman Phys. Rev. Lett., 28 1136 (1972)

15:15

DC8 Transport Properties of Mo in High Magnetic Fields.* R. FLETCHER, QUEEN'S UNIV., Kingston, Ontario. --Previously obtained data on other compensated metals W and Cd[1-3] has, in some respects, not been in accord with theory. The present data was taken with the field parallel to [100] on a sample with RRR ∿ 5000 at fields up to 4T. The Nernst-Ettinghausen coefficient is again higher than expected and yields a density of states identical to that obtained from specific heat measurements. The two methods of extracting the lattice thermal conductivity provide results in substantial agreement with each other (unlike the case of W[3]). The magnetoresistivity does not increase as B^2. The slope is highest at rather low fields and decreases at high fields in a fashion similar to that of Fe[4] but not W or Cd.

1. R. Fletcher, J.L.T. Physics 22, 39-59, (1976).

2. R.J. Douglas and R. Fletcher, Phil. Mag. 32, 73, (1975).

3. R. Fletcher, Phil. Mag. 32, 565, (1975).

4. R.V. Coleman et. al., Phys. Rev. B8, 317, (1973).

15:30

DC9 Electrical Resistivity of Cr-Au and Cr-Pd Alloys from 77K to 700K.* A. EROGLU, S. ARAJS, K. V. RAO, and C. A. MOYER, Department of Physics, Clarkson College, Potsdam, N.Y. 13676.--Electrical resistivity (ρ) has been measured as a function of temperature (T) of binary Cr alloys containing 0.27, 0.54, 0.60 at.% Au and 0.99, 1.48, 1.99 at.% Pd. Au decreases the Néel temperature (T_N) linearly with a rate of 32K/at.% Au. The T_N vs Pd concentration curve has a small minimum followed by a maximum at about 1.5 at.% and a further more rapid decrease with higher Pd concentrations. The behavior of ρ and T_N will be discussed from the viewpoint of a two-band theory of itinerant electron antiferromagnets.

* Work supported by NSF.

TUESDAY, JUNE 15, 1976
ROOM 2B
Chairman: W.J.L. Buyers

POSITRONS

13:30

DD1 Measurement of the "Lamb Shift" of the first Excited State of Positronium*
S. BERKO, *Brandeis University*
The work of Canter, Mills, and Berko leading to the measurement of the fine structure of the first excited state of positronium will be reviewed. An efficient positronium formation technique was discovered,[1] using a slow positron beam incident on solid surfaces. Measurements of the $2\gamma/3\gamma$ annihilation-yield ratio indicate a positron-to-positronium conversion ratio of up to 80%. A small fraction of the positronium atoms were formed in the first excited state: single photons transmitted through a narrow interference filter peaked near the positronium 2430-A Lyman-α line were observed[2] in coincidence with the annihilation γ's of the ground state. Finally the $2^3S_1 - 2^3P_2$ energy splitting was measured by inducing rf transitions and observing a resonant increase in the Lyman-α emission.[3] The experimental result of 8628.4 ± 2.8 MHz is within three standard deviations of the theoretical value and confirms the $R\gamma\alpha^2$ radiative corrections to a few percent.

*Work supported by the National Science Foundation.

[1]K. F. Canter, A. P. Mills, Jr., and S. Berko, Phys. Rev. Lett. 33, 7 (1974).
[2]K. F. Canter, A. P. Mills, Jr., and S. Berko, Phys. Rev. Lett. 34, 177 (1975).
[3]A. P. Mills, Jr., S. Berko, and K. F. Canter, Phys. Rev. Lett. 34, 1541 (1975).

14:15

DD2 Designs for a New Positron Angular Correlation Machine.* R.J. DOUGLAS and A.T. STEWART, Queen's Univ., Kingston, Ont.-- The position-sensitive gamma ray detectors that have been "spun off" high energy physics offer a large improvement in the state-of-the-art of positron-annihilation angular correlation machines.[1] Our design for a high-resolution, two-dimensional angular correlation machine exploiting these detectors will be presented and discussed.

[1] A.P. Jeavons et al, I.E.E.E. Transactions on Nuclear Science, NS-22, 297 (1975).

14:30

DD3 The Future of Angular Correlation Measurements.* A.T. STEWART and R.J. DOUGLAS, Queen's Univ., Kingston, Ont.-- A wide range of interesting experiments will be made possible by the new types of angular correlation apparatus now being built. Some topics in the electron structure of metals and alloys, defect structures, positron dynamics and positronium in condensed phases will be mentioned.

14:45

DD4 A Positron Annihilation Study of Defect Recovery in Electron-Irradiated α-Zr. G.M. HOOD+, M. ELDRUP*, and O.E. MOGENSEN, Danish AEC, Roskilde, Denmark.-- The presence of vacancy defects in α-Zr, irradiated at room temperature with 1.5 MeV electrons, has been indicated by positron annihilation measurements. Isochronal annealing studies showed nearly continuous recovery up to 550°K for one grade of Zr. Purer specimens exhibited no measurable recovery below 450°K, which suggests this temperature as a lower limit to the free monovacancy migration temperature. This is equivalent to a vacancy migration energy of about 1.5 eV or higher. The recovery spectrum of the less pure Zr may be explicable in terms of a wide spectrum of interstitial mobilities.

+Permanent address: A.E.C.L., Chalk River Nuclear Laboratories, Ontario, Canada.

*Visiting at Queen's University, Kingston, Ontario, Canada.

15:00
DD5 Positron Trapping Rates in Various Defects in Metals. B.T.A. McKEE, Queen's Univ., Kingston.--Measurements of the positron decay spectra in well specified samples containing various defect systems have yielded values for the magnitude of the positron trapping rate and its temperature dependence. Vacancies, dislocations, grain boundaries and voids have been included. The information on the positron trapping rates and any temperature dependences can be used to gain further understanding of the trapping mechanism for positrons in metals. The values of positron trapping rates are also useful for determining the limit of sensitivity of positrons for trapping at various defects.

*Supported by the National Research Council of Canada.

15:15
DD6 Source Effects of Positron Annihilation in Copper.* N. K. DAVE and R. J. LEBLANC Univ. de Moncton, Moncton, N.-B. -- In order to observe the contribution of positron annihilating in the source material and its temperature dependence for a Na^{22} source deposited on nickel foil, positron lifetime and doppler broadened annihilation lineshape were measured in annealed samples of 6N purity copper for different source conditions. The lifetime results show that the second component is mainly due to annihilations in the source material whose value depends upon the thermal treatment of the source material. No appreciable effect is observed on lifetimes and annihilation lineshapes due to source supporting foil or the sample surface conditions.

*Supported by National Research Council and C.R.U.M.

15:30
DD7 Positron Annihilation in Heat Treated Alloy Steel.* R. J. LEBLANC, N. K. DAVE and R. L. BANERJEE, Univ. de Moncton, Moncton, N.-B. -- Positron lifetimes are measured in alloy steel samples annealed at 1450°F and on those tempered at various temperatures from 300° - 600°F. The tempered samples were previously temperature hardened by oil quenching from the austenizing temperature of 1550°F. The results show that the main lifetime component is dependent upon the relative concentration of the austenite phase. The effects of decrease in austenite concentration at higher tempering temperatures are compared with x-ray results[1].

[1]Studies of Retained Austenite in Heat Treated Alloy Steel. (To be published) R. L. Banerjee and B. L. Averbach.

*Supported by National Research Council and C.R.U.M.

15:45
DD8 The Effect of Positron-phonon Scattering on Positron Trapping at Defects in Metals. T. MC MULLEN, Queen's Univ.--A fully quantum mechanical theory of the influence of positron-phonon scattering on the trapping rate of positrons by defects in metals is discussed in an attempt to bridge the gap between the predictions of the quantum mechanical golden rule for freely propagating positrons and those of the classical diffusion picture. Nonequilibrium many-body theory is used to formulate the problem in order to include positron annihilation in a natural way, and the positron-phonon self-energy used is that given by lowest order perturbation theory. For weak trapping the result is the golden rule, although the initial positron distribution to be used includes the positron-phonon interaction. For stronger trapping, the effect of the trap on the surrounding positron distribution is included in calculating the probability that the positron annihilates from the trapped state. This produces a depletion of the positron distribution in the vicinity of the trap as time progresses, and the results are interpreted in terms of the shape and size of this depleted region.

TUESDAY, JUNE 15, 1976
Room 2D
Chairman: J. Beaulieu

OPTICS III-LASERS

13:30
DE1 Optically Pumped Far Infrared Lasers
J.R. IZATT, *Université Laval*

9:45
DE2 Laser Chimique HF Continu de dimensions réduites. L. BERTRAND et J.M. GAGNE. Ecole Polytechnique - Le laser chimique HF à onde continue réalisé au laboratoire d'optique de l'Ecole Polytechnique est présenté. Basé sur la réaction exothermique $F + H_2 \rightarrow HF^*(v) + H$ $v = 1, 2, 3$, il utilise les atomes de fluor produits par une décharge micro-onde dans un mélange SF_6 + He. L'axe optique est perpendiculaire aux flux des gaz réactifs qui forment entre eux un angle de 72°. La longueur du milieu actif est de 5 cm. Différents paramètres tels que générateur micro-onde, vitesse de pompage et mélange des gaz ont été étudiés. La puissance maximum obtenue est de 16 W pour une puissance uhf de 2200 W et un débit de pompage de 160 ℓ/s. L'efficacité chimique est alors de 3%. Le rayonnement se compose de 14 raies correspondant aux transitions Pv(J) de vibration-rotation de la molécule HF. Lorsqu'une cavité optique sélective est utilisée le laser fonctionne successivement sur 12 raies. Le gain non saturé de plusieurs transitions est de 0.11 cm^{-1}.

10:00
DE3 High Efficiency, High Illuminance Short Laser-Pulse Generation (F-RAAT).* P.A. BELANGER, LROL, Laval Univ. -- In a regenerative amplifier driven by a short injected pulse before the laser threshold (RAAT)[1,2] one of the mirror is changed for a focusing retro-reflector. This focusing device consists of a highly focusing lens (F) and a spherical mirror (R = F) enclosed in a vacuum chamber. The focus of the lens is at the center of curvature of the spherical mirror, this device (cat eye) is equivalent to a plane mirror. At each transit the short pulse is focused at the center of the chamber. After some transits the whole energy of the amplifier is drained and a high illuminance short pulse comes across the focus. This system is suitable for experiments on non absorbing gases (e.g. multiphoton ionisation) and even on saturable absorbing gases (e.g. isotope separation of SF_6). The possibility of synchronizing the injection of a solid target (e.g. x-ray generation, fusion experiment) at the focus will be discussed. A 15 cm^2 aperture system of 1.5 ns CO_2 laser pulse will be presented.

[1] P.A. Bélanger and J. Boivin, Digest of CLEA, IEEE.J. Quant. Electron., QE-11, no 9, 1975.
[2] P.A. Bélanger and J. Boivin. Can. J. Phys. March,1976.

10:15
DE4 High-Power Short Pulse Propagation in a Low Loss Regenerative Amplifier at 10.6 μm.* M. PICHE and P.A.BELANGER, LROL, Univ. Laval. -- Previous experiments on short pulse amplification by injection into a regenerative amplifier above threshold (RAAT)[1,2] used a low reflectivity (salt) coupling mirror. In this communication we present new results in which a high reflectivity mirror is used instead of the coupling mirror of the regenerative amplifier. The internal pulse is observed through the small hole used for injection. The experiment is performed with a 15 cm^2 aperture system. The effects of varying the total small signal gain and the nitrogen concentration will be shown. The first limitation to high power nanosecond pulse generation with this technique appears to be the optical breakdown inside the gain medium.

[1] P.A. Bélanger and J. Boivin, Digest of CLEA, IEEE J. Quant. Electron., QE-11, no 9, 1975.
[2] P.A. Bélanger and J. Boivin, Can.J.Phys. March, 1976.

* Supported by the National Research Council of Canada and the Education Department of Quebec.

10:45
DE5 Opération d'une Source Laser CO2-TEA Monomode Longitudinal pendant une Période Continuelle de Huit Heures. A. GIRARD, Gen-Tec Inc.--En insérant un laser CO2 continu (CW) à basse pression dans la cavité d'un laser CO2-TEA, nous obtenons une émission-laser monomode axial et transverse de même que monoraie dans un régime d'impulsion-laser de courte ou de longue durée. A partir d'un modèle fondé sur une approche similaire à celle de Gilbert et al.[1], mais tenant compte de la présence de l'amplificateur CW, nous proposons une description théorique détaillée de la sélection de mode dans un laser hybride CO2 CW-TEA. Nous en tirons les conditions nécessaires et suffisantes pour une émission monomode stable. L'application de ces conditions à un système expérimental a permis d'obtenir une émission-laser monomode pendant une période continuelle de huit heures, à un rythme d'une impulsion par seconde.

[1] J. Gilbert, J.L. Lachambre, F. Rheault et R. Fortin, Can. J. Phys. 50, 2523 (1972).

11:00
DE6 Single mode CO_2-laser pulses of high power.* J. MEYER, Univ. of British Columbia.-- Measurements of mode beating in pulses from a hybrid high pressure/low pressure CO_2 laser system show that the ratio of dominant over residual longitudinal mode intensities is an exponential function of the gain in the low pressure section. Ratios of better than 10^6 have been achieved. The maximum obtainable power from such a laser system however, is limited to powers of a few MW. Single longitudinal mode pulses of 200 MW can be achieved by seeding an unstable resonator cavity with pulses from a hybrid laser system. The results indicate that a ratio of dominant over residual mode intensities of better than 10^6 have been achieved.

*This work was supported by the Atomic Energy Control Board.

11:15
DE7 Contrôle de la Durée de l'Emission de Sortie d'un Laser CO2-TEA de 50 nsec à plus de 100 μsec. A. GIRARD, Gen-Tec Inc.--En ajustant la composition du mélange gazeux et les caractéristiques du résonateur, on montre expérimentalement et théoriquement que le même laser CO2-TEA peut émettre des impulsions de sortie d'une durée à mi-hauteur ajustable de moins de 50 nsec à plus de 100 μsec. Appliquée à différents types de laser CO2-TEA[1,2], cette technique permet d'en obtenir une densité d'énergie de sortie de plus de 3 J/litre pour une impulsion-laser de 100 μsec à mi-hauteur. Utilisée dans des interactions laser-cibles de métal et de plastique, cette impulsion de 100 μsec permet d'atteindre une efficacité d'extraction (gr/J) à pression atmosphérique égale à la limite supérieure observée dans le vide.

[1] M.C. Richardson, A.J. Alcock, K. Leopold et P. Burtyn, IEEE J. Quant. Electr. QE-9, 2 (1973).

[2] J.L. Lachambre, J. Gilbert, F. Rheault, R. Fortin, M. Blanchard, IEEE J. Quant. Electr., QE-9, 459 (1973).

11:30
DE8 Compression d'une Impulsion Laser par un Colorant Organique Fluorescent.* D. FAUBERT et S.L. CHIN, LROL, Univ. Laval..-- Une étude expérimentale et théorique a été réalisée sur la propagation d'une impulsion laser dans un colorant organique. On observe que l'énergie de la première partie de l'impulsion est emmagasinée dans les niveaux énergétiques du colorant, sous forme d'inversion de population. Lorsque la deuxième partie de l'impulsion interagit avec le milieu, elle est amplifiée par le processus d'émission stimulée. En plus de cette amplification, la largeur à demi-hauteur et le temps de montée de l'impulsion à la sortie du colorant s'en trouvent réduits. Un modèle théorique utilisant les équations d'évolution a été élaboré. Expérimentalement, on utilise un laser à Nd:verre et un crystal de deuxième harmonique KDP pour générer des impulsions de quelques nanosecondes (largeur à demi-hauteur) à 5300 Å que l'on propage dans l'uranine en solution dans la glycérine. Des résultats typiques montrent une largeur à demi-hauteur et un temps de montée de 2 à 3 fois plus courts.

* Recherche partiellement supportée par le Conseil National de Recherches du Canada.

11:45
DE9 Etude d'un Laser CO2-TEA à Décharges de Préionisation Multiples. A. GIRARD, Gen-Tec Inc.-- Nous presentons une nouvelle approche pour l'utilisation de la préionisation dans le laser CO2-TEA. Le contrôle du délai entre la préionisation et la décharge principale d'un laser à double discharge pointe-grille[1] permet d'utiliser différents mélanges gazeux (100% à 60% d'hélium, rapport CO2/(CO2+N2) de 1 à 0) et de fortes excitations (150 J/litre). L'addition d'une autre source de préionisation (type Lamberton-Pearson[2]) entraine une augmentation générale des performances (100% à 45% d'hélium, rapport CO2/(CO2+N2) de 1 à 0 et des pompages jusqu'à 200 J/litre) tout en utilisant un circuit de décharge fort simple et sans ajouter de gaz tampon dans le mélange. Nous proposons une explication qualitative basée sur la compréhension des différents processus de production et de perte électroniques dans le plasma-laser.

[1]M.C. Richardson, A.J. Alcock, K. Leopold et P. Burtyn, IEEE J. Quant. Electr. QE-9, 2 (1973).

[2]H.M. Lamberton et P.R. Pearson, Electr. Lett. 7, 141 (1971).

TUESDAY, JUNE 15, 1976
ROOM OB
Chairman: D.C. Baird

PHYSICS EDUCATION SYMPOSIUM

13:30
DF1 Physics Education: Some Personal Views
L. KERWIN, *Université Laval*

Towards Motivation and Mastery in Learning Physics

14:15
DF2 Gaming and Simulations as Motivators
G.M. BOYD, *Concordia University*

14:45
DF3 Cultural Influences on Physicists
C.S. KALMAN, *Concordia University*

15:15
DF4 Enseignement individualisé en physique à Laval
Y. CHASSE, *Université Laval*

15:45
DF5 The Unitary Transformation: The Keller Modular Approach to Teaching Physics
S.D. ROSNER, *University of Western Ontario*

16:15
DF6 Undergraduate Physics Curriculum - A Need for Fresh Outlook. SYED ZIAUDDIN, Laurentian Univ. Sudbury, Ontario. - The advantages and the disadvantages of the present undergraduate programs in physics are discussed. Alternatives are suggested to make physics more attractive and win the more able student to study physics.

16:30
DF7 High School Physics Education in Newfoundland and Labrador. H.C. WEIR, Memorial Univ., and W. WALSH, Bishop's College, St. John's, Newfoundland.--The history of high school physics education in Newfoundland and Labrador is traced, and the contributions of various groups, including the Canadian Association of Physicists, are examined. The present course is described, and the extent of teacher and student dissatisfaction with it is assessed. Several potential replacement textbooks have been evaluated; the results are presented, along with a description of the evaluation criteria used, and the techniques employed. The paper concludes with a look, albeit speculative, at the future of high school physics education in this province.

TUESDAY, JUNE 15, 1976
ROOM 2C
Chairman: R.R. Haering

13:30
DG1 The Conduction Band of Deformed Zinc Blende III-V Semiconductors. W. HOWLETT and S. ZUKOTYNSKI, Univ. of Toronto. - The effect of deformation on the dispersion relation of the conduction band in the zinc-blende III-V semiconductors has been analysed. The conduction band eigenstates in the undeformed material are those given by Kane's $k\cdot p$ perturbation theory, namely k-dependent linear combinations of the s and p-like states at the centre of the zone. The interaction matrix describing the effect of deformation is calculated in the s-p manifold, and then diagonalized within the doublely degenerate conduction band eigenstates for the undeformed crystal. Thus the deformed energy spectrum contains as parameters the deformation potentials of the s and p states at the centre of the zone. Furthermore, the deformation produces non-uniform energy shifts as one goes deeper into the band, an effect which must be considered in the determination of the transport properties of deformed, degenerate n-type materials. This method has proven to be analytically simpler than previous calculations which attempted to diagonalize the combined $k\cdot p$, spin orbit and deformation interaction within the 8 fold manifold of conduction and valence band states at $k = 0$. The splitting of the conduction band degeneracy by the deformation is also considered.

13:45
DG2 Calculation of the Ideal Resistivity of K and Na. ROGER TAYLOR and C.R. LEAVENS, Phys. Div., N.R.C., Ottawa and R.C. SHUKLA, Brock University--The phonon-limited ideal resistivity has been computed over a substantial range of temperatures (2K to melting for K and 20K to melting for Na) employing a first principles calculation of the form factor and phonon spectrum. No parameters were adjusted to fit experimental data, yet the agreement obtained with experiment is very good. The phonon frequencies were calculated using the Dagens et al[1] model potential and the Geldart and Taylor[2] screening. The form factors were calculated using the same model potential and screening as well as the non-local electron-electron vertex correction of Rasolt.[3] Our results suggest that phonon drag may not be a significant effect in K even at 2K.

[1]L. Dagens, M. Rasolt and R. Taylor, Phys. Rev. B 11, 2726 (1975).
[2]D.J.W. Geldart and R. Taylor, Can. J. Phys. 48, 167 (1970).
[3]M. Rasolt, J. Phys. F 5, 2294 (1975).

14:00
DG3 First Principles Calculation of the Electronic Contribution to the Thermal Conductivity of Potassium. C.R. LEAVENS and ROGER TAYLOR, Phys. Div., N.R.C., Ottawa--Recently Shukla and Taylor calculated the electrical resistivity of potassium using a fundamental description of the lattice dynamics and electron-phonon coupling and obtained very good agreement with experiment. Precisely the same description has been used to calculate the electronic thermal conductivity of potassium from 1 to 330K. When the correct energy dependence of the electron distribution function is incorporated in the calculation, very satisfactory agreement with experiment is obtained.

14:15
DG4 Calculation of the Volume and Temperature Dependence of the Electron-Phonon Mass Enhancement of Potassium and Sodium* MARTINUS VAN DER SCHANS and R.C. SHUKLA, Brock University--The renormalized effective mass of the electron due to the electron-phonon interaction (λ) in potassium and sodium has been computed over a wide range of temperature and volume employing a fundamental calculation of the form factor and the phonon spectrum. It was found that the ratio of λ at finite temperature to that at 0°K, $\lambda(T)/\lambda(0)$, reached a maximum in the range $0 < T < 50$°K for sodium and $0 < T < 30$°K for potassium. With increasing volume there was a slight increase in the maximum and the entire curve shifted towards the lower temperature.

* Work supported by National Research Council of Canada

14:30
DG5 Some Model Calculations of the Electrical Resistivity of Liquid Titanium.* J. R. Todd**, and J. S. Brown, Univ. of Vermont, U.S.A. -- Calculations are presented of the electrical resistivity of molten Ti based upon the construction of a variety of muffin-tin potentials incorporating exchange-correlation in different ways and treating the influence of neighbors in two approximations of physical influence, namely the fcc 14-neighbor approximation of Mattheiss and the RFA (renormalized free atom approximation). The ion core potentials are built from Hartree-Fock-Slater atomic wavefunctions for the configuration $(3d)^3(4s)^1$. The resistivities are based upon the recent Evans, Gaspari, Szabo, Ziman (1973) T-matrix extension of the Ziman model, using experimental structure factors from x-ray studies of Waseda (1975). Exchange-correlation is treated in the Slater, Kohn-Sham-Gaspar, and Hedin-Lundqvist approximations. Trends are discussed based on these models.

* Research supported under Contract No.ERDA (11-1)-3551 by the United States Energy Research and Development Administration.
** Based upon research submitted by J. R. Todd in partial fulfillment of the M.S. degree.

14:45
DG6 The Band Structure of Cadmium Arsenide at Room Temperature. J.P. JAY-GERIN[1], M.J. AUBIN and L.G. CARON, Groupe de recherches sur les Semiconducteurs et les Diélectriques et Département de Physique, Université de Sherbrooke, Sherbrooke, Québec.
Electron effective mass values obtained from room-temperature magneto-Seebeck and Hall measurements on Cd_3As_2 have been gathered from the literature. Using Kane's model for an α— Sn type inverted band structure, the dispersion relation for the conduction band has been obtained along with a $\Gamma_6 - \Gamma_8$ energy gap of 0.19 eV. Combining these results with the available room-temperature optical data, the relative positions of other bands have been obtained. The heavy-hole valence band whose maximum is displaced from Γ by $\sim$ 10% of the distance to the Brillouin zone edge has a possible small overlap with the conduction band. The energy separation between the minima of the two conduction bands at Γ is 0.4 eV. The proposed band structure is shown to be consistent with all available data.

[1]. On leave of absence from Centre de Recherches sur les Très Basses Températures, C.N.R.S. and Service Basses Températures, Centre d'Etudes Nucléaires, Grenoble, France.

15:00
DG7 The Influence of the Magnetoresistance in the Field Modulation Technique. P. L. LI, B. HOYT, B. E. PATON, Dal. Univ. - In the field modulation technique, the induced voltage is only a function of the magnetization modified by a simple Bessel function provided the modulation field $h_0 \cos \omega t$ completely penetrates through the sample and there is no complication due to the sample magnetoresistance (MR). When magnetic breakdown occurs, the normal MR is saturated and the oscillatory part is greatly enhanced. In this case, the induced voltage will also be a function of the MR as well. Theoretical caluclations from Maxwell's equations indicate that the quadrature signal is proportional to the magnetization as above and the inphase signal will contain a mixture of magnetization and MR oscillations in the first approximation. Experimental studies in Zn needle Fermi surface, using field modulation technique, indicate that the primary contribution is due to the MR rather than the magnetization. For $\omega > 70$ Hz, the inphase signal dominates and scales as ω^2 In agreement with the theoretical calculations.

15:15
DG8 Application of cubic-harmonic expansions in LCAO type calculation in solids. K.S. SONG and K.L. MALWAL, Dept. of Physics, Univ. of Ottawa.--The problem associated with the evaluation of large number of multicenter integrals required in a LCAO type calculations of energy bands or defect calculation of solids is treated along a new approach. Instead of evaluating the integrals individually, a matrix element of the hamiltonian is handled en bloc. The wave functions (LCAO) and the crystal potential are expanded in a series of cubic harmonics around a fixed center, thereby reducing a matrix element into one single radial integration. Combined with LCAO constructed from Gaussian-type-orbitals, this method gives excellent results in energy band calculation of Li[1]. Application of the present approach to calculation of defects in solid, such as F center in alkali halides, is under way.

1) K.S. Song and K.L. Malwal, Phys. Rev. B15 (May 15) 1976.

15:30
DG9 Electronic Band Structure of Tungsten by Empirical Pseudopotential Method. C. GUHA SRIDHAR, NASA-Ames Research Center, J.F. ALWARD and C.Y. FONG, U. C. Davis, California. --- The electronic energy band structure of the transition metal tungsten is obtained by fitting a nonlocal empirical pseudopotential to optical reflectivity data. The calculated reflectivity spectrum of tungsten shows good agreement up to 5 eV with the experimental results of Weaver, Olson and Lynch[1]. The band structure, the imaginary part of dielectric constant, the reflectivity spectrum and the Fermi energy will be presented. The results will also be compared with available APW calculations.

[1] J. H. Weaver, C. G. Olson and D. W. Lynch, Phys. Rev. B 12, 1293 (1975).

15:45
DG10 A Dynamical Theory of Vacancy Diffusion. LEON GUNTHER, Tufts U.--We have developed a theory for describing diffusion in solids via vacancies. The approach allows us to follow diffusion over time scales comparable to the mean jump time. Thus we are able to study the effect of vacancy diffusion on experiments, such as the Mossbauer effect, which can probe this short time regime and for which previous theories[1] which describe the long time behavior alone are inappropriate. The theory reveals the existence of diffusive modes which are analogous to the acoustic and optical modes of lattice vibrations.

[1]For example, K.S. Singwi and A. Sjolander, Phys. Rev. 119, 863(1960).

16:00
DG11 Vibrational Coupling of 2s and 2p States of the F Center in KCl.* J. M. DEKLE and R. H. BARTRAM, Univ. of Conn.--Ham's vibronic model for the relaxed excited state of the F center involves the coupling of nearly degenerate 2s and 2p electronic states by odd-parity (Γ_4^-) vibrational modes.[1] Actually, the electron-lattice interaction involves very many modes, but it can be represented approximately in terms of a single set of modes with an effective coupling constant and effective frequency.[2] Preliminary values of these quantities for KCl have been calculated by a Green's function method from an empirically parametrized breathing-shell model of the lattice dynamics,[3] and point-ion model wavefunctions, and are compared with values inferred from a variety of experiments.[1]

*Supported by NSF Grant No. DMR 74-02604

[1]F.S. Ham, Phys. Rev. B8, 2926 and 2945 (1973).

[2]M.C.M. O'Brien, J. Phys. C: Solid State Phys. 5, 2045 (1972).

[3]J.R.D. Copley, R.W. Macpherson and T. Timusk, Phys. Rev. 182, 965 (1969).

16:15
DG12 New Energy-Momentum Calculation for the Free Frohlich Polaron. Y. LEPINE and D. MATZ, Université de Montréal. We have calculated the energy-momentum dependence of a free, large polaron, by employing a new theory[1], which is valid and manifestly translationally invariant for all coupling strengths. The equation of motion of this theory includes the Fock approximation and renormalized vertex corrections in a non-perturbative way. Furthermore, for the ground state energy the equation is variational, and we obtain an approximation to the latter by use of a gaussian trial spectrum. (1) We find a stable energy momentum curve for values of energies larger than one phonon energy above the zero momentum ground state. This is due to the correlated behaviour of those virtual phonons which in other theories give rise to spontaneous emission, to form internal bound states. Their spontaneous emission is therefore inhibited for translational motion. (2) We also find a first order phase transition at some critical momentum, at which the polaron dynamics switches to a phase described by a theory of Matz and Burkey[2], which included the Fock approximation only.

1. D. Matz, Can. J. Phys. 51, 1187 (1973)
2. D. Matz and B. C. Burkey, Phys. Rev. B7,3487 (1971)

16:30
DG13 Equivalence of the Feynman and Green's Function Fock Approximation Solutions to the Polaron Ground State Energy. D. MATZ, G. BADER, and J. MALEBRANCHE, Université de Montréal. By using a new dynamical theory of the large (Frohlich) polaron problem[1], we have succeeded in showing that the "translational invariant" variational path-integral solution for the ground state energy of the large polaron given by Feynman[2], incorporates only the dynamics of the Fock approximation of a polaron nonperturbative Green's function theory. The absence of vertex corrections in Feynman's solution, and the fact that his solution to the Fock approximation gives a lower ground state energy than that given elsewhere for the Fock approximation[3], raises some intriguing questions, which will be discussed.

1. D. Matz, Can. J. Phys. 51, 1187 (1973)
2. R. P. Feynman, Phys. Rev. 97, 660 (1955)
3. D. Matz, Can. J. Phys. 53, 2665 (1975)

16:45
DG14 Interface states of one-dimensional crystals. L. Andrade, E. Uribe. Facultad de Ciencias-Universidad Nacional Autonoma de Mexico.- Energy levels at the interface of two different one-dimensional semi-infinite crystals in close contact are calculated by means of the scattering matrix method of Saxon and Hutner. Localized interface energy levels with wave functions exponentially damped away from the interface, can occur under certain conditions. We also did analogous calculations for two different crystals, both contaminated by an impurity atom.

TUESDAY, JUNE 15, 1976
ROOM 1A
Chairman: C. Keen

13:30
DH1 Definition of the Lower Crust by Measurement of Surface Wave Group Velocities. AUBREY FRICKER C.A.P. - Surface wave measurement offers a relatively economic means to study the lower crust. Group velocities can be measured to better than 0.01 km/sec. and with well understood measurement covariance between the individual data. This is a sound basis for linear inversion. The thickness of the crust can only be determined within eight kilometers. Velocities can be determined to within one percent, but represent an average over a range of depths. The resolution ranges from less than 5km in the upper crust to about 10km in the lower crust and upper mantle. The most serious limitation of group velocity measurement is that the path length required is unlikely to fit a simple model. Studies on two lines in the Canadian Shield show the importance of critical interpretation.

13:45
DH2 Isostatic Adjustment of the Sverdrup Basin to Sediment Loading. J. F. SWEENEY and CHRISTOPHER BEAUMONT, Earth Physics Branch, Ottawa and Dal. Univ., Halifax. The stratigraphy of the Sverdrup Basin demonstrates three phases of subsidence, late Paleozoic (330-225 mybp), early Mesozoic (225-124 mybp) and late Mesozoic (124-74 mybp). During these phases of exponentially decaying rates of subsidence, the periphery of the basin experiences mild uplift that migrates inward toward the basin centre, suggestive of the response of a viscoelastic lithosphere overlying an inviscid asthenosphere. Viscoelastic beam theory is used to estimate the effective viscosity of the lithosphere during these phases of subsidence. A comparison is made with Walcott's (1970) estimate of the time dependence of the apparent flexural rigidity of the lithosphere. The general applicability of the viscoelastic beam model to the response of the Earth to surface loads is critically examined in view of other processes, for example, changes in the geothermal gradient and phase changes at depth, which may be important in determining the rate of isostatic adjustment.

Walcott, R.I., J. Geophys. Res. 75, 3941, (1970)

14:00
DH3 The Thermal Regime of Downwarped Lithosphere and the Effect of Varying the Subduction Angle. L.J. SYDORA, F.W. JONES and R.ST.J. LAMBERT, University of Alberta - The local temperature regime of a downgoing slab is considered by using a quasi-dynamic numerical approach. A general computer program in which the dip angle of a two dimensional slab may take any arbitrary value or may change with depth is used to investigate the thermal regimes of various slab configurations and the associated heat flow at the surface. The model assumes a simple shear mechanism for the descent of the lithosphere into the mantle, which is consistent with the known stress pattern in subduction zones.

14:15
DH4 Crustal Cross-sections: Evidence from Seismic Velocities in Rocks D. FOUNTAIN (U. Mont.), M. SALISBURY (SUNY,Binghamton), N. CHRISTENSEN (U. WASH.)-- A cross-section of the oceanic crust based on ophiolites (e.g., Bay of Islands) and DSDP and dredge haul data show Layer 2 to consist of basalts underlain by metabasalts (zeolite to greenschist) with metagabbros (greenschist to amphibolite) comprising the top of Layer 3. The remainder of Layer 3 is gabbroic on top of a peridotite mantle. A section of continental crust, based on unique surface exposures of deep crustal levels (e.g., Ivrea Zone), diatreme xenoliths and general properties of high grade metamorphic rocks, shows considerable lateral and vertical variation in chemical composition (with mafic rocks generally at lower levels) and an increase in metamorphic grade with depth (greenschist at shallow levels increasing to granulite at depth). This entire metamorphic sequence overlies a peridotite mantle. Seismic velocities of rocks from each sequence are compatible with the known structure of the crust. Although thicknesses and overall chemical composition varies for continental and oceanic crust, the seismic structure in both is, in large part, determined by the nature of metamorphism within the sequence.

14:30
DH5 Forty-Five North Revisited. M.J. KEEN. Geology Dept., Dalhousie Univ., Halifax, N.S. - The Mid-Atlantic Ridge at 45°N is still one of the few regions of the world's ocean ridge systems studied in considerable detail. However, since the completion of the greater part of the work in that area a number of studies of the crestal regions of other ridges - some spreading quickly, some slowly - have been made. Consequently I will attempt to consider the results of the studies at 45°N in a global context, concentrating pargicularly upon the significance of the seismic work and the bathymetry upon the structure of the crust and uppermost mantle.

14:45
DH6 Traveltime and Amplitude Interpretation of a Marine Deep Seismic Sounding Survey S.J. MALECEK* and R.M. CLOWES Univ. of B.C., Vancouver - A two-ship marine seismic system for recording near-vertical incidence to wide-angle reflected waves and refracted waves with penetration from the ocean bottom to the upper mantle (deep seismic sounding or DSS) has been developed. In 1974, two reversed 75 km DSS profiles were recorded in the Explorer Ridge region of the NE Pacific, one parallel and the other perpendicular to the ridge. Data recorded at distances beyond 4 km were stacked, filtered, statics- and amplitude-corrected before compilation as record sections. An initial model from first arrival data was altered until an amplitude and traveltime fit was obtained by comparison of the observed data with synthetic seismograms. This interpretation required the introduction of velocity gradients. The profile run across the ridge showed no anamalous behaviour as the ridge was crossed; the profile on the Juan de Fuca plate, paralleling the ridge, exhibited traveltime branch offsets and delays. These have been interpreted as due to faulting.
*Now at Mobil Oil Corp., Denver, Colorado.

15:00
DH7 Application of Asymptotic ray theory to seismic body waves in anisotropic media. F. HRON and P. DALEY, Institute of Earth and Planetary Physics, University of Alberta-- Asymptotic ray theory has been applied to the propagation of seismic body waves in anisotropic homogeneous layers. General formulae have been simplified for a special case of transversely isotropic layers in the program for the computation of synthetic seismograms. A high degree of efficiency in computation has been achieved due to the concept of dynamic and kinematic analogs used in partial ray expansion.

15:15
DH8 Resonance Absorption of Gravitational Radiation in the Earth's Crust* - OLIVER G. JENSEN, McGill Univ. -- The theory of resonance absorption of plane gravitational waves incident on a layered earth has been developed and applied to various earth crustal models. In comparison with a homogeneous earth,(1) crustal layering is found to enhance, greatly, the radiation generated seismic surface motions at certain resonant frequencies. Under certain conditions, the resonance quality Q is limited only by the absorption of elastic energy in the earth materials. It appears that well located seismographs could provide an effective means of detection of gravitational waves.

(1) Dyson, F., Astro phys. J. 156, 529 (1969).

*Supported by NRC.

15:30
DH9 Current Trends in Canadian Seismic Risk Analyses and their Uncertainties. D.H. WEICHERT, Earth Physics Branch, E.M.R. - The Canadian Building Code has contained earthquake provisions for some time and the Milne-Davenport risk calculations have become routinely accepted. Recently, the concern for nuclear power plant safety has renewed the interest in seismic risk in Canada as well as elsewhere. Because of the low risk levels generally demanded for nuclear power plants, the older approaches have been critically reexamined and new techniques sought. Although all analyses involve parametric extrapolations, non-parametric statistics should really be used to discuss the uncertainties of these seismic risk estimates. To arrive at building design parameters, the uncertainties in the methodology of the risk calculation must be further compounded with uncertainties in earthquake magnitude determination and regional seismic wave propagation. The complexities of near-source strong motion seismology will be illustrated with recent experiences from the Guatemala earthquake.

15:45
DH10 Deformation of Porous Elastic Solids by R.J. WITHERS and E. NYLAND, I.E.P.P., U.of A. - The problem of deformation and stress build up in a porous elastic solid is described. The solution is shown to be solveable by transform methods for a general loading history and results are presented. For other than the layered space it is necessary to use variational techniques and the lagrangian is given. The solution is thus amenable to finite element techniques.

16:00
DH11 A Variational Approach to Shear Heating by E. NYLAND and T.SPANOS, I.E.P.P, U.ofA.- Approximate solution of the coupled Navier - Stokes - heat flow equations can be done by methods originating in the calculus of variations. The solution for viscous shear for viscosity is of geophysical interest. We illustrate the interaction of thermal gradients, shear fields and inhomogeneities in this shear heating problem. The approach can be generalized to multiphase flows.

16:15
DH12 Variations on Lithospheric Thickness . D.S. CHAPMAN, Univ. of Michigan - The base of the lithosphere is identified as the depth at which the geotherm attains a specified fraction of the depth-dependent mantle melting temperature. Such a thermal definition of the lithosphere-asthenosphere boundary is equivalent to an iso-viscous rheological definition. By relating geotherms parametrically to surface heat flow through the use of steady state heat flow-heat production models for continents and time dependent cooling models for oceans, estimates may be made of the regional variation of temperature with depth, and hence of lithospheric thickness. Such estimates made from heat flow data are in good agreement with lithospheric thickness estimates derived from seismological data. In particular, the lithosphere is seen to thin systematically westward from the Canadian Shield to the Canadian Cordillera. Temporal changes in the thermal models dictated by decay of heat sources indicate that the lithosphere under the Canadian Shield was thinner by a factor of three or more

16:30
DH13 A Variational Approach to Long Period Earth Oscillations. D. E. SMYLIE, York Earth Sciences and A.C.I.G. - The use of Hermite cubic splines pioneered by Wiggins, Buland and Gilbert in variational solutions to Earth oscillation problems has been extended to the Coriolus coupled case. This permits the calculation of eigenperiods for free oscillations on a rotating Earth with periods close to a day which are otherwise intractable. Study of inertial oscillations, wobble and core undertone modes then becomes possible. A summary of recent progress on this problem will be given.

16:45
DH14 Deep Drilling Reveals the Complexities of the Physical Properties of the Oceanic Crust. F. AUMENTO, Department of Geology, Dalhousie University, Halifax, Nova Scotia, B3H 3J5. Deep penetration of the oceanic crust on the Mid-Atlantic Ridge, on the islands of Bermuda and Sao Miguel, Azores, have shown that the physical properties (magnetic, seismic and heat flow) of the upper part of the oceanic crust are at least as complex as might have been expected from a continental environment. Indeed, had such detail been available to us at the beginning of our oceanographic investigations we might have had extreme difficulty in formulating the very effective hypotheses of the composition of the oceanic crust, of sea floor spreading and of plate tectonics. However, we are now in a position to ratify some of the assumptions used, and to show how the sum effect of the complex properties of the oceanic crust correlates with the geophysical models in vogue.

17:00
DH15 High Pressure Geophysics, Piezomagnetism, and Magnetic Properties of the Crust and Upper Mantle

R. S. CARMICHAEL and J. KIM, Dept. of Geology, Michigan State University, East Lansing, Michigan USA

-- Rock properties are affected by conditions of confining pressure and directed (tectonic) stress in the crust and upper mantle. High-pressure experiments are underway with a nonmagnetic chamber capable of pressures to 10 kilobars, simulating conditions to a depth of 30 km. Initial work concerns magnetic properties--remanent magnetization, susceptibility, and anisotropy--of magnetite and rocks. There are reversible and irreversible stress-induced changes. Geophysical applications are in geopiezomagnetism for earthquake prediction, paleotectonics, interpretation of deep-seated magnetic anomalies, and geodynamics.

DH 16

13:30
DI1 Flow Effect Between Moving Arc and The Ambient Gas. B. JEAN, HUU-HUNG MAI and G. ABEL, INRS-Energie, U. du Québec. -- A simple differential interferometer[1] is used, in conjunction with high speed photography, to observe the passage of a magnetically driven arc in air at atmospheric pressure. A careful correlation between interferometric and photographic results reveals the existence of a zone of refractive change in the gas immediately preceding the visibly luminous region of the subsonic arc. A presentation will be made of apparent changes within this refractive zone as a function of arc current.

(1) U. Kogelschatz, Applied Optics, Vol. 13, No. 8, pp 1749 (1974).

13:45
DI2 Double-Slit Streak Photography of Arc Motion.

HUU-HUNG MAI, B. JEAN and G. ABEL, INRS-Energie, U. du Québec. -- The role played by cathode and anode roots in the propagation of a magnetically driven arc is elucidated by the simultaneous streak recording of both regions on the same photograph. Two parallel slits, at the anode and cathode rail surface respectivelly, are imaged onto the recording plane of the high speed camera. Streak photographs of the interaction between the arc and a transverse air jet are interpreted in terms of arc root motion at both electrode surfaces across the air barrier. An extension of this recording method is suggested using fibre optics bundles.

14:00
DI3 Distribution de quantités électriques et magnétiques dans la section d'un arc soufflé. D. BHATTACHARYYA, R. BOLTON et M.G. DROUET, Direction Sciences de base, IREQ, Varennes, Québec, Canada, J0L 2P0 -- A l'aide de deux techniques expérimentales distinctes, on mesure les profils, longitudinal et latéral, de courant dans un arc de 700 A, brûlant dans l'air ambiant et soufflé à 165 m^{-1} par un champ magnétique transversal de 700 G. Les électrodes de cuivre sont espacées de 1.6 mm. A partir des profils, on obtient les contours de densité de courant par une inversion numérique, ce qui permet le calcul du champ de force j x B de striction et de soufflage dans la section de l'arc. Une expansion en moments a été développée pour faciliter ce calcul.

14:15
DI4 Magnitude of Corona Point Discharge Current.* SEVILLE CHAPMAN, Buffalo, New York.--The magnitude of corona point discharge current is calculated by an approximate quantitative theory. Using plausible values for one adjustable constant, current i agrees exactly with experiment. For an isolated point of potential V_p in a wind of speed w, $i = 1.315\epsilon_o w(V_p - V_{op})$, (Eqn. I), or for a point of height h in an ambient field E_o $i = 3.9\epsilon_o kE_o(V_p - V_{op})$, (Eqn. II), where $V_p = E_o h$, ion speed v is w or kE_o depending upon circumstances, k is ion mobility, and V_{op} is a starting voltage. The model involves a space charge sphere of radius $r_s = 1.44kV_p/4v$ plus a downstream space charge cylinder, and explains the variation of current, or lack of it, with point potential, ambient field, polarity, ion mobility, wind speed, geometrical factors, and altitude as it affects mobility and the plasma about the point. One consequence of the variation of r_s is that many points on a tower in a weak field and strong wind can yield many times the current of one point, whereas the same array in a strong field under a thundercloud or in light wind may yield no more, possibly less, current than one.
*This work is supported by the Office of Naval Research.

14:30
DI5 Hypersonic Shock Generation and Propagation Through Gas-Solid Suspension.* L. BERNIER, J.M. GUAY and K. DIMOFF, INRS-Energie, U. du Québec--Refinements in recording techniques and discharge switching[2] confirm improved performance of a thermoelectrically driven shock generator[3] when an auxiliary exploding wire circuit governs diaphragm rupture before onset of the main discharge[4]. Increased apparent shock speeds and enhanced shot-to-shot reproducibility are observed. The effect of the exploding wire on electron density profiles in the shock-heated zone is explored by 70GHz microwave interferometry. Comparison is also made with hypersonic propagation through a suspension of solid nickel microparticles (30μm mean diameter) in argon (<5 Torr). Preliminary results of microparticle bonding on a metallic surface by reflected shock will be presented.

[1]G.Saint-Hilaire, J.M. Guay and K. Dimoff, J. Phys. E., 8, 277 (1975).
[2]Idem, Rev. Sci. Instr. 45, 7471 (1974).
[3]M.G.R. Philips and F.L. Curzon, Can. J. Phys. 49, 1982 (1971).
[4]K.Dimoff and B. Jean, Phys. in Canada, 29, no 4, p. 15 (1973).

14:45
DI6 RF-Floated Electrostatic Probes in RF-Produced Plasmas*, R.R.J. GAGNE and A. CANTIN, Laval Un.- When electrostatic probes are used in rf-produced plasmas it is essential, in order to obtain correct estimates of electron temperature (Te) and charge density (Ni), that no or negligible rf voltage be present across the plasma-probe junction. A new technique has been devised[1] which forces the electrostatic probe to follow the rf potential of the plasma to within 0.1V p-p. Measurements in argon, over a range of pressures from 10 μHg to 5 Torr, have shown that Te in an rf discharge is not higher than in a dc discharge and is very likely determined by free-fall losses rather than ambipolar diffusion losses as is generally believed (for values of $pr \lesssim 20$ Torr -cm). This behavior agrees with published results as determined by microwave radiometry and spectral-line intensity. The rf-floated probe technique also made it possible to obtain ion current curves which, unaffected by rf voltage, permit the obtention of reliable estimates of charge density using the appropriate probe theories.

(1)R.R.J. Gagné and A. Cantin "Electrostatic Probe Behavior in weakly Ionized rf Plasmas", Final Report to Defence Research Board.on Grant No. 9510-63.

15:00
DI7 The Surfaguide: A Waveguide Plasma Source Using Surface Waves. M. MOISAN, V. GLAUDE, P. LEPRINCE*, G. MITCHEL, Z. ZAKRZEWSKI**, Université de Montréal. A R.F. structure, made from standard waveguide elements, is used to generate long columns of plasma by propagating m=0 surface waves. Two sources have been studied, one in the S-band(2.45GHz) and the other in the X-band (10.3GHz). In the first case, the principal goal was to achieve an efficient transfer of high R.F. power to plasma. We have obtained a 10mm-diameter H_2 plasma column 115cm long with density in excess of $10^{12}cm^{-3}$ by coupling 96% of 2.4 kW CW at 0,5 Torr. In the X-band experiment the aim was to create high density plasma in capillary tubes up to atmospheric pressure. The general characteristics of the plasma column produced by a waveguide structure seem to be the same as those of the surfatron(1). The ionisation rate is higher because of the higher excitation frequency.

* Université Paris-XI
** Polish Academy of Sciences

(1) M. Moisan, V. M. M. Glaude, Z. Zakrzewski, paper presented at this meeting.

15:15
DI8 Some properties of an Unmagnetized Plasma Column Sustained by a Surface Wave*. M. MOISAN, V. M. M. GLAUDE, Z. ZAKRZEWSKI**, Université de Montréal. It has been shown before (1) that the surface wave launched by an appropriate microwave device is able to sustain a long unmagnetized plasma column. To determine the mechanism of wave propagation and the structure of the column, measurements of axial distribution of the electron density and also of the amplitude and wavelength of the surface mode were performed. The results show the existence of regions of distinctly different properties. A self-excited parametric instability was studied. Both the discrete and noisy spectra of ion modes associated with this instability were observed, depending on the conditions of generation of the instability.

* Supported in part by the National Research Council of Canada.

** On leave from Polish Academy of Sciences.

(1) M. Moisan, C. Beaudry, P. Leprince, IEEE, Trans. on Plasma Sci. PS-3, 55-59 (1975).

15:30
DI9 A Comparison of Saturation Concentrations of Metastable States of Argon in a Positive Column and in a Surfatron-type R.F. Discharge. M. MOISAN and A. RICARD+, Université de Montréal. It is known that a saturation appears in a positive column when one increases the discharge current: beyond a certain point the metastable concentration becomes independent of the current, reaching a saturation point. One sees a similar process, depending on the R.F. power, in a surfatron-type discharge. However in this case the saturated concentration of $3p^54s$ obtained (via the absorption method) between 0.02 and 0.4 Torr (26 mm.-diameter tube) are at least twice as high as those obtained in a positive column of the same diameter at the same pressure. Between 0.4 and 1 Torr, the concentrations in both discharges seem the same. This increase in the saturation concentration may be due to a difference in the radial density profile and in the energy distribution of the electrons between the two types of discharge. A surfatron discharge, as well as being stable, (for example, absence of striations) could therefore permit an increase in gain of certain gas lasers.

+ Laboratoire des Plasmas, Université Paris XI 91405-Orsay, France

TUESDAY, JUNE 15, 1976
16:45

ANNUAL BUSINESS MEETINGS

ROOM:			CHAIRMAN:
	2B	Division of Aeronomy and Space Physics	D.J. McEwen
	1B	Division of Atomic and Molecular Physics	T. Oka
	1A	Canadian Geophysical Union - A Joint Division of CAP/GAC	D.I. Gough
	2A	Division of Condensed Matter Physics	D.R. Taylor
	1C	Division of Nuclear Physics	J.B. Warren
	2D	Division of Optical Physics	C. Richard
	2F	Division of Particle Physics	H.C.S. Lam
	0B	Division of Physics Education	D.C. Baird
	2E	Division of Plasma Physics	A.J. Alcock
	2C	Division of Theoretical Physics	R.T. Sharp

TUESDAY, JUNE 15, 1976
ROOM 0B
Chairman: M. De Celles

L'ENSEIGNEMENT DE LA PHYSIQUE AU QUEBEC

19:00
DJ Partie I: Méthode d'enseignement aux niveaux secondaire et collégiale
Partie II: Table ronde sur les programmes de physique au Québec

WEDNESDAY, JUNE 16, 1976
ROOM 1B
Chairman: P. Depommier

9:00
EA1 β^+-Decay of ^{106}In.* H. HUANG, J.K.P. LEE, B.P. PATHAK, McGill University.--The levels of ^{106}Cd populated in the decay of the two isomers of ^{106}In have been investigated using β- and γ- spectroscopy measurements. The half-lives of the two isomers of ^{106}In have been established to be 5.2 ± 0.2 min and 6.1 ± 0.1 min, respectively, and their spins are deduced. The sequence of levels in ^{106}Cd show the usual trend of $J^\pi = 0^+, 2^+, 4^+, 2^+$ characteristics of this mass region. The observed energy spacings and the γ-decay properties are discussed in terms of the systematics of the Cd and Te nuclei.

*Work supported by the Atomic Energy Control Board.

9:15
EA2 Level Structure of ^{126}Cs and ^{126}Xe.* B.P. PATHAK, L. LESSARD, L. NIKKINEN, McGill University.--Low-spin excited levels in ^{126}Cs and ^{126}Xe have been investigated from the decays of ^{126}Ba and ^{126}Cs using β- and γ-ray spectroscopic techniques. Spin and parity assignments have been done on the basis of observed γ-decay properties and the deduced log ft values. The low-lying members of the ground state quasi-rotational band and the quasi γ-band head have been identified. The position of the first excited 0^+ level has been found to be at 1313 keV. The observed decay characteristics of the excited states are compared with the predictions of the collective model.

*Work supported by the Atomic Energy Control Board.

9:30
EA3 Structure of ^{141}Sm from the Decay of ^{141}Eu.* J. DESLAURIERS, G. KENNEDY, S.C. GUJRATHI, S.K. MARK, McGill University.--The structure of ^{141}Sm has been investigated through the decay of ^{141}Eu. A level scheme comprising 17 excited states has been constructed. The beta decaying ground state of ^{141}Eu has been determined to have $J^\pi=5/2^+$; its half-life has been observed to be 40.0 ± 0.4 sec. From beta end-point measurements, the total decay energy of ^{141}Eu has been established as Q_{EC}=6.03 ± 0.08 MeV; this value will be compared with predictions of mass formulae. The strucuture of ^{141}Sm will be discussed in the light of the systematics of the N=79 isotones.

9:45
EA4 Levels in ^{152}Sm Populated by the (t,α) Reaction*. C. R. HIRNING and D. G. BURKE, McMaster Univ.--The ^{153}Eu(t,α)^{152}Sm reaction has been done using 15 MeV tritons from the Los Alamos Scientific Laboratory model FN tandem accelerator. The reaction products were analyzed in a Q3D magnetic spectrometer, and detected with a helical cathode position sensitive detector[1] at the focal surface. Many previously unknown levels above the pairing energy gap have been populated. Several two quasiparticle state assignments are proposed on the basis of relative cross-sections and energies, and on the basis of an (α,2nγ) study[2] of ^{152}Sm. The theoretical calculations and their success in describing two quasiparticle states in ^{152}Sm will be discussed.

10:00
EA5 Observation of ΔN=2 Mixing of States in $^{155}_{64}Gd_{91}$. O. P. JOLLY and J. C. WADDINGTON, McMaster Univ.--High resolution (~5 keV) angular distribution studies of the ^{155}Gd(d,t)^{154}Gd reaction have been done at the McMaster University FN Tandem Accelerator Laboratory. The reaction products were analyzed with an Enge type magnetic spectrograph. This study shows characteristic ℓ=0 transitions for four levels populated at 2376, 2443, 2648 and 2683 keV. Usually, in the Nilsson model, matrix elements between orbitals differing by two in the principal quantum number, N, are neglected. On this basis only two strong ℓ=0 transitions are expected. However as has been seen previously in the odd neutron nuclei, ΔN=2 mixing between $1/2^+[400]$ and $1/2^+[660]$ neutron orbitals has led to a fragmentation of the reaction strength. The observed levels are members of rotational bands formed by the parallel and anti-parallel coupling of these orbitals with the target ground state $3/2^-[521]$. The levels at 2376 and 2443 keV have been assigned as the band heads of $1,K^\pi=1,1^-$ configurations and the levels at 2648 and 2683 keV as the band heads of $I,K^\pi=2,2^-$ configurations. Other rotational members of these bands have also been identified.

10:15
EA6 Levels in ^{157}Ho and ^{159}Ho*. O. STRAUME. D. G. BURKE and J. PANAR, McMaster Univ.--The structures of ^{157}Ho and ^{159}Ho have been studied by the (^{3}He,d) and (α,t) reactions using beams of 24 MeV ^{3}He from the McMaster FN Tandem Van de Graaff accelerator and 30 MeV ^{4}He from the M.P. Tandem Van de Graaff accelerator at the University of Rochester. The reaction products were analyzed in Enge type magnetic spectrographs and detected with photographic emulsions giving peak widths (FWHM) of ~15 keV of (^{3}He,d) and ~12 keV for (α,t). The (^{3}He,d) angular distributions and (^{3}He,d) to (α,t) cross-section ratios give ℓ-values for many of the levels populated. The ground states of ^{157}Ho and ^{159}Ho are known to be the $7/2^-[523]$ Nilsson orbital and in the present experiment the orbitals $7/2^+[404]$, $5/2^+[402]$ and $1/2^-[541]$ have been assigned to strongly populated low-lying levels. Tentative assignments are also given for the $1/2^+[411]$ and $3/2^+[411]$ orbitals, and the (K_o-2) γ-vibrations based on the $5/2^+[402]$ states have been observed in both nuclei. Relative spectroscopic factors are extracted and compared with predictions obtained from a Nilsson model calculation with pairing and Coriolis coupling included.

*Supported by the National Research Council of Canada.

10:30
EA7 The Level Structure of ^{157}Tb.* N.C. SINGHAL, J.V. THOMPSON and M.W. JOHNS, McMaster U.--In beam γ-ray spectroscopy has been used to study high spin states in ^{157}Tb. These states were populated by the ^{154}Sm (^{7}Li, 4n) ^{157}Tb reaction with 36 MeV ^{7}Li beams from the McMaster Tandem Accelerator. States with excitation energies up to 2583 keV ($31/2^-$) in the $3/2^+$ [411] ground state band and 2085 keV ($27/2^+$) in the 5/2 [532] band have been observed through gamma-gamma coincidence measurements and gamma-ray yield functions from 24-36 MeV. Angular distribution measurements are being planned. The effect of the Coriolis terms on the energy level spacings in the ground state rotational band is being studied.

*Research Supported by the National Research Council of Canada.

10:45
EA8 Gamma-Ray Angular Distribution Measurements from the ^{162}Dy(n,n'γ)^{162}Dy Reaction.* H.R. HOOPER, J.M. DAVIDSON, D.M. SHEPPARD, P.W. GREEN, and G.C. NEILSON, Univ. of Alberta--The recent development of a small-sample technique[1] has made possible the study of levels in ^{162}Dy using γ-ray angular distributions from the ^{162}Dy(n,n'γ)^{162}Dy reaction. Agreement with previous spin-parity assignments[2] has been found for the following levels: 888 keV, 2^+; 1148 keV, 2^-; 1275 keV, 1^-; and 1357 keV, 3^-. A γ-ray previously reported[2] at energy 1275 keV has been resolved as a doublet with a peak separation of 2.9 ± 0.2 keV.

*Work supported in part by the AECB of Canada.
1. J.M. Davidson *et al.*, Bull. Am. Phys. Soc. Ser. II 20, 1155 (1975).
2. A. Backlin *et al.*, Phys. Rev. 160, 1011 (1967).

11:00
EA9 Evidence for a Five-Quasiparticle Isomer in ^{177}Ta L. BUJA-BIJUNAS, J. C. WADDINGTON, McMaster Univ. and T. L. KHOO, Michigan State Univ.--Recent interest in the study of many-quasiparticle states in ^{176}Hf has prompted a similar study of high spin states in ^{177}Ta. Experiments at McMaster and Michigan State Universities using the ^{170}Er(^{11}B,4n) and ^{176}Lu(α,3n) reactions have located a high spin isomer at 2826.9 keV. This isomer decays with a half life of approximately 70ns by 555 and 790 keV transitions to previously identified 3 quasiparticle states[1]. Delayed and prompt γ-γ techniques were used to isolate the γ-rays feeding and de-exciting this isomer.

[1]D. Barneoud, S. Andre and C. Foin, Phys. Lett. 55B, 443 (1974).

11:15
EA10 Interacting Boson Model and the Sphericity of the Yrast Band. H. OGATA, Department of Physics, University of Windsor, Windsor, Ontario N9B 3P4.--The interacting boson model (IBM) in the SU(5) representation is applied to the yrast band of even-even nuclei in and around the deformed region of A=150-190. By introducing a sphericity parameter, x, both rotational and vibrational limits are very well described in the second order perturbation. Energy levels of a wide variety of isotopes, spherical and deformed as well, are fitted by a two-parameter r.m.s. minimization method, and the backbending feature is reasonably reproduced in between these two limits. Plots of relative energy spectrum of these nuclei show a remarkable regularity throughout the whole region.

11:30
EA11 Inelastic Processes in the ^{184}W(p,t) Reaction at 35.2 MeV*. L. PH. ROESCH, O. ABOU-ZEID, W.R. FALK, P. DEBENHAM and M.J. CANTY, Univ. of Manitoba--Angular distributions for tritons from the reaction ^{184}W(p,t)^{182}W have been measured over the angular range from 15 to 80° at a proton bombarding energy of 35.2 MeV. The WO_3 target of thickness 150μgm/cm^2 (enriched to 99.91% ^{184}W) was prepared by evaporation onto a carbon backing of 40μgm/cm^2. An overall energy resolution of 60 keV was obtained. Analysis of the data yielded angular distributions for the 0^+, 2^+, 4^+ and 6^+ states of the first rotational band and the 0^+ and 2^+ states of the β-band. At 35.2 MeV an angular momentum transfer of L=4 is favoured, compared to L=0 at proton energies of 18 MeV, applicable to the previous investigations on similar reactions[1]. Preliminary coupled channel analyses indicate that inelastic effects are very important in this reaction at 35.2 MeV.

[1] C.H. King, R.J. Ascuitto and N. Stein, Phys. Rev. Lett. 29, 71 (1972).
* Supported in part by the AECB of Canada.

11:45
EA12 Intermediate Coupling States in ^{205}Tl.* J.M. DAVIDSON, H.R. HOOPER, P.W. GREEN, D.M. SHEPPARD, and G.C. NEILSON, Univ. of Alberta--Recent evidence has shown that the low-lying levels of ^{205}Tl are well represented by the intermediate coupling of a single hole in the closed Z=82 proton system to the vibrational states of the ^{206}Pb core. In the present work, we have studied the excited states of ^{205}Tl using γ-ray angular distributions from the ^{205}Tl(n,n'γ)^{205}Tl reaction. These angular distributions were recorded and analyzed using a small-sample technique developed by the authors.[1] A spin limit of J = (5/2,7/2) has been deduced for the ^{205}Tl excited state at 925 keV. Further results will be presented and compared to theoretical calculations based on the above model.

*Work supported in part by the AECB of Canada.
[1]J.M. Davidson *et al.*, Bull. Am. Phys. Soc. Ser. II 20, 1155 (1975).

12:00
EA13 Determination of the muonic nuclear polarization of ^{208}Pb and ^{209}Bi from combined electron scattering and muonic atom X-ray data. D.W.L. SPRUNG, X. CAMPI* & J. MARTORELL†, McMaster University, Hamilton, Ontario.

The nuclear polarization energy E_{NP} is a significant correction to the $1s_{\frac{1}{2}}$ energy level of the muonic atom. Chen[1]) gives E_{NP} = 6 keV for lead while Scheck[2]) found an additional 3.2 keV from the $1h_{\frac{9}{2}}$ proton in bismuth. Using recent "model independent" methods[3]) for analysis of combined electron and muon data[4]), we have deduced E_{NP} = 4.96 ± 0.7 keV for Pb and 4.4 ± 2.0 keV in Bi. These values are significantly smaller than previous determinations[4]) which used muonic data only. In our method, the electron data constitute a severe constraint on the shape of the nuclear charge density.

1 M.Y. Chen, Phys.Rev.C 1 (1970) 1167
2 F. Scheck, Zeit.f.Phys. 172 (1963) 239
3 J.L. Friar & J.W. Negele, Nucl.Phys.A212 (1973) 93
4 D. Kessler et al.,Phys.Rev.C 11 (1975) 1719

* Perm. address, Inst.de Phys.Nucleaire, Orsay, France
† Pres. address, S.I.N., 5234-Villigen, Switzerland

WEDNESDAY, JUNE 16, 1976
ROOM 1C
Chairman: J.S. Fraser

9:00

EB1 Multiple Interaction Processes in Ge(Li) Detector Pulse Formation.* R. CHUN, L. L. GADEKEN+ and B. C. ROBERTSON, Queen's Univ. at Kingston--The contribution of multiple interaction processes to pulse shape generation in coaxial Ge(Li) detectors is calculated using a Monte Carlo technique. The results are compared with point interaction calculations and experimental pulse shape measurements. Multiple interaction processes are found to be significant, and their inclusion leads to good agreement with experimental information.

*Work supported by the Atomic Energy Control Board of Canada

+Present address: Pattern Analysis and Recognition Corporation, Rome, N.Y.

9:15

EB2 Figure of Merit (FOM) for Testing Goodness-of-Fit in Gamma-Ray Spectrum Analysis.* G. BALIAN and N.W. EDDY, Concordia University.--The traditional chi-squared test for quality of fit when applied to a gamma-ray spectral peak has several undesirable features. It is inordinately sensitive to errors (residuals) in the region of the peak tails; the occasional large residual in an otherwise satisfactory fit can grossly inflate the chi-squared value; it can be sensitive to different peak shapes and to the use of different response functions; and it can be misused to indicate overly optimistic qualities of fit. The authors have modified the standard chi-squared formula and designated the result "figure of merit" (FOM).

*Work supported by the Atomic Energy Control Board.

9:30

EB3 Proton Induced X-Ray Emission From Heavy Elements Using 20-50 MeV Protons*. J.S.C. McKEE, C.P. RANDELL and S.F.J. WILK, Univ. of Manitoba--High resolution K_α and K_β spectra for self-supporting lead, tantalum, gold and indium targets have been obtained using a 5mm planar Ge(Li) detector with no Compton suppression. The production mechanism of satellite peaks resolved on the high energy side of K_α and K_β X-ray groups excited in tantalum has been determined, and on the basis of these measurements it is now estimated that heavy elements are detectable at concentrations of ppm or better.

* Supported by the AECB of Canada.

9:45

EB4 On the Analysis of Precision Multichannel Lifetime Spectra D.A.L. PAUL, Univ. of Toronto, Toronto M5S 1A7--It is shown that even with the simplest multichannel timing circuit the random coincidence spectrum is more complex than has previously been thought. The breakdown of random coincidences into types is discussed and an analytic formula for the time distribution of coincidences is obtained for a true spectrum which is a simple exponential decay. When the start pulse rate is much smaller than the decay rate, or when the efficiency of the stop detector is small, the new formula reduces to that derived by Coleman and Griffith.[1]

[1]Coleman, P.G., and Griffith, T.C., 1973 J. Phys. B 6, 2155.

10:00

EB5 High Density γ Converters, R.J. Douglas, A.T. Stewart, Queens University, L. Bird, A.A. Raffler, Carleton University.--Results are presented for the prototype γ detector to be used in the electron momentum spectrometer at Queens University. The high density converter is used in conjunction with multiwire proportional chambers to measure the position of γ rays from positron annihilation.

10:15

EB6 Energy Resolution Improvement Through Kinematic Correction With a Position Sensitive Detector*. W.R. FALK, O. ABOU-ZEID, L. PH. ROESCH, Univ. of Manitoba--The full acceptance of the high resolution beam analysis system at the University of Manitoba Cyclotron Laboratory produces a beam on target which typically has an angular spread of ±2°. The resulting kinematic energy spread and/or angular resolution are frequently unacceptable, and these effects may normally be reduced only at the expense of beam intensity. A technique has been developed that simultaneously greatly decreases the effect of the kinematic energy spread and improves the angular resolution while utilizing the full beam intensity. This is achieved by shifting the usual beam waist on target to a point downstream. The energy resolution improvement for g.s. α-particles from the $^{12}C(p,\alpha)^{9}B$ reaction is approximately a factor of three (to a value of 60 keV).

[1] Annual Report 1973/74, Cyclotron Laboratory, University of Manitoba.

* Supported in part by the AECB of Canada.

10:30

EB7 The Proton Spectrometer at TRIUMF. P. KITCHING, W.J. McDONALD, G.M. STINSON, and A.N. JAMES,* Univ. of Alberta; and E.D. EARLE, AECL, Chalk River--One of the facilities soon to be available in the proton experimental area at TRIUMF is a medium resolution proton spectrometer. This instrument, the first stage of a high resolution system, consists of a quadrupole and a vertical dipole and can be run in a 'large angle' or 'small angle' configuration by moving the quadrupole back from the target. The table below lists the design parameters for the two operating modes. Detectors at the focal plane consist of two multi-wire proportional chambers and a drift chamber. Current status of the system will be discussed.

Design Parameters for Medium Resolution System

	Large Angle	Small Angle
Forward Angle	20°	10°
Bend Plane Acceptance	± 20 mr(± 1.2°)	± 18 mr(± 1.1°)
Non Bend Plane Accep.	± 50 mr(± 2.8°)	± 16 mr(± 1°)
Solid Angle	3.1 msr	1.2 msr
First Order $\Delta p/p_0$ 1)	± 0.034%	± 0.033%
Momentum Acceptance	± 5%	± 5%

1)For beam spot ± 2.5 mm and ± 1 mm detector resolution.

*On leave from the University of Liverpool.

10:45

EB8 The TRIUMF π^0 Detector.* D.F. MEASDAY, D. BERGHOFER, M.D. HASINOFF, R. MACDONALD, M. SALOMON, J. SPULLER and T. SUZUKI, Univ. of B.C., J.K.P. LEE, McGill Univ., P. DEPOMMIER, J-M POUTISSOU and R. POUTISSOU, Univ. de Montréal.-- Two large NaI crystals have been commissioned at TRIUMF for the detection of hundred MeV γ-rays. One measures 18"ϕ × 20" long (TINA) and the other 14"ϕ × 14" long (MINA) Their energy resolution for 130 MeV γ-rays is about 5% and 8% respectively and the timing resolution is about 3n-secs. When used in coincidence, they are an effective π^0 detector and their performance and prospects will be discussed.

11:00

EB9 Commissioning of the TRIUMF Stopped π-μ Channel A. OLIN, D.A. BRYMAN, J.A. MACDONALD, P.A. REEVE, M. SALOMON, J.S. VINCENT, TRIUMF, G.A. BEER, G.R. MASON, R.M. PEARCE, L.P. ROBERTSON, Univ. of Victoria, J.-M. POUTISSOU, Univ. of Montreal* — Measurements of the characteristics of pion and muon beams available from the TRIUMF stopped π-μ channel are reported. Fluxes, spatial distributions, and the energy spread of the beams have been measured for Be and Cu production targets and for different ranges of transmitted momenta as selected by slits in the midplane. In addition to muon beams produced by pions decaying in the channel, a beam of muons at the channel momentum, produced from π decays in the vicinity of the production target, has been obtained. This beam has a high stopping density and small spot size, and may be conveniently tagged by its time of flight. The optical parameters of the channel will be compared with design values.

* Supported by AECB.

11:15

EB10 Control of Phase Disturbances in a High Power 100% Duty Factor Linac. J. McKEOWN, J.S. FRASER and G.E. McMICHAEL, AECL, Chalk River, Ontario. -- The graded-β section of the Chalk River Electron Test Accelerator has accelerated a beam of 20 mA to 1.5 MeV. This accelerator is used to model the behaviour of a 1 GeV proton linac in a neutron factory to breed fissile material. An experimental study has been made of the phase stability of the accelerator rf system with varying beam loading and the major disturbances identified. The largest effect is associated with the changes in phase shift across the klystron power amplifier. The accelerating structure admittance angle changes by 4° when the rf power is divided equally between the beam and the structure. Using reactive beam loading theory the mean phase angle for maximum transmission is calculated. The phase control system for the accelerating field[1] keeps the effect of these disturbances to less than 1°.

1 J. McKeown, Nucl. Inst. & Meth. 121 (1974) 509-516.

11:30

EB11 A Technique for the Measurement of low B^{10} Concentrations in CANDU Moderator. R. T. JONES and A. OKAZAKI, AECL, Chalk River. -- B^{10}, in boric acid dissolved in the D_2O moderator, is used as a coarse reactivity control in some CANDU reactors. There is a need for methods to measure B^{10} concentration especially at low levels when the B^{10} to B^{11} ratio has been altered by burnup. A technique to measure concentrations in the range 0 to 125 parts per billion B^{10} has been developed. A small sample of the solution (~ 1 ml) is evaporated to dryness on an aluminum planchet which is subsequently irradiated with thermal neutrons. Alpha particles from the $B^{10}(n,\alpha)Li^{7}$ reaction are counted during the irradiation with a silicon surface barrier detector. Counting samples prepared from standard solutions concurrently with the unknown enables the concentration of the unknown to be measured to an accuracy of ± 6 ppb.

11:45

EB12 Electron-Positron Shower due to a Neutron Source* P.S. TAKHAR , Royal Military College, Kingston, Canada.-- Electron-positron shower in the vicinity of a neutron source was investigated, by a number of large area cosmic-ray counters. The neutron source was on the first floor, and the shower experiments were performed on the second floor. The radiation from the source, produced shower in the concrete floor. The shower intensity above the neutron source was four times than the normal cosmic ray shower. Elsewhere on the floor the counting rate varied with the distance. The absorption coefficients for the electron-positron shower were 0.0030 ± 0.0001 cm^{-1} and 0.0026 ± 0.001 cm^{-1} depending upon the shielding material. These were much lower values compared to the data obtained from cosmic-ray experiments. Finally an analysis of the gamma and x-ray spectrum of the shower producing radiation will be reported. The radiation emitted by the neutron source will be discussed in terms of electron-positron shower.

*Work supported by D.R.B. of Canada Grant No. 9510-51.

EB13

WEDNESDAY, JUNE 16, 1976
ROOM 2A
Chairman: L. Kerwin

ATOMIC PHYSICS II

9:00

EC1 The L_2-L_3 Coster-Kronig Transition Probability at Z = 96.* R. W. FINK and D. W. NIX, Chemistry, Georgia Tech. Atlanta--Dual-parameter coincidence measurements with high resolution Si(Li) and Ge(HP) x-ray spectrometers were performed with the same source of ^{244}Cf used by McGeorge & Fink[1]). The present method eliminates possible errors arising from single-channel windows used earlier. Both $K_{\alpha 1,2}$ gating with observation of coincident L x rays and L_{α} gating with observation of coincident $K_{\alpha 1,2}$ x rays were performed and very careful corrections applied for overlap of $K_{\alpha 1}$ events into the $K_{\alpha 2}$ gate and for L_{β}, L_{γ}, and continuum events into the L_{α} gate. The present result for the L_2-L_3 Coster-Kronig transition probability is f_{23} = 0.209 ± 0.022(2σ), compared to 0.188 ± 0.010(2σ) (ref. 1) and 0.226 ± 0.034(2σ) (ref. 2). The systematics of high-Z values of f_{23} will be discussed in the light of the new measurement at Z = 96.

1) J. C. McGeorge and R. W. Fink, Z.Physik 248, 208 (1971)
2) M. R. Zalutsky and E.S.Macias, Phys.Rev. A11,71 (1975)

*Supported in part by the U. S. Energy Research & Development Administration

9:15

EC2 Measurements of Stopping Powers Using Proton Induced X-Ray Emission.* J. K. KLIWER, R. E. MARSHALL and D. N. TANG, University of Nevada, Reno--Stopping powers of keV protons in thin films deposited on thick substrates are measured by observing characteristic x-rays generated from the substrate.[1] The uniformity and thickness of the films are monitored simultaneously with the collection of stopping power data.

*Supported by the Research Advisory Board, University of Nevada, Reno.

[1]A. Johansen, S. Steenstrup and T. Wohlenberg, Radiat. Eff. 8, 31 (1971).

9:30

EC3 Non-characteristic X-rays Produced in Heavy Ion-Atom Collisions. J. C. WADDINGTON and W. R. STOTT, McMaster Univ.--During heavy ion-atom collisions continuum x-rays are produced which extend in energy well above the characteristic x-rays of the projectile and target atoms. Beams of Br and C ions with ~1 MeV/nucleon of energy have been used to study the continuum between 15 and 40 keV produced in collisions with thin self-supporting targets of gold. Angular distributions of the

continuum photons will be presented. Theoretical predictions of the angular distribution of the photons in a symmetric collision[1] predict a $1/2 + 1/4 \sin^2\theta$ dependence. The experimental angular distributions of the photon cross sections from the assymetric collisions are peaked forward of 90°. A Doppler shift correction of the measured spectra indicate the photons originate from a system moving with the centre of mass velocity of the colliding system. Experiments have also been conducted to determine the excitation function for the production of continuum photons.

[1] B. Müller, R.K. Smith and W. Greiner, Phys. Lett. 53B (1975) 401.

9:45

EC4 L x ray Emission from Double Vacancy Atomic States in Indium. R.W. FINK, Georgia Institute of Technology,* P.A. INDIRA, I.J. UNUS and P. VENUGOPALA RAO, Emory U.-- Experimental studies of the decay of multiple vacancy atomic states are scarce because of the inherent difficulty in isolating these species of atoms. In the present work, double vacancy states, created in the K Auger transitions following the electron capture decay of ^{113}Sn (115d), are studied by observing L x rays in coincidence with the K conversion electrons and L conversion electrons from the 393 kev transition. The ratio of these two coincidence rates is related to the average L-x-ray yield, $\bar{\omega}_L$ (xy) where x or y or both are L vacancies. Two Si(Li) detectors in fast coincidence with each other are employed to observe Indium L x rays (∿3.5 kev) and the conversion electrons. It is found that ω_L(xy) is not more than 15% higher than the values estimated on the assumption that there is no difference between the decay properties of single- or double-vacancy atomic states.

*Supported in part by USERDA in the School of Chemistry.

10:00

EC5 Cross sections for the Electron Stripping of Nitrogen Ions in some Rare Gases between 35 keV and 150 keV. H. C. SUK and B. HIRD, University of Ottawa.--

The measurement of σ_{12} cross sections with an absolute accuracy of about 10% will be described. The second order target thickness corrections were found to be important even though relatively few of the ions were stripped in their passage through the gas target.

The two state, quasi-adiabatic theory of Rapp and Francis, in the approximate form used by Lee and Hasted fits both the absolute magnitudes and the energy variation remarkably well, though it is theoretically difficult to justify an application of this theory to electron stripping reactions.

10:15

EC6 Target Thickness effects in Single Collision Cross section Measurements. B. Hird and H.C. Suk, University of Ottawa.-- In most beam-gas measurements of atomic collision cross sections, single collision conditions are assumed if the number of ions in the final state is a linear function of the gas pressure, and is relatively small compared to the number of ions in the initial state. The conditions under which this single collision assumption is justified are examined theoretically. It is found that multiple collisions can be important even though both criteria are apparently obeyed quite well.

The exact differential equations for the relative populations of three, mutually interacting, ion species are solved as a function of the distance through the gas target, and a relation, valid to third order in the target thickness, is obtained in terms of the interaction cross sections.

An example is given of an experiment where the final state ion population shows both a linear dependance on the target gas pressure, and is small compared to the incident beam population, but where the use of the usual single collision cross section formula would lead to considerable error in the measured cross section.

10:30

EC7 Formation of D^- by Charge Exchange of keV Deuterium Ions in Cesium Vapor.* A. S. SCHLACHTER†, J. WARREN STEARNS†, F. ROUSSEL††, P. PRADEL††† and G. SPIESS†††, Lawrence Berkeley Laboratory†, C.E.N./Saclay††, and Stanford Research Institute†††--A high intensity source of D^- ions is desirable for the CTR neutral injection program and for certain particle accelerators. One important method of producing D^- is by charge exchange in a suitable target. One of the most widely-used targets is cesium vapor. There are, however, discrepancies as large as a factor of 2 in published values of the equilibrium yield of D^- in cesium at low keV energies. We shall present results from two different experiments for $F_{-\infty}$ in the energy range 1-5 keV. Preliminary results show 20% at 1 keV, dropping to 6% at 5 keV.

*Work partially supported by the U.S. ERDA.

10:45

EC8 Angular and Energy Distributions of Proton - Carbon Foil Electrons Emitted Close to the Beam Direction.* W.MECKBACH†,K.C. CHIU and J.WM.MCGOWAN, Univ. of Western Ontario -- Cusp shaped distributions were obtained: a) as a function of angle when the elecron velocity equals in magnitude that of the ions; b) as a function of energy at zero angle with respect to the ion beam. Our results are in qualitative agreement with those of Duncan and Menendez[1] in that with increasing ion energy the half widths of the measured angular distributions decrease, while those of the energy distributions increase. This result can be interpreted in terms of the theories of Salin[2] and Macek[3]: By representing the measured angular- and energy distributions as a function of the absolute ion - electron velocity difference it is found that the half widths of the resulting distributions are independent of the ion energy.

*Supported by the National Research Council of Canada.
†Visiting Fellow, Centre Chemical Physics, on leave of absence from Centro Atomico Bariloche,CNEA, Argentina.
[1]M.M. Duncan and M.G. Menendez, Phys.Rev.A 13,566(1975)
[2]A. Salin, J.Phys.B.2,631 (1969)
[3]J. Macek, Phys.Rev.A 1, 235 (1970)

11:00

EC9 Optical Radiation Produced in Low-Energy Ion-Surface Scattering at Grazing Incidence. N. H. TOLK, W. HEILAND,* S. Y. LEUNG, J. C. TULLY and J. KRAUS, Bell Laboratories.--We have observed optical radiation emitted from excited neutral atoms which have undergone neutralization and excitation due to low-energy (6 keV) ion-surface scattering at grazing incidence (60°-80° angle of incidence). Ultraviolet, visible and infrared photons are detected downstream following grazing incidence collisions using H^+, H_2^+, H_3^+, He^+, Ne^+ and Ar^+ projectiles and Mo, Zr, Mg and Cu target surfaces. Broadband continuum radiation has been observed in addition to line radiation from both backscattered and sputtered particles. The effect of oxygen pressure, target orientation, and projectile energy on the intensity distribution and polarization of the observed radiation will be discussed.

*On leave from Max-Planck Institute for Plasma Physics, Garching, Germany.

11:15

EC10 G-2 Resonance Observed in Monoelectron Oscillator. R. VAN DYCK, JR., P. EKSTROM, and H. DEHMELT, U. of Washington.--Essentially as proposed by us (1973 & 1974) the G-2 resonance at $\nu_s = \nu_s - \nu_c + \nu_m$ has been observed by making a single electron see an effective, adjustable (<10 μG) rotating magnetic field at ν_s, the spin frequency, occurring as the sum of a forced-axial-motion frequency ν_d = 59.415890 MHz and $\nu_c - \nu_m$ = 51206.11

MHz, the frequency of the $4^{o}K$ thermal cyclotron motion through the inhomogeneous static field of a ∿30 G deep magnetic bottle superimposed upon a strong ∿18.3 kG field. Spin flips, induced at a rate ∿1/min, were detected by continuously monitoring the bottle-related shift $\delta\nu_z \simeq (m + n + \frac{1}{2})$ 2.5 Hz of the axial resonant frequency ν_z = 59.4101 MHz and focussing on the minimum values, 2.5 & 0 Hz, corresponding to n = 0, m = ±½, which occur as the electron jumps frequently between the cyclotron levels, n, and rarely between the spin levels, m. The minimum ν_d-linewidth of ∿500 Hz realized so far is primarily due to the continuous ν_z- monitoring. Pulsed operation promises a 100 fold sharper line. With the measured ν_m = 34.464 KHz, our preliminary value of $a = (\nu_s - \nu_c)/\nu_c$ is 0.001159655(5). D. Wineland and P. Schwinberg have made important contributions to this NSF supported work.

11:30

EC11 Intermdediate-energy Positron Scattering in Neon and Argon J.S. TSAI, L.P. LEBOW and D.A.L. PAUL, Univ. of Toronto, Toronto, M5S 1A7--Positron total cross sections have been measured on argon and neon at energies between 25 eV and 300 eV. The new results have been extrapolated upwards in energy to about 4KeV where they would join smoothly on to the total Born cross curves, combined with the new results and with previously published results for low energies, allow evaluation of the integral for use in the sume rule

$$a_s + f_B(o) = -\frac{1}{2\pi}\int_o^{\infty} \sigma(k)dk$$

For neon our data lead to a scattering length $a_s = (-0.53 \pm 0.15)a_o$ in fair agreement with one of the theoretical models of Montgomery and LaBahn. For argon an estimate of the true value of $f_B(0)$ has been made based on the value $f_B^{HF}(0) = -8.7a_o$ obtained from Clementi wave function for the ground state of argon, and we find $a_s = (-2.8 \pm 0.7)a_o$.

WEDNESDAY, JUNE 16, 1976
ROOM 2B
Chairman: D.J. McEwen

ATMOSPHERIC AND SPACE PHYSICS

9:00

ED1 Modelling of Electron Aurora
A.V. JONES, *Herzberg Institute of Astrophysics, N.R.C.*
Methods are discussed of calculating the height distributions and intensities of auroral emission features from an initial primary electron energy distribution. For indirect excitation processes the ion and neutral chemistry and electron temperatures must be considered.

9:40

ED2 Extreme UV Auroral Excitation, Predictions and Observations
C. ZIPF, *University of Pittsburgh*

10:20

ED3 Electron Impact Production of Highly Excited (12-25 eV) Atmospheric Gases
P. MARMET, *Université Laval*
Discrete energy levels have been measured above the first ionization threshold of N_2, O_2, CO, CO_2, NO an H_2O from perturbations detected in the ionization efficiency curve. Data are obtained from a crossed beam experiment between monoenergetic electrons and molecular gases. Foreign ions and ionic fragments are carefully eliminated by filtering the ions of interest through a quadrupole mass filter. Signal to noise ratios as high as 10^5 are obtained. In general results show that immediately after the collision a large number of excited negative ion states are formed, competing with highly excited Rydberg series converging to ionic limits. This is immediately ($T \sim 10^{-14}$ or 10^{-13} sec.) followed by autoionization. This throws new light on the understanding of the ionization and excitation mechanism by electron impact. Results will be shown and discussed.

11:00

ED4 Laboratory Studies of $O(^1D_2)$ Reactions of Atmospheric Interest
H.I. SCHIFF, *York University*
There is increasing concern over possible depletion of the earth's ozone shield by human activity. The ozone budget is largely controlled by reactions with the oxides of nitrogen (NO_x) and with HO. These reactive species derive mainly from reactions of $O(^1D_2)$ atoms with N_2O in the case of NO and with H_2O, CH_4 and H_2 in the case of HO. The $O(^1D_2)$ atoms are produced by the uv photolysis of O_3 and are lost mainly by non-reactive quenching collisions with N_2 and O_2. Absolute cross sections for the reactions with atmospheric gases have been measured using a time-resolved laser photolysis system. The temperature dependences of these cross sections have also been determined over the range 131-393 K.

11:40

ED5 Auroral and Airglow Emissions in the Polar Cap Observed by ISIS-2 Auroral Scanning Photometer.* S. ISMAIL and L.L. COGGER, Univ. of Calgary.--Diffuse auroral emissions in the entire polar cap at 5577 and 3914Å were observed by the ISIS-2 Auroral Scanning Photometer. Regions of soft particle precipitations in different sectors of the polar cap were determined from 5577/3914Å intensity ratios. Ratios in the morning and afternoon sectors indicate that they result from a combination of characteristic daytime and nighttime precipitations. The ratios in the central polar cap are compatible with the observations of polar rain by ISIS-1 and ISIS-2 Soft Particle Spectrometers. 5577Å airglow intensities were also measured over the winter polar cap and compared with high and mid-latitude intensities. It was found that a maximum in 5577Å airglow can occur at any winter latitude. This implies that the latitudinal distribution of atomic oxygen is also nonuniform and that regions of enhanced atomic oxygen concentration can occur at any latitude.

*Supported by the National Research Council of Canada.

WEDNESDAY, June 16, 1976
ROOM 2C
Chairman: M. Sayer

SOLID STATE PHYSICS RESEARCH IN INDUSTRY

9:00
EE1 The Physics of Integrated Circuit Lithography.
K.A. PICKAR, *Bell-Northern Research*

The complexity of integrated circuits has increased by approximately a factor of two per year since 1960. This incredible growth rate, made possible by a multidisciplinary synthesis of the skills of physicists, electrical engineers, chemists and material scientists, characterizes this technology as the fastest evolving in history. A limiting step in future advances, requiring further application of these disciplines, is the lithographic process, the definition of fine line patterns required to fabricate these devices. As current minimum line widths of 5 m are decreased, the wavelength of light becomes a fundamental limit for optical photolithography. However, even in the 1 m to 2 m regions, other problems intervene which require new methods of exposure. We will discuss two possible approaches, electron beam and X-ray lithography. The technique of plasma etching as a substitute for wet chemistry will also be covered. In all cases, attention will be given to physical limits. These considerations are applicable to the fabrication of other devices including integrated optical circuits, Josephson junction logic circuits, surface acoustic wave transducers and high frequency discrete transistors. These new techniques together with the already well-developed ion implantation technology, are being combined to give a rationalized process sequence to assure at least several more generations of complexity doubling in the next decade.

10:00
EE2 Surface Physics Research in Industry
Y.C. CHENG, *Xerox Research Centre of Canada Ltd.*

Research in surface physics is discussed from the viewpoint of its importance to several industrial research activities. Problems related to integrated electronics, integrated optics and electrophotography are presented. The role of surfaces in metal-oxide-semiconductor structures are discussed. Research on different aspects of surface physics problems, such as surface states, two-dimensional electron gases, surface phonon scattering, surface mobility, surface roughness scattering, and other related topics will be reviewed. Surface problems in integrated optics will be examined. Thin film waveguides and the role of surface scattering in propagation loss is reviewed. Examples are given on some methods in making components for integrated optical structures; difficulties and related research activities are presented. Finally, brief mention will be made on the role of surface physics research in the field of electrophotography.

11:00
EE3 Research in Electrophotography
G. HARTMAN, *Xerox Research Centre of Canada Ltd.*

Current research on charge exchange at interfaces between materials in the context of conventional and novel electrophotographic systems will be reviewed. Of particular interest are charge exchange processes between metal-polymer-interfaces and from photoconductors into polymers and insulating liquids. Several electrophotographic processes will be described to illustrate the commercial importance of the charge exchange phenomena reviewed.

WEDNESDAY, JUNE 16, 1976
ROOM 2D
Chairman: A.H. Morrish

MAGNETIC PROPERTIES OF SOLIDS

9:00
EF1 Zeeman Splitting of the E1 and E2 Excitons in MnF_2. W. C. EGBERT and W. M. YEN, Univ. of Wisc.-Madison--We have measured the effective g factors of the E1 and E2 excitons in MnF_2 by applying axial magnetic fields up to 70 kOe. A simple theory describes the excitons and shows that the difference in g factors, $\Delta g = g(E2) - g(E1)$, tests for sample-dependent variations in the crystalline strain field. Comparison of our results to earlier experiments indicates that such variations are in fact not seen in Δg or in the magnetic circular dichroism (MCD) spectrum, which in this theory is also affected by strains in the crystal. In addition, by estimating one reduced matrix element, measurements of Δg can be used to compute the coefficients which describe the mixing of $^4T_1$ states in E1 and E2. Zeeman and MCD spectra taken with stress and an axial magnetic field simultaneously applied are proposed to clarify understanding of the MCD spectrum of the one magnon sidebands.

9:15
EF2 Néel Temperatures of Binary Chromium Alloys. C. A. MOYER, Department of Physics, Clarkson College of Technology, Potsdam, N. Y. 13676.--A critical comparison of theory with experiment is given for the Neel temperature vs concentration of binary chromium systems containing small amounts of various solutes. A wide spectrum of behavior is observed experimentally, much of which can be understood qualitatively on the basis of changes in the Fermi level of the chromium host. We formulate this idea quantitatively in a rigid band model having spherical electron and hole pockets of unequal size at the Γ and H points of the Brillouin zone. The predictions of this model are examined for arbitrary solute concentrations. The model successfully describes the saturation observed upon alloying chromium with electron-rich elements like ruthenium, and may also account for the anomalous oscillations found in the chromium-aluminum system. The oscillatory behavior of T_N in chromium-aluminum alloys is contrasted with that reported for chromium-cobalt and chromium-palladium alloys.

9:30
EF3 Magnetic Phase Diagram of Cr-rich Cr-Si Alloys. K.V.RAO and S. ARAJS, Clarkson College, Potsdam, N.Y.--Among the various Cr-transition metal alloys, the Cr-Fe alloy system is highly anomalous: e.g., a large first-order jump is observed in the elec. resis. at T_N, for conc. above 2 at%Fe. The only other system with such rare features, almost identically, is the Cr-rich Cr-Si one.[1] In the absence of neutron diffraction studies, the pressure dependence of T_N, is a convenient tool for classifying the nature of the various magnetic phases. We have made such a study on the same alloys that were used in ref.1. It is found that unlike in Cr-Fe alloys where the magnetic transition is Para-incommensurate-commensurate (P-I-C) type with $dT_N/dP \simeq 15$K/Kbar, for the Cr-Si system this pressure derivative is found to be large, $\sim$ 35K/Kbar in alloys which exhibit the pronounced discontinuous transition. Initially, the transition is P-C type changing to P-I at higher pressures. This behaviour in both Cr-Fe & Cr-Si alloys goes against what is expected from the electron to atom ratio rule.[2] A detailed phase diagram and possible explanations for these results will be given.

[1] S.Arajs,K.V.Rao, L.Hedman & H.U.Åström,LT14 3,1136 (75)
[2] R.Nityananda, A.S.Reshmwala and A.Jayaraman, Phys. Rev. Lett., 28 1136 (1972)

9:45
EF4 Magnetic Study of Pd-Ag and Pd-Rh Alloys Containing Fe Atoms.* J. I. BUDNICK, T. J. BURCH, W. A. HINES, A. H. MENOTTI and R. PAOLINO, Univ. of Conn. and V. CANNELLA, Wayne State Univ.--Magnetic measurements are reported for alloys of composition $(Pd_{1.00-x}Ag_x)_{0.98}Fe_{0.02}$ (where x = 0.05, 0.10, 0.25, 0.33 and 0.50) and $(Pd_{1.00-y}Rh_y)_{0.99}Fe_{0.01}$ (where y = 0.01, 0.04, 0.07, 0.50 and 0.75) for temperatures 3 - 77°K and RT, and fields up to 20 kOe. These results, supplemented by previous data, enable an analysis of the dependence of effective magnetic moment per dissolved Fe atom, μ, and ordering temperature, T_c, on the host matrix susceptibility, χ_o in the light of existing theories. The Pd-Ag alloys containing Fe are ferromagnetic for $x \leq 0.33$ with a linear dependence of T_c upon χ_o while μ increases gradually with χ_o. The x = 0.50 composition shows a "spin-glass" behavior. Pd-Rh alloys containing Fe are ferromagnetic for $y \leq 0.20$, however, both μ and T_c are double-valued functions of χ_o. The y = 0.50 and 0.75 alloys are paramagnetic down to 3°K. These results illustrate the striking difference in behavior between a transition metal addition (Rh) to Pd and a noble metal addition (Ag) to Pd as well as the inapplicability of a simple rigid band model.

*Supported in part by the Univ. of Conn. Res. Found.

10:00
EF5 Thermal Expansion Anomalies in Alpha-Uranium.* M. O. STEINITZ and D. A. TINDALL, St. Francis Xavier University.--Thermal expansion measurements on alpha-uranium have been carried out in the temperature range 4.2°K-50°K. A capacitance technique was used, utilizing a new cell design allowing rapid sample changes and the use of samples of any shape. Improved values for the discontinuous length changes along the a, b and c axes at the 22°K and 37°K phase transitions were obtained and compared with previous results using strain gages[1] and with specific heat measurements,[2] and measurements of the pressure dependence of the transition temperature.[3]

[1] M. O. Steinitz, C. E. Burleson and J. A. Marcus, J. Appl. Phys. 41, 5057 (1970).
[2] J. Crangle and J. Temporal, J. Phys. F:Metal Physics, 3, 1097 (1973).
[3] E. S. Fisher and D. Dever, Solid State Comm., 8, 649 (1970).

10:15
EF6 Magnetic Phase Transition in $Mn_{1.98}Fe_{0.02}Sb$.* C. BLAAUW, G. R. MACKAY and W. LEIPER, Dalhousie Univ.- In Mn_2Sb a ferrimagnetic-antiferromagnetic phase transition is known to occur as a result of impurity doping, caused by exchange inversion at a critical value of the lattice parameter[1]. Using the Mossbauer effect of Fe^{57} and Sb^{121} we have studied this transition in $Mn_{1.98}Fe_{0.02}Sb$. The Fe saturation hyperfine field changes from 80 kG in the ferrimagnetic region at $T>T_t$ to 50 kG at $T<T_t$. Also a spin transition is observed through a change in sign and magnitude of the quadrupole interaction. The inferred change in alignment from the c-axis to the basal plane is similar to results found in related systems. The Sb saturation hyperfine field is 224 kG and the temperature dependence at low temperatures is very small. The results are discussed in terms of current theories of magnetic interactions in concentrated magnetic alloys.

[1] H. S. Jarrett, Phys. Rev. 134A, 942 (1964).

*Supported by NRC and the Faculty of Graduate Studies at Dalhousie University.

10:30
EF7 Local Moment - Spin Density Wave Interaction in Dilute CrFe and CrCo Alloys. F.T. HEDGCOCK, J.O. STROM-OLSEN and D.F. WILFORD, Eaton Electronics Lab, McGill Univ., Montreal, Quebec, Canada
The susceptibility of several CrFe and CrCo alloys has been measured between 2°K and 350°K, and the magnetization and magnetoresistance measured to 60kOe at both 4.2°K and 1.06°K. The susceptibility of CrFe obeys a Curie law below T_N while that of CrCo is temperature independent. This contrast is reflected in the field dependence of the magnetization and magnetoresistance of CrCo which is only a few % of that observed in CrFe. We have quantitatively explained this contrast through a model first proposed by Lomer which explicitly includes an interaction, Δ, between local moments and the chromium spin density wave (S.D.W.).

10:45
EF8 Magnetic Anisotropy of Mg-Mn Alloys. J.L. BENCHIMOL, F.T. HEDGCOCK and J.O. STROM-OLSEN, McGill University, Montreal, Quebec -- Magnetic anisotropy has been measured in three single crystals of Mg containing 80, 175 and 315 p.p.m. manganese in the temperature range of 1.8°K to 300°K at maximum fields of 8KG. The symmetry of the crystal introduces in the expression for the energy of the local spin a term which varies as AS_z^2 with A equal to 7.5 milli °K and independent of concentration. The inclusion of this term leads to an expression for the susceptibility anisotropy consistent with that observed i.e. proportional to T^{-2}.

11:00
EF9 Magnetic Moment Changes in Heusler Alloys due to Ti, V, and Cr Substitution.* C.C.M. CAMPBELL and C.V. STAGER, McMaster U.-- The Heusler alloys are a series of local moment ferromagnets, usually containing Mn, with a magnetization of $\sim 4\mu_B$ per molecule. Magnetic measurements are reported for the alloy series, $Ni_2Mn_xT_{1-x}Sn$, where T is Ti, V or Cr. Samples were prepared at Mn concentrations corresponding to x = 1, 0.8, 0.6, 0.4, 0.2 and 0.0 for the Ti and V series. For $x < 0.4$, the samples of the Cr series are polyphase. Susceptibility studies on all three series show Curie-Weiss behaviour and indicate an effective moment of $\sim 5\mu_B$/Mn atom. Interpretation of the magnetization results suggests that an atom of Ti contributes $\sim -1\mu_B$, V makes no contribution, and Cr gives $\sim +1\mu_B$ to the magnetic moment of the alloys. This change of sign from negative to positive with increase in atomic number can be interpreted, if an important cause of the ferromagnetic coupling in Heusler alloys is the superexchange mechanism.

*Research supported by the National Research Council of Canada.

11:15
EF10 High Field Twist Effect in Invar Alloys*
O. CAPORALETTI and G.M. GRAHAM, Univ. of Toronto--It has been observed that Invar rods undergo a twisting deformation in response to a high magnetic field parallel to the longitudinal axis of the sample at low temperatures. The twist is of the order of 0.1" $KO_e^{-1}cm^{-1}$ and reversible with field changes up to 100 KO_e. The effect is consistent with a canted magnetic structure with a net azimuthal component of magnetization of the order of 1% of the saturation magnetization. It is suggested that this is a macroscopic manifestation of the antiferromagnetic interactions believed to be present in these alloys.

* Work supported by the National Research Council of Canada.

11:30
EF11 Resistance and Magnetoresistance of Amorphous Alloys. R.W. COCHRANE and J.O. STROM-OLSEN, McGill University.--We have examined the resistivity of a number of amorphous alloys, most of which order ferromagnetically, from 1 to 300 K in magnetic fields up to 45 kOe. The resistivity of the "as deposited" samples shows a characteristic minimum with a ln T dependence at low temperatures. For the ferromagnetic alloys the magnetic field does not alter these characteristics but does contribute a magnetoresistance which saturates at low fields with the magnetization. Furthermore, $\rho(T)$ varies smoothly through T_c to better than 2 parts in 10^6. Annealing at temperatures up to the crystallization point does not significantly alter this behaviour, in spite of some marked changes in the mechanical properties. Crystallization, however, removes the resistance minimum and the ln T dependence reinforcing the conclusion that these anomalies are structural in origin.

11:45
EF12 Surface Corrections to the Landau Diamagnetic Susceptibility.* R.K. BHADURI, and B.K. JENNINGS, McMaster U.--The steady value of the diamagnetic susceptibility of a uniform noninteracting electron gas is given by the usual Landau value. The question arises as to whether or not this value is affected by the presence of a surface potential. This question is investigated in both the zero and high temperature limits by using the Wigner-Kirkwood expansion of the electronic partition function in the presence of a weak magnetic field. Explicit expressions for the susceptibility are derived for electrons in a smooth arbitrary potential barrier, and by taking some simple examples, it is shown that the surface corrections to the susceptibility vanish at high temperature, while at zero temperature small correction terms may persist.

*Work supported by the National Research Council of Canada.

WEDNESDAY, JUNE 16, 1976
ROOM 2E
Chairman: J.R. Derome

THEORETICAL PHYSICS II

9:00 Broken Symmetries
EG1 L. MICHEL, *Institut des Hautes Etudes Scientifiques Bures sur Yvette France et Centre de Recherche Mathematique Universite de Montreal*

9:30
EG2 Speculations on Quarks
G. KARL, *University of Guelph, Guelph, Ont.*

10:00
EG3 Schemes of Generalizing Dynamical Systems. C. A. LINCOLN, State University of New York, College at Fredonia.--Some of the attempts at systematically generalizing dynamical systems are reviewed with special attention paid to the themes of (1) Lagrangian dynamics and Lagrangian field theories[1] (2) Sudarshan's scheme of generalizing by formulations in terms of Lie Algebras[2] and (3) geometrical schemes as in general relativity and unified field theories. Generalization schemes based upon formulations in terms of C* albebras[3] and propositional calculi[4] are proposed and some of their limitations discussed. An additional scheme for generalizing non relativistic quantum mechanics is suggested and examined briefly.

[1] G. R. Gruber, Foundations of Physics, 1, 227, 1971.
[2] E.C.G. Sudarshan, Lectures in Theoretical Physics, 1961 Brandeis Institute, W. A. Benjamin, 1962.
[3] G. C. Emch, Alg. Methods, in Stat. Mech. and Quant. Field Theory, Wiley-Interscience, N.Y. 1972.
[4] J. M. Jauch, Found. of Quant. Mech., Addison Werley, Reading, Mass.,1968.

10:15
EG4 Quantum Mechanics and Electromagnetic Theory: Unification in Markov Processes, John R. Fanchi and R. Eugene Collins, University of Houston. It is shown that the Smoluchowski equation for a diffusional type Markov process, or random walk, in space-time is mathematically equivalent to a set of coupled equations having the form of Maxwell's equations and the Klein-Gordon equation including the vector and scalar potentials. Thus the vector and scalar potentials, with the phase of the wave function carry all information inherent in the transition probability density.

10:30
EG5 Quantum Mechanics: A Hilbert Space Formalism for Probability Theory, R. Eugene Collins, The University of Houston, Houston, Texas 77004. We show that the Born representation of a probability density as $\psi^*\psi$ with $\psi \epsilon L^2$ is necessary to correct a defect in classical probability; this is the key element in exhibiting classical probability theory in a Hilbert Space format. Using this we derive the Schrodinger equation for an electron in an external field specified by vector and scalar potentials and the complete operator formalism for expectation values directly as elements of a classical probability formalism.

10:45
EG6 Statistical Effects of the Motion of an oscillator Interacting with a Radiation Field. S.V. GODOY and E. BRAUN, Facultad de Ciencias, Universidad de México and Universidad Autónoma Metropolitana (Izta palapa).-- The motion of a quantum oscillator interacting with a quantized radiation field is studied. The exact solution shows that the motion of the oscillator is described by a Langevin-type equation in which the friction force and the effective frequency depend on time. The physical conditions under which these properties become constant are studied. The stochastic force becomes a gaussian process and in the limit of long times and weak coupling has an autocorrelation function with the usual delta behavior.

11:00
EG7 On Dirac Strings* W.-T. NI, and H.C. YEN, National Tsing Hua University. Hsinchu, Taiwan, Republic of China.—It is known that a classical monopole field can be derived from a vector potential having a half-line singularity (Dirac string). For a magnetic monopole of strength g_o at the origin,we obtain a vector potential having a singularity on an arbitrarily fixed curve $\theta=\alpha(r)$, $\phi=\beta(r)$;explicitly, the potential is given by

$$A_{[r]} = g_o \Delta^{-1}[\alpha'(r)\sin\theta\sin(\beta-\phi) + \beta'(r)(\cos\alpha - \cos\theta)]$$
$$A_{[\theta]} = -g_o r^{-1}\Delta^{-1} \sin\alpha\sin(\beta-\phi)$$
$$A_{[\phi]} = g_o r^{-1}\Delta^{-1}[\sin\alpha\cos\theta\cos(\beta-\phi) - \cos\alpha\sin\theta]$$

where $\Delta = 1 - \cos\alpha\cos\theta - \sin\alpha\sin\theta\cos(\beta-\phi)$. Comparison with Wentzel's[1] integral expression is discussed and generalization to the case of curved space is made.

* Supported in part by the National Science Council, Republic of China.

1 G. Wentzel, Suppl. Prog. Theor. Phys. 37 & 38, 163 (1966).

11:15
EG8 AN ALTERNATE APPROACH TO THE TIME DEPENDENT PERTURBATION* PRAKASH CHAND and FRANKLIN CABRERA. Universidad de Los Andes. In the usual approach of time dependent perturbation theory the knowledge of previous term is essential to write a term. Furthermore, the master equation is also used to equate the coefficients of small perturbing parameter to find the perturbation to any order. Starting with the interaction picture a set of rules are defined to enable to write perturbation term to any order has been discussed that all types of perturbation cannot be solved in closed form. The whole approach is very physical and the necessity and use of interaction picture is emphasized.

* Supported by a grant from CONICIT

▾ Based on the thesis of Cabrera

EG 9, 10, 11

WEDNESDAY, JUNE 16, 1976
ROOM 1A
Chairman: P. Vanicek

GEODESY

9:00
EH1 Nano Variations in Gravity due to Seasonal Groundwater Movements: Implications for the Gravitational Detection of Tectonic Movements. A. LAMBERT AND C. BEAUMONT* (E.P.B.) *(Now at Dalhousie University) Six nanogravity surveys have been made at two coastal areas of Eastern Canada in order to study the gravity changes associated with seasonal groundwater fluctuations. The repeated surveys made with a LaCoste and Romberg model D gravimeter, D6, demonstrate that: 1) Seasonal changes in gravity differences ($\sim$100nm/s^2) at Cap Pelé, a region of relatively simple hydrogeology, are in good agreement with well and piezometer measurements, and 2) the corresponding changes ($\sim$120nm/s^2) at York Point, a region of complex hydrogeology suggest a different interpretation of seasonal groundwater flow from that inferred from piezometer measurements alone. The results demonstrate that normal variations in groundwater may obscure gravity changes associated with tectonic movements and earthquake precursory effects. When normal variations in groundwater are known or are not significant, the results demonstrate that tectonic gravity changes as small as 20-30nm/s^2 may be detected at the 90 percent confidence level with the LaCoste and Romberg D meter. Such a gravity change corresponds to a 'free-air' change in elevation of $\sim$1cm.

9:15
EH2 On the Interpretation of Repeated Geodetic Surveys for Geophysical Ends by E.NYLAND, I.E.P.P., U.of A. - The theory involved in transforming changes in geodetic survey observations to movement on faults is linear as long as the geometry of the tectonic drive is fixed. Interpretation using theories developed for undetermined linear systems is therefore useful. The non-linear problem of determining geometry is best approached by studying source parameters with optimum accuracy by non-linear optimization methods.

9:30
EH3 Geodetic Surveys in Monitoring Tectonic Measurements in Peruvian Andes by A. CHRZANOWSKI, Univ. of N.B., E. NYLAND, Univ. of Alta., and P. POLAK, Univ. of N.B. - A survey methodology for monitoring strain changes in the Peruvian Andes with an accuracy of 10^{-5} or better is being developed by the authors. A test micro-geodetic network of 12 points with distances ranging from 200 to 1500 metres was established in 1975 over a fault with known activity at an elevation of about 4500 m. The unusual problems of geodetic surveying at very high altitudes and the requirements of geophysically significant data led to a very stringent evaluation of various surveying instruments and procedures. The network was surveyed with the Wild T-2 theodolite and HP-3800 infrared EDM instrument. Error analysis of the adjusted network indicate that the required accuracy may be achieved using the employed survey techniques. The network will be remeasured once a year. Geodetic levelling and a set of mechanical devices with continuous recording of strain changes will be added to the survey programme in the future measurements.

9:45
EH4 Analysis of Step by Step Adjustment Procedures for Large Horizontal Geodetic Networks. P. GAGNON. Université Laval. - An adequate treatment of the actual North American horizontal geodetic network would clarify its definition and increase its use as well as the resulting benefit to the scientific community and to the society in general. These facts have been recognized and the task of the redefinition of the North American geodetic networks has been recently undertaken. A major part of this task is the global adjustment of the horizontal network. This paper discusses of the appropriate procedure to be used to solve the problem of the readjustment of the Canadian horizontal geodetic network in the context of the redefinition of the whole North American horizontal geodetic network. The problem of least square adjustment is defined. The characteristic of horizontal geodetic network are given. A partitioning scheme for large horizontal network is proposed. Various step by step procedures are analysed and compared with the simultaneous procedure.

10:00
EH5 Special Relativity and Annual Aberration in Long Baseline Interferometers. W. H. CANNON, R. B. LANGLEY, W. T. PETRACHENKO, CRESS and Physics Dept. York Univ. and A.I.A.S. - The annual aberration of starlight by the earth's orbital velocity is a classical phenomenon discovered and correctly explained by Bradley in 1725. The effect of aberration is to displace the apparent position of a star by about 20" arc. The effect of annual aberration on the position of a radio source is easily observable with a long baseline interferometer which can determine the position of a radio source with an accuracy of ±0".01 - ±0".1 arc. Recently there has been some interest in the use of L.B.I. as a means of testing the theory of relativity. The classical analysis of the response of a long baseline interferometer predicts that it should be insensitive to the effects of annual aberrations. It follows that the observation of the effects of annual aberration in a long baseline interferometer constitutes a test of special relativity to a precision of about ±0.1%.

10:15
EH6 Geodetic and Astrometric Measurements Using the Algonquin-Chilbolton Long Baseline Interferometer*. W. H. CANNON, R. B. LANGLEY, W. T. PETRACHENKO, CRESS and Physics Dept. York Univ. and A.I.A.S.- In March, May, and June of 1973 three separate long baseline interferometry (L.B.I.) experiments were carried out at 2.8 cm using the 46m radio antenna at Algonquin Park, Ontario, Canada and the 25m radio antenna of the Appleton Laboratory at Chilbolton; England. Fringe frequencies obtained from the interferometer in each of these experiments were used to determine a number of geodetic and astrometric parameters. Approximately 4000 separate fringe frequency measurements were used in this analysis. Results will be presented which will indicate that the 5251km equatorial component of the interferometer baseline had an r.m.s. deviation from the mean of 105 cm. in length and 15 x 10^{-3} "arc in orientation between the three experiments.

*Supported by the National Research Council of Canada.

10:30
EH7 Response of an aquifer near Ottawa to the Alaskan earthquake of 1964. D.R. BOWER and K.C. HEATON* Earth Phys. Br. (*now with Dept. of Physics, York University, Toronto) - Coincident with the Alaskan event the water level in a deep uncased well near Ottawa showed a small initial rise then a decrease of 30 cm followed by a decay back to the original level over a period of 2 days. This is suggestive of a residual dilatation with subsequent fluid diffusion. It is shown that this explanation is consistent with the diffusion and elastic properties of the aquifer estimated independently from a slug test, from the earth tide response and from the response of the well level to atmospheric pressure. A simple saturated, porous half space is assumed.

10:45
EH8 Geoid Determination from Astrogeodetric, Gravimetric and Doppler Satellite Data. By Saburi John and Alphonce Mutajwaa - U.N.B. - The geoid referred to the geodetic ellipsoid is conventionally computed from astrogeodetic deflections. In most parts of Canada, astrogeodetic coverage is poor so that deflection coverage has to be enhanced using gravity data. To obtain absolute geoidal heights, one may use geoidalheights derived from doppler satellite positioning as constraints. In this paper such a geoid has been computed and used in an adjustment of a geodetic network in Eastern Canada.

11:00
EH9 Improved Marine Navigation Error Modelling through System Integration. DAVID WELLS. Bedford Institute of Oceanography - Radio navigation accuracy is most significantly influenced by errors in modelling radio wave propagation; satellite navigation by errors in modelling ship's velocity; and log and gyro navigation by errors in modelling ocean currents. Passive ranging (rho-rho) radio navigation is also influenced by errors in modelling clock synchronization and drift. The characteristics of these and other secondary influences, established during several cruises at the Bedford Institute of Oceanography, are reviewed. They are complementary in the sense that in each case the error modelling can be improved by measurements from other systems. The mathematical design of a novel integrated navigation system based on this approach is described.

WEDNESDAY, JUNE 16, 1976 — ELEMENTARY PARTICLES - EXPERIMENTS
ROOM 2F
Chairman: P.M. Patel

9:00
EI1 Excitation of New States of Matter by High Energy Neutrinos
D. CLINE, *University of Wisconsin*

9:40
EI2 Measurement of the $\bar{K}^{*-} \to \bar{K}^{0} \gamma$ Radiative Decay
D.G. RYAN, *McGill University*

10:15
EI3 Particle Search Results from Fermilab
J.A.J. MATTHEWS, *Michigan State University*

10:55
EI4 $K\pi$ and $K\pi\pi$ Results from a 13 GeV $K^{\pm}p$ Experiment
R. CARNEGIE, *Carleton University*

11:35
EI5 Deep Inelastic Muon Scattering
H. ANDERSON, *University of Chicago*

EJ. 1 2 3 9

EK 1 — 8.

WEDNESDAY, JUNE 16, 1976
ROOM 1C
Chairman: A.E. Douglas

Annual General Meeting of the Canadian Association of Physicists

14:00
FA1 Presidential Address: A Political Role for the CAP?
A.E. DOUGLAS, *President CAP, National Research Council of Canada*

14:30 Break

14:45 Annual Business Meeting

17:30 Réception - gracieuseté de l'Université Laval

19:30 Banquet

THURSDAY, JUNE 17, 1976 SEANCE PLENIERE
ROOM Théâtre de la cité universitaire Pavillon des Sciences de l'administration INTERACTION LASER - MATIERE
Chairman: ~~C. Bédard.~~ ?

9:00
GA1 Laser Plasma Interaction Experiments for Fusion
H.G. AHLSTROM, *Laser Plasma Interaction Group - Lawrence Livermore Laboratory*

yes

9:40
GA2 Laser Plasma Interaction
D. HENDERSON, *Laser Theory Group, Los Alamos Scientific Laboratory*

10:20 Café

10:40
GA3 Laser Isotope Separation Experiments at LASL
~~R. JENSEN, Laser Isotope Separation Group~~ - *Los Alamos Scientific Laboratory*
To be read by D Henderson.

11:20
GA4 To Be Announced

GA5 R. Gentry

THURSDAY, JUNE 17, 1976 NUCLEAR PHYSICS II-SELECTED TOPICS
ROOM 1B
Chairman: J.M. ROBSON

13:30
HA1 Use of Tensor Polarized Deuterons to Measure Spin and Parity
J.A. KUEHNER, *McMaster University*

14:15
HA2 Fundamental Experiments with a Neutron Interferometer
A. OVERHAUSER, *Purdue University*

15:00
HA3 Symmetry Properties of Atomic and Nuclear Interactions
P. KABIR, *University of Virginia*

15:45
HA4 Neutral Current Effects in Muonic Atoms
G. FEINBERG, *Columbia University*

THURSDAY, June 17, 1976
ROOM 1C
Chairman: D.R. Taylor

13:30

HB1 Interaction of Helium with Vacancies in Metals

E.V. KORNELSEN, *National Research Council, Ottawa*

A description will be given of a technique based on thermal desorption which allows the interaction of injected Helium with lattice vacancies in metals to be studied in some detail. Supporting computations of the binding energies of various gas/vacancy complexes will also be discussed.

14:15

HB2 Neutron Scattering Studies of the Dynamical Structure of Liquid ^{4}He

E.C. SVENSSON, *Atomic Energy of Canada Ltd. Chalk River, Ont.*

Recent neutron-scattering studies at Chalk River which have elucidated several aspects of the dynamic structure of liquid ^{4}He will be discussed. These include studies of: (i) The phonon dispersion at low wave vectors ($0.2 \lesssim Q \lesssim 1.0$ Å^{-1}) for T = 1.0 K and pressures in the range $0 \leq P \leq 24$ atm. Direct evidence is obtained for anomalous (upward) dispersion in a range $0 < Q < Q_-$ where Q_- decreases with increasing P. (ii) The behavior of the complete scattering function $S(Q,\omega)$ for selected values of Q, P and T. These studies give evidence for strong interference between one-phonon and multiphonon scattering processes which qualitatively explains several features found in earlier studies and which indicates that liquid He is very "anharmonic". No evidence is found for the existence of two-roton bound states. (iii) The "free-particle" scattering at large Q ($6 < Q \lesssim 12$ Å^{-1}). Oscillations in the widths of the distributions persist throughout this region and a simple model suggests that these oscillations have their origin in similar oscillations in the He-He scattering cross section which occur because of the quantum scattering of identical particles. No sharp structure in the lineshape attributable to scattering from the condensate atoms is observed. (iv) The scattering in the non-superfluid phase, $T > T_\lambda$, and comparison with hydrodynamic theory. A triple-peaked lineshape consisting of a central Rayleigh component (entropy fluctuations) and a Brillouin doublet (sound waves) is observed for $Q = 0.11$ Å^{-1} at T = 4.2 and 3.6 K at saturated vapor pressure (SVP). At T = 2.3 K and SVP there is evidence for a transition at $Q \sim 0.3$ Å^{-1} from the first-sound to the zero-sound mode of propagation.

15:00

HB3 Far-Infrared Studies of Excitons and the Electron-Hole Liquid in Germanium

T. TIMUSK, *McMaster University*

Starting from the original proposal by Keldysh that excitons could condense at low temperature in Germanium to form metallic fluid droplets and subsequent confirmation by Pokrovsky this new phase of matter has been studied extensively by a variety of techniques. Far-infrared measurements, first done at the Lebedev Institute in Moscow, are particularly suitable for this study. The exciton gas, too, can be studied with high resolution in this spectral region and at high temperature and high exciton density a third phase, the electron hole plasma, can be seen as a seperate absorption at very low energy (1 meV). We present recent results on far-infrared spectra of all three phases and attempt to trace the phase boundaries. The exciton spectrum consists of several sharp lines in the 2 to 4 meV region with a long photo-ionization continum extending to 7 meV with a hydrogenic $\nu^{-8/3}$ frequency dependance. At higher temperatures new lines appear which can be interpreted as arising from the 1.0. meV excited state of the exciton. At still higher temperatures (15K) a continuous absorption with $\nu^{-2.7}$ power dependance appears at 1 meV characteristic of a free electron-hole plasma. The absorption of the electron hole fluid at 9 meV is also discussed in particular in doped samples where the droplets are very small and the plasma appears to be very highly damped.

THURSDAY, JUNE 17, 1976
ROOM 2A
Chairman: R.L. Armstrong

13:30
HC1 G-2 Resonance Observed in Monoelectron Oscillator. R. VAN DYCK, JR., P. EKSTROM, and H. DEHMELT, U. of Washington.--Essentially as proposed by us (1973 & 1974) the G-2 resonance at $\nu_d = \nu_s - \nu_c + \nu_m$ has been observed by making a single electron see an effective, adjustable (<10 μG) rotating magnetic field at ν_s, the spin frequency, occurring as the sum of a forced-axial-motion frequency ν_d = 59.415890 MHz and $\nu_c - \nu_m$ = 51206.11 MHz, the frequency of the 4^0K thermal cyclotron motion through the inhomogeneous static field of a ∿30 G deep magnetic bottle superimposed upon a strong ∿18.3 kG field. Spin flips, induced at a rate ∿1/min, were detected by continuously monitoring the bottle-related shift $\delta\nu_z \approx (m + n + \frac{1}{2})$ 2.5 Hz of the axial resonant frequency ν_z = 59.4101 MHz and focussing on the minimum values, 2.5 & 0 Hz, corresponding to n = 0, m = $\pm\frac{1}{2}$, which occur as the electron jumps frequently between the cyclotron levels, n, and rarely between the spin levels, m. The minimum ν_d-linewidth of ∿500 Hz realized so far is primarily due to the continuous ν_z- monitoring. Pulsed operation promises a 100 fold sharper line. With the measured ν_m = 34.464 KHz, our preliminary value of $a \equiv (\nu_s - \nu_c)/\nu_c$ is 0.001159655(5). D. Wineland and P. Schwinberg have made important contributions to this NSF supported work.

13:45
HC2 EPR Determination of Crystal Field Splitting in Ti_4O_7.* J.F. HOULIHAN and DAVID P. MADACSI, Penn State Univ. --Until recently, attempts to describe the crystal field environment of the Ti^{3+} ion in the mixed valence (Magnelli) phases of the titanium - oxygen system, Ti_nO_{2n-1}, have been hindered by a lack of single crystal EPR data. Recently, however, the authors have reported single crystal EPR results for Ti_3O_5, and an LCAO determination of crystal field splitting parameters based on the g-shift results with the assignment of D_{2h} symmetry for the Ti^{3+} site.[1] The results of this determination were found to be consistent with available optical, x-ray, and (polycrystalline) EPR data. Single crystal EPR results recently obtained have now permitted the extension of this analysis to Ti^{3+} ions in the next homolog in this series, Ti_4O_7. Rhombic crystal field splitting parameters thus obtained will be compared to available optical and x-ray data.

[1] J.F. Houlihan, D.P. Madacsi, and L.N. Mulay, Mat Res. Bull. 11, 307, 1976.

*Supported by the fund for Scholarly Activity of Penn State University.

14:00
HC3 NMR Line Width in Amorphous NiP.* H. E. SCHONE and P. A. GUSTAFSON, College of William and Mary.--We have studied the P^{31} NMR knight shift and line width for electroplated amorphous NiP alloy films. The line width has a field dependent part arising presumably form an inhomogeneous knight shift. The residual zero field width should be dipolar, corresponding to the contributors of phosphorous neighbors, and we compare it to various models for the P-P correlation function in this material. We find that the knight shift (K) has little or no composition dependence from 20 to 25% phorphorous and that K differs from its value in the corresponding crystalline material and from the value obtained in amorphous NiP obtained by electroless deposition.[1]

*Work supported by NASA.

[1] L. H. Bennett, Bull. APS 20, 644 (1975).

14:15
HC4 An NMR Study of Molecular Motions in Solid Fluoropentummine Cobalt (III) Chloride* E.C. REYNHARDT, A. WATTON and H.E. PETCH, University of Victoria--Molecular motions have been studied in a powdered sample of Fluoropentammine Cobalt (III) Chloride by using pulsed and c.w. NMR techniques. Activation energies of 1.8 and 2.4 kcal/mole associated with threefold reorientations of ammine groups have been isolated. At higher temperatures half of the complex ions execute rapid anisotropic reorientations with an activation energy of 6 kcal/mole. The other ions remain stationary up to 360°K where the complex changes structure or decomposes. Good agreement between relaxations and second moment measurements has been obtained. The motions are discussed in terms of structural features observed in other ammine complexes.

*Supported by the National Research Council.

14:30
HC5 NMR Study of Ionic Motions in Two Ammonium Bisulphates* A. WATTON, E.C. REYNHARDT and H.E. PETCH, University of Victoria--
Proton spin-lattice relaxation times and second moments in the temperature range from 77°K to 400°K have been measured for two ammonium bisulphates - the Ferroelectric NH_4HSO_4 and the ani Ferroelectric $(NH_4)_3H(SO_4)_2$. The low temperature phases of both materials show evidence of the same ionic motions - NH_4^+ reorientations around two and three fold axes with activation energies ∼ 2kcal/mole. The high temperature region in both materials is again characterised by similar mechanisms - the self diffusion of one half of the NH_4^+ groups. However, in the region of the upper phase transition of NH_4HSO_4 an ionic motion is evident which apparently is absent from the $(NH_4)_3H(SO_4)_2$ dynamics.

*Supported by the National Research Council.

14:45
HC6 A Proton FFT Study in the Isotropic Phase of CBOOA.* J. VISINTAINER AND E. BOCK, Univ. of Manitoba, R. Y. DONG and E. TOMCHUK, Univ. of Winnipeg.--Proton line shapes and relaxation measurements have been studied in the liquid crystal N-p-cyanobenzylidene-p-n-octyloxyaniline (CBOOA) using the technique of Fast Fourier Transform (FFT) spectroscopy. The proton spin-lattice relaxation time T_1 above the nematic-isotropic phase transition was measured, at several Larmor frequencies, for the resolved peaks of the FFT spectra. The critical temperature dependence T_{1cf}, the T_1 due to critical order fluctuations, was thus studied for each spin species. The critical temperature behavior of CBOOA will be compared with the predictions of a model based on short-range nematic orientational order fluctuations.[1]

[1] R. Y. Dong, E. Tomchuk and E. Bock, Can. J. Phys. 53, 610 (1975).

*Supported by the National Research Council of Canada.

15:00
HC7 Proton Longitudinal Relaxation Time Measurements in Gaseous Hydrogen Chloride and Hydrogen Iodide.* WALLACE KALECHSTEIN, CLAUDE LEMAIRE and ROBIN L. ARMSTRONG, Univ. of Toronto--Measurements of the proton longitudinal relaxation time T_1 through the region of the characteristic minimum at 61 MHz and 299 K in gaseous hydrogen chloride and hydrogen iodide are presented. In each case, the relaxation process is dominated by the spin-rotation interaction which has been independently studied using molecular beam techniques. The present results provide a conclusive test for available relaxation theories. In particular, a single correlation time model for the collision modulated spin-rotation interaction is found to be consistent with the proton magnetic relaxation data.

*Supported by the National Research Council of Canada.

15:15
HC8 EPR and Spin-Lattice Relaxation of the Jahn-Teller System Cu^{2+} in Zinc Bromate Hexahydrate. A.JESION, Y.H. SHING and D.WALSH, McGill University.--The anisotropic EPR spectrum for the Jahn-Teller system $Cu^{2+}:Zn(BrO_3)_2 \cdot 6H_2O$ has been measured at 4.2°K. The angular variation of this spectrum shows that the ground state is a strain stabilized vibronic doublet with tetragonal symmetry. The principal axis of the g tensor was determined to be 12.5 ± 2 degrees away from the [100] crystal axis. Accurate spin-lattice relaxation measurements were carried out by pulse-saturation techniques at X-band frequencies within the temperature range 4.2°K to 1.3°K, for three concentrations of Cu^{2+}. Relaxation times within this temperature interval varied from 12 to 50 μs for all samples. This rate is at least four orders of magnitude faster than for Cu^{2+} in Tutton salts which is free of Jahn-Teller complications.

15:30
HC9 **Proton Susceptibility of $^{13}CH_3D$.*** **R.F. CODE, J. HIGINBOTHAM and B. WOOD, Univ. of Toronto.--The magnetic susceptibility of protons in solid $^{13}CH_3D$ has been measured as a function of temperature from 26 K to 2 K. Previously, only the temperature range below 4.2 K had been measured. Furthermore, the use of ^{13}C as an internal thermometer enables systematic errors to be eliminated. The nuclear spin wavefunctions of the protons in solid CH_3D can have either A or E type symmetry. Evidence for an increase in the relative amounts of the A type symmetry species at low temperatures will be discussed.**

***Supported by the National Research Council of Canada and the Research Corporation.**

15:45
HC10 High Frequency Paraelectric Resonance in KI:OH^-. FRANK BRIDGES and WILLIAM M. KELLY, U.C. Santa Cruz.--We have used harmonic generation techniques to observe paraelectric resonant transitions in the KI:OH^- system at frequencies of up to 150 GHz. As a result we have made a more accurate determination of the uncorrected dipole moment of OH^- in this system, 1.26 ± .07eÅ. Our new data confirm the existence of a low-lying excited multiplet previously postulated[1], and it is found to be lower than expected, within 100 GHz of the ground state multiplet. The new zero-field splittings which have been found occur at approximately 97, 102, 120, 140 and 150 GHz. The features of the data are in good agreement with those predicted[2]. We will discuss the implications of the existence of this excited multiplet.

†Supported by the National Science Foundation.
[1]Frank Bridges, Sol. State Comm. 13, 1877 (1973).
[2]Frank Bridges, Phys. Stat. Sol. (b) 65, 743 (1974).

16:00
HC11 Strongly Bound and Weakly Bound Water, and Moisture Content of Wood by Proton Magnetic Resonance. A.J. NANASSY, Eastern Forest Products Laboratory, Ottawa. The sorbed water in wood produced two overlapping PMR spectral components, one broad and one narrow. The spectrum could be resolved instrumentally for the narrow component. The integrated absorption intensity of the narrow component changed linearly with the wet-mass or moisture content (MC) up to 22% at 25°C: the slope of the straight lines for six wood species examined were the same. Sorption hysteresis produced three such straight lines with slightly different slopes for a specimen. The true dry-mass and the MC of a specimen up to 22% can be calculated from the wet-mass, the slope (a constant), and a single PMR spectrum of the narrow component. The ratio of the mass of the strongly bound water to that of the weakly bound water was found to be about unity at the critical moisture content. CMC is defined by the MC at which the integrated absorption intensity of the broad component as a function MC reaches the upper value.

16:15
HC12
Mossbauer study of the changes induced in hexavalent iron compounds by gamma radiation.
A. Jimenez R. *, H. Arriola S. *, P. Ramos R.* y A Cruset **. -- The decomposition by gamma radiation of some hexavalent iron compounds was studied using the Mossbauer effect in the following way; the samples were cooled to 77° and 293° K, respectively and the following dosages, 10, 20, 30, 40, 50, 100 and 150 Mrads and then, at the same temperatures the spectra were obtained.

Since these compounds easily reduce in a humid atmosphere, care was taken in the preparations, working always under inert and dry atmosphere until the samples were sealed.

The isomeric shifts, quadrupolar splittings and oxidation state ratios are given. The intermediate valence states, $Fe^{3.5}$ or Fe^{4+} were not detected.

* Centro de Estudios Nucleares, U N A M (Mexico).
** Centre de Recherches Nucleaires, Estrasburg (France).

16:30
HC13 Design of a liquid helium cryostat for Mossbauer Spectroscopy. A. Jimenez R. *, H. Arriola S. *, J.M. Ramos ** y A. Cruset ***. -- A cryostat for liquid helium was designed in order to cool samples for Mossbauer studies, with such a geometry that makes possible high transparency for X-rays around 10 Kev.

This consists of a 12 litre cylinder with 0.38 mm thick stainless steel walls, surrounded by a 6 litre cylindre for liquid nitrogen as a thermic shield. There are two possible modes of operation, the horizontal mode, that is, cooling directly the sample infront of an aluminized mylar window and the vertical mode, which fixes the sample as well as the source inside the cryostat.

* Centro de Estudios Nucleares, U N A M (Mexico).
** Instituto de Fisica, U N A M (Mexico).
*** Centre de Recharches Nucleaires, Estrasburg (France).

Mossbauer Spectra at 290°, 77° and 4°K are shown.

THURSDAY, JUNE 17, 1976
ROOM 2B
Chairman: J. Destry

13:30
HD1 The Study of Organic Molecules on Surfaces by Electron Tunnelling
J.G. ADLER, *University of Alberta*

The use of both elasticaly and inelasticaly assisted electron tunelling in the study of thin layers of organic compounds deposited or absorbed on surfaces will be discussed. Experimental techniques both for measurement and sample preparation will be presented. A number of results for different molecular species will be presented. In addition the use of inelastic electron tunneling to determine the vibrational spectrum of the molecular species involved, along with the use of elastic magnetic scattering to determine the presence of radicals will be illustrated by results obtained on a simple aromatic molecule (benzene).

14:15
HD2 The Kinetics of Magnetic Flux Penetration into Superconductors.* B.K. MUKHERJEE, H.D. WIEDERICK, J.P. PENDRYS and D.C. BAIRD, R.M.C., Kingston.-- We are carrying out an experimental investigation of the kinetics of magnetic flux penetration into superconductors under non-equilibrium conditions. The specimens used have different geometries and their κ values are in the pure Type-I to improve Type-II range. The magnetic flux is produced internally, by passing a current through the superconductor, or externally, in which case it is generated by a solenoid surrounding the specimen. We describe the experiments and present a preliminary discussion of our results.

*Work supported by Defence Research Board of Canada Grant No. 9510-21.

14:30
HD3 HELICAL PROPAGATION OF FLUX JUMPS IN WIRES OF TYPE II SUPERCONDUCTORS CARRYING A CURRENT IN LONGITUDINAL FIELDS. R. Boyer and M.A.R. LeBlanc. U. of Ottawa, Canada and J.F. Bussière, Brookhaven National Laboratory. -We have measured the velocity of propagation of flux jumps along wires of NbZr, NbTi, Nb and V carrying steady transport currents and magnetized in an axial magnetic field. The speed of propagation is monitored by two small pick up coils embracing the wire and spaced along the length. For the Nb and V samples we also placed a saddle-shaped pick up coil along a section of the wire circumference. With this arrangement we detect a succession of pulses between the two main pulses as the flux jump advances. The dependence of f the frequency of these pulses and v_z the axial velocity on the current I are correctly described by the relations:
$f=v_z K^2/2\pi R$ and $v_z=v_o (1+kI^2) / (I+KI^2)^2$ where v_o is the velocity when I=0, R is the wire radius. k and K are adjustable parameters which can be estimated from the model leading to these relations. The model visualizes that the flux jump follows a helical path corresponding to the configuration of flux lines near the surface of the wire.

14:45
HD4 Rotation Induced Voltages in Superconductors.* C. PURCELL, B. L. BLACKFORD, G. STROINK, Dal. Univ. - On the basis of simple arguments one expects that centrifugal forces acting on the electrons in a rotating conductor will generate a small radial electric field with a magnitude proportional to the square of the rotation rate. An attempt was made to detect a rotation induced E.M.F. in normal and superconducting cylindrical samples. The method employed sliding superconducting contacts developed especially for this experiment, to draw a current from the rotating specimen. A Clarke SLUG was used to measure the induced current. The observed E.M.F.'s were several orders larger than the expected rotation induced voltages and appeared to be an artifact generated by the sliding contacts. The exact nature of the observed E.M.F.'s is still not clear.

*Supported by the National Research Council of Canada.

15:00
HD5 Increase in Critical Currents and Decrease in A.C. Losses in Wires and Ribbons of Type II Superconductors in Longitudinal Magnetic Fields. R. GAUTHIER, J.P. LORRAIN and M.A.R. LEBLANC, U. of Ottawa and A. LACHAINE, U. of New Brunswick, Fredericton, Canada.- We have investigated the increase in current carrying capacity and the decrease in hysteresis losses in wires and ribbons of type II superconductors NbZr, NbTi, NbTa, V and VTi in static longitudinal magnetic fields. For the wires the current is always fed in from an external source and we continously monitor the magnetization along the length of the specimen as I is impressed and varied through half and full cycles. For the ribbons the current is introduced by induction, i.e. by applying a transverse field $H_\perp$ directed along the flat surface. In this situation we trace the locus of the // and $\perp$ components of the magnetization during half cycles ($H \to 0 \to H$) and full cycles ($+H \to 0 \to -H$) in various static $H_{//}$. We account for these results and data on A.C. losses with a simple model exploiting (i) the critical state concept $F_L = F_p$ where F_L is the Lorentz force and (ii) the empirical expression $d\theta/dx = kF_p B^2$ to describe the change in direction of the vortices. Here k is a parameter of the sample and $F_p(B)$ is the pinning function used in (i).

15:15
HD6 Magnetization of Type II Superconducting Disks Rotating in Magnetic Fields. R. BOYER and M.A.R. LEBLANC U. of Ottawa, Canada.- We have investigated the changes in configuration of magnetic induction threading disks of type II superconductors (V and VTi) subjected to continuous rotation in static magnetic fields directed $\perp$ to the axis of rotation Z. The magnetic moment of the disk is monitored via two orthogonal pick up coils separately feeding electronic integrators and the Y axes of a X-Y_1-Y_2 recorder whose X-axis is driven by a signal proportional to the angle of rotation θ. One pick up coil monitors the magnetization // to the applied field H and the other $\perp$ to H and Z. We have examined the behaviour occuring during rotation starting with 4 types of initial field profiles across the thickness of the disk. These profiles are established by first cooling through T_c to 4.2°K in (i) various H_i whose magnitude is then maintained, (ii) $H_i = 0$ then raised to H_f, (iii) $H_i > H_{c2}$ then a) decreased to H_f or b) lowered through 0 to $-H_f$. We account for the evolution of the magnetic moment and its components for all initial states with a simple model which exploits the critical state concept and the expression $d\theta/dz = kJ_c(B)$ for the change in direction of the vortices where k is a constant of the sample.

THURSDAY, JUNE 17, 1976
ROOM 2C
Chairman: C. St-Pierre

13:30

HE1 High Power TEA-CO_2 Laser Induced Polymerization of Ethylene*. S.L. CHIN. LROL, Université Laval.--Complex molecules under a short pulse irradiation of a TEA-CO_2 laser can easily be dissociated into different fragments.[1,2] These dissociated fragments or radicals can be used to induced chemical reactions; for example, polymerization. A 100-MW double discharged TEA-CO_2 laser was used to induce the polymerization of ethylene gas at pressures ranging from ∿ 17 atm. to ∿ 62 atm. at room temperature. The polymerization product, apart from the fine carbon particles, was mainly tetradecane ($CH_3(CH_2)_{12}CH_3$) (∿ 80%) and Octadecane ($CH_3(CH_2)_{16}CH_3$) (∿ 20%).

1. N.R. Isenor et al., Can. J. Phys. 51, 1281(1973).

2. V.N. Bagratashivili et al., Opt. Commun.,14, 426, (1975).

* This work was supported in part by a grant from the Imperial Oil Limited, Canada.

13:45

HE2 Maintenance of the Canadian Unit of EMF with the Josephson Effect. G. H. WOOD, National Research Council, Ottawa--A suitably biased superconducting Josephson junction serves as a very precise frequency-to-voltage transducer in which the proportionality factor is the ratio of fundamental constants 2e/h. The exploitation of this phenomenon to maintain the Canadian unit of emf (the volt, V_{NRC}) in terms of these constants, rather than the electrochemical potential of saturated Weston standard cells, will be described. Results to date are very promising and delineate the areas where improvements will be made to reduce the experimental uncertainty to the required 0.05 to 0.10 ppm level.

14:00

HE3 Coaxial Acoustic Resonator.* T. TIEDJE, W.N. HARDY and R.R. HAERING, Univ. of B.C. -- A new resonance technique has been developed for measuring ultrasonic attenuation and the speed of sound in small needle-like samples. A longitudinal acoustic mode is excited in the sample by applying an a.c. voltage across the plates of the capacitor formed by placing the end of the sample close to a flat electrode. The acoustic resonance is detected by measuring the time dependent capacitance between the other end of the vibrating sample and another flat electrode. The detector circuit uses a 500 Mhz carrier and is presently capable of measuring acoustic oscillations less than .1 A° in amplitude. Preliminary room temperature measurements have been made to determine the limitations on sample size. The principal advantage of the technique is that acoustic bonds are not required.

*Supported by the National Research Council of Canada.

14:15

HE4 Energy and Resource Recovery From Solid Waste: Collection Methods. ARTHUR C. MEYERS III*, Technical Environmental Resource Research Associates, Inc., Ames, IA -- The collection of mixed municipal refuse (MMR II) accounts for approximately 85% of the total cost of MMR II disposal. In this study only the energy aspects of the collection methods were considered. The conventional household collection consists of bulk removal of the total solid waste from a neighborhood and its transfer to a distant dump site. Increased energy costs combined with increasing distances to acceptable landfill sites has caused rapid increases in collection costs. One can add to this the problem of growing material scarcities. An analysis was made of the resource and energy content of MMR II as a function of mass, volume and separation ease. Various collection, separation, and compaction techniques were considered. Also selective separation of specific items such as aluminum, steel and/or newspaper were considered. The optimum solution depends explicitly on the market for the recycled materials or the energy produced. Results from combining different possible collection methods with recovery systems will be presented.

*Current address: 1612 Burnett, Ames, IA 50010

14:30

HE5 A Systematic Study of Energy Conservation Methods Applicable to Residential Buildings. ARTHUR C. MEYERS III*, Institute of Basic and Applied Research, Inc., Arvada, CO and Solar Energy Tech Research, Inc., and THOMAS C. JOHNSON, Solar Energy Tech Research, Inc., Arvada, CO-A systematic study has been made of the various methods available to conserve energy use in residential buildings. The study considered two major areas of energy conservation. One, how the buildings themselves might be designed or modified to require less energy consumption to maintain predetermined conditions. Two, how the inhabitants of the building might organize their environment for minimum energy consumption. The study emphasis, even for new systems and techniques of energy conservation, was the use of currently available technology. Analysis of various conventional construction methods provided the baseline data for all subsequent considerations. The improved systems proved to be highly cost effective. The actual degree of improvement over conventional systems needed to make a specific new system economically viable depends on the local climatic conditions, the cost of available energy sources, etc.

*Current address: 1612 Burnett, Ames, IA 50010

14:45

HE6 Gradient Correction to Exchange and Correlation Energies and Chemisorption.* L.M. KAHN, Battelle Columbus Labs., Columbus, Ohio 43201 and M. RASOLT, Battelle Columbus Labs., and Ohio State University, Columbus, Ohio 43210--The effect of the gradient correction to the exchange and correlation energies on chemisorption properties is examined using the evaluation of B_{xc} arrived at by Rasolt and Geldart.[1] Quantities common to the study of chemisorption are calculated for various forms of the energy functional within the linear response approach.[2] It is found that the change in the potential and density, induced by a point charge in the vicinity of a metal's surface, due to the gradient correction, is larger than the contribution of the local correlation term but of opposite sign. The dipole moment induced by a point charge is increased by the gradient term. Calculation of the properties of alkali chemisorption, where the adion is represented by a pseudocharge density, shows that the gradient correction tends to lower the binding energy by about 10% (creating closer agreement with experiment), while leaving the equilibrium adion-metal separation unaltered.

* Submitted by John F. Devlin

(1) M. Rasolt and D.J.W. Geldart, Phys. Rev. Lett. 35, 1234 (1975).

(2) S. C. Ying, J. Smith, and W. Kohn, Phys. Rev. B11, 1483 (1975).

15:00

HE7 Perturbed γ-ray directional correlation studies of In(III) complexing in Aqueous Solutions*. G. R. DEMILLE, D. L. LIVESEY, K. MAILER and S. P. TURNER, University of New Brunswick.--Studies of the time-integrated perturbation factor $G_2(\omega)$ for the γ-ray directional correlation in ^{111}In provide insight into the complexing of In(III) in aqueous solutions. Measurements have been performed over a range of pH values from extreme acid to extreme alkaline conditions. The results support the suggestion[1] that at low OH^- concentrations the predominant species is $[In(H_2O)_6]^{3+}$ while at high OH^- concentrations the species $[In(OH)_6]^{3-}$ is formed. In each extreme case the electric field at the ^{111}In nucleus is symmetrical and no perturbation is observed. At intermediate OH^- concentrations, strong perturbations of the directional correlation indicate the presence of an electric field gradient due to partially de-protonated complexes $[In(H_2O)_n(OH)_{6-n}]^{(n-3)+}$. Information concerning the perturbation may be derived from time-dependent factors $G_2(t)$.

[1] J. Celeda and D.G. Tuck. J. Inorg. Nucl. Chem. 36, 373 (1974).

*Supported by N.R.C. funds.

15:15

HE8 Identification of Sources of Atmospheric Sulphur Compounds by Sulphur Isotope Abundances* H.M. BROWN**, H.R.KROUSE**, and A.LEGGE***, The University of Calgary For short time intervals, ambient SO_2 concentrations at a given site often approximate a two source model in which one source (background) is constant in emission rate and isotopic composition while the other (industrial stack) is fixed in its isotopic composition but varies in its emission. For this model, a plot of isotopic composition vs. conc.$^{-1}$ gives a straight line intersecting the y-axis at the isotopic composition of the industrial emissions. Studies near sour gas processing plants in Alberta show that the concentration and isotopic composition of the background is dependent upon wind direction. Consequently we are designing an array of high volume samplers wherein each sampler will be triggered for a selected wind direction. In this way, a polar plot with isotopic composition as the radial co-ordinate and the angle as direction should delineate multiple sources of atmospheric sulphur compounds.

*Supported by N.R.C. of Canada and UNISUL
**Dept. of Physics ***Environmental Sciences Centre

THURSDAY, JUNE 17, 1976
ROOM 1A
Chairman: E.R. Pounder

GENERAL GEOPHYSICS

13:30

HF1 An Analytical Representation of the Geomagnetic Field in Canada at Year 1975. E. DAWSON and L. NEWITT, Energy Mines and Resources.--The 1975 magnetic charts of Canada were produced by a least-squares analysis of 65,440 component observations made between 1955 and 1973. To reflect desired wavelengths of approximately 1000 km it was necessary to divide the map area of 31 million km^2 into 4 quadrants with a 10% overlap. In each quadrant polynomials were determined for rectangular magnetic field components x(north), y(east) and z(vertical). These polynomials were 6th order in latitude and longitude and cubic in time. X and Y were analyzed together using Maxwell's curl-free condition (Curl H)Z=0. From these polynomial expressions 2° grid values in DHZ were computed. These values were used to derive the final charts using a standard contouring package. A comparison of the model to the input gives an r.m.s. fit of 173 nT. An examination of the charts produced shows that the magnitude of the field in Canada has increased slightly since 1970.

13:45

HF2

Subsurface geological mapping using aeromagnetic data: the case of the Appalachians of southern Quebec. SEGUIN, MAURICE K.-, Department de Géologie, Université Laval, Québec, G1K 7P4, Canada. - An interpretation of the aeromagnetic (AM) data covering the area bordered by longitudes 71°00'W to 72°00'W and latitudes 45°00'N to 46°00'N is presented. In the northern sector (St. Sylvestre area), the chloritoschists of the Tibbit Hill (metavolcanic and lowermost unit of the Oak Hill group) is extending to a minimum depth of 5 Km and thinning out to the northeast. To the southeast, a fold in the Pennington dyke indicates a first phase of folding along an east-west axis. The depth extent of this tyke is about 1 Km. Further south, the AM data suggest that the Becancour dome is a doubly folded structure with fragments of the ophiolite around it. The depth extent of the ophiolite located on the northwestern side of the dome is about 8 Km; the dip is 75-80° SE on the average. The depth extent of a band of complex located on the southeastern side of the dome is of the order of 2.5 Km only and the dip is towards the north west. A large synclinal structure is thus present in this region; the complex is deeply seated on the northwestern side.

14:00

HF3 Séismicité Induite dans la Région du Réservoir de Manic 3. F. ANGLIN et G. LEBLANC, Energie, Mines et Ressources Canada. - Depuis novembre 1974, en coopération avec l'Hydro-Québec, la Direction de la Physique du Globe à Ottawa surveille la séismicité près des barrages de la rivière Manicouagan, à l'aide d'une station séismographique reliée par télémetrie. Au début d'août 1975, le remplissage du réservoir de Manic 3 débuta; à la mi-septembre des petites secousses situées à 80 km de la station se produisirent. On soupçonna une relation de causalité et on avertit l'Hydro-Québec de la possibilité d'un cas de séismicité induite. Des stations portatives furent envoyées à Manic 3. Le 23 octobre 1975, le choc principal se produisit, avec une magnitude de 4.3; il fut suivi par plus de neuf cents micro-tremblements. La région où la séismicité fut induite se situe à 9 km en amont du barrage de Manic 3.

14:15

HF4 Microséismicité de la Région Baie St-Paul - La Malbaie 1974. G. LEBLANC et G.G.R. BUCHBINDER, Energie, Mines et Ressources Canada. - Au cours de l'été 1974, la Direction de la Physique du Globe déploya un large réseau de séismographes sur les deux rives du St-Laurent, entre Baie St-Paul et Tadoussac. Les hypocentres de trente-sept microchocs furent déterminés et les solutions des mécanismes de rupture obtenues pour six. Ces nouveaux résultats confirment ceux de l'expérience de 1970 quant à la localisation de la zone active et au taux des ruptures. La complexité des mécanismes de faille ne permet pas encore une explication unifiée de la séismo-tectonique locale.

14:30

HF5 Slowness and Azimuth Measurements from the La Malbaie Temporary Array. D.J. HEARTY, Univ. of West. Ont. London, Ont., C. WRIGHT, Seis. Div. DEMR, Ottawa and R.F. MEREU, UWO-In the summer of 1974, the Canadian Seismology Division of the Earth Physics Branch of the DEMR conducted a microearthquake survey near La Malbaie, NE of Quebec City. Twenty-two stations were installed along the shores of the St. Lawrence River. In addition to the local earthquakes, 18 teleseismic events over the distance range 35° to 150° were also recorded during the two month period of the experiment. By employing the

network as a seismic array, we were able to measure the slowness (dT/dΔ) and apparent azimuth for the signals from these earthquakes. Comparisons of these measurements with expected values for a spherically symmetric earth revealed that the ray paths for six events originating in the Panama-Colombia Border region had encountered lateral inhomogeneities in structure. One possible interpretation for this bias could be the presence of a crustal structure located beneath the array and dipping to the southeast. The data from the La Malbaie temporary array is at present being compared with additional data which was obtained over the past year at the new tripartite array operated by the University of Western Ontario near London, Canada.

14:45
HF6 Heat Flow Through Lower Continental and Oceanic Crust - A Unified Interpretation of the Dependence on Tectonic Age. HAMZA, V.M., Inst. Astr. Geof., Univ. São Paulo - Linear relations between heat flow and heat generation observed in different continental plutonic provinces has provided reliable estimates of heat flow through lower continental crust. It is found that these 'reduced heat flow values' decrease as the tectonic age of the province increases. A careful examination however reveals that the dependence of reduced heat flow on age is significantly different from the well-known dependence of surface heat flow on age for continental regions. Since the main difference between continental and oceanic regions is the presence in the former of a felsic radioactive upper crust, a physical basis exists for comparing heat flow from below upper crust in continental regions with near surface heat flow in oceanic regions. A plot of reduced continental and oceanic heat flow values against their respective ages suggest a continuous and overlapping trend of decreasing heat flow with age, thereby indicating the existence of a uniform heat flow age pattern for continental and oceanic regions. This uniform heat flow age relation suggests that the vertical temperature distribution in the lithosphere is a function of its tectonic age.

15:00
HF7 On Permanent Deformation of the Lithosphere by Solid Earth Tides.* H.H. SCHLOESSIN, Dept. of Geophysics, U.W.O., London, Ont.--In a 1952 paper Nadai dealt with a visco-elastic model for the tidal deformation of the outer homogeneous rock shell (100 K) of the earth. He computed the displacements and the principal stresses and strains generated by the vertical and horizontal components of the tidal acceleration. In the present discussion the problem is extended to determine the effects of varying crustal thickness (ζ) and topography (H) on horizontal (u) and vertical (v) components of elastic displacement of a shell of continental and oceanic lithosphere: $u=-u_o(R,\zeta)\sin 2\theta$ and $v=v_o(R,\zeta)/4(1+3\cos 2\theta)$ with $\cos\theta=\cos\phi\cos\lambda=\cos\phi\cos(\omega t)$. Displacements can be computed from observed relationships between depth of the Moho, ζ, orthometric height, H, and Bouguer anomalies, Δg. Global variations are obtained from the surface area distribution with H. Partial relaxation of the mean value of stress, over the diurnal cycles, causes incremental permanent strains depending on P and T.

A. Nadai, 1952. Trans. Am. Geophys. Union, 33, 247.

* Work supported by the N.R.C.

15:15
HF8 Heat of Radioactive Decay in the Earth's Inner Core. KEITH L. MCDONALD, P. O. Box 2433, Salt Lake City, Utah.—Since the heat equation[1] is linear the particular integral u_{ij} for the sum H of heat sources of coefficients H_{ij} (denoting the i^{th} active element of the j^{th} disintegration chain), is the sum of the individual u_{ij}. Thus, with $\beta^*=\beta_i$, we attach subscripts i,j to the previously written[1] $u_{-i}(r,t)$ and sum over i,j. The steady state heat source $H(r)=H_o\rho^{-\gamma}$ entails 4 spherical cases, simply evaluated: $u_{pi}(\rho)=-[H_oR^2/k_o(\beta^*-\gamma+2)]\rho^{-\gamma+2}$, $\beta^*\neq\gamma-2$, $=-[H_oR^2/k_o]\rho^{\gamma-2}\log\rho$, $\beta^*=\gamma-2$; $=[H_oR^2/k_o(\gamma-1)]\log\rho$, $\gamma=1$, $\beta^*=\gamma+2$. Thus, $H=\Sigma_i H_i\rho^{-\beta_i}$, $H_i=\Sigma_j H_{ij}$, $\beta^*=\beta_i$. Of the 4 heavy element chains we omit N_p since it is reduced by 10^{-3} in only 22 million yr. Nil ^{235}U is less abundant than ^{238}U in ratio 1/139.[2] With half-life $T_{\frac{1}{2}}=8.52\times10^8$ yr, ^{235}U was 0.149 as abundant as ^{238}U 4.6x10^9 yr ago, when earth was formed, and has produced comparable heat, but most of which long ago escaped; for $v_r=0.03$ cm/sec. a heat cell would require 235 yr to pass thru core fluid and if $v_r=2.5$ cm/yr a solid mantle convection cell would need 116x10^6yr in ascending 2900 km, a reasonable lifetime. ^{232}Th has $T_{\frac{1}{2}}=13.9(\times10^9$yr) compared to 4.50 for ^{238}U. For crustal igneous rocks Th is 2.56 times more abundant[2] and should decrease with depth due to gravitational settling. Due to the long lifetimes of these 2 parents compared to their daughters, no quasiparents[1] are important in the formalism and sensibly all core heat derives from the 2 chains.

[1]K. L. McDonald. Bull. A. P. S., 20 (12), 1501 (1975).
[2]H. Jeffreys, The Earth (Cambridge U. Press, 1959), Ch. 9.

15:30
HF9 Conduction Heat-Loss Scaling in Open Field Line Geometry,* T. K. CHU, L. C. JOHNSON, Princeton U.--The cooling of a finite-length plasma column due to conduction loss at the column ends, where the confining magnetic field lines are intercepted by a cold material wall, is considered. A heat-loss scaling in density, temperature, and column length is obtained by matching the solution of the interior heat diffusion equation to that of the heat flow equation near the boundary. The resulting temperature profile along the field lines agrees with published θ-pinch experimental results and predicts a potential drop toward the wall. The scaling, when applied to the scheme of CO_2-laser heating of a long, magnetically confined plasma column, sets a limit on electron heating for a given plasma column length, and determines electron-ion equilibration and ion energy loss times. The propagation speed of a cooling wave, originating from the wall and propagating into the plasma interior, is found to be small when compared to that of a laser-induced heating wave. Therefore, conduction loss during laser heating can be neglected.
*Work supported by USERDA Contract E(11-1)-3073.

15:45
HF10 Goos-Hänchen Shift at a Shock-Wave Type of Moving Interface. KAISER S. KUNZ and JAMES R. NEWHOUSE, New Mexico State U.--We have generalized the calculations of Goos-Hanchen shift to apply to a moving interface between a stationary medium 1 and stationary medium 2 with permittivities ε_1 and ε_2, respectively. The presence of the moving interface introduces Doppler shifts in the frequencies and propagation vectors of the reflected and transmitted waves and, in addition, destroys the continuity of the tangential components of the electric field E and the magnetic field H at the interfaces. We have obtained formulas for the angles of reflection and transmission for such a moving interface. The evanescent wave associated with total reflection is best described in a coordinate system (primed) moving with the interface. One finds, however, that the real and imaginary parts of the complex propagation vector are no longer at right angles to each other. In the primed coordinate the reflection coefficient R' has unit magnitude. That is not true of the reflection coefficient R in the original unprimed coordinate system.

16:00
HF11
THE UPPER MANTLE OF SOUTHERN BRITISH COLUMBIA.
A.J. WICKENS, Seismology Div., EPB., Dept. of Energy, Mines & Resources.

A concentration of temporary and permanent long period stations were used to observe Rayleigh and Love waves over a region bounded by Vancouver Island on the west and a parallel line approximately 400 kilometers to the east. Significant variations in the upper mantle shear velocities were detected, particularly in the eastern sector where a prominent low velocity region was required to fit the data.

16:15
HF12 APPLICATIONS OF A SQUID GRADIOMETER TO AIRBORNE GEOMAGNETIC MEASUREMENTS M.B. Burbank & J. Vrba, Canadian Thin Films Ltd. The potential of gradient sensitivities of 10^{-5} gamma/foot within a single instrument design make a SQUID gradiometer an attractive airborne geomagnetic survey tool. In addition to the elimination of diurnal variations, discrimination of local anomalies from large regional variations and enhancement of near surface structure from deeply-buried structure, significant analytical leverage results from the gradient tensor data measured by a SQUID gradiometer. An analysis with regard to anomaly location, anomaly classification and depth determination is reviewed for various model geometries.

16:30
HF13 Gravity Study of Great Impact J.F. SWEENEY Earth Phys. Br. - The 65km in diameter Manicouagan circular structure in eastern Quebec has been attributed to hypervelocity impact by either a large meteorite or a cometary body and has also been described as the eroded remains of a resurgent caldron. Two-dimensional modelling of gravity data obtained over this feature combined with rock density measurements and seismic constraints is most consistent with a meteorite impact origin of the structure. Resurgent caldron models generate broader gravity anomalies than observed and comet impact models do not account for the residual gravity high observed over the center of the structure. Excavation of a transient cavity produced by meteorite impact is limited to crustal depths between 2 and 8km on the basis of gravity model calculations.

16:45
HF14 Seismic Body Waves in Anisotropic media: Synthetic Seismograms. C.M. KEITH, Seismology Div. E.P.B., Dept. of Energy, Mines & Resources. Synthetic seismograms and particle motion diagrams are computed for simple, layered Earth models containing a layer of anisotropy. The presence of anisotropy couples P, SV and SH wave motion so that P-waves incident on the anisotropic layer from below produce P, SV and small amplitude SH waves at the surface; both the P velocity and the amplitudes of the converted phases vary with azimuth. Significant SH amplitudes may be generated even when the wavelength of the P wave is much greater than the thickness of the anisotropic layer. Incident SV or SH waves may each generate large amplitudes of both SV and SH motion. This strong coupling is largely independent of the degree of velocity anisotropy of the medium. The arrivals from short-period S waves exhibit S-wave splitting but arrivals from longer period S waves superpose into a modified waveform. This strong coupling does not allow the arrival of separate phases with pure SV and SH polarisation except along directions of symmetry where the motion decouples.

THURSDAY, JUNE 17, 1976
ROOM 2D
Chairman: N.H. Burnett

PLASMA-MAGNETIC CONFINEMENT, WAVES, INSTABILITIES

13:30
HG1 Mesures spectroscopiques de la concentration électronique d'un plasma dense créé par un Z-pinch*. J. MERCIER, INRS-Energie, Varennes, Québec, Canada, J0L 2P0; C.R. NEUFELD, P. NOEL et A. ROBERT, Direction Sciences de base, IREQ, Varennes, Québec, Canada, J0L 2P0 -- Nous présentons des résultats de mesures effectuées sur un plasma d'hydrogène créé par un Z-pinch de taille moyenne. Des photos obtenues par caméra rapide montrent que la première compression du pinch demeure stable pendant 0.5 µsec. Le profil de la raie H_β (4861 Å) émise par le plasma a été mesuré photoélectriquement et sa largeur pendant la période stable du pinch a été évaluée. Nous avons obtenu des spectres très larges (≥ 1500 Å), ce qui indique un plasma de haute densité (s'approchant de $10^{19}cm^{-3}$). Des calculs de compression indiquent également une densité élevée.

* Ce travail a bénéficié d'une bourse du Conseil national de recherche.

13:45
HG2 Experimental Study of a Non Circular Cross Section Tokamak Plasma. FRANCOIS MARTIN, M.I.T. Pressure profiles gotten by Thomson scattering on the Rector tokamak are studied as a function of the equilibrium field curvature. Stable plasmas have been obtained for index of curvature varying from n = +1. to n = -1.5. A feedback system maintains a stable vertical plasma position for negative index of curvature. There is a 40% increase in plasma current for a n = -1.1 plasma and a 60% increase for a n = -1.5 plasma over a circular plasma. The peak electron temperature and electron density do not change significantly as a function elongation. Limiting β is obtained by cold gas injection. Scaling of q, β_p and β as a function of plasma cross section will be discussed.

14:00
HG3 Calcul du potentiel vecteur dû à une distribution arbitraire de courant azimutal. J.P. MATTE et G. LAFRANCE, INRS-Energie, Université du Québec.--- Nous montrons comment la méthode de la "matrice de capacité"(1), d'abord mise au point pour calculer le potentiel électrique dû à une distribution de charge et en présence d'électrodes, peut être modifiée pour permettre le calcul du potentiel vecteur A dû à des bobines et au courant azimutal du plasma. Nous discuterons des applications à l'étude de la machine à confinement électromagnétique (champ B avec minimum et bouchage électrostatique) KEMP-II.

1 R.W. Hockney, "Methods in Computational Physics", Vol. 9, Academic Press, 1970; B. Alder, S. Fernback, M. Rotenberg, éditeurs, p. 162.

14:15
HG4 Rapid Electron Thermal Conduction in a Turbulent Heating Experiment.* A. HIROSE and H.M. SKARSGARD, Univ. of Saskatchewan--A non-uniform rf electric field (3V/cm, 1.8 MHz) applied to a toroidal argon plasma has been found to turbulently heat both electrons and ions with remarkable efficiency. The intensity of the electric field and thus the Joule dissipation are a maximum near the outer edge of the plasma. However, anomalously rapid electron thermal conduction takes place, and the thermal energy generated mainly at the plasma periphery can be quickly transported (within several µsec, across 2 cm) to the plasma center where the Joule heating is negligible. Fluctuation measurements have revealed the presence of high frequency (100 MHz < f < 300 MHz) noise which may be responsible for the enhanced electron thermal conductivity.

*Research supported by the Atomic Energy Control Board

14:30
HG5 Alfven and Ion Acoustic Instabilities in a Non-uniformly Compressed Plasma Flow.* Y. NISHIDA and A. HIROSE, Univ. of Saskatchewan--It has been shown that in a non-uniformly compressed plasma flow ($\vec{\nabla} \cdot \vec{V} \neq 0$), Alfven and ion acoustic modes can become unstable, provided they propagate perpendicular to the flow. The finite $\vec{V} \cdot \vec{\nabla}$ term modifies the equation of continuity of perturbed ion density and affects the dispersion relations of the modes. For both modes, the growth rate is given by $-\vec{\nabla} \cdot \vec{V}/2$. and if the flow velocity decreases in the downstream direction the modes can be unstable.

*Research supported by the Atomic Energy Control Board

14:45
HG6 Spatial Evolution of Non-linear Cylindrical Ion Acoustic Waves.* T. CHEN and L. SCHOTT, Univ. of Saskatchewan--Ion acoustic waves with peak to peak density perturbations $\Delta N/N \sim 0.45$ are excited with a cylindrical probe in a low pressure argon plasma ($p = 2.4 - 4 \times 10^{-4}$ Torr, $N \simeq 10^9$ cm^{-3}, $T_e \simeq 1$ eV). With increasing distance from the exciter an initial impulse disturbance evolves through a soliton-like stage and decays finally into a wave train whose shape is related to the Airy function. The significance of the cylindrical geometry of the waves for the solutions of the Korteveg de Vries equation is discussed. The observed asymptotic waveforms are in qualitative agreement with those predicted by the theory.

*Research supported by the Atomic Energy Control Board

15:00
HG7 Reduction of Anomolous Diffusion Losses by Dynamic Stabilization of a Magnetoplasma. S.Q. MAH, H.W.H. VAN ANDEL, and J.TEICHMANN, U. de Montréal- Experimental work on the dynamic stabilization of dissipative drift modes in a R.F. Plasma has been continued[1]. The stabilization results from the addition of a small oscillating azimuthal component B_ϕ to the main axial magnetic field B_o. The occillating component is produced by passing an alternating current at 100 kHz through a conductor placed parallel to the plasma column. Drift instabilities present in this plasma can be made to disappear at stabilising currents such that $B_\phi/B_o \leq .01$. It has been shown that under certain conditions the stabilization results in a dramatic increase in electron density, which corresponds to a reduction in anomolous diffusion losses due to the instability. Measurements of the phase difference between perturbations in density and potential show that dynamic stabilisation reduces this phase difference, which is consistent with a reduction in anomolous diffusion, and a damping of the unstable drift mode.

[1]H.W.H. Van Andel, S.Q. Mah, and J.Teichmann, Physics Letters 50A, 403 (1975)

15:15
HG8 Trapped Particle Instabilities Excited by a Whistler Wave in a Collisionless Plasma. E. MARQUIS and J. TEICHMANN*, University of Montreal. Theory of instabilities due to particles trapped by a whistler mode propagating along the magnetostatic field in a collisionless plasma is developed. Three types of instabilities, propagating in the direction of the whistler mode, were analysed: the longitudinal electrostatic mode already known[1] and two new electromagnetic modes having transverse polarisation. The most unstable mode has right circular polarisation and the phase velocity close to the phase velocity of the trapping mode. It is shown that the instability domain depends strongly on the equilibrium distribution of trapped electrons.

1. Palmadesso P., Schmidt G., Phys. Fluids 15, 485 (1972).

* Work supported by the National Research Council of Canada.

15:30
HG9 MHD Theory of Dynamic Stabilization of Drift-Dissipative Instabilities. J. de CARUFEL and J. TEICHMANN*, University of Montréal. A MHD theory of dynamic stabilization of dissipative drift modes in a collision dominated fully ionized plasma is developed. The stabilizing field is a low-impedance electromagnetic field with a dominant azimuthal magnetic component. In comparison to the previous theory[1], the present study takes into account the full set of transport equations. The corresponding dispersion relation has been analysed numerically. It is shown that a strong reduction of the growth rate of the basic drift mode takes place when the frequency of the external field, Ω, is larger than the dominant collision frequency ν_{ei}. In case when $\Omega \ll \nu$ stabilization of the drift wave takes place for a threshold amplitude of the stabilizing magnetic field which is $10^1 - 10^2$ times larger than in the previous case.

1. Lepechinsky D., Rolland P., Teichmann J., Nuclear Fusion 11, 297 (1971).

* Supported by the National Research Council of Canada.

HG 10

THURSDAY, JUNE 17, 1976
ROOM 2E
Chairman: H.E. Johns

13:30
HH1 On the Voltage-Current Characteristics of Biological Membranes. S. J. YAO, Univ. of Pittsburgh, Pittsburgh, -- The voltage-current characteristics(V/I) of biological membranes generally exhibits two distinct regions. At the high voltage region, the ionic current varies with the applied potential (▲V) according to the Butler-Volmer equation. This high voltage region phenomenon has been ascribed to the interfacial electron-transfer at the membrane/electrolyte boundary. At the low voltage region,i.e., the displacement from resting potential is less than 50mV, the current responds linearly with ▲V. Thus far, no suitable explanation has been proposed. In this report, the low voltage region is considered as the subthreshold. We believe that no electron transfer should occur in the subthreshold. The current should be mainly cation migration current and thus the V/I linear. Electron-transfer becomes dominant only when ▲V exceeds the subthreshold at which the membrane Fermi-level matches that of the redox electrolyte.

1. L. J. Mandel, Nature, 225, 450 (1970).

13:45
HH2 Configuration Linéaire Optimale d'Electrodes pour la Mesure "in vivo" d'Impédance Spécifique. P.N. ROBILLARD et Y. POUSSART, Univ. LAVAL.

La mesure "in vivo" de l'impédance spécifique des structures cérébrales sous-corticales ne révèle qu'une résistivité apparente. En effet le système de 4-électrodes, utilisé pour effectuer cette mesure, perçoit les structures avoisinantes. Il s'agit alors d'élaborer un système d'électrodes qui, tout en étant précis pour le milieu étudié, ne subit que peu d'influence des milieux voisins. Une simulation par ordinateur de tous les arrangements linéaires possibles a démontré qu'une configuration bi-dipolaire, (dipole courant et dipole tension) augmentait la résolution spatiale d'environ 50% en regard du système conventionnel. Ces données ont été vérifiées expérimentalement en milieu connu. Il appert que, dans les conditions identiques, la configuration bi-dipolaire accroit la précision de la mesure de la résistivité d'au moins 5% sur toutes autres configurations. Dans le contexte cérébral, où l'on retrouve une hétérogénéité résistive élevée, une réduction de 50% du champ de perception du système favorise une interprétation plus exacte de la résistivité apparente.

14:00
HH3 Etude Théorique et Expérimentale des Propriétés Electriques de la Microélectrode de Verre à Bout Ouvert
R.Plamondon et S.Gagné. Université Laval

La connaissance quantitative de la jonction électrique fait la pointe d'une microélectrode de verre avec le milieu électrolytique environnant est essentielle si l'on veut réduire au minimum les perturbations produites par la sonde elle-même, lors d'enregistrements électrophysiologiques. Une étude en ce sens est donc effectuée à l'aide d'un modèle théorique permettant de prédire la résistance et le potentiel de pointe d'une microélectrode. Ce circuit équivalent tient compte de la diffusion ionique, de la conduction dans la double couche électrochimique et de celle à travers le paroi de verre. La comparaison entre les résultats expérimentaux et les prédictions théoriques est ensuite présentée. Cette analyse offre de nombreux avantages pratiques quant à l'utilisation des microélectrodes de verre en milieu cellulaire, pour la mesure des potentiels de repos, des potentiels d'action et même des résistivités de solutions biologiques.

14:15
HH4 Syndrome général d'adaptation sous l'effet du champ magnétostatique, Hubert Laforge, psychologue; Maurice-K. Seguin, physicien; Mario Moisan, psychologue.

Sous un champ magnétostatique on observe un ralentissement, suivi d'un arrêt presque total de la croissance du rat; le sommeil est réduit progressivement de 20 à 30% avant de revenir à un niveau voisin de la normale; la performance sous DRL-10 secondes est soumise à des fluctuations qui sont en corrélation avec les perturbations qui affectent sommeil et activité.

Les sujets ont été soumis, un seul à la fois et de façon continue, pendant plus de 20 jours, à un champ magnétostatique vertical atteignant 2800 oersteds. Les variables physiologiques et comportementales observées révèlent une évolution caractéristique des phases du syndrome général d'adaptation : choc, contre-choc, résistance. On peut considérer que le champ magnétostatique a, dans les circonstances étudiées, un effet général non spécifique similaire à celui d'autres agents stressants. Ces résultats permettent de lever plusieurs des ambiguïtés laissées par les recherches précédentes, suggèrent la poursuite de ces investigations sur le système endocrinien et mettent en lumière la nécessité de procéder à des expositions chroniques plutôt que de courte durée.

14:30
HH5 Photodimerisation of 1-Methylthymine Studied by Neutron Diffraction. B.M. POWELL and P. MARTEL, Atomic Energy of Canada Ltd., Chalk River, Ontario.--Polycrystalline samples of 1-methylthymine were irradiated by 254 nm ultraviolet radiation. The photon flux at the specimen position was ~10^{16} photons $cm^{-2}.s^{-1}$. and irradiation times of 1½, 6, 12, 47 and 72 hours were used. The primary photoproduct in the solid state is expected to be a molecular dimer produced by the formation of a cyclobutane ring between adjacent planar molecules. Measurements by UV spectrophotometry showed that dimer concentration increased with irradiation time, and for the longest irradiation it was 52%. The elastic neutron scattering spectrum of the irradiated samples was measured and compared with the corresponding spectrum of the unirradiated sample. Simple ideas of the mechanism of dimer formation suggest that the intensity of the (102) powder line should decrease linearly with increasing dimer concentration. This relationship was observed from the experimental powder spectra. However, several other changes are observed in the powder spectra, indicating significant structural distortions in addition to the formation of dimers. These changes are interpreted as the formation of a triclinic lattice.

14:45
HH6 In Vivo Determination of N Using Pu-Be Sources.*J. MERNAGH, K.G. McNEILL and J.E. HARRISON, Univ. of Toronto--The Birmingham group have shown[1] the possibility of using the 10.8 MeV neutron capture gamma ray of ^{15}N for quantitating nitrogen in the body. A major problem is neutron capture by iodine in the detecting crystal, largely solved in Birmingham by the use of a pulsed neutron beam and gated circuits. We show that a viable signal/background ratio can be obtained from body nitrogen using Pu-Be neutron sources and heavy shielding of source and detector. Using four 5 Ci Pu-Be sources, two 5"x4" NaI crystals and 10 minutes measurement, about 1500 net counts (2700 gross) are obtained from a normal volunteer, compared with a background of about 1200 counts.

The feasibility of using neutron sources for N studies may allow hospitals without cyclotrons to use this technique in the future.

15:00

HH7 An Evaluation of Albedo Neutron Dosimeters, D.W.O. ROGERS, Physics Division, National Research Council, Ottawa; Murray Walsh, Nick Teekman and Brian Orr, Central Health Physics, Ontario Hydro, Pickering--Film badges are insensitive to much of the neutron dose received by personnel at CANDU reactors since it is from intermediate energy neutrons. To detect these neutrons, various personnel dosimeters based on using LiF TLD's to measure the albedo thermal neutrons from the body have been developed elsewhere. We have done a series of measurements with monoenergetic neutrons from 20 keV to 14 MeV to measure their responses. The $^{45}Sc(p,n)$ reaction was used to produce neutrons at 20 keV while the more standard $^{7}Li(p,n)$ and $t(d,n)$ reactions were used at the other energies. Our results are considerably different from previous experimental results[1] for the lower energy neutrons and are in much better agreement with calculated results.[2] A discussion of the principles of operation of the dosimeters will be given along with estimates of their overall accuracy and sensivity.

[1]Hoy, Health Physics 23 (1972) 385.
[2]Alsmiller and Barish, Health Physics 26 (1974) 13.

15:15

HH8 Automated Protein Analysis by Proton Activation*. D.A. DOHAN and K.G. STANDING, Univ. of Manitoba--Proton activation analysis may be used to determine the protein content of grain[1]. A computer controlled system for rapid processing of large numbers of samples has been constructed, and tested at a rate of 2 analyses per minute. The reproducibility of the results is ~ 1%, close to the value expected from counting statistics. The apparatus has already been used for routine testing of several thousand grain and oilseed samples. Possible extension of the technique to measurements on single kernels will be discussed.

* Supported by a contract with Supply and Services, Canada and Agriculture Canada.

[1] D.A. Dohan, K.G. Standing and W. Bushuk, Cereal Chem. 53(1), 91, (1976).

15:30

HH9 Trace Levels of Radioactivity in Fundy Coastal Organisms.* B. L. TRACY, Univ. of New Brunswick (Saint John Campus)--Preliminary investigations have been carried out on the radioactive content of selected marine organisms and water samples taken from along the Bay of Fundy coast near Saint John, N.B. A high-resolution, low-background Ge(Li) detector system has been used. The seaweeds Ascophylum nodosum, Fucus vesiculosis, and Rhodymenia palmata (dulse), and the molluscs mytilus edulis (mussel) and Littorina littorea (periwinkle) have been studied. Traces of the fall-out fission products ^{137}Cs, ^{141}Ce, ^{144}Ce, and possibly ^{106}Ru have been observed, along with members of the naturally-occurring uranium and thorium decay series. Concentration factors of the radionuclides in the marine organisms as compared to ambient sea water have been determined. Implications for the proposed nuclear power station at Pt. Lepreau, N.B., are discussed.

15:45

HH10 Mossbauer emission spectroscopy of ^{57}Co substituted in apo-carbonic anhydrase. G. LAAUW, Dalhousie Univ., A. LACHAINE, D.L. LIVESAY and K. MAILER, Univ. of New Brunswick.--The catalytic activity of the enzyme carbonic anhydrase depends on the presence of a zinc or cobalt ion at a well-defined site in the molecule. Information about the molecular field at this site may be obtainable from the Mossbauer spectrum at ^{57}Fe derived from ^{57}Co substituted for the zinc atom which is normally present. Preliminary data indicate a marked quadrupole splitting, possibly related to the interaction seen in perturbed directional correlation experiments on $^{111}Cd^{m}$ substituted in the enzyme. Detailed analysis is required to establish the charge states in ^{57}Fe following electron capture and to allow for possible bond disruption effects.[2] The method should be of wide application to biomolecules containing metalloenzymes where ^{57}Co can be substituted for divalent metal ions which normally activate the enzymes.

[1]Bauer, et al. Phys. Rev. L. 32, 340 (1974).

[2]Cardin et al. Biochem. Biophys. Acta 371, 44 (1974).

*Supported by N.R.C. funds.

16:00

HH11 Hydrophobic Groups Are Components of the Organic-Inorganic Interaction in Calcified Tissues.* A. ROUFOSSE, J.B. LIAN, AND M.J. GLIMCHER, Harvard Med. Sch., Dept. Orthop. Surg., Children's Hosp. Med. Ctr., Boston.--A comparative ESR study of a free radical previously identified as $(CH_3)_2$-C-R in x-ray irradiated enamel and bone is conducted in a series of native and chemically modified calcified tissues. These experiments indicate that the organic configuration yielding this radical is present in embryonic tissues, remains present during tissue maturation and is intimately associated with their inorganic phase. An indication of the nature of R is obtained by comparing the ESR signals and amino acid compositions of several different pathological calcifications. The radical is found only in tissue containing apatitic calcium phosphate. The matrix proteins of these calcified tissues are enriched in acidic amino acids and leucine. They also contain the new calcium binding amino acid, γ-carboxylated glutamic acid. Interactions between leucine side chains through hydrophobic forces can provide the 3-dimensional steric configuration necessary for the initiation of mineral deposition onto the organic matrix.

16:15

HH12 Force as an Operational Construct in Psychology. D.W.GRIESINGER, Union College, Schenectady, N.Y.--Lewin[1] introduced into psychology the concept of psychological force but was unable to specify an equation of motion, relating force to behavior. Physical analogs prove helpful in developing Lewin's ideas. The effort exerted by a hungry rat seeking food at the end of a linear runway can be defined as proportional to the gradient of a maximally smooth scalar field, whose source is the food in the goal box. This assumption leads to a direct analog between potential energy and utility in psychology. If a Newtonian equation of motion is used with this definition of force, the results compare favorably with Hull's[2] data on rat running behavior.

[1]K. Lewin. Contrib. to Psychol. Theory 1, Whole No.4(1938)

[2]C.L. Hull. J. Comp. Psychol. 17, 393 (1934)

16:30

HH13 How Safe Are Microwave Ovens?
W.M.ZUK, M.H. REPACHOLI and D. LECUYER; Radiation Protection Bureau, Health and Welfare Canada.
Under the provisions of the Radiation Emitting Devices Act of 1970, the Radiation Protection Bureau has the responsibility for the development and implementation of statutory standards to control potentially hazardous radiation emitting devices. In October 1974 standards of design, construction and performance for microwave ovens were promulgated as Regulations under the Radiation Emitting Devices Act. In addition to other safety requirements, the Regulations limit microwave leakage to a maximum of 1 mW/cm^2 under conditions of minimum operating load. In implementing the microwave oven Regulations, the Radiation Protection Bureau has surveyed microwave ovens sold in Canada, and has found that many ovens exceed the maximum permissible leakage level. In most cases the leakage occurs because of inadequate seals around the doors or poorly designed interlocks that allow the doors to be partially opened while the oven is on. The design, construction and performance criteria, inspection procedures and results will be provided. Methods for improving the safe use and operation of existing ovens will also be given.

THURSDAY, JUNE 17, 1976
ROOM 2F
Chairman: H.R. Glyde

13:30
HI1 Thermal Expansion of $SrTiO_3$ Near its Structural Phase Transition.* H.W. WILLEMSEN and P.P.M. MEINCKE, Univ. of Toronto--The linear thermal expansion coefficients in the <001> and <110> directions of monodomain[1] single crystals of $SrTiO_3$ near its structural phase transition at T_c = 106.8K are reported. These measurements show the existence of pronounced shape, orientation and history dependent effects in the background thermal expansion coefficient both above and below the transition temperature. This behaviour is ascribed to the impurity and defect induced electret effect.[2] The influence of this mechanism on the observed transition temperature and critical behaviour will be described.

*Work supported in part by the National Research Council of Canada.

[1]K.A. Müller, W. Berluger, M. Capizzi and H. Grünicher, Sol. State Comm. 8, 549 (1970).

[2]H. Weik and V.L. Lambert, Phys. Rev. Lett. 10, 51 (1963).

13:45
HI2 Far Infrared Reflectivity of Alkali Halide Host-Defect Systems.* B.P. CLAYMAN, Simon Fraser Univ. -- To date, measurements of the impurity-induced optical activity in alkali-halides have been restricted to energies below and above the optic band. By using a novel dual cavity system[1], I have compared the reflectivity spectra of pure and doped alkali halide single cyrstals over the region from 10 to 333 cm^{-1} at resolutions exceeding 1.0 cm^{-1}. In KI:Cl^- the resonant modes and gap modes which had previously been observed in transmission were seen as dips in the reflectivity. In addition, new resonances near the gap edge at 90 and 98 cm^{-1} were discovered. There was also a pronounced narrowing and decrease in strength of the Reststrahlen band. Measurements are proceeding on other host-defect systems.

[1]R.W. Ward, Infrared Physics 15, 1 (1975).

*Supported in part by the N.R.C.

14:00
HI3 The Dispersion of Acoustic Phonons in $SnSe_2$. B. M. POWELL* S. JANDL+ and J. L. BREBNER+, *AECL Chalk River; + University of Sherbrooke, University of Montréal. We present here preliminary results of an investigation on phonon dispersion curves in the semiconducting layer structure $SnSe_2$ obtained by inelastic neutron scattering at AECL, Chalk River. Using a simple model the results are analysed to give a value of the interlayer interaction which is found to be similar to that of other layer structures. A group theoretical analysis of phonon symmetries and the corresponding atomic displacements for different wave vectors is also given.

14:15
HI4 Search for Short-Range-Order Effect in Low Temperature Specific Heat of Ag-Au. DOUGLAS L. MARTIN, Physics Division, N.R.C., Ottawa -- It has been shown[1] that long-range order (LRO) in Cu-Au alloys changes the specific heat by ∿20% at ∿10K. X-ray work shows short-range-order (SRO) in Ag-Au alloys but no LRO. There is some dispute whether the time effects studied in the electrical resistance of Ag-Au[2,3] refer to the creation of SRO (homogeneous SRO) or more complicated processes such as the formation of coherent SRO phase boundaries (inhomogeneous SRO). Experiments are currently in progress to see whether the low temperature specific heat of Ag-50at%Au depends on thermal history. Preliminary results show no significant change suggesting, if confirmed, that either (a) SRO has little effect on that part of the lattice vibration spectrum affecting specific heat results in the 3 to 30K range studied or (b) room temperature SRO equilibrium occurs quickly (∿1h) in the specific heat sample (∿200g).

[1] D.L. Martin, to be published
[2] K. Lücke and H. Haas, Scripta Met. 7, 781 (1973)
[3] W. Schüle and G. Crestoni, Z. Metallk. 66, 728 (1975)

14:30
HI5 Resonant Phonon Scattering in One-Dimensional Antiferroelectric Praseodymium Compounds*. J.P.HARRISON, J.T.FOLINSBEE and D.R. TAYLOR, Queen's Univ.--Recent experiments on Praseodymium Ethyl Sulphate and Praseodymium Chloride have shown that these systems can be described as 1-D XY systems with the interaction between n.n. Pr^{3+} ions (along the c axis) arising from electric dipole-dipole coupling[1]. Whilst at 0.4K $PrCl_3$ undergoes 3-D ordering, no evidence of 3-D ordering has been observed in PrES down to 0.1K. The thermal conductivity of PrES has been measured from 0.15 to 1.5K. The data, which vary roughly as T^5, are described very well by a model in which 'Debye phonons' are resonantly scattered by a doublet of splitting 0.75K. This splitting is a measure of the coupling of the Pr^{3+} dipoles to their n.n. dipoles. The success of this model lends further credence to the identification of the anomaly in the thermal conductivity of $PrCl_3$ with conduction by soft modes associated with the 3-D phase transition.

[1]J.P. Harrison, Jan P. Hessler and D.R. Taylor (to be published).

14:45
HI6 Phonon Reflection at a Si-^{3}He Interface*. J.T. FOLINSBEE and J.P. HARRISON, Queen's Univ.--The reflection coefficient, R, for ballistic phonons normally incident on a Si-^{3}He interface has been measured, using heat pulse techniques, in order to learn more about heat flow across He-solid interfaces (Kapitza Resistance). The results show that for phonon temperatures from 2K to 7K almost all longitudinal phonons are reflected at the interface (R ≈ 1), whereas transverse phonons have R ≈ 0.5. These results are qualitatively similar to results of other groups for ^{4}He-solid interfaces[1], but as yet have no good theoretical explanation. Further research is in progress to measure R for phonons with temperatures below 1 K.

[1]C. Guo and H.J. Maris, Phys. Rev. A10, 960 (1974).

*Supported by the National Research Council.

THURSDAY, JUNE 17, 1976
ROOM OB
Chairman: M. Séguin

13:30
HJ1 Vertical Motion of Precambrian Shield From Magnetic Overprinting. E.J. Schwarz. Geological Survey of Canada - Remanent magnetisation in a host rock is modified near a younger intrusion because of heating and subsequent cooling in a magnetic field. In general, the magnetic direction of the younger intrusion differs from the original, older, direction of the host rock. It is shown that by thermal experiments on the remanent magnetisation and by calculation of the thermal effect of the younger intrusion, the ambient temperature of the host rock at the time of intrusion can be estimated. In the case of the norite of the Sudbury Irruptive, this comes to 170°C at the time of intrusion (1250 my) of the NW trending diabase dike swarm. Taking a geothermal gradient at that time of 30°C/km, a depth of 5 km of the present erosion surface is obtained. This suggests a cumulative vertical motion of that order of magnitude in the last 1250 M y.

13:45
HJ2 Magnetism of the Lower Ordovician St. George's Limestone and the Rotation of Western Newfoundland.* E. R. DEUTSCH and K. V. RAO, Memorial Univ. of Nfld.-- Limestones from ten sites (62 samples) of the St. George's Formation, Port-au-Port Peninsula, were found to possess a weak natural remanence in the range <0.1 - 2.5 microgauss, typically directed southward and inclined +50° to +60°. Only 24 samples were strong enough to treat further. High-field isothermal magnetization curves showed the magnetic carrier in different samples to be hematite, magnetite or both. "Hematite" samples were unaffected by alternating-field (AF) treatment to 800 oersteds, while in the "magnetite" samples both AF and thermal demagnetization (300 oe, 500°C) produced well-grouped, shallow, positive, southward directions. St. George's limestone from two sites at Cape Norman, northern Newfoundland, behaved similarly. Fifteen AF-treated Port-au-Port "magnetite" samples gave a reverse paleomagnetic pole at 30°N, 119°E (dp,dm = 2°,3°). This is not significantly different from the pole reported for the mid-Ordovician Trenton (New York) limestones, consistent with the absence of a post-Cambrian rotation of western Newfoundland.

14:00
HJ3 Paleomagnetism of granite bodies from the Central Mobile Belt of Newfoundland. G. S. MURTHY, Physics Dept., Memorial Univ. Newfoundland, St. John's, Newfoundland--- The ages of granites from the Central Mobile Belt of Newfoundland are crucial in choosing one or other of the models proposed for the tectonic development of the island of Newfoundland. While field relations and structural studies suggest a pre-mid Ordovician age for most of the granites, Rb-Sr ages of late Devonian age are reported for the same bodies in the literature. A paleomagnetic study of five of the granite bodies is undertaken with the express purpose of deciphering the ages by paleomagnetic means. Oriented samples were collected from Locker's Bay, Middle Brook, Aspen Cove, Deadman's Bay and Ragged Harbour granites of which the first two are found to have a significant NRM mean direction. Alternating field demagnetization seems to be useful in eliminating secondary components of magnetization. Paleomagnetic results of these granite bodies are discussed and tentative age relations are proposed.

HK

14:15
HJ4 Magnetism of the Cloud Mountain Lavas, Northwestern Newfoundland.* K. V. RAO and E. R. DEUTSCH, Memorial Univ. of Newfoundland.-- Three flows of the gently dipping Cloud Mountain plateau basalts were sampled at 10 sites on Canada Bay. Their age is pre-Bradore and may correspond to the reported[1] radiometric date of 605 ± 10 m.y. for the Long Range dikes. The intensity of natural remanence of the samples ranged from 8×10^{-3} to 8×10^{-2} gauss and natural Koenigsberger ratios ranged from 0.4 to 35. Alternating-Field demagnetization to 100 peak oersteds (optimum value) greatly improved within-flow and between-flow groupings. Thermomagnetic measurements indicate that the component thus isolated is stable singledomain magnetite. Its mean direction after tilt correction corresponds to a reverse paleomagnetic pole at 5°N, 172°E (dp,dm= 2°,4°, N=3 flows). This is not significantly different from the pole reported for the very late Precambrian Franklin diabase in northern Canada.

[1]V. Stukas and P. H. Reynolds, Earth Planet. Sci. Lett., 22, 256 (1974).

14:30
HJ5 Paleomagnetic Evidence for a Joining of Structural Provinces during the Early Proterozoic.* C. K. Seyfert and Michael D. Cavanaugh, Buffalo State University College.--The apparent polar wander (a.p.w.) paths of the Slave and northwestern Churchill provinces do not coincide with the a.p.w. path of the Superior Province for poles older than 1750 M.Y. Paleomagnetic poles from the Wyoming, Eastern Nain, southeastern Churchill, and Southern provinces fall on the a.p.w. path of the Superior Province. Deformation in the Churchill Province approximately 1750 M.Y. ago was probably the result of a collision of a plate which included the Slave and northwestern Churchill provinces with a plate which included the Superior Province, the southeastern Churchill Province, and the Wyoming and Eastern Nain Provinces. A strong secondary magnetization was introduced in several units at the time of this collision.

*Submitted by J. E. MACK, JR.

THURSDAY, JUNE 17, 1976
ROOM 2A

17:00 CAP COUNCIL

Chairman: R.J.A. Lévesque

AUTHOR INDEX/INDEX DES AUTEURS

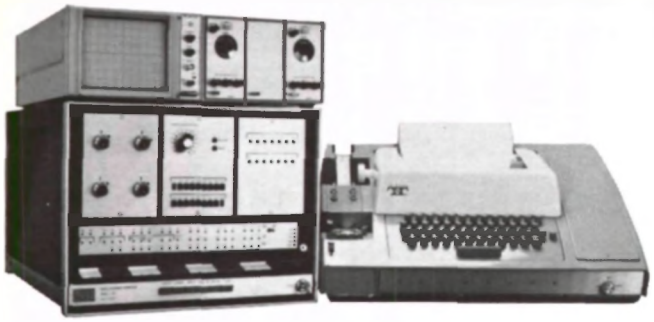

Check the New Nicolet 1180 laboratory data system

FEATURE: *The NIC-1180 is a complete "turnkey" system with a wide range of software.*

BENEFIT: The system is delivered and installed with software and training provided at time of installation so system can be put to use immediately. NMR, FT-IR, EPR and Laser Raman applications software, in addition to general laboratory data collection and processing software are currently offered.

FEATURE: *Field-expandable memory is 20-bit word, MOS solid state.*

BENEFIT: This word length is optimal for signal averaging and high-dynamic-range frequency analysis applications. It offers a more efficient instruction set, minimizes the requirements for double precision arithmetic, and permits up to 80K of memory to be easily addressed.

FEATURE: *Optional analog-to-digital converters (ADC's) are offered.*

BENEFIT: The choice of standard 12-bit, 333 kHz ADC or optional 15-bit, 48 or 90 kHz; 8-bit, 5 MHz ADC's; or 15-bit pulse counting buffer permits the user to choose the most appropriate bandwidth or resolution.

FEATURE: *Direct memory access is provided through two concurrent DMA ports.*

BENEFIT: Operating at rates up to one million transfers to memory per second, DMA permits, for example, concurrent memory accessing by the ADC and the disk memory.

FEATURE: *A seven-level, vectored priority interrupt scheme is provided*

BENEFIT: This feature supports a multi-task environment. For instance, acquisition, processing and plotting can be conducted simultaneously.

FEATURE: *A hardware Read Only Memory (ROM) program loader is included.*

BENEFIT: Containing programs for tape readers and disk memory systems the ROM eliminates time-consuming "bootstrap" program loading through the switch register.

FEATURE: *Many arithmetic and logic functions required for high speed data processing are hardwired.*

BENEFIT: Fixed point and floating point operations are executed quickly. Divide, signed multiply, bit inversion and 60-bit shift are hardwired and allow a 4K FFT computation in 2.5 seconds.

FEATURE: *Four front panel parameter knobs provide user interaction in CRT display routines.*

BENEFIT: These controls permit determination of the start point and width of the displayed data and entry of phase correction constants, integration, baseline and slope correction factors and other data manipulation operations.

FEATURE: *Real-time alphanumeric displays are provided on the CRT.*

BENEFIT: A 64-character ASCII character generator provides up to 30 characters per line to display number of sweeps made while acquiring time domain data or scale factors, peak positions, and intensities during frequency domain measurements.

FEATURE: *Many peripheral interfaces are built into the NIC-1180 main frame.*

BENEFIT: These include two channels of RS-232C of which one can be used for a Teletype. All common baud rates from 110 to 38,400 bauds, and one channel each for high speed reader and high speed punch are built in. Provisions have also been made for the new Hewlett-Packard Interface Bus (HPIB).

FEATURE: *A complete list of optional peripherals includes every conceivable need.*

BENEFIT: The list of peripherals includes CRT terminals, tape readers, tape punches, cartridge and "floppy" disk memories, X-Y plotters, line printers, magnetic tape recorders, a signal conditioner, and a pulse programmer.

For more details or to discuss your proposed NIC-1180 application please telephone or write.

NICOLET CANADA LIMITED

23-1616 Matheson Boulevard
Mississauga, Ontario L4W 1R9
Telephone: 416/625-3901

ADDENDA AND CORRIGENDA

CONGRES CONJOINT ACP-APS-SMF 1976 - CAP-APS-SMJ JOINT CONGRESS

Sunday, June 13 :
Note change of room

	19:30	1E	C.A.P. Council

Wednesday, June 16 :
Added sessions

EJ	9:00	OB	Mexican Physical Society; invited papers
EK	9:00	1E	Optics and Lasers IV

Thursday, June 17 :
Added session:

HK	13:30	1E	Atomic and Molecular Physics III

Note change of room

	17:00	2D	C.A.P. Council

PROGRAM CHANGES

SESSION AD

Chairman J. Marton ~~is~~ replacing J Shanahan

SESSION AE

AE 4 withdrawn

SESSION AI

AI 13 added (see HF 9)

SESSION BC

BC 5 withdrawn

BC 11 withdrawn

BC 12 withdrawn

SESSION BF

BF 4 withdrawn

SESSION DE

DE 9 to be presented by A Weingartshofer

SESSION HC

HC 10 withdrawn

SESSION HE

HE 2 withdrawn

SESSION HF

HF 9 transferred to HI 13

HEJ

SESSION HH

HH 9 withdrawn

ADDENDA AND CORRIGENDA

CONGRES CONJOINT ACP-APS-SMF 1976 - CAP-APS-SMJ JOINT CONGRESS

Sunday, June 13 :
Note change of room

	19:30	1E	C.A.P. Council

Wednesday, June 16 :
Added sessions

EJ	9:00	OB	Mexican Physical Society; invited papers
EK	9:00	1E	Optics and Lasers IV

Thursday, June 17 :
Added session:

HK	13:30	1E	Atomic and Molecular Physics III

Note change of room

	17:00	2D	C.A.P. Council

Congrès ACP-APS-SMF
1976
CAP-APS-SMF Congress

Programme/Program

Additions, Changes, Deletions

A session of invited papers on selected topics will be held on Wednesday morning, June 16 in Room OB.

A number of post-deadline papers have been added at the end of sessions as indicated. As well two sessions have been added, on optics and lasers, and on atomic and molecular physics.

Two papers have been withdrawn: BC5 The Electronic absorption spectrum of NH2 by J.W.C. Johns, D.A. Ramsay and S.C. Ross

HH10 Mossbauer emission spectroscopy of ^{57}Co substituted in apo-carbonic anhydrase by C. Blaauw, A. Lachaine, D.L. Livesey and K. Mailer

MONDAY, JUNE 14, 1976

EF13

11:15
AH10 The Behavior of the Magnetic Properties of MgEu Alloys Under Deformation. C. R. BURR and R. G. PIRICH, SUNY-Binghamton.-- For a series of alloys of Eu in Mg we have measured the magnetic susceptibility. For temperatures above 30K the magnetic susceptibility follows a Curie Weiss law for these alloys. Below 30K the susceptibility gradually becomes temperature independent as T decreases. We have deformed some of the dilute alloys of this series and have discovered that the magnetic susceptibility at room temperature decreases for increasing deformation. Our interpretation based on this data and on Mossbauer data[1] is that the deformation is producing a valence alteration in some of the ions. We later annealed the alloys and remeasured the susceptibility and these results will be exhibited.

[1] J. D. Phillips, et al., Bull. Amer. Phys. Soc. 21, 440 (1976).

- GEOPHYSICS-ELECTRO MAGNETIC METHODS I

EF14

11:30
AH11 X-Ray Studies of MgEu Alloys as a Function of Eu Concentration. R. G. PIRICH and C. R. BURR, SUNY-Binghamton.-- A series of alloys of the Mg-Eu system which range in concentration from very dilute alloys of Eu in Mg up to 33 atomic percent Eu have been prepared. The phase diagram of the Mg-Eu system[1] indicates that there is no solid solubility of Eu in Mg, and that the intermetallic compounds Eu_2Mg_{17}, $EuMg_2$ and EuMg form. Powder patterns for the alloys are obtained with an X-ray diffractometer at room temperature. Our results, which are consistent with the phase diagram, show the existence of the different phases which appear up to 33 atomic percent Eu. The positions of these peaks have been accurately fitted using a computer and the results of the fit will be presented.

[1] W. Muhlpfordt and W. Klemm, J. Less-Common Metals 17, 127 (1969).

OPTICAL PROPERTIES OF SOLIDS

16:30
BD13 Angle Resolved Synchrotron Photoemission from Ni(001).* G. J. LAPEYRE, R. J. SMITH, and J. ANDERSON, Montana State U.--We present initial results of a study of angle resolved photoemission from Ni(001) for photon energy 10eV<hν<28eV. In certain emission directions valence band structure is observed as low as -4.2eV (below E_F). This indicates a d-band width substantially larger than hitherto observed experimentally and more in accord with band structure calculations. Initial state structure is also observed 6 to 7eV below E_F which may be due to the lowest lying s-p band. Normal emission, which samples the Γ-X(Δ) line in the Brillouin zone shows only a single sharp peak, about 1eV wide and abutting the fermi level. The absence of any splitting of this peak may have implications regarding the detailed band structure and possibly the magnetic state of the outermost layers of the crystal.

*Supported by AFOSR No. 75-2872; Synchrotron Center supported by NSF Grant No. 144-F805.

16:45
BD14 Thermally Stimulated Luminescence Emission and Charge Release in Magnesium Oxide. FRICIS DRAVNIEKS and JOHN E. WERTZ, University of Minnesota, Minneapolis. The interpretation of thermally stimulated emission and of charge release curves of irradiated solids is greatly simplified by the use of a hyperbolic (rather than a linear) temperature scan.[1] The previous analysis has been extended to second-order processes. Both the thermoluminescence curves and the charge-release curves of x-irradiated MgO have been resolved into peaks corresponding to first-order and to second-order processes.

[1] A. Halperin, M. Leibovitz and M. Schlesinger, Rev. Sci. Inst. 33 1168 (1962)

17:00
BD15 Thermal Studies of Maya Blue.
A. GRINBERG and A. de YTA, Universidad Autónoma Metropolitana, Unidad Azcapotzalco, Mexico, D. F. The enigmatic pigment used by the ancient Mayas in decorating pottery, murals and other types of artwork, known as Maya Blue, has been under investigation by the archaeologists since 1931. Its stability towards mineral acids and alkalis, including aqua regia and boiling nitric acid, one of the most puzzling characteristics of this pigment, has contributed to increase the interest in the elucidation of its composition and the preparation techniques employed in the Maya region; in fact, it is not found elsewhere in the wold. Until now there is agreement only in that the inorganic base is a colourless clay mineral called attapulgite; whether the colour is due to an organic (indigo) or an inorganic substance in still under dispute. We have used differential scanning micro-calorimetry, thermogravimetry and differential thermal analysis to characterize and compare samples of attapulgite and Maya Blue of different origins, synthetic blues and some organic pigments, to establish more definite correlations and to throw some light in to this long controversy.

TUESDAY, JUNE 15, 1976

THEORETICAL PHYSICS I

11:45

CF8 Recursive Analysis of a Periodic System.* D. N. PETCHER and C. A. UZES, University of Georgia.--The motion of a single particle in a periodic lattice can be described by recursion equations constructed from energy eigenstate matrix elements of a complete set of circular functions. The equations are analyzed by transforming them into a set of characteristic eigenvalue equations. The particle's charge density can be obtained directly from the eigenvectors of the characteristic matrix, while band gaps, direct transitions, and energy eigenvalues are given by the roots of the characteristic equations. The procedure is a modification of a recursive mechanics method, originating from Heisenberg's New Tamm-Dancoff method, developed for non-linear oscillators.

*Research supported by the Air Force Aerospace Research Laboratories, Air Force Systems Command, United States Air Force, Contract F33615-75-C1177.

CONTINENTAL CRUST & MATHEMATICAL GEOPHYSICS

17:15

DH16 Seismic Properties of the Oceanic Crust - A Review. M.J. PURDY, Woods Hole Oceanographic Institution - During the last decade there have been significant advances in seismic refraction techniques at sea including the use of ocean bottom seismometers. These advances have made it possible to carry out controlled seismic refraction experiments on and near ridge crests where the rough topography and rapidly changing tectonic environment makes the acquisition of good data difficult. The higher quality data now available has revealed more details of the crustal structure and has enabled the development of the oceanic crust with time to be described. These new techniques and some of the more important results will be discussed.

WEDNESDAY, JUNE 16, 1976

NUCLEAR TECHNIQUES & INSTRUMENTATION

12:00

EB13 A 50 cm long Position Sensitive Heavy Ion Counter for the Chalk River QD³ Spectrometer. W.G. DAVIES, N.C. BRAY, G.C. BALL, J.S. FORSTER, J.J. HILL and W. McLATCHIE,* AECL Chalk River, Ontario--A new 50 cm long position sensitive heavy ion counter has been built for use with the Chalk River high resolution QDDD magnetic spectrometer. The counter consists of two 1.5 cm x 1.5 cm x 50 cm proportional counters, the first of which is position sensitive, followed by a 7 cm deep x 1.5 cm high gridded ion chamber. The position signal is obtained by charge division on the 0.01 mm dia. high resistance (164 Ω/cm) anode wire. The particles enter through an 833 μg/cm² aluminized mylar pressure window which allows the counter to operate in the range from 26 to 1000 kPa (20-760 Torr) of isobutane. The whole counter assembly is moved and accurately positioned by a computer controlled stepping motor using a rack on pinion drive. The counter has position resolution of about 1 cm and a total energy resolution of about 1.4% measured in an experiment to produce ^{19}N and ^{22}O in the $^{18}O + ^{208}Pb$ reaction. Results of this experiment will be presented.

*Permanent address: Queen's University, Kingston, Ontario.

THEORETICAL PHYSICS II

11:30

EG9 Stability of e, p, $\bar{e}$, $\bar{p}$ (Descriptive). R. B. DRISCOLL, P.O. Box 637, Oakland, Ca. 94604. -- Elementary particle consists of N pointlike particles (PPs) in mutual circular orbit (rad. a) with orbital velocities C_n = C = 3×10^{10} cm/sec. In its inertial frame PP_n emits flux of massive (say 10^{-60}gm) Ritz field particles (FPs) which decay from weak to strong to electric with respective decay constants w,s,0[1] and whose density D is anisotropic for acceleration $C^2/a \neq 0$.~ PP_n at time $-t_n$ has mass m_n, charge g_n. Its FPs with emission velocity C have lab velocity $\vec{V}_n$. Flux ϕ_n is absorbed by PP (orbital vel.= C) at $\vec{a}$, time = 0. Colinear flux ϕ_n^* of induced FPs is emitted by PP. FPs emitted rearward by PP_n at PP have zero lab vel., relative absorption vel. = $-C$, zero lab emission vel., of which PP absorbs flux ϕ_n, inducing colinear (in inertial frame) flux ϕ_n^*. FP momentum fluxes exert "field force" on PP keeping it in mutual orbit; similarly for N-1 other PPs. Cf. suppl. prog.

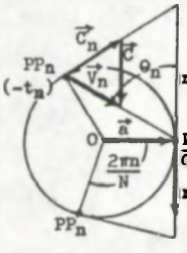

[1] R.B. Driscoll, Bull. Am. Phys. Soc. 20, 828(EC8)(1975).
[2] Alfred O'Rahilly, Electromagnetic Theory. Dover,504('65).

11:45

EG10 Propositional Calculus of Dynamical Systems.* G. R. COOPER, C. A. LINCOLN State Univeristy of New York, College at Fredonia. Generalized dynamical systems are looked at in terms of propositional calculus.[1] Association of propositional calculus with various algebras is made in an attempt to ascertain viability of the propositional calculus as a generalization scheme. The harmonic oscillator is involved, for an example, with the discussion of appropriate propositions as projection operators, the Boolean lattices of the propositions and compatible and incompatible propositions.[2]

[1] J. M. Jauch, Found. of Quant. Mech., Addison Wesley, Reading, Mass., 1968.
[2] G. Fano, Math. Methods of Quant. Mech., McGraw-Hill, Inc., New York, 1971.

12:00

EG11 Anharmonic Oscillator Energies with Recursion Matrix Mechanics.* C. A. UZES, University of Georgia.--The Heisenberg Tamm-Dancoff recursion equation for nonlinear oscillators is converted into a meaningful characteristic energy eigenvalue problem via an infinite dimensional basis transformation of the form SAT, where A is a matrix representing the recursion equation and where S is not the inverse of T. This procedure, appropriate to the situation where the recursive matrix A is not orthogonal or Hermitean, is numerically seen to lead to convergent approximation sequences for energy eigenvalues for several non-linear oscillators. The matrix elements of SAT are defined by summable but nonconvergent infinite series. In each order of approximation eigenvalues exist which are locally independent of the single parameter upon which S and T depend, a fact which implies that this recursive method belongs to an as yet not defined variational principle. As the approximation order is increased the eigenvalues are numerically seen to converge to the proper limits for several different oscillators.

WEDNESDAY, JUNE 16, 1976
ROOM: 0B
Chairman: R.J.A. Lévesque

INVITED PAPERS-SELECTED TOPICS

9:00 New Theoretical Results on the PD -H System
EJ1 A.A. VALLADARES, L.E. SANSORES, *Universidad Nacional Autonoma De Mexico*

9:45 Systematics of Nuclear Masses and the Shell Model
EJ2 M. BAUER, *Instituto De Fisica, Universidad Nacional Autonoma De Mexico*

10:30 3-Equation of State for Simple Fluid
EJ3 F. DEL RIO, *Universidad Autonoma Metropolitana Mexico*

11:15 A Universal Equation of State for Shock Compressed Materials
EJ4 F.C. Prieto, Instituto de Fisica, Universidad Nacional de Mexico

WEDNESDAY, JUNE 16, 1976
ROOM: 1E
Chairman: J.W.Y. Lit

LASERS AND OPTICS

9:00
EK1 High Energy Single Longitudinal Mode (SLM) Pulse from a Tandem of TEA-CO_2 Laser.* R. DAIGLE and P.A. BELANGER, LROL, Laval. Univ.-- High power SLM pulses have been generated with a similar set up of tandem lasers previously used by one of us[1] for regenerative amplification of a short laser pulse. For this experiment the short pulse master oscillator is replaced by a low power SLM oscillator. This low power SIM pulse is injected in a high power TEA-CO_2 laser through a small hole in one of the mirrors. For a given range of the time of injection the output of the high power laser consists of a smooth high power pulse. A parametric study of this experiment (time of injection and attenuation of injection signal) will be presented together with an analysis of the effects due to the Fabry-Perot resonance for different configurations of the optical resonator. As in the RAAT system[1,2], the advantage of this method is that it requires no additional optical elements in the high energy laser beam. The results obtained to date consist of a 15 joule smooth pulse of 100 ns MWHM.

1 P.A. Belanger and J. Boivin.Digest of CLEA, IEEE J. Quant. Electron., QE-11, no 9, 1975.
2 P.A. Belanger and J. Boivin. Can. J. Phys. March,1976
* Supported by a Grant of the Education Dept. of Quebec.

9:15
EK2 Ultrashort-Pulse Generation by Lasers with Saturable Absorbers.* T.K. LIM and M.M. DENARIEZ-ROBERGE, LROL. Laval Univ. -- A theoretical model is presented for the ultrashort-pulse (USP) generation by lasers with saturable absorbers. In this model, the laser gain medium is approximated as a two-level system as treated previously by other authors[1,2]. On the other hand, the absorber is described by a four-level system which is characterized by a two-stage absorption process and the various pertinent relaxation times. It is shown that generation of USP is possible even if the overall recovery time of the absorber is long compared to the cavity round-trip time. In addition, evolution of the USP from noise-like field distribution is investigated using parameters appropriate for solid-state lasers with organic dyes as saturable absorbers. It is indicated that the influence of excited-state absorption and photoisomer formation of the absorber on the characteristics of the laser output can be accounted for by the present model.

1 P.G. Kryukov and V.S. Letokhov, IEEE J. Quant. Electron. QE-8, 766 (1972).
2 J.A. Fleck, Jr., Phys. Rev. B, 1, 84 (1970).

9:30
EK3 Etude Comparative des Méthodes permettant d'extraire un Signal Faible d'un Fond Continu à Variation lente.* H.H. ARSENAULT, LROL, Univ. Laval.-- Les données expérimentales sont quelquefois superposées à un continuum beaucoup plus intense que le signal auquel on s'interesse, et qui cache complètement celui-ci. C'est le cas, par exemple, des courbes d'ionization obtenues en spectroscopie par collision électronique. Diverses méthodes ont été proposées pour se débarrasser du fond: le redressement par lissage[1] et les méthodes de redressement par dérivation[2] sont les principales. Une analyse de ces diverses méthodes permet de constater que celles-ci comportent toujours un compromis entre la réduction du fond et la détectabilité du signal, entre la distorsion et le rapport signal sur bruit des structures d'intérêt. Les données ayant une structure large sont les plus difficiles à extraire convenablement, mais sauf pour certains cas très spéciaux, les diverses méthodes ne sont pas équivalentes.

1 R. Carbonneau, E. Bolduc et P. Marmet, Can.J. Phys. 51, 505 (1973).
2 R.G. Dromey, J.D. Morrison et J.C. Traeger, Int.J. Mass. Spectrom. 6, 57 (1971).
* 9:45
EK4 Propriétés Statistiques des Images Entachées de Speckle et Intégrées à l'aide d'une Ouverture Finie.* G. APRIL et H.H. ARSENAULT, LROL, Univ. Laval. -- Lorsqu'on observe une image à l'aide d'un détecteur de dimensions finies, il en résulte une intégration du signal et du bruit. On peut également soumettre l'intensité mesurée à une transformation logarithmique, afin de restreindre l'étendue dynamique du signal, comme cela se produit intrinsèquement lors d'un enregistrement sur émulsion photographique. Quand il s'agit de speckle (bruit multiplicatif), ces transformations entraînent que, dans certaines conditions, le bruit rémanent devient gaussien et indépendant du signal. En ajustant les divers paramètres disponibles, il est possible d'améliorer le rapport signal sur bruit, de réduire l'aliasing causé par l'échantillonnage ou de réaliser une compression de l'information dans les images traitées.

* Subventionné par le Conseil National de Recherches du Canada.

10:00
EK5 New Method for Improvement of Image Quality in Holographic Microscopy.* C.J. BUDHIRAJA and S.C.SOM, LROL, Laval Univ.-- It is well known that image quality in high-magnification holography is severely degraded by coherent and speckle noise. As a result, it is difficult to attain a resolution of the order of 10^2 lines/mm or more in holographic reconstruction. A new approach to the problem, which is appropriate for holographic microscopy, has previously been explored[1,2]. We have now adapted the technique to holographic microscopy of the usual microscopic specimens. This method can be used to reduce noise in the reconstructed image as well as to improve image contrast. The physical basis of the method will be discussed with reference to the experimental arrangements that w have used. Illustrative results will also be present d.

1 S.C. Som and C.J. Budhiraja, Opt Commun., 12, 143 (1974).
2 S.C. Som and C.J. Budhiraja, Appl. Opt. 14. 1702 (1975).

* Supported by the National Research Council of Canada.

10:15
EK6 La Modulation Spectrale au Service de la Vélocimétrie Doppler.* P. CIELO et C. DELISLE, LROL, Univ. Laval. -- La modulation spectrale s'obtient par interférométrie à différence de marche supérieure à la longueur de cohérence de la source lumineuse qui éclaire l'interféromètre. La présente a pour but de montrer tant théoriquement qu'expérimentalement comment il est possible de faire de la vélocimétrie Doppler à partir du phénomène de la modulation spectrale. Cette nouvelle approche rend dorénavant possible la mesure de la vitesse d'un objet se déplaçant à une vitesse supérieure au mètre/seconde au moyen d'une source à spectre large, tel qu'une source de lumière blanche. Sur le plan expérimental on a mesuré la vitesse d'un prisme rétroréflecteur monté sur la jante d'un disque en rotation. C'est une lampe à filament de tungstène qui a servi de source.

* Subventionné par le Conseil National de Recherches du Canada.

10:30
EK7 Application of the Projection Operator Techniques to Light Scattering by Dilute Gases.* A. ZARDECKI, LROL, Laval Univ.-- Starting from the familiar projection operator formalism of Zwanzig, a new simple computational scheme for determining the dynamic structure factor of a dilute gas is developed. The procedure amounts to a perturbation approach in which the scalar product of the particle velocity and the momentum transfer vector is regarded as a small parameter. Explicit results of the calculated Rayleigh-Brillouin spectrum of light scattered from H_2, D_2 and HD are given. The theory is applicable both to atomic and molecular gases.

* Supported by the National Research Council of Canada.

10:45
EK8 Fabrication et Modes d'un Disque Optique Intégré.* D. VINCENT et J.W.Y. LIT, LROL, Univ. Laval. -- A l'aide d'un masque très simple, nous avons réalisé un disque optique formé d'une couche mince diélectrique déposée sur un substrat en verre. Ce disque possède une porte par laquelle un mode guidé par une lame à l'extérieur du disque peut pénétrer dans le disque. Une fois à l'intérieur, le mode, en plus d'être guidé par la lame, peut aussi être guidé par le bord du disque: ceci ressemble aux "whispering gallery modes" bien connus en acoustique. Les modes fondamentaux ont la forme de polygones fermés dont le nombre de côtés augmente à mesure que l'ordre du mode-disque augmente. Suivant l'inclinaison du bord du disque le front d'onde du mode-disque est plus ou moins déformé. Enfin, on peut le faire sortir par la porte où le mode-lame est entré. Nous présenterons les détails de la technique de fabrication et ses problèmes, quelques photos des modes fondamentaux et aussi comment nous envisageons réduire la déformation du front d'onde.

* Subventionné en partie par le Conseil National de Recherches du Canada.

THURSDAY, JUNE 17, 1976

MAGNETIC RESONANCE-RELAXATION, MOSSBAUER

16:45
HC14 NMR in ^{3}He adsorbed on Argon plated Grafoil at Low Temperatures. S.G. Hegde and J.G. Daunt, Stevens Inst. of Tech.- - - Argon plated Grafoil, with its enhanced surface homogeneity , has been used as a substrate to investigate monolayer and submonolayers of adsorbed ^{3}He in the temperature range of 0.4K to 4.2K using Steady State NMR. Resonance linewidth changes as a function of temperature and coverage closely follow the behaviour observed for corresponding coverages of ^{3}He adsorbed on bare Grafoil.[1] Near-monolayer coverages (0.9 and above) exhibit approximately Gaussian lineshapes with constant linewidths in the temperature range 0.40K-1.3K, which however are narrower than expected from rigid lattice dipolar interactions, indicating motional narrowing due to tunneling . Above 1.3K, marked motional narrowing occurs.

1.S.G.Hegde,E.Lerner and J.G.Daunt, Phys.Letters, 49A, 437 (1974)

PLASMA-MAGNETIC CONFINEMENT, WAVES INSTABILITIES

15:45
HG10 Profil radial d'une colonne de plasma faiblement ionisé. J.P. NOVAK, Direction Sciences de base, IREQ, Varennes, Québec, Canada, J0L 2P0 -- L'équation de Boltzmann a été employée en approximation des treize moments pour calculer le profil radial d'une colonne de plasma faiblement ionisé stationnaire et libre dans l'espace. Le modèle simple, développé pour un faible degré d'ionisation, est basé sur l'hypothèse de collisions électron-atome dominantes. Cependant, les collisions impliquant les ions sont incluses dans l'équation de quantité de mouvement parce que la diffusion radiale est considérée comme ambipolaire. Un ensemble de six équations différentielles est obtenu pour les températures des atomes et des électrons,pour les écoulements de chaleur, la vitesse de diffusion des électrons et la densité électronique. Des calculs numériques ont été exécutés pour des décharges dans l'argon entre 0.1 et 1 atmosphère et pour des courants entre 0.1 et 1 ampère. L'application des équations non-stationnaires au canal du leader dans de grands intervalles est également discutée.

THURSDAY, JUNE 17, 1976
ROOM: 1E
Chairman: E.J. Knystautas

13:30
HK1 Etude de l'interaction postérieure à la collision dans les fonctions d'excitation des états liés de l'hélium.* D. ROY, A. DELAGE et J.-D. CARETTE, Laboratoire de physique atomique et moléculaire, Centre de Recherches sur les atomes et les molécules, Univ. Laval Québec. Au moyen d'un spectromètre électronique de haute résolution, nous avons mesuré dans la région d'autoionisation la section efficace d'excitation électronique des principaux états liés de l'hélium (n = 2 à 8) par diffusion inélastique d'électrons monocinétiques. Ces mesures ont aussi été réalisées pour des pertes d'énergie fixes égales et supérieures à l'énergie d'ionisation. De façon régulière, on observe dans ces courbes les ions négatifs temporaires $(2s^22p)^2P$ et $(2s2p^2)^2D$, ainsi que des singularités dont les déplacements sont conformes à l'existence d'une interaction postérieure à la collision entre les électrons diffusés et éjectés. Nos résultats seront comparés à ceux qui ont été obtenus par le groupe de Read (Manchester).

13:45
HK2 Section efficace différentielle d'excitation et forces d'oscillateur du Xe I par collisions électroniques. J.D. CARETTE, A. DELAGE et D. ROY, Laboratoire de Physique atomique et moléculaire, Centre de recherches sur les atomes et les molécules, Univ. Laval, Québec. Un faisceau d'électrons monocinétiques ($\Delta E_{\frac{1}{2}}$ = 30 meV), animés d'une vitesse imposée, est projeté sur une cible de Xe. Un analyseur électrostatique d'énergie est utilisé pour obtenir le spectre de pertes discrètes d'énergie des électrons incidents. Chacune correspond à un niveau d'énergie décrit par un état électronique de XeI. Une des quantités physiques qui est mesurée est la section efficace différentielle et relative d'excitation, $\sigma(E,\theta)$, ces divers niveaux d'énergie. Ces mesures donnent accès à l'efficacité relative d'excitation par impact électronique de chacun des états électroniques en fonction de l'énergie des électrons incidents et de l'angle des électrons diffusés. Les forces d'oscillateur optiques, généralisées et effectives des transitions de l'état fondamental de l'atome à ses divers états excités peuvent être calculées à partir de l'amplitude des pics des spectres en fonction du changement d'impulsion.

14:00
HK3 Fonctions d'excitation différentielles de quelques états électroniques du krypton I. A. DELAGE, D. ROY et J.-D. CARETTE, Laboratoire de Physique atomique et moléculaire, Centre de recherches sur les atomes et les molécules, Univ. Laval, Québec. Différentes mesures de section efficace décrivant l'interaction entre des électrons et les atomes ont pu mettre en évidence plusieurs types de perturbations dans la région d'autoionisation des gaz rares causées par la formation d'ions négatifs et la présence des niveaux neutres autoionisants; aussi ces mesures constituent-elles des outils puissants pour étudier les niveaux d'énergie de ces atomes. Nous avons mesuré les fonctions d'excitation différentielles à 0^0 des niveaux 5s, 5s', 5p et 6s + 4d du krypton dans la région d'énergie s'étendant de 22 à 28 eV. Les nombreuses singularités observées sont interprétées en termes de résonances Feshbach et de cuspides de Wigner; elles seront comparées aux résultats obtenus en transmission et par électroionisation. L'étalonnage de l'énergie est obtenu au moyen de la résonance $4s^24p^55s^2(^2P_{1,2})$ qui apparaît dans le canal 6s + 4d dans ce domaine d'énergie dû à un effet de collision multiple; ce phénomène y sera aussi discuté.

(recherche subventionnée par le CNRC et le MEQ).

14:15
HK4 Rotational "Dipole States" of Molecular Negative Ions.* W. R. GARRETT, Oak Ridge National Laboratory, Oak Ridge, Tennessee 37830. -- Some molecules are able to bind an extra electron to form a stable negative ion in which the valence orbital is very external in character, with low binding energy and large average radius. Strongly polar closed shell molecules fit in this category. In systems of this type, the electron binding energy is measurably influenced by rotational motion of the nuclei.[1] This breakdown in the Born-Oppenheimer approximation leads to rotational energy states of a negative ion which are uncharacteristic of the neutral molecules. The shift in energy of the rotational levels as a function of total angular momentum, J, is determined by the moment of inertia and the dipole moment of the polar molecule.

*Research sponsored by the Energy Research and Development Administration under contract with the Union Carbide Corporation.

[1]W. R. Garrett, Phys. Rev. A11, 509 (1975).

14:30
HK5 Excitation de la couche interne $(2a_1)$ de la molécule d'eau. D. LEFAIVRE et P. MARMET, Université Laval. --Plusieurs niveaux neutres de H_2O ont pu être observé par impact électronique entre 12 et 32 eV. La configuration électronique de la molécule est : $(1a_1)^2\ (2a_1)^2\ (1b_2)^2\ (3a_1)^2\ (1b_1)^2$. La position en énergie de niveaux neutres résultant de l'excitation de couche $(2a_1)$, $(1b_2)$ ou $(3a_1)$ a pu être déterminée. Le cas particulier de la couche $(2a_1)$ est qu'il est un nouveau membre d'une série isoélectronique que nous décrirons.

Nous tenons à remercier le Conseil National des Recherches pour l'octroi No A-3169 ainsi que le Ministère de l'Education du Québec qui ont rendu ce travail possible.

14:45
HK6 ESR Spectra of OD in $^2\Pi_{\frac{3}{2}}$ (J=3/2) v= 0-5 States.* H. RASHID, K. P. LEE and K. V. L. N. SASTRY, Univ. of New Brunswick.--The ESR spectra of OD have been observed in various vibrational states of the electronic ground state $^2\Pi_{\frac{3}{2}}$. The Λ-doubling frequencies, the g-factors and the hyperfine interaction constants were determined for the vibrational states v= 0,1,2,3,4 and 5 by a least squares fitting of the experimental field values obtained at several microwave frequencies. The results will be discussed and compared with the calculated ones.

*Supported by the National Research Council of Canada.

15:00
HK7 Reaction of Vibrationally Excited HBr and I. C.C. BADCOCK, W.C. HWANG, and J.F. KALSCH, Aerospace Corp.--The reaction between vibrationally excited hydrogen bromide and iodine atoms has been investigated. Iodine atoms are generated by 400 ns pulses of 580 nm radiation from a flashlamp pumped dye laser. HBr is excited by 2 μs pulses from a transverse discharge pumped chemical laser operating multiline. The reaction volume is near the inlet to a molecular beam sampling mass spectrometer. Both possible products of the reaction HI and Br (as BrI) have been detected and are sensitive to the IR laser power. The only thermodynamically feasible reaction is from HBr (v=2), ΔH=1.8 kcal/mole, and from HBr (v=3) which is not significantly populated. Based on detailed balance, the reaction shows a vibrational acceleration of over 10^8 for reaction from the v=2 level of HBr.

15:15
HK8 On the Formation of Positive and Negative Ions in Gaseous UF_6.* R. N. COMPTON, Oak Ridge National Laboratory, Oak Ridge, Tennessee 37830. -- Total cross sections for the production of positive and negative ions by electron impact on UF_6 have been determined. The positive ion cross section reaches a maximum value of 17.5±3 Å^2 at 160 eV. The cross section for producing UF_5^- has a maximum value of 2.7±0.5 Å^2 at 2.15±0.05 eV. Also, reactions between orthogonal crossed beams of fast (0-50 eV) alkali atoms (Na, K, Cs) and UF_6 have been studied. The product ions observed are UF_6^-, UF_5^-, and F^- in order of increasing reaction threshold energy. The following thermodynamic quantities are estimated from the collisional ionization data: $EA(UF_6) \geq 5.1$ eV; $EA(UF_5) = 4 \pm 0.3$ eV; $D(UF_5\text{-}F) = 3 \pm 0.3$ eV.

15:30
HK9 Influence of Temperature on Thresholds for Reactions of the Type $A + MF_n \rightarrow A^+ + MF_n^-$.* R. N. COMPTON, P. W. REINHARDT, Oak Ridge National Laboratory, and C. D. COOPER, University of Georgia.--Recently, molecular electron affinities have been deduced from measurements of the threshold energies for the formation of positive and negative ion pairs from orthogonal crossed beam reactions of fast alkali atoms with room temperature molecules. Slight corrections (~ 0.1 eV) to these electron affinities are expected due to the effect of internal energy in the target molecules. Reaction thresholds for alkali (Cs, Na) collisions with SF_4, SF_6, SeF_6, and TeF_6 have been determined as a function of target gas temperature from room temperature to 900°K and the observed energy shifts are 0.0005, 0.0005, 0.0007, and 0.0002 eV (LAB)/°K respectively. The electron affinity of SF_4 is determined to be 0.77±0.2 eV.

*Research sponsored by the Energy Research and Development Administration under contract with the Union Carbide Corporation.

15:45
HK10 Spectrométrie électronique à basse énergie appliquée à l'étude des surfaces métalliques.* A. ADNOT et J.D. CARETTE, Laboratoire de Physique atomique et moléculaire, Centre de recherches sur les atomes et les molécules, Univ. Laval, Québec. On présente un spectromètre électronique de haute résolution conçu pour détecter les pertes d'énergie associées aux vibrations des molécules ou atomes adsorbés sur les surfaces. Un exemple sur le système Acier Inox. 304/oxygène est présenté. On montre que cet appareil peut également fournir des diagrammes de diffraction qui, bien que partiels, car limités aux faisceaux situés dans le plan d'incidence, peuvent être utiles pour la caractérisation des surfaces monocristallines: les diagrammes de diffraction des systèmes W(100), W(100) - (4x1)O, W(100) - (2x1)O sont présentés, ainsi que les courbes I - V du faisceau (00) pour chacune de ces structures dans la région 0 - 40 eV. Les spectres de pertes d'énergie dans le domaine 0 - 500 meV seront discutés.

*recherche subventionnée par le CNRC et le MEQ.

AUTHOR INDEX/INDEX DES AUTEURS

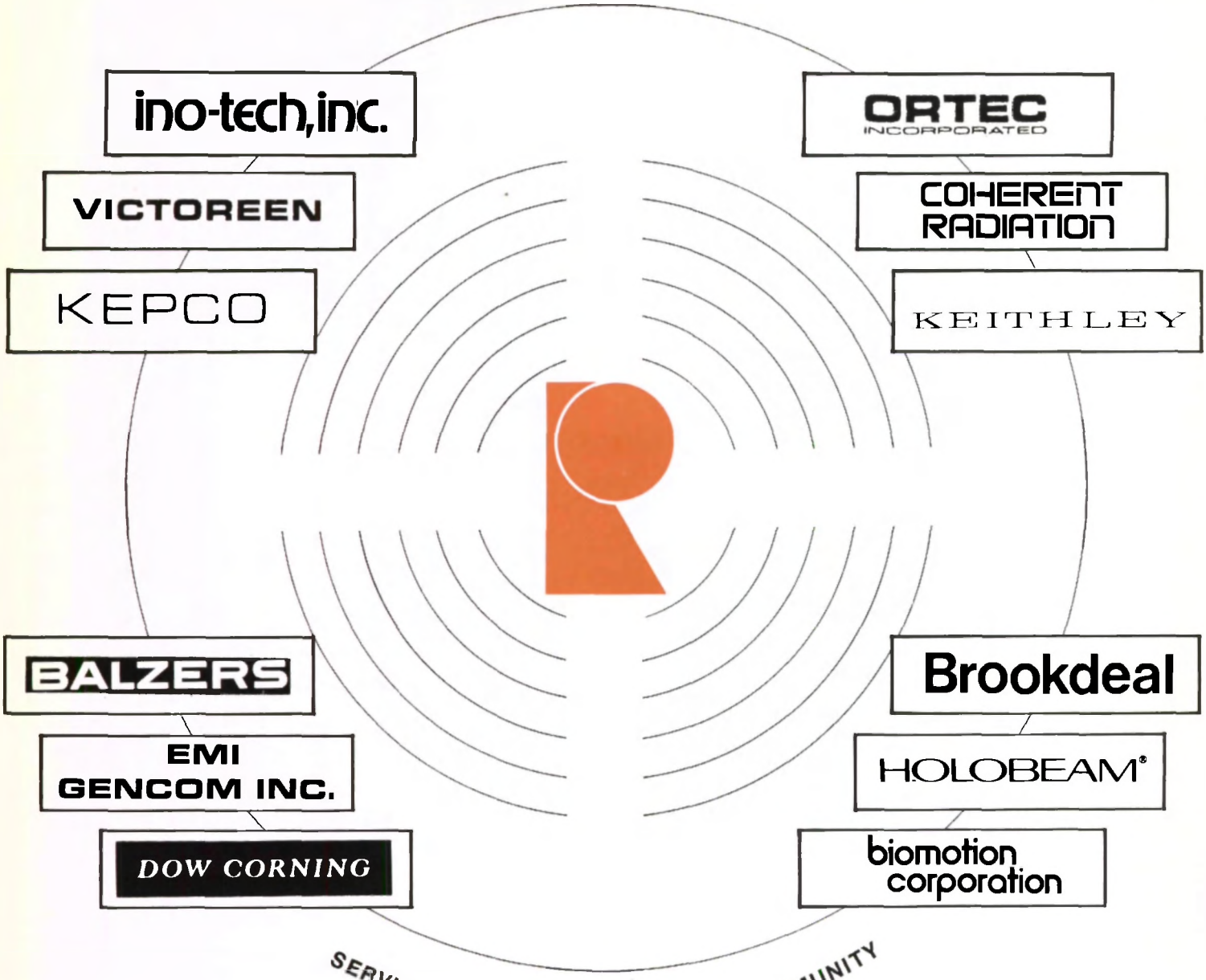

radionics limited

Head Office: Montreal
Branches in Vancouver • Winnipeg • Toronto • Ottawa

SEE US AT THE CAP CONGRESS

FOR PROVEN PERFORMANCE WITH MINI PRICES

The comprehensive line of NRC mini mounts has much to offer. The system is versatile, well thought-out and designed for easy setup to save time. The basic building blocks are comprised of the optical mounts which can be either post mounted for variable heights or on riser blocks for fixed heights. When used with NRC optical tables or BREADBOARDS, each component can be quickly lined up either with the mounting hole arrays or with the aid of a straight-edge and base clamps. This way, not only do you have the full flexibility of three dimensions but the optical axis can also be kept low for stability considerations. Many leading laboratories have now standardized, and in some cases switched midstream, to the NRC mini mounts.

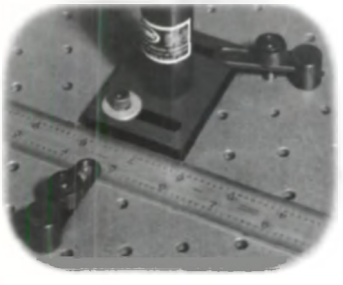

MIRROR & BEAMSPLITTER MOUNTS
Two "bail-pivot" and one gimbal design, each are kinematic and with two orthogonal tilt adjustments. The MM-1 is only 1" X 1" and for two-inch mirrors, there is the choice of either MM-2 or the Gimbal GM-2. The GM-2 is also ideal for mounting beamsplitters due to its large through aperture.

LENS MOUNTS AND LENS POSITIONERS
A combination of lens holder and lens mount allows different lenses or optical elements to be interchanged quickly with a spring loaded detent. The lens positioner has 5 degrees of freedom, X-Y-Z, and two tilts. In addition to positioning lenses, it should also prove to be useful for mounting other electro-optical devices.

OTHER USEFUL ACCESSORIES
Rotational stages, RSA-1 and RSX-1; Translation Stage, TSX-1; Translating post holders VPT-3 and VPT-4; Prism Table T-1; Filter Holder FH-1; Magnetic Bases MB-1 and MB-2; as well as various cross post clamps and base clamps.

ECONOMY
The mini series component line is also very reasonably priced. Here are some examples:

Mirror Mounts; MM-1 and MM-2	$ 22
2" Gimbal GM-2	$ 50
Lens Mount LM-1	$ 11
Lens Positioner LP-1	$180
Rotational Stage RSA-1 & RSX-1	$ 48
Translation Stage TSX-1	$ 55
Filter Holder FH-1	$ 30
Magnetic Base MB-2	$ 28

FREE 32-page catalog, packed with detailed information on over 500 stocked items, plus application notes and a holographic film selection guide as a bonus. Send for your copy today.

Better products through innovation

(NRC) newport research corporation

18235 Mt. Baldy Circle, Fountain Valley, California 92708, Phone (714) 962-7701; Telex 685535